RIPPLE-DRIFT CROSS-LAMINATION IN TURBIDITES

RIPPLE-DRIFT CROSS-LAMINATION IN TURBIDITES OF THE ORDOVICIAN CLORIDORME FORMATION, GASPÉ, QUÉBEC

By

Shyama Bijoy Bhattacharjee, M. Sc.

A Thesis

Submitted to the School of Graduate Studies

in Partial Fulfilment of the Requirements

for the Degree

Master of Science

McMaster University

October 1970

MASTER OF SCIENCE (1970)
(Geology)

McMASTER UNIVERSITY
Hamilton, Ontario.

TITLE: Ripple-drift Cross-lamination in Turbidites of the Ordovician Cloridorme Formation, Gaspé, Québec

AUTHOR: Shyama Bijoy Bhattacharjee, M.Sc. (Cal.)

SUPERVISOR: Professor R.G. Walker

NUMBER OF PAGES: xvii, 167, App. 22.

SCOPE AND CONTENTS: 49 beds of ripple-drift cross-lamination were measured in the Ordovician Cloridorme Formation of Gaspé, Québec. Most of the beds are Bouma C (cross-laminated), some are BC (parallel lamination passing up into cross-lamination) and a few are AC and ABC types (graded bedding passing up into parallel and cross-lamination).

Six climbing patterns have been recognised in the ripple-drift beds, namely: concave-upward, straight, sigmoidal, convex-upward, sinuous, and disconnected-irregular. Angles of climb range from 1 to 44 degrees. Commonly the angle of climb steepens up through the coset to about 1/2 or 3/4 of the coset thickness and then gradually flattens out until the bed is plane.

Measurements of wave length, amplitude, stoss-angle, lee-angle, angle of climb and ratio of lee- to stoss-lamina thicknesses show that the wave length continues to increase upward, and the lee/stoss

thickness ratio decreases upward through the coset. The amplitude,and stoss- and lee-angles increase upward through that portion of the coset in which the angle of climb increases upward. Simultaneously with the increase in amplitude and angle of climb, the shape of the foreset laminae becomes progressively more and more sigmoidal.

Down-current changes in lamination types were recorded in several beds. The most interesting change is from parallel lamination down-current into ripple-drift, continuing downcurrent back into parallel lamination.

ACKNOWLEDGEMENTS

The writer wishes to express his sincere gratitude to Dr. R.G. Walker, his research supervisor, for his patience, discussion and encouragement. Sincere thanks are also extended to Dr. G.V. Middleton for his comments on early versions of the manuscript.

Assistance in the field was given by K. Skipper and J.W. Pett. Thin sections were prepared by H.D. and L.J. Falkiner. J. Coward advised on computational methods. J. Whorwood showed great patience in preparing the photographs as did J. Cekr in constructing the dip compensator. Miss J. Barrett kindly undertook the typing of the manuscript.

Financial support was provided by the National Research Council of Canada and the Geological Survey of Canada.

TABLE OF CONTENTS

TABLE OF CONTENTS (continued) Page

TABLE OF CONTENTS (continued) Page

LIST OF TABLES

LIST OF FIGURES

LIST OF FIGURES (continued) Page

LIST OF FIGURES (continued) Page

LIST OF FIGURES (continued) Page

LIST OF PLATES

LIST OF PLATES (continued)

CHAPTER ONE. INTRODUCTION

1.1. Introduction

Abundant fallout of grains from suspension, in a ripple system, enables each ripple to climb up the stoss slope of the next ripple downcurrent, and results in the formation of the sedimentary structure known as "ripple-drift cross-lamination". This will be shortened to "ripple-drift" throughout the thesis.

Sorby (1859, p.143) first used the term ripple-drift "for all structures that are the effect of the action of ripples on drifted material". In a later paper (Sorby, 1908, p.171-233) he concluded that the production of this structure involves the depth and velocity of the current, the size, shape and density of the material drifted, the length and height of the ripples, and the rate of deposition. Further, on the basis of difference in structure (meaning different types of ripple-drift) he tried to "distinguish between deposits formed from deep water and those formed from shallow water" meaning thereby that in deep water sand and mud are rippled together and in shallow water, the ripples are composed of sand only.

After Sorby, brief descriptions of ripple-drift (or climbing ripples) appeared infrequently in the literature until 1950. False bedding or pseudo cross-stratification described by Spurr (1894) from glacial outwash plain deposits, show strong concentration of very coarse material (pebbles and gravels) in the troughs. Walker (1963), however, is of the opinion (quoting Jaggar, 1894) that this false bedding and the "compound cross-bedding" of Gilbert (1899) probably owe their origin to ripple migration. After Spurr, Woodworth (1901) described some steeply climbing (about 40^{o}) sets of ripple-drift showing selective accumulation of mica on the lee face of the ripples. Bucher (1919) used the term for "a small scale pattern of cross-bedding" and referred the reader to Sorby (1908). He implied that climbing was involved in this small scale pattern of cross-bedding.

McKee (1938, 1939) has illustrated steeply climbing (about 30^{o}-40^{o}) ripple-drift from the Colorado River delta and the flood plain deposits of the Colorado River. According to Allen (1969, p. 121) these "appear to have been generated by the steep climbing of small scale linguoid ripples".

Ripple-drift cross-lamination occurs commonly in fluviatile deposits (Walker, 1963; Allen, 1963; DeRaaf et al., 1964; Coleman

et al., 1964; Friend, 1965; McKee, 1965, 1966; Coleman and Gagliano, 1965; Davies, 1966; Jopling & Walker, 1968). However, this thesis will be restricted to the ripple-drift which is common in many turbidite formations.

1.2. Ripple-drift cross-lamination in Turbidites

Rather exhaustive field observations supplemented by experimental studies (Kuenen and Migliorini, 1950; Kuenen, 1951, 1965, 1966, 1967; Middleton, 1966a, b, 1967a, b, c) and simultaneous theoretical interpretations (Bagnold, 1962; Sanders, 1963, 1965; Walker, 1965; Scheidegger and Potter, 1965; Walton, 1967) have helped to maintain a rapid pace in the growth and development of the turbidite concept since 1950. Works of Dzulynski and Walton (1963), Dzulynski (1965, 1966), Dzulynski and Simpson (1966a, b) and Allen (1969) lead to some understanding of the formation of sole structures. Bouma (1962) recognised an ordered sequence of internal sedimentary structures (fig. 1) in some turbidites. Walker (1965) and Harms and Fahnstock (1965) subsequently interpreted the sequence in terms of flow regime.

The occurrence of ripple-drift cross-lamination in the C division (division of current ripple and convoluted lamination; attributable to deposition in ripple regime) of Bouma (1962), has been reported by very many workers (Sorby, 1908; Kuenen, 1953, 1967; Allen, 1960;

FIG. 1.

The complete sequence of division in an ideal turbidite, modified from Bouma (1962) by Walker (1965, fig. 1, p. 2).

Division A: attributed to formation in the antidune phase of bed transport.

Division B: attributed to formation in the plane-bed phase of transport.

Division C: attributed to formation in the ripple-bed phase of transport.

Division D: deposited from suspension with little bed-load movement.

Division E: formed by normal pelagic deposition.

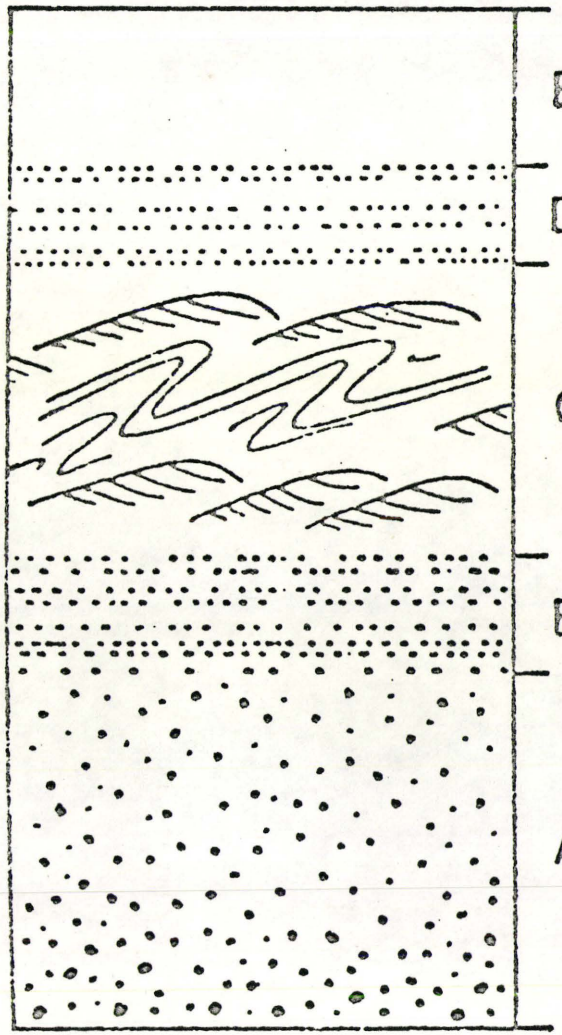
E. PELITIC DIVISION
D. UPPER DIVISION OF PARALLEL LAMINATION
C. DIVISION OF CURRENT RIPPLE LAMINATION
B. LOWER DIVISION OF PARALLEL LAMINATION
A. GRADED DIVISION

FIG. 1.

Wood and Smith, 1959; Prentice, 1960; McBride, 1962; Bouma, 1962; Sanders, 1963; Dzulynski and Walton, 1965; Reading, 1963; Walker, 1963, 1965, 1969; Jopling and Walker, 1968; Enos, 1969a, b). Experimental studies on the production of ripple-drift have been made by McKee (1965) and Kuenen (1966, 1967).

Many of these and other published works on turbidites, however, include only a brief or superficial description of ripple-drift, along with one or two photographs or diagrams. There is little quantitative data and even less experimental data.

The most important turbidite ripple-drift literature consists of papers by Sorby (1908), Kuenen (1953, 1966, 1967), Walker (1963, 1969), Jopling and Walker (1968), Sanders (1963), McKee (1965) and Allen (1970b).

Sorby (1908) described in detail the ripple-drift cross-lamination of the Langdale Slates (Ordovician, English Lake District) and included two good photographs (his plate No. XV and XVI). Some of his observations have already been mentioned. Points to be noted here are (i) the extremely fine grain size of the material, (ii) high 'concave-upward' and 'stratight' angles of climb and (iii) signs of erosion of the stoss side laminae in the lower part of the cosets.

Kuenen (1953, pl. B) described ripple-drift from the Gamlan Flags (Barmouth, Wales) and noted simultaneous upward growth and forward travel. He summarised his observations in a later paper (1967), where he included three figures (his fig. Nos. 4, 6, 7) illustrating ripple-drift cross-lamination from Pliocene rocks of the Ventura Basin, California, and the Portobello and Gamlan Flags (Lower Paleozoic of Britain) respectively. He noted that the angle of climb in these cases varies from 4^{o} to 45^{o} (average about 12^{o} = 1 in 5), and the grain size is usually between 150 and 50μ (i.e. coarse silt and fine sand). He further quoted some other good examples of ripple drift in flysch (Ballance, 1964, fig. 8 and Crowell et al., 1966, fig. 18). Kuenen (1967, p. 219) also notes that "J.R. Boersma made a field study of ripple in 'turbidites' (personal communication) and found practically nothing but climbing ripples". This is not the experience of Walker (personal communication), who has detailed measurements of 16,000 beds.

Walker (1963) originally distinguished three types of ripple-drift which he assigned to different environments. In a second paper (Jopling and Walker, 1968) a revised and genetic classification was given based upon the ratio of fallout from suspension to bed load moved by traction.

This ratio will be referred to throughout the thesis, and can be considered as:

$$\frac{\text{Rate of transfer of suspended load to bed load}}{\text{Rate of bed load transport}}$$

Type C of Jopling and Walker's classification is believed to be formed by turbidity currents. In a third paper (Walker, 1969), the geometry of ripple-drift cross-lamination was analysed. From the field data and some other available data from the literature, it was shown that the ratio of thickness of the stoss-side and lee-side laminae is the single most important factor (the other being stoss-angle) that controls the angle at which the ripples climb. Walker also noted that higher angles of climb are generally associated with thicker cosets.

Simultaneously with Walker's 1963 paper, Sanders (1963) published a theoretical approach to the problem of formation of primary sedimentary structures. He envisaged that the difference between suspension and traction is reflected in the gross structures that result from deposition by (i) tractional shifting of sand in ripples with no sand fallout from current and (ii) tractional shifting of sand in ripples during sand fallout from current (see his fig. 1). The second process leads to the formation of ripple-drift.

The work of Sanders was followed by the experimental work on ripple-drift cross-lamination of Kuenen (1966, 1967). He determined the rate of ripple migration experimentally in a circular flume. Relating the migration rate to the current velocity and the angle of climb, he tried to show that the rate of upward ripple growth in turbidite ripple-drift beds is about 0.1 cm/min.

Earlier experiments on the production of ripple-drift were published by McKee (1965). He used a wave tank, with a combination of wave action superimposed on unidirectional flow, and the resulting patterns of ripple-drift, not surprisingly, were very complex. However, he observed that the angle of climb is higher with weak currents and lower with stronger currents, and he also noted that water depth and current strength are the two main factors that cause an increase in the size of ripples upward through the bed.

The most recent contribution is the theoretical work of Allen (1970b). He proposed a quantitative model (see fig. 40) of climbing ripples and predicted several spatial patterns of climbing ripple cross-lamination types due to varied flow conditions. The model, in essence, is a theoretical treatment of the genetic classification proposed by Jopling and Walker (1968), incorporating the experimental work of Simons et al. (1965) and Bagnold (1966).

1.3. Non-climbing cross-lamination in Turbidites

In the Cloridorme Formation (Ordovician, Gaspé, Québec), and in the examples of Kuenen (1967, p. 218-19), ripple-drift cross-lamination is commoner than non-climbing cross-lamination. However, Walker (personal communication) could not confirm this relationship from his experience, and mentioned that in many sequences (e.g. the Upper Devonian of Pennsylvania, Maryland and New York State) non-climbing ripples may be very common and ripple-drift cross-lamination completely absent.

The non-climbing ripples generally consist of single sets of cross-lamination or a few sets of irregular and truncated cross-lamination. These cosets may occur singly or on top of either a graded bed or a parallel laminated bed. A characteristic feature of these beds is that the thickness of the cosets does not exceed 3 inches and rarely exceed 1 inch (Hsu, 1964, p. 379). The sands and silts are sometimes found to be better sorted than that of the associated graded beds. The cross-laminated sands may sometimes occur in discontinuous patches and may contain a deepwater fauna mixed with a transported fauna.

The occurrence of these beds in turbidite sequences has been reported from the Ordovician Martinsburg and Devonian Trimmers

Rock Formations of the central Appalachians (McBride, 1962; McIver, 1961), the Mississippian and Pennsylvanian Stanley, Jackfork and Atoka formations of the Ouachitas (Cline, 1960); the Pennsylvanian Tesnus and Haymond formations of the Marathon Basin (Cotera, 1962; McBride, 1966); the Mesozoic Franciscan group of the Coast Range and the Cretaceous and early Tertiary flysch of the Swiss Alps (Crowell, 1955; Hsu, 1960); Pliocene sandstones of the Ventura Basin (Hsu, 1964); Palaeozoic graded bedded sequences of the British Isles (Kopstein, 1954; Basset and Walton, 1960; Kelling, 1958) and in the Carboniferous graded greywackes of Germany (Kuenen and Sanders, 1956).

These cross-laminated beds associated with graded beds have often been referred to as turbidity current deposits. Natland and Kuenen (1951) suggested that these were deposited by "ripple-forming dilute turbidity currents". Hsu (1964) strongly advocated the hypothesis that these beds were initially deposited as graded beds but later they were reworked and re-deposited by the "rippling action of deep marine bottom currents". Deep marine bottom currents exist and are sometimes strong enough to ripple the deep sea bottom (Menard, 1952; Ericson et al., 1955; Emery, 1956; Heezen and Hollister, 1964; Hubert, 1964; Shepard and Dill, 1966; Stanley and Kelling, 1967).

However, despite all this work it does not presently seem possible to distinguish turbidity current formed ripples from ocean bottom current formed ripples. Probably the best clue is the ripple vs. sole mark orientations.

1.4. Current Direction in Turbidites (from Cross-Lamination and Ripple-Drift)

Crowell (1955) found a good parallelism between the cross-lamination direction and the direction of sole marks. Hsu (1964) also observed such parallelism in the Palaeozoic outcrops of the Ouachita and the Marathon Basins. McBride (1962) also noted a good agreement between the two types of directional measurements. In the Cloridorme Formation they show a fair degree of parallelism (Enos, 1969b). Current directions measured from ripple-drift and sole marks by the present author in the Cloridorme formation indicated a strong parallelism.

Prentice (1960) noted that the palaeo-current direction obtained from the measurements of flute casts do not agree with those indicated by the ripple marks and cross-lamination. Basset and Walton (1960) reported that the current direction indicated by cross-lamination measurements does not show any preferred orientation, while the current direction obtained from flute cast measurements in the same rocks do show good preferred orientation.

Adjacent beds of ripple-drift showing current directions differing by almost 180° were noted by the present author and Enos (1969b, p. 696) on several outcrops of the Cloridorme formation.

1.5. Previous Work on the Present Area

The Middle Ordovician rocks exposed along the north coast of Gaspé peninsula (Fig. 2) were described briefly by McGerrigle (1959). Enos (1969a) named these rocks the Cloridorme formation and made a detailed study. The general description of the formation given here is based on the work of Enos (1965, 1969a, b).

The Cloridorme formation is divided into three constituent structural blocks (with uncertain stratigraphic relationship) namely: Eastern, Central and Western (Fig. 2). Enos erected 14 stratigraphic members, viz. α_1 to α_3, β_1 to β_7 and γ_1 to γ_4 respectively. The formation consists of 7700 m ("with an uncertainty factor of 2") of greywacke, calcisiltite, and dolostone interbedded with argillite, and is exposed in a narrow belt 80 miles long and 12 miles wide along the northern Gaspé coast, Québec.

The entire sequence, assigned to the 'Orthograptus truncatus intermedius Zone' of Berry (1960), is considered as age equivalent to the upper part of the Normanskill formation (Enos, 1969a;

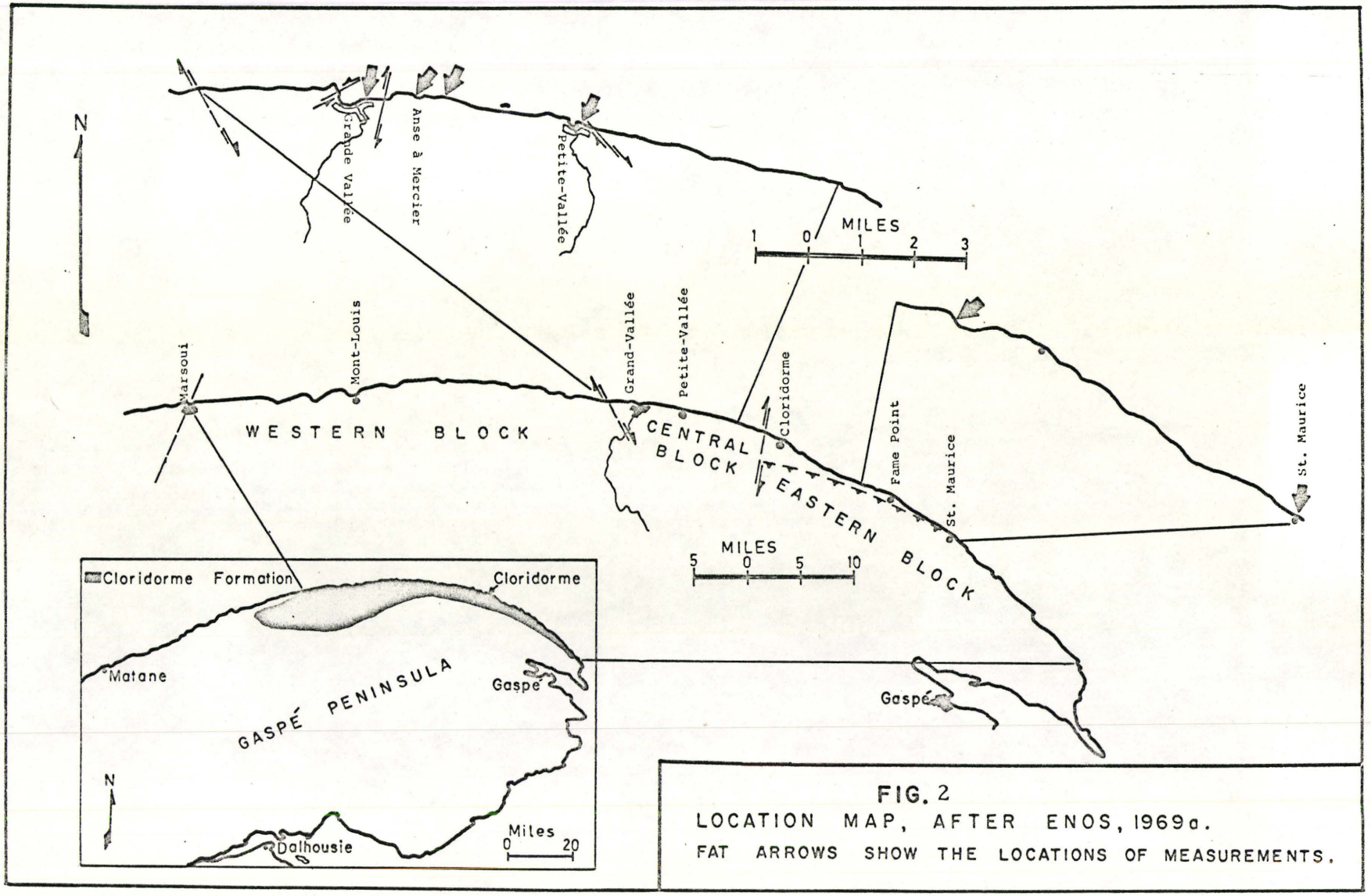

FIG. 2
LOCATION MAP, AFTER ENOS, 1969a.
FAT ARROWS SHOW THE LOCATIONS OF MEASUREMENTS.

Berry, 1962). However, from an analysis of the graptolite faunas of the Gaspé north shore, Riva (1968) found it impossible to interpret the Gaspé fauna in terms of the Berry's 'Zone' of the Ordovician sequence of Texas. Riva concludes that more than one graptolite zone is included in the Cloridorme Formation. The formation as a whole forms a part of the geosynclinal assemblage of the folded Appalachians, extending from south-eastern Tennessee to Newfoundland. The Cloridorme Formation, although faulted and overturned, has not suffered extensive metamorphism.

From a detailed study of the stratigraphy, sedimentary structures and lateral variation in the greywacke sequence, Enos (1969a,b) concluded that these rocks were deposited by turbidity currents, which periodically invaded the quiet pelagic mud and ooze environment. Current directions were longitudinal and mainly to the west except in the upper two members (i.e. γ_2 and γ_3) where easterly directions are found. From the tentatively inferred en echelon configuration of the members, Enos suggested that they were wedges built successively towards the west as the elongate trough was filled from the eastern end.

Following Enos, Parkash (1969) made a detailed study of the sedimentary structures, textures and fabric of 8 greywacke beds and

concluded that the beds were deposited by "low concentration, highly turbulent" turbidity currents. This type of work is made possible only by the superb coastal exposures.

Walker (1969) measured a sequence of 61 turbidite beds, including 15 beds of ripple-drift, at Petite Vallée harbour (one of the four localities of the area studied by the present author), and made some geometrical conclusions which will be fully discussed later. Skipper (1970) correlated a sequence of beds from the β_1 member for a distance of 7.5 miles and described the occurrence of some antidune beds and certain unusually thick turbidites displaying "a sequence of internal sedimentary structures different from the typical 'Bouma Sequence'". At the same time, Pett (1970), from a study of the morphology of flutes (1511 flutes measured in total) from different members of the Cloridorme formation (including a few from other formations), demonstrated that there exists a continuum of flute shapes independent of the bed types (A, B, C of Bouma, 1962) except that wider flutes tend to be present on the soles of A beds (Pett and Walker, 1971).

The excellent coastal exposures of the rocks of the Cloridorme Formation have made the sequence one of the best of its kind in the world

and present an ideal situation to study the different aspects of turbidites that have been fascinating sedimentologists since 1950.

1.6. Area of Present Study and the Problem of Cloridorme Ripple-Drift

After a reconnaissance survey along the northern Gaspé coast, four localities were selected for the purpose of present study. They are: (1) St. Maurice, (2) Fame Point, (3) Petite Vallée and (4) Grande Vallée (Fig. 1). At all of these places, except St. Maurice, the beds are overturned. Table 1 shows the dip and strike of beds in the respective localities. At St. Maurice, the bed measured belongs to the α_3 member of the eastern structural block. The beds measured at Fame Point belong to the β_1 member of the central structural block. The beds measured at Petite Vallée and Grande Vallée belong to the β_7 member of the central structural block. In all the localities the mean current direction is parallel to the strike of the beds.

A total of 49 ripple-drift beds were studied (Table 1). Of these, bed 477 of St. Maurice, beds 5, 7, 8, 9 and 10 of Petite Vallée Harbour and beds 1 and 2 of Grande Vallée (East of Anse à Mercier) were studied in detail. The features that distinguish the ripple-drift of the Cloridorme turbidites from other ripple-drift are the spectacularly thick cosets (range 2 to 75 cm), the consistently large wavelengths

PLATE 1.

View of the ripple-drift beds at Petite Vallée. Bed 7 is to the right (AC with a little B). Bed 6 lies on bed 7. Overlying bed 6 is a very thin unnumbered bed. Overlying the unnumbered bed is bed 5. Stratigraphic top is to the left. Current from top ⟶ bottom, east to west.

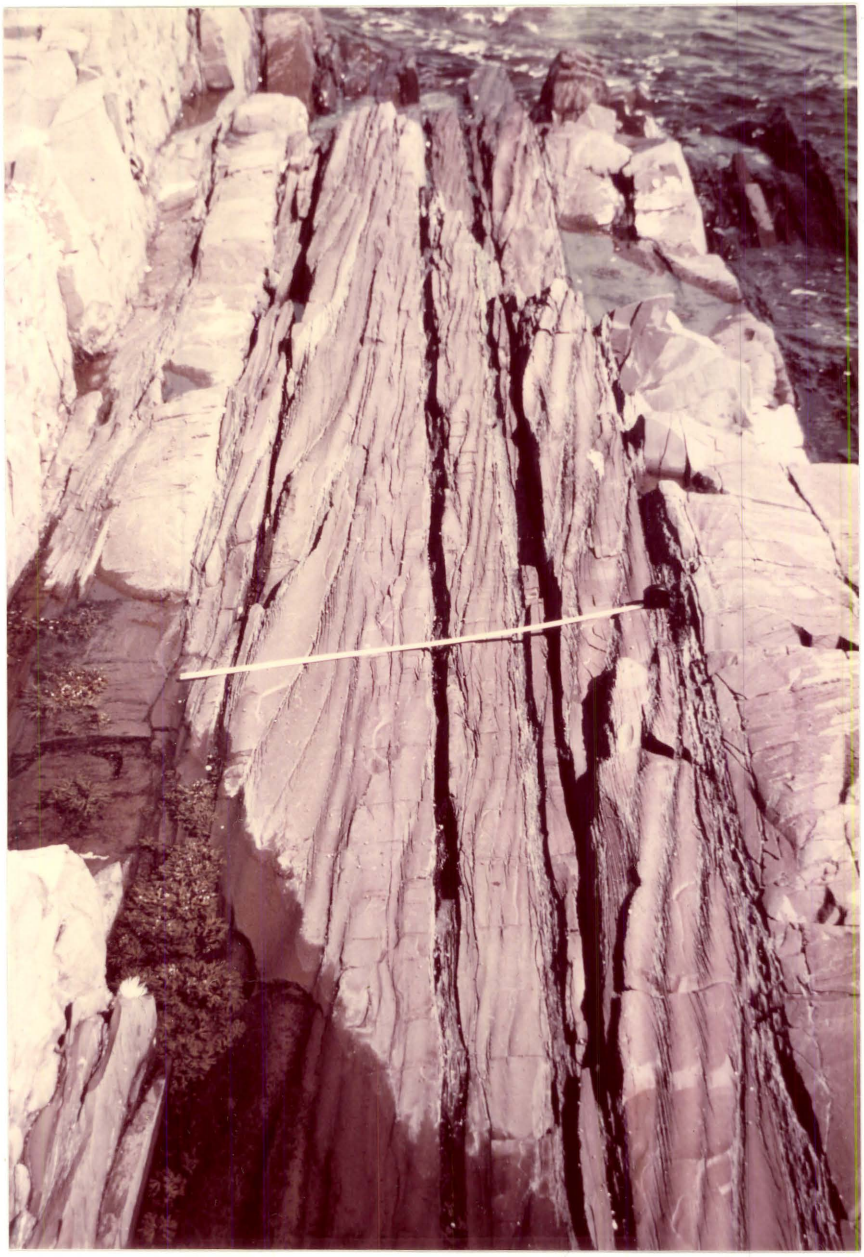

PLATE 2

View of bed 8 of Petite Vallée. Stratigraphic top is to the right and flow east to west (bottom to top of picture). Note the gradual decrease in angle of climb and wave length downcurrent.

PLATE 3.

View of the wave-cut platform, east of Anse à Mercier, Grande Vallée, showing bed 1 (lower right) and bed 2 (lower left). Stratigraphic top is to the right.

PLATE 4.

View of beds 1, 2 and 3 at Petite Vallée, Note thick parallel sided cosets. View facing east, current flow from east to west.

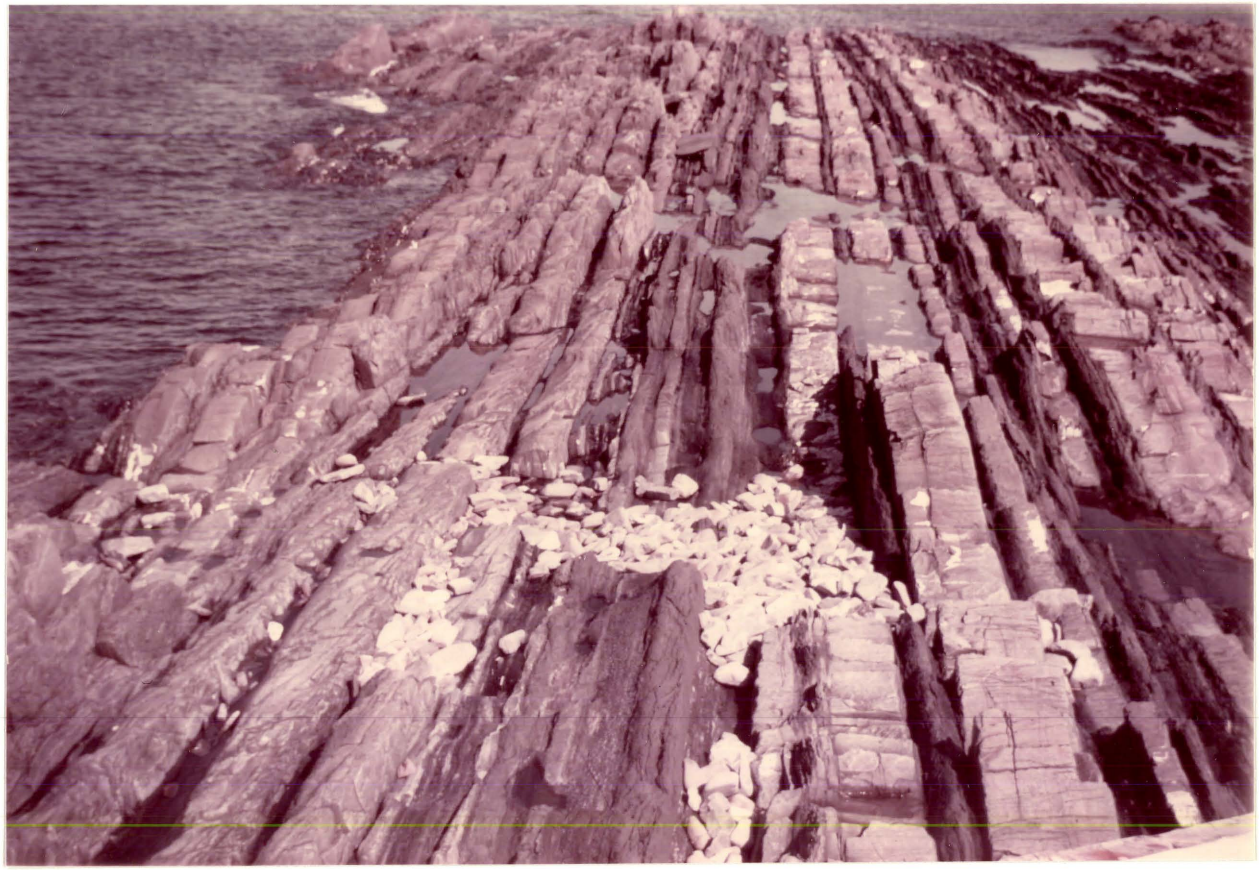

(range 13 to 84 cm) and comparatively small amplitudes (range 0.4 to 5.2 cm). The ripple-drift beds are spectacularly parallel-sided and can be followed along strike on the wavecut platform for more than 100 metres without any apparent significant change in their character. In most of the beds, individual laminae can be traced from stoss-side to lee-side, across the ripple system. Signs of erosion of stoss-side laminae are fairly common in the lower part of a coset. The wide range (1 to 44 degrees) of the angle of climb is in good harmony with the wide (6 types, see Fig. 6) variety of the spectacularly displayed climbing patterns. Current directions measured from ripple-drift cross-lamination are close to the mean direction of flow given by sole marks in all the localities studied. Surprisingly, in some of the beds the current direction deduced from the ripple-drift is opposite to the regional East-to-West palaeoflow direction. Some of these characteristics and many others were noted earlier by Walker (1963, 1969) and Jopling & Walker (1968). However, a detailed field investigation of the turbidity-current-formed ripple-drift has not been undertaken previously. It is therefore difficult at present to relate some of the field observations to the experimental work of Kuenen and the theoretical work of Allen.

In his experiments, Kuenen (1966, 1967) has tried to assess the growth rate of the turbidite ripple-drift beds from the experimentally determined rate of ripple migration and current velocity, combined with data on the angle of climb obtained from field measurements. His main conclusion indicates rates of upward growth of ripples for about 0.1 cm/min.

Recently Allen (1970b) published a theoretical analysis of ripple-drift cross-lamination and predicted that for various types of flows, different sequences of types of ripple-drift cross-lamination would be formed. However, no work has been done in the field in determining different sequences of turbidite ripple-drift, and hence one of the main objectives of this study is to see whether Allen's theory does in fact account for the field observations.

The primary purpose of this study, therefore, is to investigate the morphology of turbidite ripple-drift and to evaluate the findings in terms of the published experimental and theoretical results.

TABLE I

Data on strike and dip, bed thickness, current direction and number of ripples measured

TABLE - I

LOCATION	Member (Enos, 1969)	Strike and Dip of Beds	Bed Number	Bed Thickness in centimetre A	B	C	No. of measurement Stations on The Bed	No. of Ripples measured at each station (average)	Total No. of Ripples measured on The Bed	Exposed measurable Bed-Length in feet	Local Mean Palaeo-Flow Direction (Enos, 1969)	Ripple-Flow Direction ****	Sole-Mark Direction ****
St. Maurice (North of Church)	σ_3	S. 297° D. 40°→207°	* 477	0	8	70	24	5	118	900'	307°	306°	303° **301°
West of Fame Point	β_1	S. 282° D. 85°→192°	* 666	0	0	11.2	1	3	3	40'	274°	281°	---
			* 700	0	0	9.4	1	3	3	"		"	---
			* 701	0	0	7.5	1	3	3	"		"	---
			* 702	0	0	14.5	1	3	3	"		"	---
			* 759	0	0	6.5	1	3	3	"		278°	281°
			* 765	0	0	8.0	1	3	3	"		"	"
			* 772	0	0	5.9	1	3	3	"		286°	---
			* 773	0	0	4.8	1	3	3	"		284°	---
			* 774	0	0	5.1	1	3	3	"		281°	---
			* 790	0	0	9.8	1	3	3	"		286°	---
			* 791	0	0	14.5	1	3	3	"		"	---
			* 793	0	0	12.5	1	3	3	"		283°	---
			* 794	0	0	8.5	1	3	3	"		284°	---
			* 795	0	0	11.7	1	3	3	"		281°	---
			* 798	0	0	9.0	1	2	2	"		286°	---
			* 799	0	0	6.5	1	3	3	"		"	279°
			* 800	0	0	5.5	1	3	3	"		"	281°
			* 801	0	0	7.3	1	3	3	"		"	"
			* 899	0	0	23.0	1	3	3	"		289°	287°
			*1013	0	0	5.8	1	3	3	"		281°	---
			*1014	0	0	2.6	1	3	3	"		"	---
			*1015	0	0	4.7	1	3	3	"		"	---
			*1021	0	0	5.0	1	3	3	"		286°	---
			*1030	0	0	5.6	1	3	3	"		288°	290°
			*1031	0	0	6.1	1	3	3	"		"	"
			*1033	0	0	9.0	1	3	3	"		286°	291°
			*1034	0	0	5.1	1	3	3	"		"	"
			*1035	0	0	4.6	1	3	3	"		"	"
			*1036	0	0	3.6	1	3	3	"		291°	288°
			*1038	0	0	5.1	1	3	3	"		293°	---
Petite Vallée Harbour, East.	β_7	S. 272° D. 80°→182°	1	0	0	32.0	1	6	6	300'	270°	261°	---
			2	0	0	57.0	1	6	6	"		265°	285°
			3	0	0	35.0	1	4	4	"		261°	---
			4	0	0	7.0	1	4	4	"		247°	---
			5	0	0	38.0	17	4	71	340'		254°	266°
			6	0	0	3.4	1	4	4	"		250°	---
			7	52	2	22.5	17	4	73	"		246°	259°
			8	0	5	20.8	12	4	42	"		249°	273°
			9	0	0	60.0	10	5	50	250'		255°	---
			10	0	0	28.0	4	4	15	260'		***81°	---
East of Anse à Mercier Grande Vallée	β_7	S. 277° D. 75°→187°	1	0	2	25.0	1	4	4	300'	269°	***112°	---
			2	0	5	12.0	5	4	20	"		268°	271°
			3	0	0	17.0	1	4	4	-		277°	277°
Anse à Mercier West, G. Vallée	β_7	S. 272° D. 75°→182°	4	8	2	70.0	1	4	4	25'	269°	222°	244°
			5	0	0	58.0	1	4	4	"		260°	---
			6	0	0	75.0	1	4	4	"		272°	---
East of Harbour G. Vallée	β_7	S. 279° D. 78°→189°	7	0	0	25.0	1	2	2	50'	273°	***87°	---
			8	0	0	65.0	1	4	4	"		***113°	---

N. B. → Amount and direction of dip.

* Those with asterisk are Bed Nos. of logged sections, others are ordinary serial Nos.

** Orientation direction of Graptolites.

*** Current directions in these beds are opposite to the regional current direction.

**** Mean of several measurements.

CHAPTER TWO. PARAMETERS AND THEIR MEASUREMENT

2.1. Parameters

Fig. 3(A) (after Walker, 1969) shows the model of a climbing ripple and explains the terminology used in describing the geometrical parameters. In the text the author has conveniently used some shorter forms of these terms and/or some letter symbols to designate these parameters. All these terms (including some others not shown in fig. 3-A), symbols and their precise explanations are given in Table II.

Explanations of a few other terms, frequently used in the text, are given below:

Measured Angle of Climb: This indicates the actual angle of climb measured in the field and is given the symbol ϵ. The term angle of climb, wherever used, refers to this measured (actual) angle of climb only. In certain places the term "measured angle of climb" has been used (instead of 'angle of climb') to avoid any confusion that might arise between the terms "measured angle of climb" and "computed angle of climb".

Computed Angle of Climb: Symbol used for this term is ϵ', and it refers to the angle of climb computed from the values of actual measurement of the parameters β, α, t_L and t_S, using the equation (Walker, 1969, p. 387) given below:

$$\tan \epsilon' = \frac{-(t_L \sin \beta + t_S \sin \alpha)}{(t_S \cos \alpha - t_L \cos \beta)} \qquad (1)$$

Coset thickness: The term refers to the vertical thickness of sets of ripple-drift cross-lamination contained in a bed (for details see Allen, 1968, p. 99, Fig. 5.2). The terms 'thicker coset' and 'thinner coset', sometimes used in the text, refer to coset thicknesses greater than and smaller than 10 cm respectively.

2.2. Field Measurement Procedures

On the basis of the simple geometry explained in Fig. 3-A, ripple data were recorded in the field on pre-designed sheets. A sample copy of the data sheet is enclosed in Appendix 1(a).

Most of the column headings in the data sheet are self-explanatory. However, a few need a little clarification. "Position on Bed" - indicates the distance in feet from an arbitrary zero bench mark on the bed. "Position on Bed" when recorded as 0.0 indicates only one measurement station on that particular bed. All measurements except "Positions on Bed" were recorded in centimetres. Under "Bed

FIG. 3.

A. Model of a climbing ripple showing the terminology used.

B. Field procedures for measurement of stoss-angle lee-angle and ripple shapes. Details explained in the text.

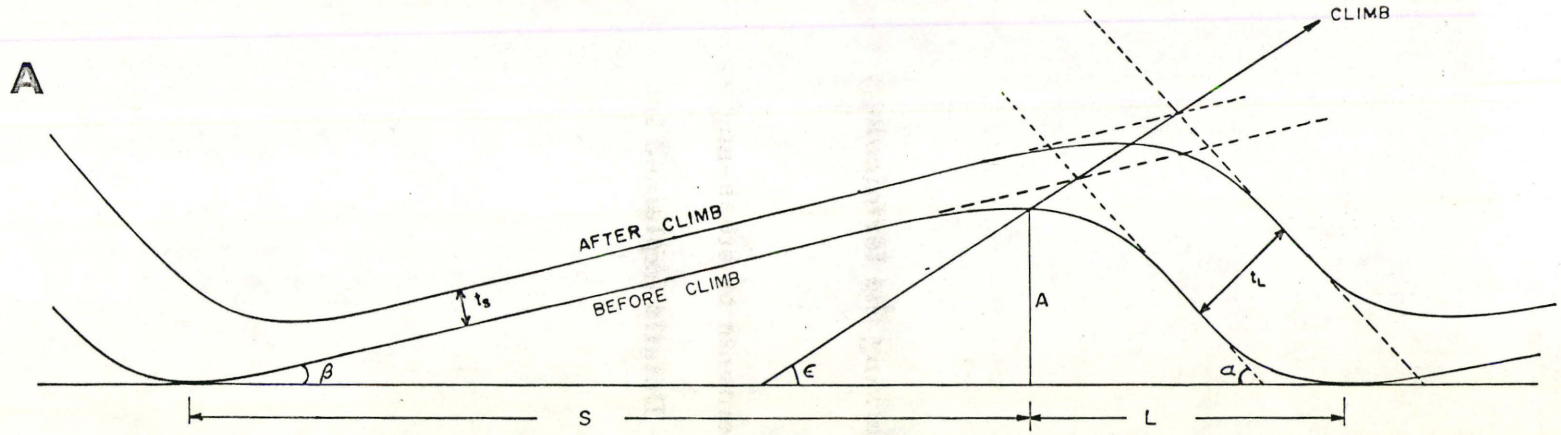

MODEL OF A CLIMBING RIPPLE SHOWING THE TERMINOLOGY USED

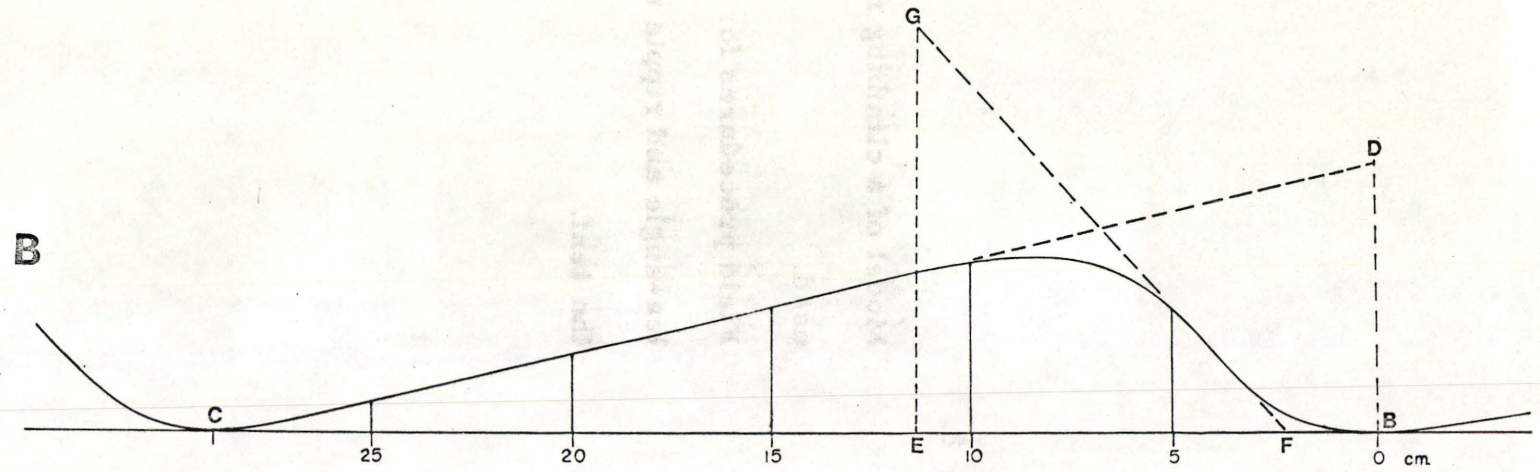

S = projected length of the stoss side; L = projected length of the lee side; A = amplitude; S+L = wave length; t_S = thickness of the stoss laminae; t_L = lee side thickness of the same laminae β = stoss angle; α = lee angle; ϵ = angle of climb.

FIG. 3

TABLE II

Terms and symbols used and their explanation.

TABLE II

Term	Symbol	Explanation
Wave length	W (= S+L)	Length from trough to trough of a ripple.
Amplitude	A	Perpendicular height from the base to the crest of a ripple.
Lee length	L	Projected length of the lee side.
Stoss length	S	Projected length of the stoss side.
Stoss-angle	β	Inclination of the stoss-slope with respect to the base (i.e. line joining the trough points) of a ripple.
Lee-angle	α	Inclination of the lee-slope with respect to the base of a ripple.
Stoss-thickness	t_S	The perpendicular thickness of a single or a set of laminae on the stoss side of a ripple.
Lee-thickness	t_L	The perpendicular thickness of the same single laminae or the same set of laminae on the lee side of the same ripple.
Angle of climb		The angle between the base of a ripple (assumed to be parallel to the base of a coset) and the line joining the crests of successively superposed ripples from bottom upward and forward through a ripple-drift coset.
Ratio of Lee-to-Stoss side lamina thickness	t_L/t_S	
Ripple Index	RI	$RI = \frac{W}{A} = \frac{\text{Wave length}}{\text{Amplitude}}$
Ripple Symmetry Index	RSI	$RSI = \frac{S}{L} = \frac{\text{Stoss-length}}{\text{Lee-length}}$

Thickness" A-B-C indicate Bouma's (1962) divisions of a turbidite bed. "Inter" means interturbidite, i.e. argillite.

After selecting the ripple-drift bed for measurement, the 'Positions on Bed' (i.e. stations) were chosen and marked by paint. The interval between stations (in case of beds studied in detail) was not regular but was determined by the nature of exposure.

At each station on the bed, angle of climb, stoss-angle, lee-angle, t_L, t_S, wave length, amplitude, lee length and ripple shape were measured.

The angle of climb, the stoss-angle and the lee-angle were calculated in the laboratory from horizontal and vertical length measurements made in the field.

Fig. 4 illustrates the measurement procedure of the angle of climb. The angle of climb at the points (i.e. 'Position within Bed') P, Q and R are then defined respectively by the angles $\angle$QPK, $\angle$ RQL and $\angle$ SRM respectively. Once the lengths AB, AC, AD and AE and the heights PB, QC, RD and SE are measured, the angles of climb at the points P, Q and R can be calculated easily. For example:

$$\angle \text{QPK (in degrees)} = \left[\tan^{-1}\left(\frac{QK}{PK}\right)\right] \times \left[\frac{180}{\pi}\right] \text{ where}$$

$$QK = QC - PB \text{ and } PK = AC - AB$$

FIG. 4.

Field procedure for measurement of Angle of Climb, Position on Bed and Position within Bed. Details explained in the text.

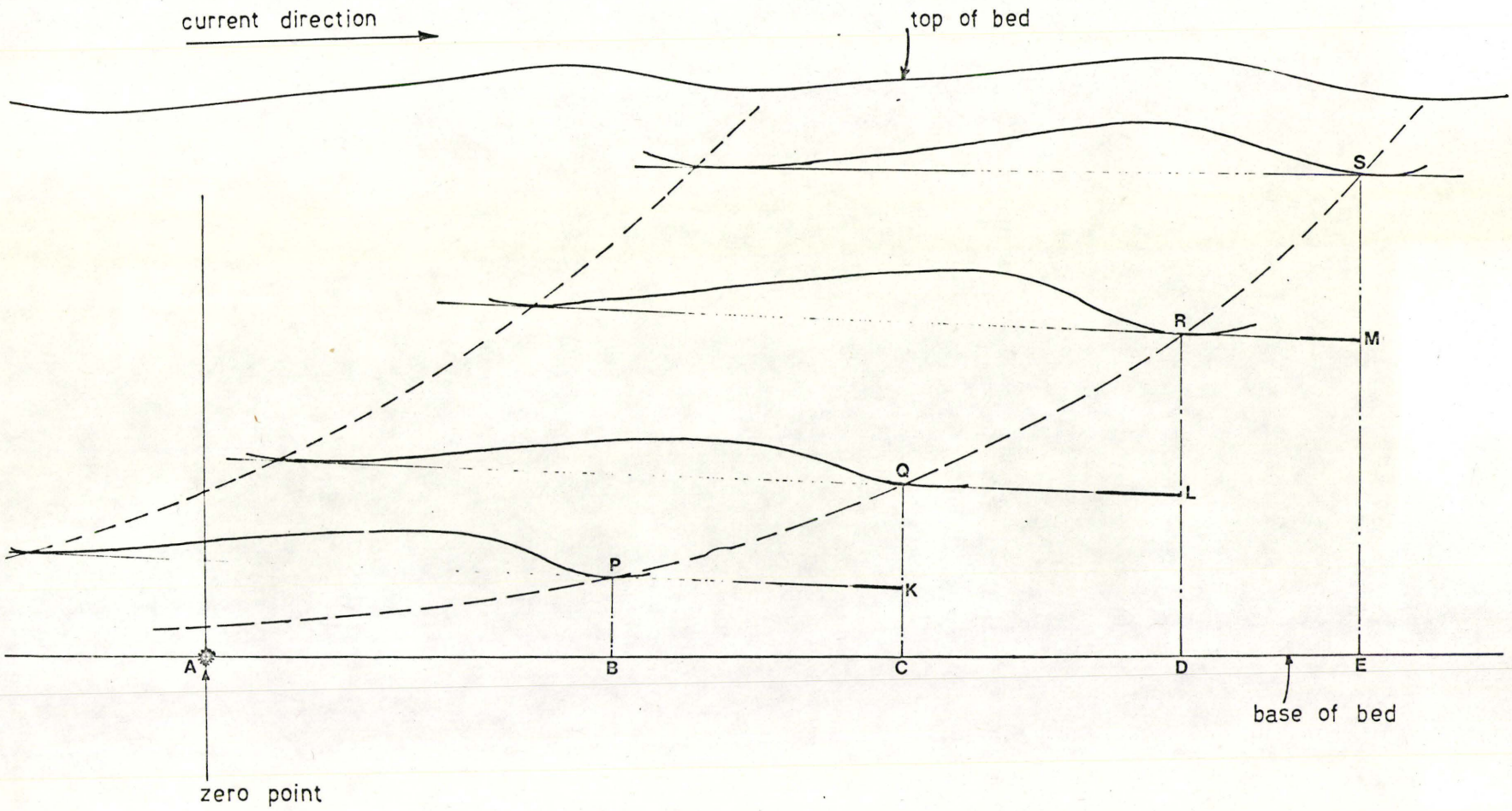
current direction
top of bed
S
R
M
Q
L
P
K
A
B
C
D
E
base of bed
zero point

FIG. 4

In fig. 4, the angle of climb has been shown as a line passing through the troughs of the subsequently superposed ripples upward through the coset. This scheme was adopted in the field for data recording because of the ease of recognising the angle of climb from the ripple troughs, where from the sea had etched out the softer clayey sediments leaving thereby a slightly depressed dark line (see Pl. 2).

The methods of measurements of the stoss- and lee-angles are illustrated in Fig. 3B, where the lengths BC and EF and the heights DB and GE, laid out arbitrarily, were recorded in the field. Then the required angles are given by:

$$\text{Stoss-angle } (\angle BCD) \text{ in degrees} = \left[\tan^{-1}\left(\frac{DB}{BC}\right)\right] \times \left[\frac{180}{\pi}\right]$$

$$\text{Lee-angle } (\angle EFG) \text{ in degrees} = \left[\tan^{-1}\left(\frac{GE}{EF}\right)\right] \times \left[\frac{180}{\pi}\right]$$

In order to minimize errors in such measurements, lengths of the bases of the triangles were usually chosen to be as large as possible.

Depending on the thickness of the coset, measurements of these parameters were made at every station on 3, 4, 5 or 6 selected (well defined) ripples from different levels (see fig. 4) in the bed along the angle of climb.

Palaeocurrent data on ripple-drift cross-lamination and sole marks were recorded with the help of a dip compensator (described by Enos 1969b; Parkash, 1969, p. 16) in conjunction with a Brunton compass. Current directions in the ripple-drift beds were recorded at each station from the line of intersection of the lee side laminae with the wave eroded stoss side planes (see Pl. 5) exposed along the base of the beds.

While recording the ripple shapes, the base of every ripple was marked at 5 cm intervals and the vertical heights at those points were recorded as shown in fig. 3(B).

2.3. Rock Samples

Rock samples, one from the bottom and one from the top of every coset were collected. In all cases the samples were from near the crest on the stoss-side of a ripple. Similar samples located a couple of hundred feet apart (see Table VI) were collected from the beds that were studied in detail. From bed 477 at St. Maurice, three similar samples from the base, the middle and the top of the coset were collected at 4 stations (0', 300', 600' and 900' points). In addition, one oriented specimen of a complete ripple was obtained from each of the three localities at Grande Vallée, Petite Vallée and St. Maurice. Fig. 8 shows the number of the bed and the exact position of the extracted ripple specimen within each bed at these three localities.

2.4. Laboratory Methods

Data Processing: Direct measurements of W, A, L, t_S, t_L and coset thickness were possible in the field. But the final values of the measurements of α, β, ϵ, ϵ', S, RI and RSI were later calculated in the laboratory (523 measurements of each in total) with the help of a computer. Both raw and processed data are given in the Appendix 1(c) and 1(d) respectively.

Grain Size Analysis: In this study two different methods were used for two different sets of collected samples. (1) The samples collected for the purpose of studying the relationship between (i) coset thickness and maximum grain size, (ii) angle of climb and maximum grain size, (iii) wave length and maximum grain size, and (iv) ripple index and maximum grain size, were analysed by using binocular microscope. (2) The samples collected for the purpose of studying grain size distribution across ripples were analysed in thin section by the help of the shadowmaster using a magnification of X100.

Modal Analysis: This was done with the help of a shadowmaster using X100 magnification. A total of 100 counts (taken to be sufficient for such analysis; see Parkash, 1969, p. 66) were made using a 5X20 rectangular grid.

Statistical Analysis: Graphic Mean (M_Z) and Inclusive Graphic Standard Deviation (σ_I) were calculated (after Folk, 1968; p. 45-46) for four parameters W, A, RI and RSI.

Correlation coefficients were calculated for each two parameters plotted and the results are shown on the plots. The significance of the correlation coefficients was evaluated by means of comparison with standard tables (Table A-30a; Dixon and Massey, 1957, p. 468). The calculations of correlation coefficients was done using the standard formula:

$$r = \frac{xy}{\sqrt{(x^2)(y^2)}}$$

where $x = X - \bar{X}$ and $y = Y - \bar{Y}$.

2.5. Accuracy of Measurements

A high degree of accuracy can only be achieved in the case of easily measurable parameters such as Wave Length and Lee Length (L). Measurements of Amplitude, Stoss-angle, Lee-angle, Angle of Climb, t_L and t_S were more difficult to make and hence they are less accurate. All these measurements were made with extreme caution and were recorded after several checks. However, in each of the different types of measurements as mentioned above, the accuracy is about ±10%.

In all the four localities (Grande Vallée, Petite Vallée, Fame Point and St. Maurice) measurements of the geometrical parameters of the ripple drift were made on vertical sections through the beds and the vertical sections were parallel to the palaeoflow direction. Hence, no correction was necessary for oblique sectioning.

The accuracy of measurements of flow direction from ripples and sole marks are probably about $\pm 10^{o}$ degrees.

The accuracy of grain size measurements done with the help of (i) the binocular microscope and (ii) the shadowmaster are ±0.01 mm and ±.005 mm respectively.

CHAPTER THREE. DESCRIPTION OF RIPPLE-DRIFT

OBSERVATIONS AND RESULTS

3.1. General Sedimentology of Ripple-Drift Bearing Rocks

Composition and Texture:

Ripple-drift beds occur in all the three dominant lithologies of the Cloridorme formation, namely: Calcisiltites, Calcareous wackes and greywackes.

Ripple-drift cross-lamination is infrequently present in calcareous wackes and even more infrequently present in graywackes. Calcareous wackes, containing more than 10% argillaceous matrix, but more sparry calcite cement than matrix, may grade vertically and perhaps laterally into type-1 calcisiltites by decrease in both grain size and degree of recrystallization. Three types of graywackes were distinguished by Enos (1969a) on the basis of sedimentary structures, approximate matrix content, distinctness of contacts and colours. With the downcurrent increase of matrix type-1 graywackes may grade to type-2.

Of the two types of calcisiltites distinguished by Enos (1969a), the more abundant type-1 is characterised by thin beds, by ripple-drift and convoluted lamination and by relatively little matrix. Some beds of type-1 are darker at the top, suggesting an increase in argillaceous content, hence grading. The terrigenous grains (largely quartz)are angular, equant to elongate, moderately well sorted and 0.01 to 0.09 mm in diameter. The carbonate grains, largely irregular single crystals, a few polycrystalline, are 0.005 to 0.08 mm in diameter. The carbonate content of type-1 varies between 45 and 82 percent. The matrix (excluding carbonate) varies between 2 and 32 percent, and is mainly chlorite with some carbonaceous material.

Type-2 calcisiltites exhibit spectacularly thick cosets of ripple-drift. Type-2 is distinguished from type-1 "by the presence of parallel lamination or false bedding, or both, by an average matrix content of 18 percent versus 11.6 percent in type-1 calcisiltite, and by an average thickness of 24 cm about 7 times that of type-1 calcisiltites" (Enos, 1969a, p. 20). The median grain size (both terrigenous and carbonate grains) is about 0.02 mm. The quartz grains are moderately well sorted. The carbonate grains are dominantly single crystals but a few of them are polycrystalline.

Some of the data relevant to the present topic are tabulated below (see Table III) from Enos' work (1969a, b).

For the present purposes, it should be noted that the bed 477 of St. Maurice represents a mixed lithology, with calcareous wacke in the lower half of the bed and calcisiltite type-1 in the upper half of the bed. All of the 30 beds measured near Fame Point are type-1 calcisiltites. All the beds measured at Petite Vallée and at Grande Vallée are calcisiltite type-2.

Sole Marks:

Table III shows the frequency of occurrences of different types of sole marks in different lithologic units. Out of 49 beds studied by the present author, sole marks were recorded from 20 beds only. No flute casts were observed at the base of the ripple-drifted beds. The only type of sole marks present were the shallow longitudinal ridges, which are usually poorly developed except in bed 5 of Petite Vallée (see Pl. 6) and in bed 2 of Grande Vallée, where they were found to be fairly well developed, with small cuspate crossing bars.

Current Direction:

The data on current directions measured from ripple-drift and sole marks are presented in Table I. Graptolite orientation direction was measured only in bed 477 of St. Maurice. Fan-shaped orientations of

TABLE III

(A) Petrology of the dominant rock types of the Cloridorme Formation (from Enos, 1969a, b)

(B) Characteristics of dominant rock types.

(C) Lithology of α_3, β_1 and β_7 Members.

A. PETROLOGY OF DOMINANT ROCK TYPES OF THE CLORIDORME FORMATION (Enos 1969 a , Table 1)

	Number of samples	Matrix: Total argillaceous matrix	Matrix: Chlorite (distinguishable)	Matrix: Carbonaceous material	Matrix: Carbonate, cement and (or) matrix	Grains*: Quartz: Total quartz	Quartz: Monocrystalline quartz	Quartz: Polycrystalline quartz	Quartz: Chert	Grains*: Feldspar (plagioclase)	Grains*: Rock fragments: Total rock fragments	Rock fragments: Serpentine	Rock fragments: Volcanic	Rock fragments: Granitic	Rock fragments: Schist (quartz rich)	Rock fragments: Gneiss	Rock fragments: Carbonates	Rock fragments: Sandstone (largely graywacke)	Rock fragments: Siltstone (some calcisiltite)	Rock fragments: Shale	Grains*: Mica	Grains*: Fossil fragments	Grains*: Pyrite (authigenic)	Grains*: Heavy minerals	Grains*: Unknown, opaque
Calcisiltite, type 1	5	11.6	..	..	62.4	80	80	..	..	15	3	..	..	..	..	..	..	..	..	..	2	..	tr.	..	..
Calcisiltite, type 2	3	18.0	8.1	..	47.9	65	65	..	..	17.5	6.5	..	..	..	..	..	..	..	..	..	8.8	..	1.9	..	..
Calcareous wacke	5	10.6	2.5	0.4	31.9	62.1	53.9	8.2	..	14.9	18.0	3.4	4.1	0.2	4.5	..	1.3	..	0.2	4.2	1.7	2.1	0.9	0.3	..
Graywacke, type 1	12	17.2	4.5	0.2	16.7	59.9	44.2	14.6	1.1	10.0	25.0	3.8	11.4	0.6	1.4	tr.	1.9	0.7	1.6	3.6	1.9	0.6	0.4	0.3	1.4
Graywacke, type 2	5	48.4	7.6	1.2	7.1	61.6	50.7	10.3	0.6	12.8	19.6	8.1	3.5	0.5	2.9	0.2	..	..	0.3	4.1	4.1	..	1.0	0.9	..
Graywacke, type 2, carbonate rich	5	17.4	3.4	1.1	41.3	57.6	48.6	9.1	..	17.1	16.2	1.9	9.7	0.2	2.3	..	..	..	..	2.1	3.8	1.9	0.4	0.4	2.7
Graywacke, type 3	3	19.3	11.0	0.5	8.3	16.2	11.0	5.2	..	0.9	76.2	..	3.4	..	0.6	..	61.2	3.4	6.5	1.1	..	6.6	tr.	..	..

*Calculated as 100 percent excluding matrix, except for dolostones, limestone, and dolomitic silty argillite.

B. CHARACTERISTICS OF DOMINANT ROCK TYPES (Enos 1969 b , Table 2)

ROCK TYPE	MATRIX (percentage): Argillaceous	MATRIX (percentage): Carbonate*	TEXTURE: Mean thickness of beds (cm)	TEXTURE: Maximum thickness of beds (cm)	TEXTURE: Mean maximum grain size (ϕ)	STRUCTURES (percentage of beds): Laminations	Cross-laminations	Graded beds	Flutes	Grooves	Other directional sole marks
Graywacke, type 1	17	17	27	260	-0.1	11	8	68	10	26	2
Graywacke, type 2	48	7	18	60	0.6	4	2	6	2	26	3
Graywacke, type 3	19	8	80	385	-0.9	21	3	92	47	11	10
Calcareous wacke	11	32	21	133	1.7	66	47	97	55	8	18
Calcisiltite, type 1	12	62	3	30	>4	13	24	—	3	1	1
Calcisiltite, type 2	18	48	24	150	>4	51	62	1	<1	2	<1

* Includes cement and/or detrital carbonate matrix.

C. LITHOLOGY OF $\mathcal{L}3$, $\beta 1$ and $\beta 7$ MEMBERS (Enos 1969 c , Table 4)

Member	Estimated thickness (m)	Total measured (m)	Argillite	Dolomitic silty argillite	Dolostone and limestone	Calcisiltite 1	Calcisiltite 2	Calcareous wacke	Graywacke 1	Graywacke 2	Graywacke 3
$\beta 7$	835	1500	44.1	..	0.7	6.7	9.6	0.6	31.1	7.3	..
$\beta 1$	1175	561	70.4	..	1.9	7.2	..	6.7	..	0.3	13.5
$\mathcal{L}3$	2000	52	51.9	11.3	1.0	18.1	..	17.7	..	..	..

PLATE 5.

Lines of intersection of lee side laminae with wave-eroded stoss side of underlying ripple. Current from right ⟶ left, east to west.

PLATE 6.

Longitudinal ridges at the base of bed 5, Petite Vallée.

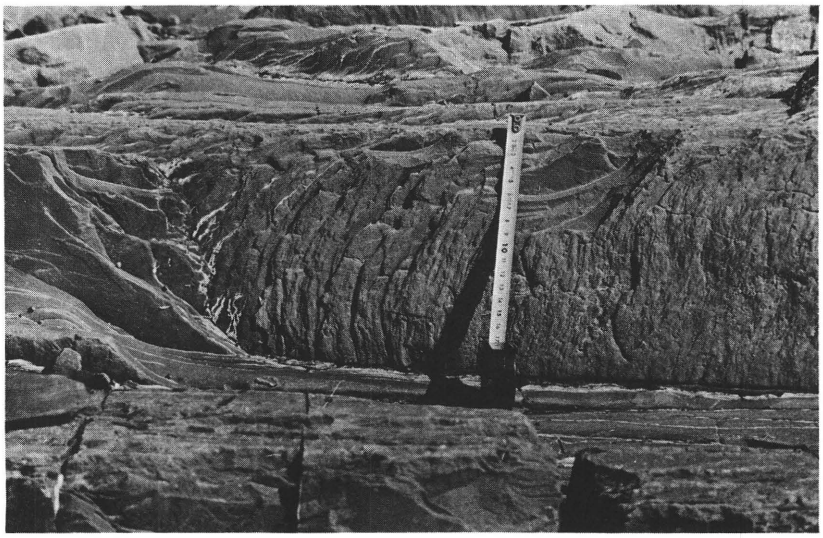

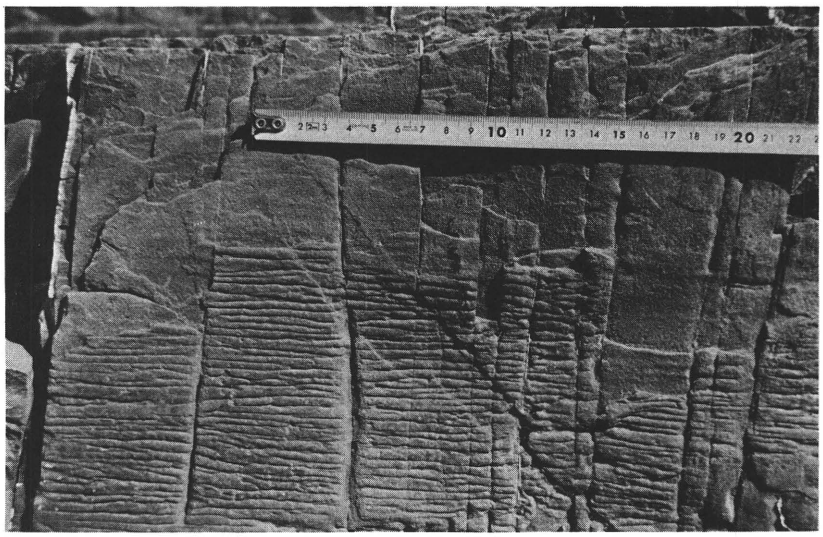
10
20

graptolite synrhabdosomes were observed in the saddles of weakly si nuous ripples (small scale dunes ?) in two cases at the top of bed 477. The local mean current directions deduced from the sole marks and graptolite orientations agree fairly well with those deduced from ripple-drift in all the four localities. These results also agree closely to the figures obtained by Enos for local mean palaeoflow directions (see Table I). Surprising occurrences of thick beds of ripple-drift, parallel lamination and both parallel lamination and ripple-drift, showing a reversal of current directions relative to the local mean palaeoflow directions were observed at Petite Vallée (2 beds, 28 and 15 cm thick), at Grande Vallée (3 beds, 27, 25 and 65 cm thick) and at Fame Point (2 beds 25 and 39 cm). Not all of them were studied in detail, hence only 4 were included in Table-II. Fig. 11 shows a schematic diagram of bed-1 of Grande Vallée.

Continuity of Beds:

Type-1 calcisiltite beds containing ripple-drift appear continuous in any outcrop, but can not be satisfactorily traced between outcrops because they lack distinguishing features.

Despite their spectacular thickness, ripple-drift beds of type-2 calcisiltite appear less persistent laterally than any other lithology of the Cloridorme Formation. Enos (1969a) noted that none of the type-2 calcisiltite beds could be traced as far as 1 mile.

The assumption that the ripple-drift beds of type-2 calcisiltite lithology exhibit a very poor lateral continuity, is evidenced by the abrupt appearance and disappearance of thick ripple-drifted beds shown in the detail correlation chart (Fig. 1.4, Parkash 1969) of Parkash, who correlated 8 greywacke beds for only a distance of 3200 yards. In another detailed correlation in unit H and the base of unit G of the β_7 Member at Grande Vallée, Enos (1969b, p. 706) observed that not one of about 56 massive type-2 calcisiltite beds was continuous throughout the 3 km interval. In the same units, out of 139 greywacke beds traced by Enos, only 46 extended throughout the interval, but 18 out of those 46 were locally discontinuous. In the β_1 Member, however, a greater continuity seems apparent from the fact that about 53 to 60 beds (type-3 greywacke and calcareous wacke only) out of 63 were found to be continuous (Enos 1969a, p. 706) for a distance of 7.5 Km.

The exposed length of ripple-drift beds in any outcrop hardly exceeds a couple of hundred feet (see Table I). Maximum exposed length traced by the present author was 1200' feet in bed 477 at St. Maurice.

A spectacular example of erosion involving a 60 cm (average) thick bed of ripple-drift was recorded from Petite Vallée (β_7 Member).

Bed 9 appeared abruptly at the upcurrent end with signs of severe local erosion and attained a thickness of 69 cm at a downcurrent distance of 50' and then gradually thinned down to 51 cm at 246 feet before it disappeared under the shore cliff. Beds 1, 2, 3 and 8 of Petite Vallée also display signs of local erosion. In β_1 (Fame Point, West) and α_3 (St. Maurice) Members no such sign of severe local erosion was observed.

Depositional Slope:

In bed 8 of Petite Vallée, an attempt was made to determine the slope of the depositional surface by tracing one individual lamina as far as possible across the ripple system. The selected lamina at the downstream end occurred 9.2 cm above the base of the bed. It could be traced upstream over 9 ripples, where it occurred 11.5 cm above the base of the bed. The distance between the two spots was 268 cm. Thus, the depositional surface was calculated to be dipping downstream at an angle of $0^{\circ}30'$ (i.e. 1/116). Walker (1969) calculated a slope of 1/100 by tracing a lamina over 38 ripples in bed 5 of Petite Vallée.

PLATE 7.

An unnumbered bed at Petite Vallée, showing a thick coset and concave-upward climb. Stratigraphic top to the right. Current from bottom ⟶ top, east to west.

PLATE 8.

View of beds 5, 6, and 7, Petite Vallée, at the 40' point. Bed 7 is AC, others are only C.

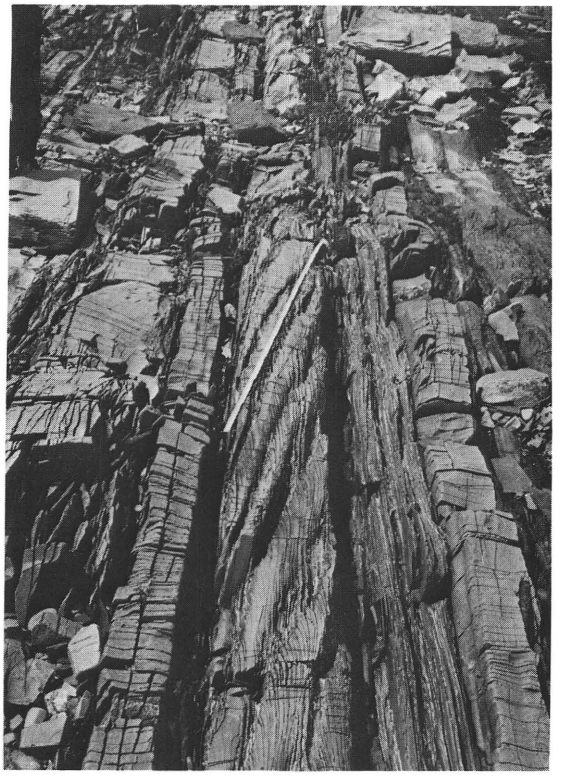

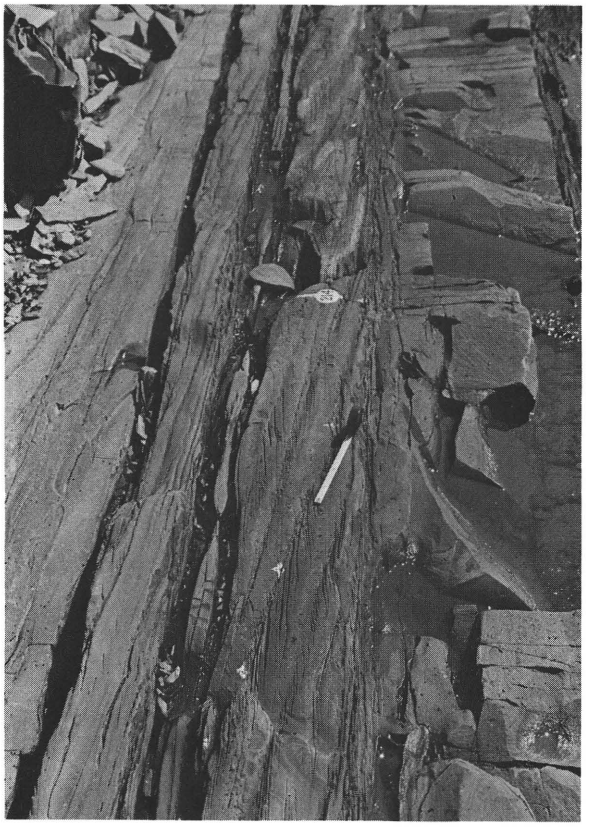

PLATE 9

Close up view of bed 5, Petite Vellée at the 259 point, interpreting type O_2 ripple-drift for bed ripple-drifted, but lower part irregularly drifted.

PLATE 10.

Close up view of bed 5, Petite Vellée at the 322 point. Note the lower irregularly drifted apart.

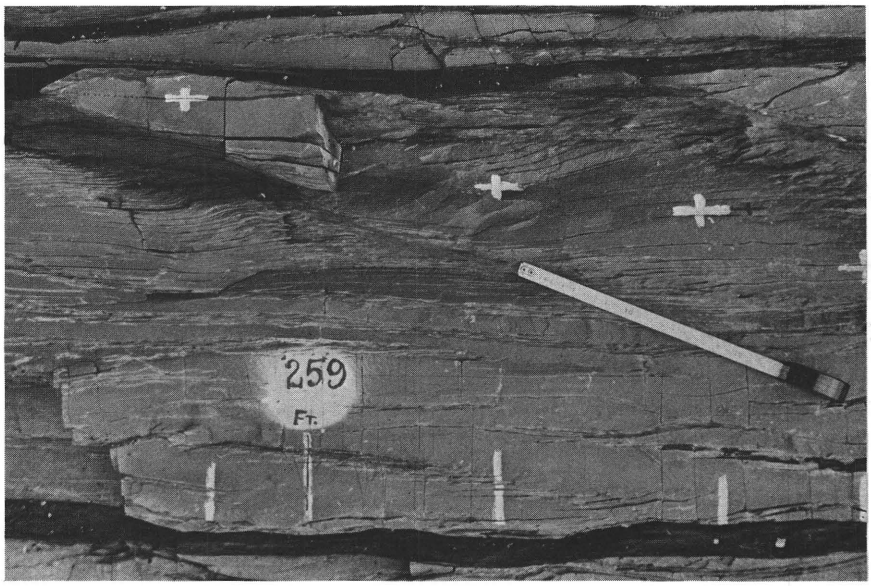
259
FT.

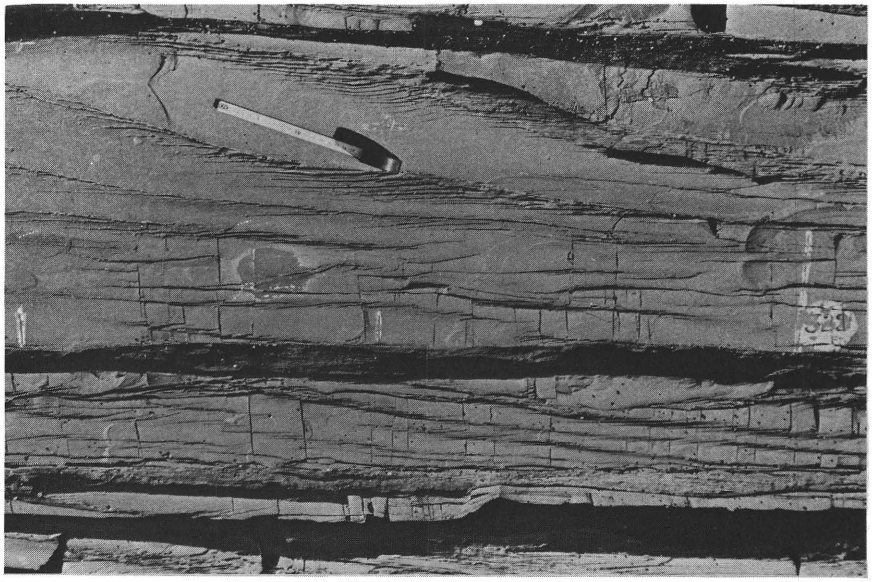

PLATE 11.

Close up view of bed 7, Petite Vallée, at the 259' point, illustrating type a_2 ripple-drift cross-lamination (ripple-drift following Bouma's A and B divisions)

PLATE 12.

Close up view of bed 7, Petite Vallée, at the 306' point, illustrating type a_1 ripple-drift cross-lamination (ripple-drift directly on top of Bouma's Division A).

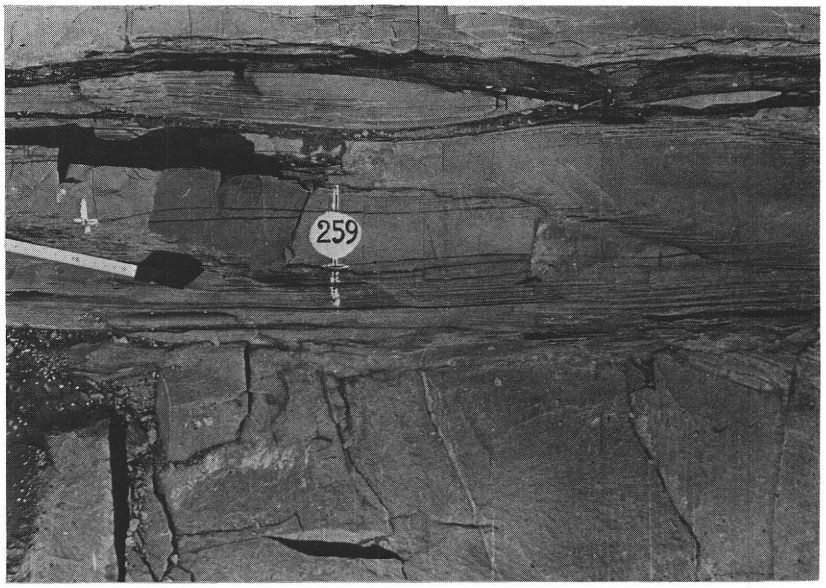
259

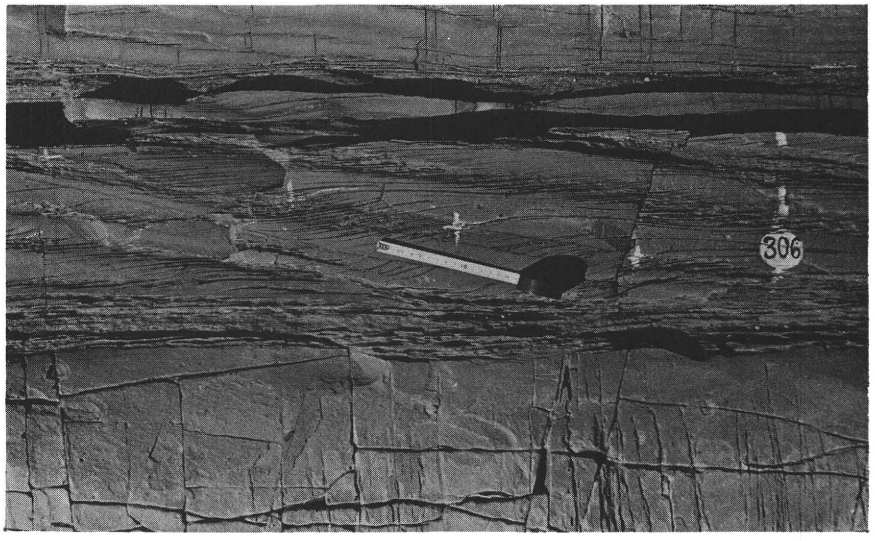
306

PLATE 13.

Close up view of bed 7, Petite Vallée, at the 40' point, illustrating type a_1 ripple-drift cross-lamination (ripple-drift directly on top of Bouma's division A)

PLATE 14.

Close up view of bed 7, Petite Vallée, at the 100' point. Bouma AC, with slightly concave-upward angle of climb.

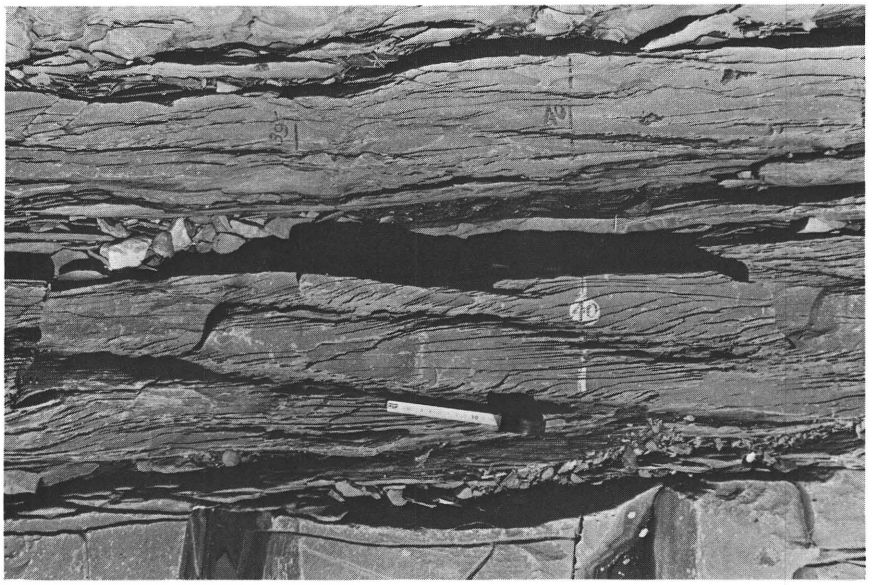
40

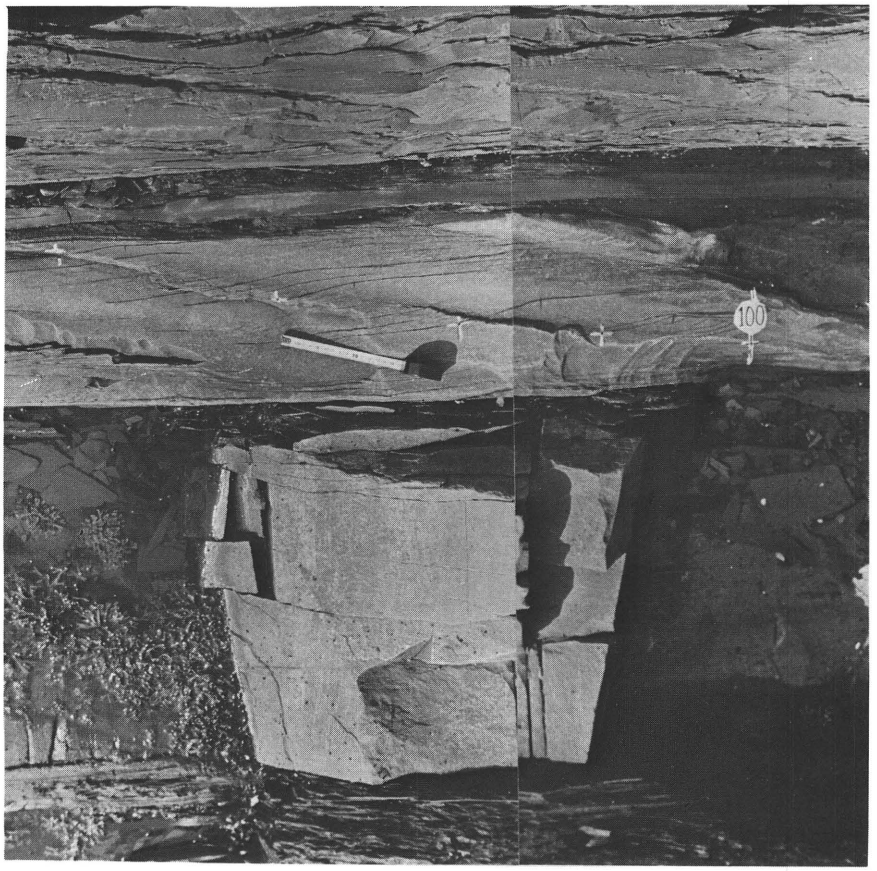
100

PLATE 15.

Close up view of bed 477, St. Maurice, illustrating type b_2 ripple-drift cross-lamination. Note the high angle of climb and overtaking of ripples at the top. Note the shape of the ripple laminae (thickest at the crest) in the middle of the regularly drifted part.

PLATE 16.

Close up view of bed 477, St. Maurice. Note the lower irregularly drifted part.

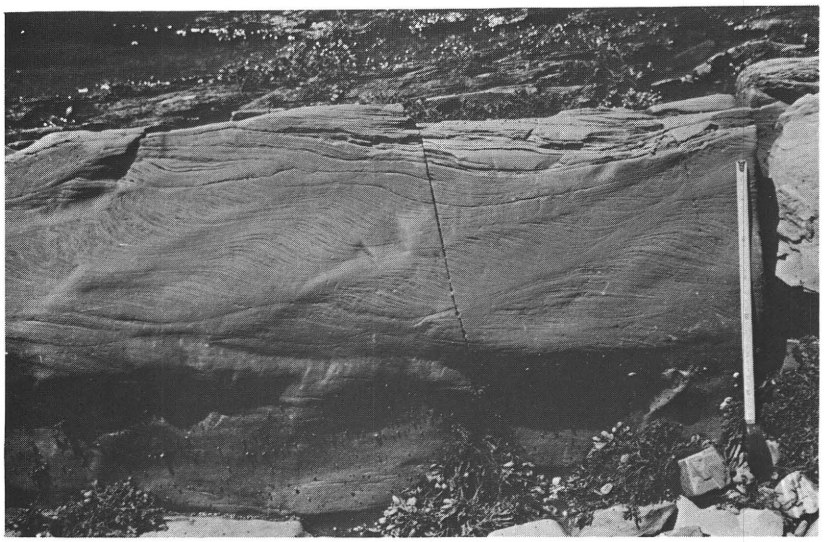

TYPES OF OCCURRENCES OF RIPPLE-DRIFT CROSS-LAMINATION

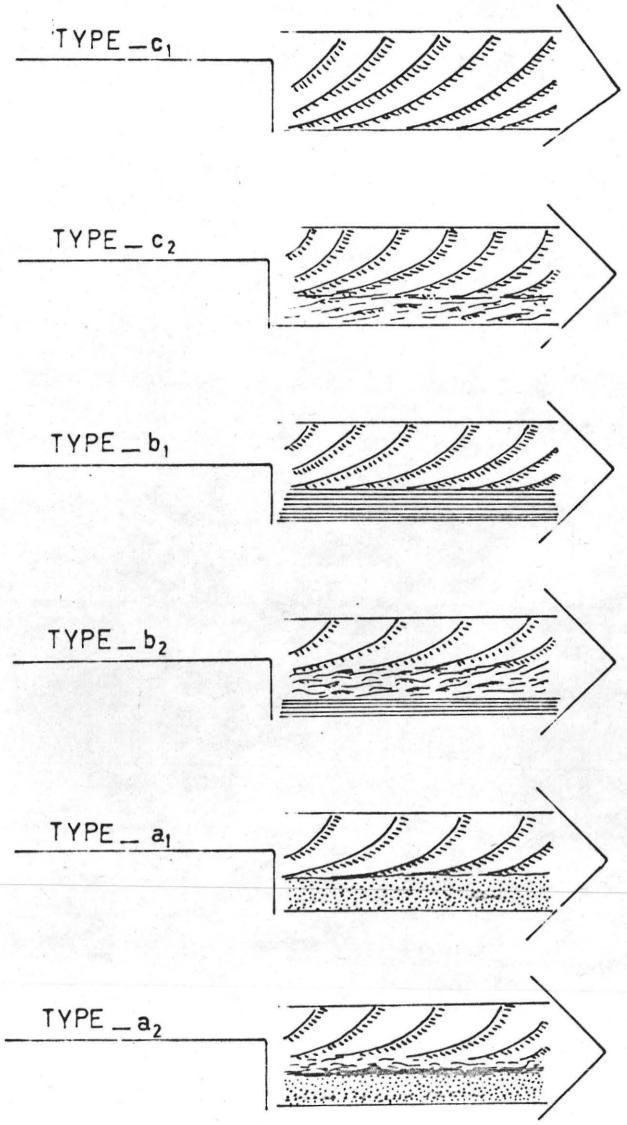

FIG. 5

3.2. Mode of Occurrence and Association of Ripple-Drifted Beds

It has already been noted that ripple-drift cross-lamination occurs in all the dominant lithologies of the Cloridorme Formation, but the frequency of its occurrence is markedly higher in type-1 and type-2 calcisiltites than any of the others.

Fig. 5 shows the various types of occurrences of ripple-drift cross-lamination in the Cloridorme turbidites in terms of A, B and C divisions of the Bouma (1962) turbidite model. Among the six types, C_1 and C_2 are most abundant and they occur separately, with argillite layers both above and below the bed. In β_7 Member (Grande Vallée-Petite Vallée area) all of the six types are present, but the apparent absence of type a_1 and a_2 in β_1 Member is surprisingly significant.

Beds 1, 2 and 3 of Petite Vallée (see Pl. 4) and the beds of Fame Point, West (see Pls. 28, 30) are the examples of type c_1. Bed 5 of Petite Vallée (see Pls. 1, 9), bed 2 of Grande Vallée and bed 477 of St. Maurice (see Pl. 15) respectively illustrate type c_2, type b_1 and type b_2. Bed 7 of Petite Vallée exhibits (see Pls. 11, 12) both of the types a_1 and a_2. Bed 4 of Grande Vallée is a good example of type a_2. Plate 39 is a spectacular illustration of type b_1. Plates 7 through 14 are illustrations of the various types of occurrences.

If the data (Table I) are analysed in terms of Bouma model for the occurrence of ripple-drift cross-lamination, it is seen that of 49 beds, 43 begin with ripple-drift (division C), 4 are BC type and 2 are ABC (doubtful AC) type.

Walker (1969, p. 384) noted that out of 15 beds containing ripple-drift (in a section of 61 turbidites at Petite Vallée), 12 begin with ripple-drift, 2 are AC type and 1 is BC; and with all the Cloridorme data included, 20 begin with ripple-drift, 2 are AC type and 1 is BC type.

Results of the analyses of bedding types (in terms of Bouma model) and ABC Index (Walker, 1967) in three thick measured sections of turbidites are given below. It is hoped that such analyses might reveal some relationship that might exist between the occurrence of ripple-drift and environment of deposition and between the ripple-drift and other associated bedding types.

TABLE IV

Total No. of Beds	Locality	Member	Bedding Types %							ABC Index %
			A	AB	ABC	AC	B	BC	C	
375	Petite Vallée	β_7	50.4	-	0.27	6.4	3.5	0.8	38.7	59
755	Fame Point, West	β_1	-	-	*2.5	-	12.4	3.8	81.2	11
532	St. Maurice	α_3	-	-	*0.75	-	29.9	10.7	58.6	21

* type-3 greywacke of Enos (1969).

3.3. General Observations on Parameters and Other Features of Ripple-Drift

Coset Thickness:

Thickness of coset is the most spectacular feature of the Cloridorme Formation ripple-drift (see Plates 1, 2, 4, 7 and 15). The average thickness is 20 cm and the range is 2 to 75 cm (see Table I). Walker (1969) reported a maximum thickness of 98 cm from Grande Vallée. These thicknesses are much above the averages for division C, 5 to 10 cm, given by Kuenen (1967) or 5 cm given by Walker (1969) or 2.5 cm given by Hsu (1964), for (non-climbing) cross-laminated beds.

Thicker cosets are frequently encountered in β_7 Member, where they occur in association with more frequently occurring A beds (see Pls. 2, 4 and Table I). In β_1 Member the cosets are much thinner (less than 10 cm) and A beds are virtually absent. In the upper part of the section measured at Fame Point, West, A beds abruptly start appearing (above bed 1059) in large numbers associated with common, thick convoluted beds and a few thicker and thinner ripple-drift beds. According to Enos (1969a, b) this upper part of the section tentatively represents the base of the β_2 Member. In the α_3 Member at St. Maurice (North of the Church), A beds are virtually absent, but the

convoluted beds are spectacularly thick and both thick and thin cosets of ripple-drift are present. In some of the beds, it appears that the original form of the convoluted lamination might possibly be traced back to ripple-drift.

Angle of Climb:

The angle of climb in the ripple-drift cosets of the Cloridorme turbidites ranges from 1^{o} to 43^{o} degrees (see Table V). These angles are comparable to those quoted by Kuenen (1967), which range from 4^{o} to 45^{o} degrees, averaging about 12^{o}. In the present case the average is 7.5^{o} degrees. This low value is due to inclusion of a larger number of thinner cosets showing very low angles of climb (see Table V).

Table V also shows the computed values (discussed earlier) of the angles of climb. They range from 2.7^{o} to 56.1^{o} averaging 9.0^{o} degrees. A comparison between the data columns shown in Table V reveals that the average values of the measured angles of climb agree very closely to the average values of the computed angles of climb. But the minima and maxima (values) differ from each other, with the latter being usually higher. This is probably due to:

TYPES OF ANGLE OF CLIMB

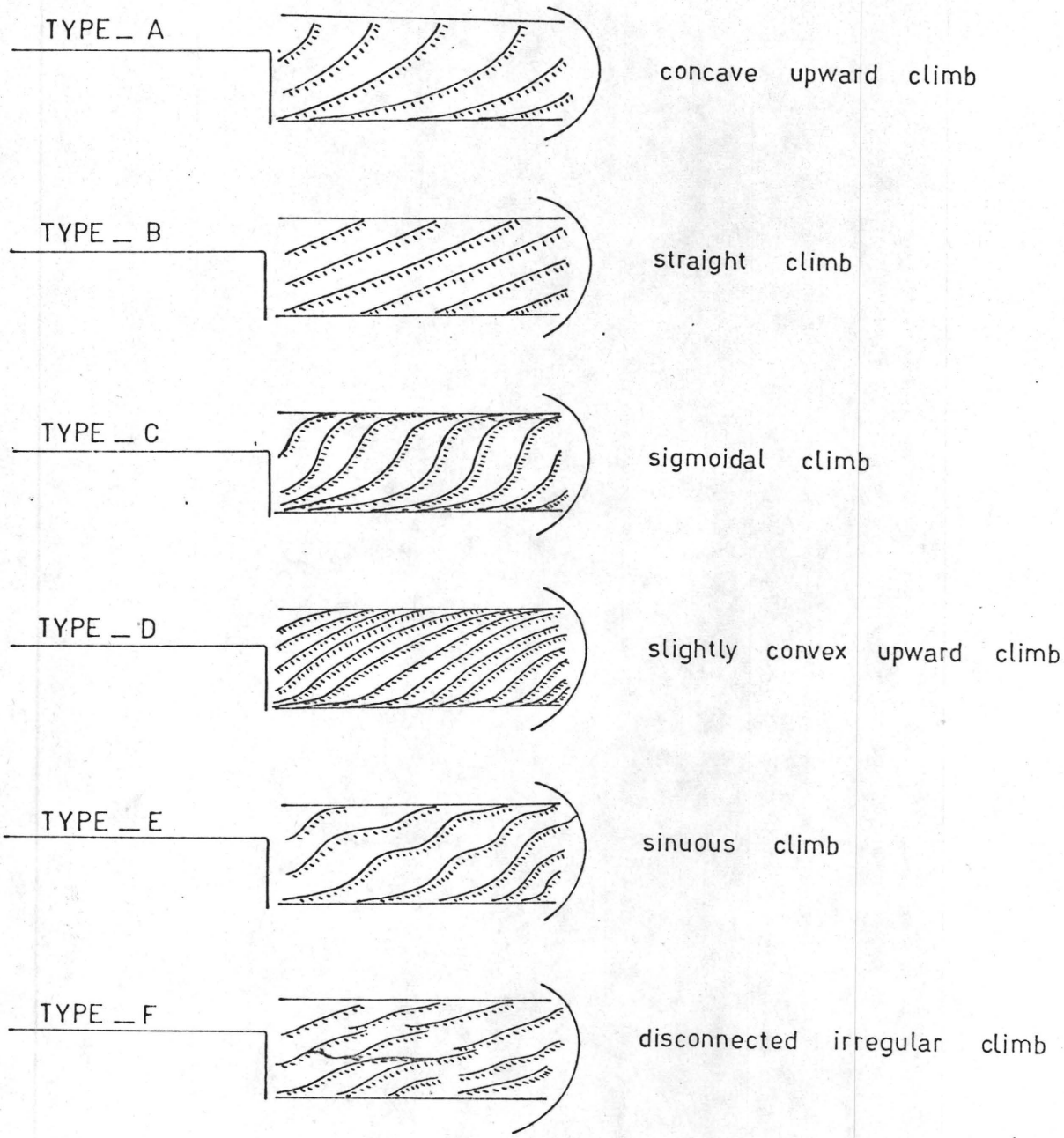

FIG. 6

TABLE V

Data on minimum, maximum and average values of the measured and computed angles of climb.

TABLE V

LOCATION	Bed Number	Bed Thickness Centimeters A - B - C	Minimum Value of Measured Angle of Climb, in Degrees	Maximum Value of Measured Angle of Climb, in Degrees	Average Value of Measured Angle of Climb, in Degrees	Total No. of Measured Values	Minimum Value of Computed Angle of Climb, in Degrees	Maximum Value of Computed Angle of Climb, in Degrees	Average Value of Computed Angle of Climb, in Degrees	Total No. of Computed Values
St. Maurice (North of Church)	477	0 8 70	2.1	36.0	16.7	73	6.1	37.6	17.0	118
West of Fame Point	666	0 0 11.2	...	...	5.7	1	6.7	7.1	6.9	3
	700	0 0 9.4	...	...	3.8	1	3.8	6.7	5.7	3
	701	0 0 7.5	...	...	5.3	1	6.3	9.2	7.9	3
	702	0 0 14.5	...	...	10.9	1	4.8	11.6	7.4	3
	759	0 0 6.5	...	...	4.5	1	6.6	7.4	6.9	3
	765	0 0 8.0	...	...	4.9	1	5.9	8.1	7.1	3
	772	0 0 5.9	1.1	3.8	2.5	2	6.3	7.7	7.0	3
	773	0 0 4.8	...	...	2.9	1	3.7	6.6	4.7	3
	774	0 0 5.1	1.1	4.7	2.9	2	6.8	7.6	7.1	3
	790	0 0 9.8	...	...	4.8	1	4.4	6.1	5.1	3
	791	0 0 14.5	...	...	7.8	1	4.5	8.0	6.4	3
	793	0 0 12.5	...	...	6.9	1	3.6	7.1	5.0	3
	794	0 0 8.5	...	...	3.6	1	2.7	8.4	5.8	3
	795	0 0 11.7	...	...	6.3	1	7.0	10.4	8.4	3
	798	0 0 9.0	...	...	6.0	1	4.4	7.7	6.1	2
	799	0 0 6.5	...	...	4.0	1	5.7	7.1	6.4	3
	800	0 0 5.5	...	...	3.2	1	4.8	5.3	4.9	3
	801	0 0 7.3	...	...	4.5	1	5.7	6.6	6.0	3
	899	0 0 23.0	14.0	16.0	15.0	2	8.7	21.1	14.1	3
	1013	0 0 5.8	...	...	4.9	1	4.6	8.5	6.6	3
	1014	0 0 2.6	...	...	5.1	1	4.3	6.8	5.5	3
	1015	0 0 4.7	...	...	3.6	1	4.4	9.1	6.7	3
	1021	0 0 5.0	...	...	7.3	1	6.9	10.4	8.3	3
	1030	0 0 5.6	...	...	2.5	1	4.8	6.3	5.6	3
	1031	0 0 6.1	...	...	3.4	1	4.2	6.6	5.7	3
	1033	0 0 9.0	...	...	5.9	1	6.0	10.0	7.5	3
	1034	0 0 5.1	...	...	2.2	1	3.3	4.6	4.0	3
	1035	0 0 4.6	...	...	2.3	1	3.1	5.9	4.7	3
	1036	0 0 3.6	...	...	2.6	1	3.3	6.3	4.9	3
	1038	0 0 5.1	...	...	4.2	1	5.9	7.0	6.5	3
Petite Valeé Harbour, East.	1	0 0 32.0	4.4	20.8	12.5	5	7.4	11.2	8.3	6
	2	0 0 57.0	8.4	28.0	18.9	5	7.7	20.7	12.5	6
	3	0 0 35.0	11.3	30.8	19.3	3	9.0	14.1	11.5	4
	4	0 0 7.0	4.3	16.6	12.4	3	5.6	8.8	7.5	4
	5	0 0 38.0	1.0	33.9	10.1	67	3.2	34.6	15.2	71
	6	0 0 3.4	2.6	8.2	4.6	3	3.7	7.5	5.1	4
	7	52 2 22.5	2.7	14.8	8.3	63	10.4	56.1	21.9	73
	8	0 5 20.8	1.0	18.2	7.8	41	9.1	28.9	19.7	42
	9	0 0 60.0	2.5	25.8	12.7	52	3.8	23.1	14.3	50
	10	0 0 28.0	2.6	24.1	11.0	12	3.7	29.2	11.0	15
East of Anse à Mercier Grande Vallée	1	0 2 25.0	...	...	7.6	1	6.0	15.9	10.8	4
	2	0 5 12.0	1.4	32.4	6.9	17	3.7	14.5	7.7	20
	3	0 0 17.0	3.2	6.7	4.7	3	6.1	10.1	8.0	4
Anse à Mercier West, Grande Vallée	4	8 2 70.0	12.5	43.3	28.1	3	9.4	33.0	20.3	4
	5	0 0 58.0	4.1	16.3	10.8	3	14.3	21.1	18.0	4
	6	0 0 75.0	7.3	12.1	9.8	3	11.1	29.2	18.0	4
Grande Vallée Harbour, East	7	0 0 25.0	2.1	2.3	2.2	2	——	——	——	——
	8	0 0 65.0	1.3	7.2	3.9	3	——	——	——	——

PLATE 17.

Bed 477, St. Maurice, showing steep concave-upward climb.

PLATE 18.

Bed 477, St. Maurice, showing steep concave-upward climb and overtaking.

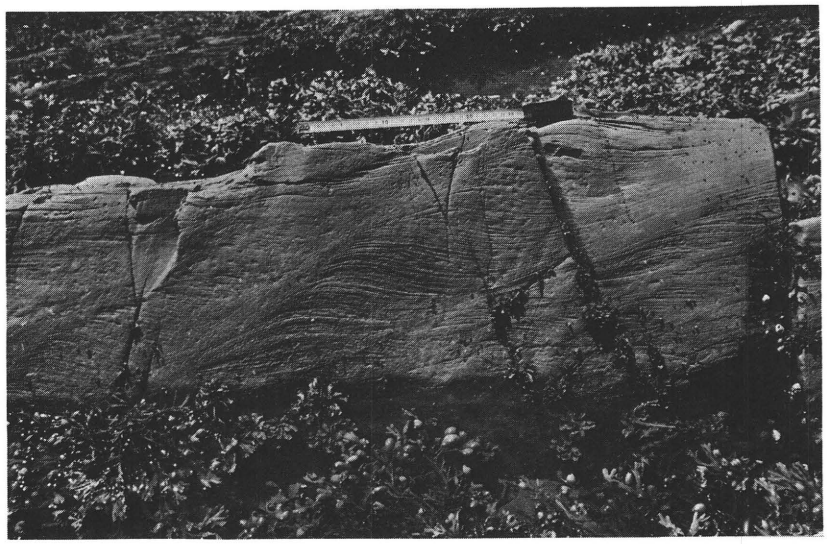

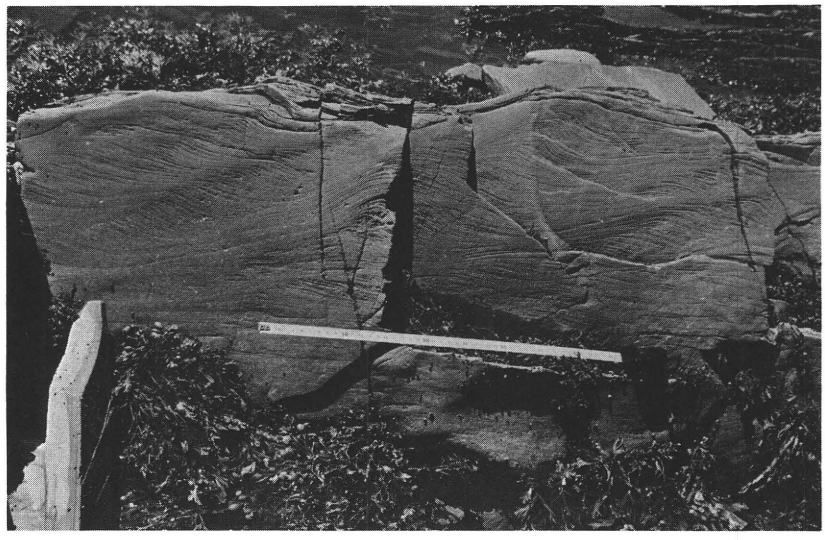

PLATE 19.

Bed 7, Petite Vallée, showing concave-upward climb

PLATE 20.

Bed 7, Petite Vallée, showing concave-upward climb.

PLATE 21.

Bed 5, Petite Vallée, at the 292' point, showing concave-upward climb.

PLATE 22.

Bed 5, Petite Vallée, at the 130' point, showing concave-upward climb. Note the increase in wave length towards the top.


292
FT.

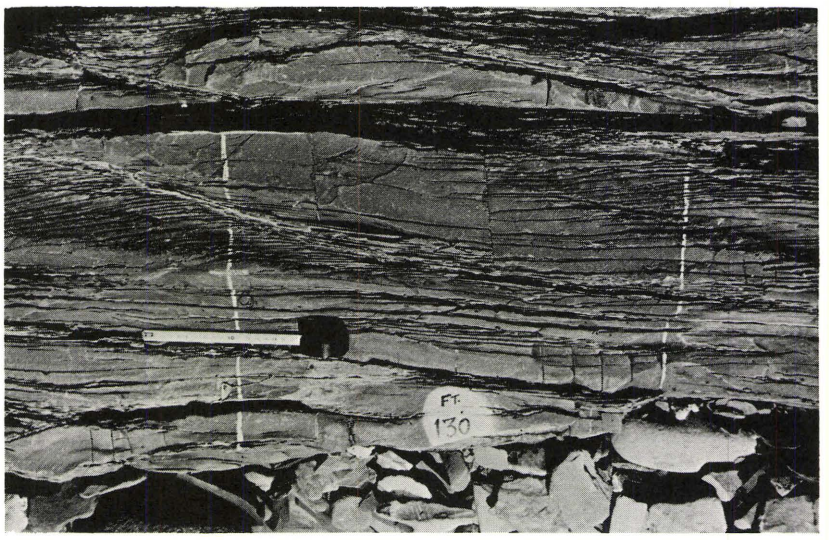
FT.
130

PLATE 23.

Bed 5, Petite Vallée, showing concave-upward climb

PLATE 24.

Bed 9, Petite Vallée, showing concave-upward and sigmoidal climb.

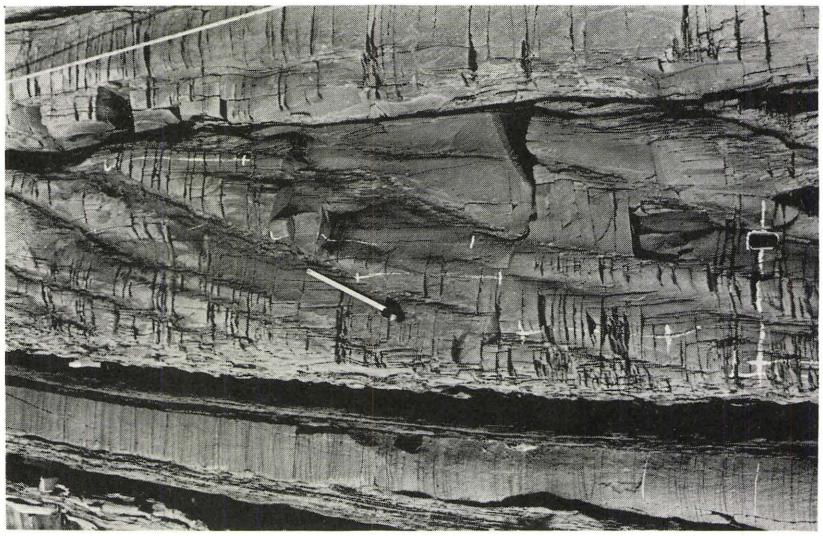

PLATE 25.

Bed 7, Petite Vallée, showing concave-upward climb.

PLATE 26.

Bed 7, Petite Vallée, showing concave-upward climb.

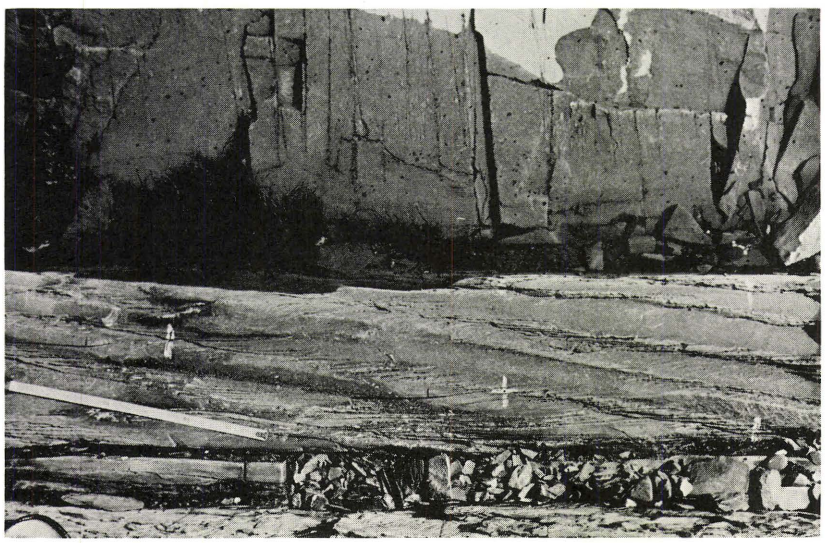

PLATE 27

Bed 7, Petite Vallée, showing the length of the climb line.

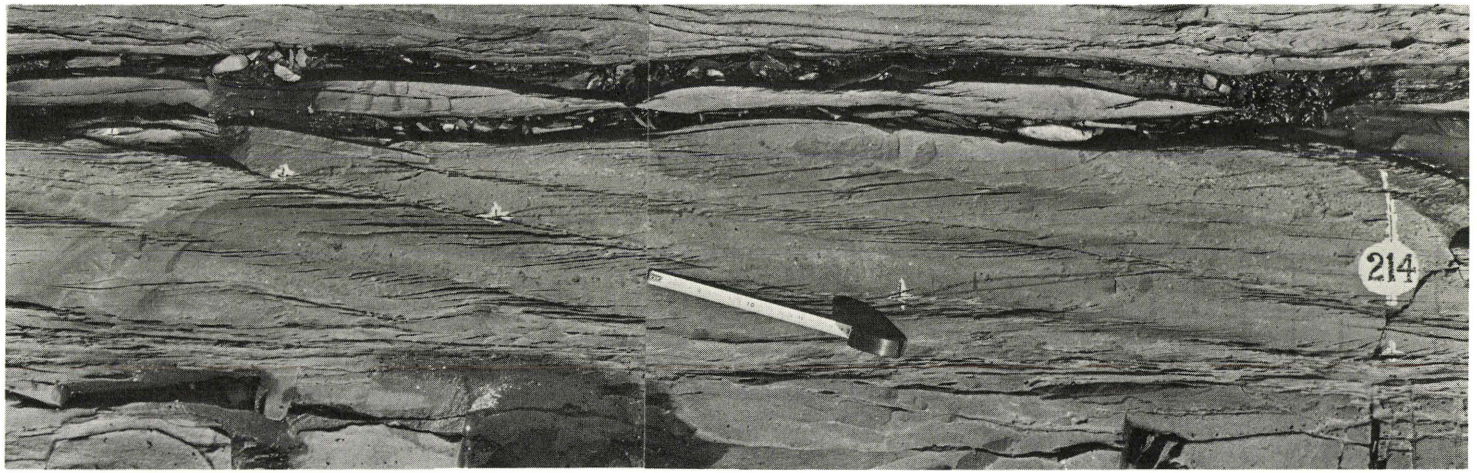
214

PLATE 28.

Beds at Fame Point, West, showing thin cosets and straight climb.

PLATE 29.

Bed 5, Petite Vallée, 191' point, showing sigmoidal climb.

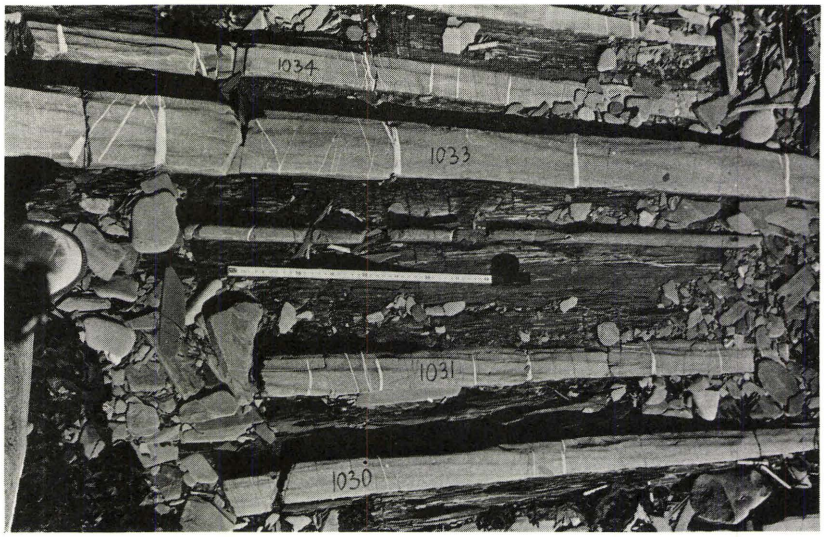
1034
1033
1031
1030

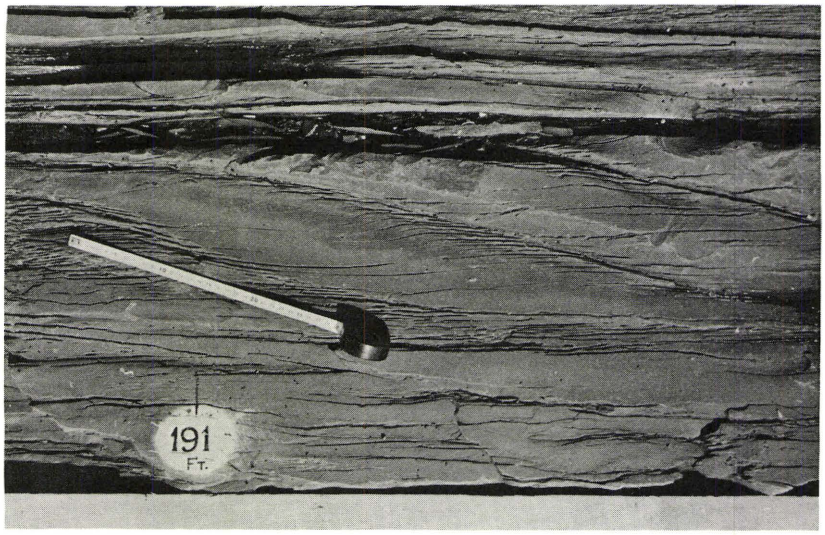
191
FT.

PLATE 30.

Beds at Fame Point, West, showing thin cosets and fairly straight climb.

PLATE 31.

A thin coset at Fame Point, West, showing erosion of stoss-laminae from the base to the top of the coset.

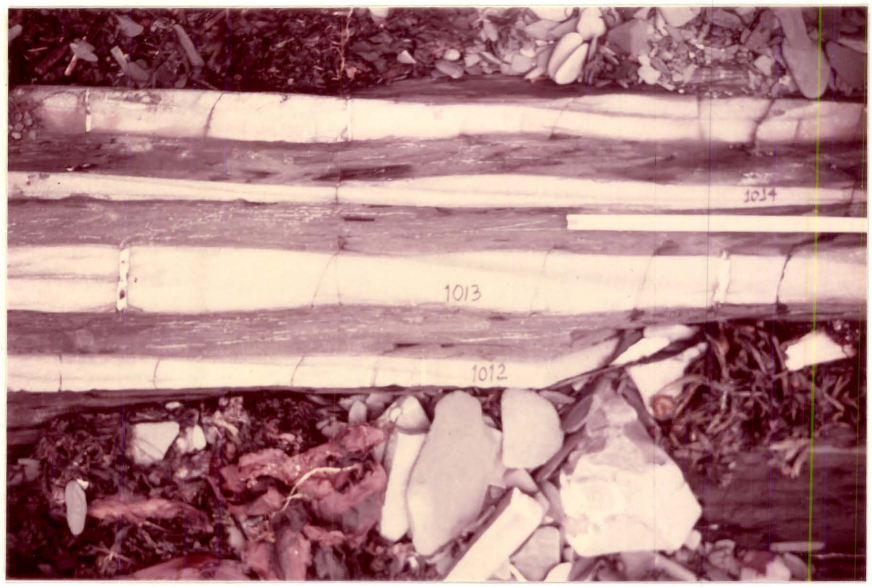
1014
1013
1012

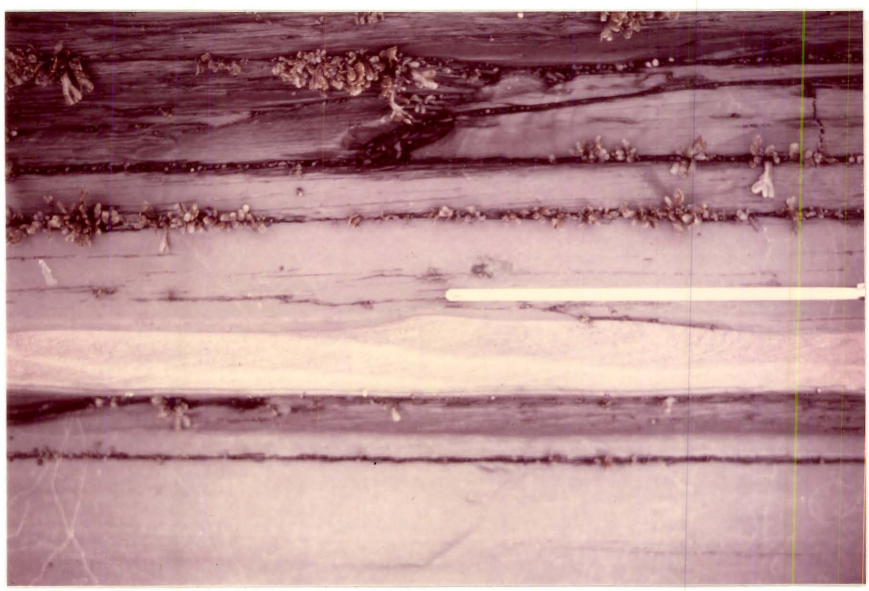

PLATE 32.

Bed 9, Petite Vallée, thick coset showing sinuous and sigmoidal climb.

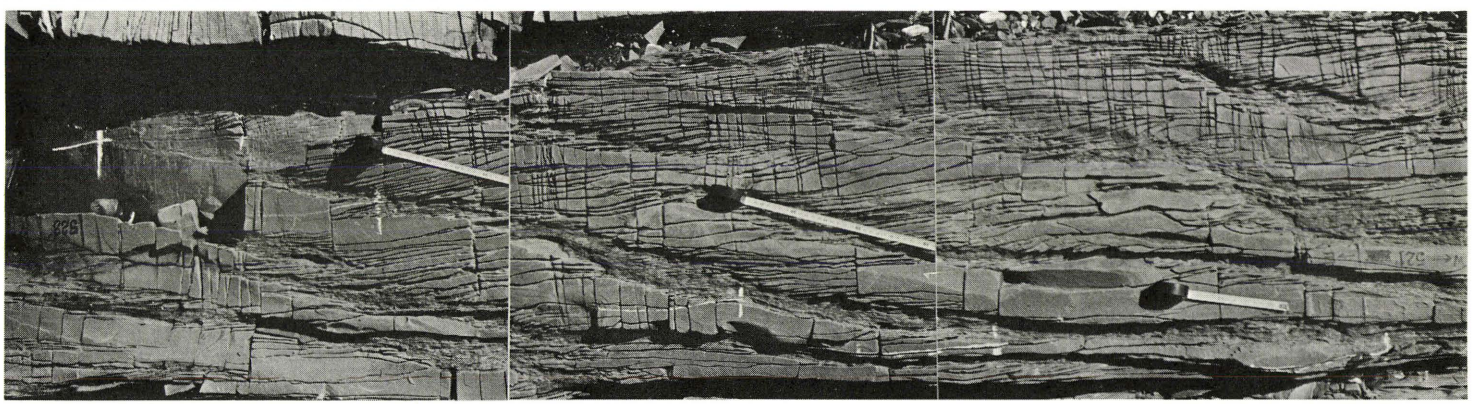

PLATE 33.

Bed 1, Grande Vallée, lower half showing load structure, upper ripple-drifted part showing disconnected-irregular climb.

PLATE 34.

Bed 1, Grande Vallée, showing sinuous climb.

(i) The values of the angles ∠QPK, ∠RQL, and ∠SRM in Fig. 4, which represent how the recorded values of the "measured angle of climb" were obtained in the field. In contrast, the "computed angle of climb" was obtained from the measurements of parameters α, β, t_L and t_S of the ripples located precisely at the points P, Q and R. The values of the "measured angles of climb" thus suffer from an averaging effect.

(ii) The cumulative effect of error in the measurements of α, β, t_L and t_S.

(iii) In the field ϵ was measured along the line joining the successive troughs (cf. fig. 4) as against along the crest in case of computed values of ϵ'. However, this difference, in all probability, is considered to be a negligible one.

The angle of climb in some beds remains constant from base to top of the coset, in some others it increases gradually upward through a coset, in still others it shows some other patterns. Fig. 6 illustrates six different types (not a rigid classification) of angle of climb observed in the field. Of these type - A (concave-upward climb with a small convex part at the top; see Pls. 2, 15 to 26) and type - C (distinctly sigmoid climb; see Pl. 29) are respectively very abundant

and common, in the thicker cosets of the β_7 member at Petite Vallée and Grande Vallée. Type-B (straight climb; see Pl. 28) usually is very common in thinner cosets and is very frequently encountered in β_1 Member at Fame Point, West. Type - D also appears to be restricted to thinner cosets. This type was observed only in bed 6 of Petite Vallée. Type - E (sinuous climb, see Pls. 32, 34) was observed in some thick cosets (e.g. bed 10, Petite Vallée). It is emphasized that the type-E is a characteristic of the cosets showing a reversed current direction (e.g. bed 10 and the unnumbered bed below bed 10 at Petite Vallée and bed 7 and 8 of Grande Vallée). Type - F commonly occurs in the lower part of a thick coset (e.g. bed 5 Petite Vallée, bed 477 St. Maurice), but sometimes may cover the entire coset thickness (e.g. bed 1 Grande Vallée). Plates 15 through 34 are illustrations of the various types of angle of climb.

t_L/t_S:

The ratio of lee-to-stoss side lamina thicknesses in the ripple-drift cosets of the Cloridorme formation ranges from 1.1 to 19.0. Measurements were made on 523 ripples and the data are tabulated in the Appendix 1(c).

FIG. 7.

A. Frequency distribution of Wave Length

B. Frequency distribution of Amplitude

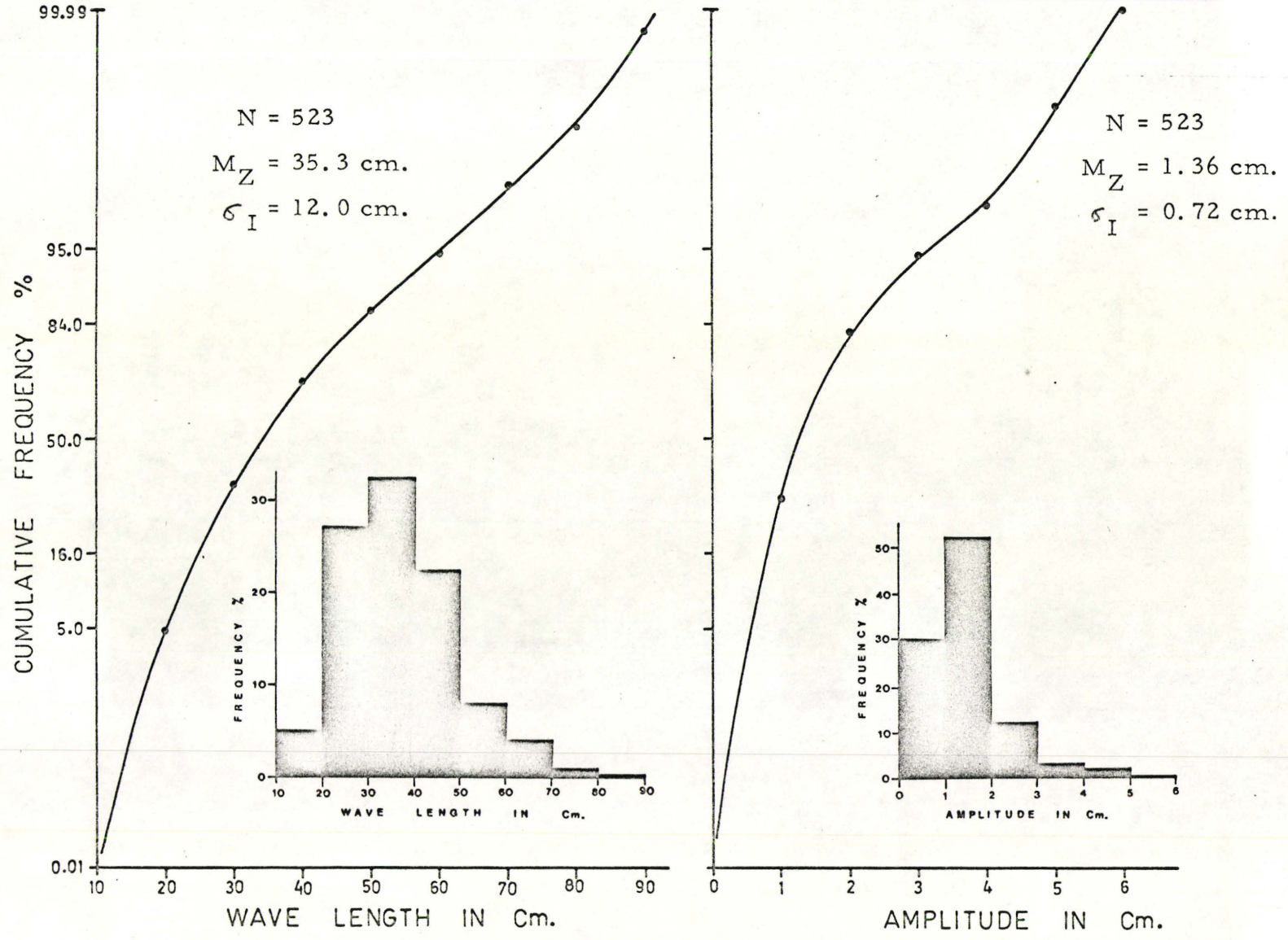
99.99
95.0
84.0
50.0
16.0
5.0
0.01
CUMULATIVE FREQUENCY %
N = 523
M_Z = 35.3 cm.
σ_I = 12.0 cm.
FREQUENCY %
WAVE LENGTH IN Cm.
10 20 30 40 50 60 70 80 90
WAVE LENGTH IN Cm.
A
N = 523
M_Z = 1.36 cm.
σ_I = 0.72 cm.
FREQUENCY %
AMPLITUDE IN Cm.
0 1 2 3 4 5 6
AMPLITUDE IN Cm.
B

FIG. 7

Wave Length:

Large wave length is one of the spectacular features of the ripple-drift of the Cloridorme turbidites. The range is from 13 to 84 cm with a mean value 35.3 cm (see fig. 7) and standard deviation 15.9 cm. Tabulated data in Appendix 1(c) include a total of 523 measurements of this parameter. These values are somewhat larger than those quoted by Walker (1969, Table I, p. 386) from the Bude Sandstones (9-15 cm), Gamlan Flags (12 cm), and Portobello Sandstone (23-32 cm).

A general field observation is that the wavelength increases upward through a coset. This is also true for some of the examples quoted above (Walker, 1969, p. 386).

Amplitude:

Collected data on this parameter (total 523, see Appendix 1(c)) shows that the range is from 0.4 to 5.2 cm, with a mean value of 1.36 cm (see fig. 7) and standard deviation 0.72 cm. Obviously some parts of some cosets of ripple-drift (e.g. uppermost part of bed 477) would best be defined as 'dune-drift cross-lamination', taking the minimum height of dunes to be 3 cm (Harms, 1969).

It was observed that amplitude continues to increase upward almost up to 1/2 or 3/4 the thickness of the coset, whereafter it decreases a little.

TABLE VI

Data on grain-size measurements.

TABLE VI

LOCATION	Bed Number	Bed Thickness in Centimeters A - B - C	MEAN SIZE OF TEN LARGEST GRAINS *Sample from Bottom of Coset mm.	Phi(ø)	*Sample from Middle of Coset mm.	Phi(ø)	*Sample from Top of Coset mm.	Phi(ø)	Sample locations, in feet.	U = Up Stream Point D = Down Stream Point
St. Maurice (North of Church)	477	0 - 8 - 70	0.09	3.47	0.17	2.55	0.08	3.65	0'	U
			0.14	2.85	0.11	3.19	0.05	4.31	300'	
			0.16	2.65	0.15	2.74	0.07	3.84	600'	
			0.15	2.74	0.14	2.85	0.08	3.65	900'	D
West of Fame Point	666	0 - 0 - 11.2	0.07	3.84	-	-	0.04	4.63	-	
	700	0 - 0 - 9.4	0.09	3.47	-	-	0.07	3.84	-	
	701	0 - 0 - 7.5	0.07	3.84	-	-	0.04	4.63	-	
	702	0 - 0 - 14.5	0.07	3.84	-	-	0.07	3.84	-	
	759	0 - 0 - 6.5	0.07	3.84	-	-	0.05	4.31	-	
	765	0 - 0 - 8.0	0.08	3.65	-	-	0.07	3.84	-	
	772	0 - 0 - 5.9	0.06	4.05	-	-	0.04	4.63	-	
	773	0 - 0 - 4.8	0.06	4.05	-	-	0.04	4.63	-	
	774	0 - 0 - 5.1	0.05	4.31	-	-	0.04	4.63	-	
	790	0 - 0 - 9.8	0.06	4.05	-	-	0.04	4.63	-	
	791	0 - 0 - 14.5	0.09	3.47	-	-	0.07	3.84	-	
	793	0 - 0 - 12.5	0.08	3.65	-	-	0.06	4.05	-	
	794	0 - 0 - 8.5	0.17	2.55	-	-	0.08	3.65	-	
	795	0 - 0 - 11.7	0.11	3.19	-	-	0.04	4.63	-	
	798	0 - 0 - 9.0	0.07	3.84	-	-	0.06	4.05	-	
	799	0 - 0 - 6.5	0.06	4.05	-	-	0.06	4.05	-	
	800	0 - 0 - 5.5	0.05	4.31	-	-	0.04	4.63	-	
	801	0 - 0 - 7.3	0.05	4.31	-	-	0.04	4.63	-	
	899	0 - 0 - 23.0	0.04	4.63	-	-	0.04	4.63	-	
	1013	0 - 0 - 5.8	0.04	4.63	-	-	0.08	3.65	-	
	1014	0 - 0 - 2.6	0.06	4.05	-	-	0.04	4.63	-	
	1015	0 - 0 - 4.7	0.08	3.65	-	-	0.06	4.05	-	
	1021	0 - 0 - 5.0	0.05	4.31	-	-	0.04	4.63	-	
	1030	0 - 0 - 5.6	0.06	4.05	-	-	0.04	4.63	-	
	1031	0 - 0 - 6.1	0.05	4.31	-	-	0.04	4.63	-	
	1033	0 - 0 - 9.0	0.05	4.31	-	-	0.04	4.63	-	
	1034	0 - 0 - 5.1	0.06	4.05	-	-	0.05	4.31	-	
	1035	0 - 0 - 4.6	0.06	4.05	-	-	0.05	4.31	-	
	1036	0 - 0 - 3.6	0.06	4.05	-	-	0.05	4.31	-	
	1038	0 - 0 - 5.1	0.63	0.68	-	-	0.11	3.19	-	
Petite Vallee Harbour, East.	1	0 - 0 - 32.0	0.20	2.34	-	-	0.16	2.65	-	
	2	0 - 0 - 57.0	0.17	2.55	-	-	0.15	2.74	-	
	3	0 - 0 - 35.0	0.18	2.49	-	-	0.15	2.74	-	
	4	0 - 0 - 7.0	0.16	2.65	-	-	0.14	2.85	-	
	5	0 - 0 - 38.0	0.08	3.65	-	-	0.07	3.84	48'	D
			0.18	2.49	-	-	0.04	4.63	322'	U
	6	0 - 0 - 3.4	0.05	4.31	-	-	0.05	4.31	-	
	7	52 - 2 - 22.5	0.08	3.65	-	-	0.04	4.63	49'	D
			0.09	3.47	-	-	0.06	4.05	320'	U
	8	0 - 5 - 20.8	0.09	3.47	-	-	0.08	3.65	-	
	9	0 - 0 - 60.0	0.10	3.31	-	-	0.08	3.65	0'	D
			0.14	2.85	-	-	0.17	2.55	246'	U
	**10	0 - 0 - 28.0	0.17	2.55	-	-	0.09	3.47	0'	U
			0.07	3.84	-	-	0.07	3.84	250'	D
East of Anse a Mercier Grande Vallee	**1	0 - 2 - 25.0	0.09	3.47	-	-	0.08	3.65	-	
	2	0 - 5 - 12.0	0.07	3.84	-	-	0.05	4.31	-	
	3	0 - 0 - 17.0	0.08	3.65	-	-	0.07	3.84	-	
Anse a Mercier West, Grande Vallee	4	8 - 2 - 70.0	0.32	1.66	-	-	0.29	1.8	-	
	5	0 - 0 - 58.0	0.38	1.42	-	-	0.36	1.5	-	
	6	0 - 0 - 75.0	0.45	1.18	-	-	0.10	3.31	-	

* All the samples were collected from near the crest (on stoss side) of the ripples.
** Current directions in these beds are opposite to the regional current direction.

Stoss-angle and Lee-angle:

In the field, characteristics of these parameters can not be compared between stations because of difficulty in remembering the sequences observed at different stations. However, a common observation is that β has a low value near the base of a coset, then it increases towards the top and decreases again before the ripples start becoming levelled at the top of the coset. No such generalisations can be arrived at in case of α. Data on α and β are given in Appendix 1(c).

Grain Size:

The mean size of the ten largest grains (see Table VI) were recorded (using a binocular microscope) from rock samples collected one from the bottom and one from the top of each of the 47 measured beds. The analysis shows that in the ripple-drifted beds, the coarsest grain size ranges from 0.04 to 0.45 mm. Of 47 beds only 3 have values higher than 0.25 mm (fine sand). It also appears that the rocks of the β_7 Member are coarser grained than those of β_1 and α_3.

Grain size distribution across 3 ripples were studied in thin sections. Results and other details are shown in fig. 8 and fig. 9. A systematic study of grain size distribution, across ripples from different levels of a climbing band, was planned. Unfortunately the plan did not succeed because it is extremely difficult to extract the samples.

However, 3 analyses, as mentioned above, may help us visualize the entire picture.

Fig. 8(i), which shows the maximum grain size distribution of a ripple located 15 cm below the top of bed 477, reveals that (a) the coarsest grains occur near the crest, (b) in general, grains are coarser on the stoss side than on the lee side, and (c) smallest grains occur near the trough. Fig. 9 (the same ripple) in addition shows that the sediment, for a considerable length of the stoss side, has a markedly low matrix content.

Fig. 8(ii) and (iii) show analyses of two ripples from the top of two other beds. It is important to note that in these two cases the maximum grain size distribution is rather haphazard as against a definite pattern observable in fig. 8(i).

Ripple Shape:

A few frequently occurring sequences of ripple shapes, observed in the ripple-drift cosets of the Cloridorme formation is given in fig. 10. It can be seen in fig. 10A that in thicker cosets, exhibiting concave-upward climb, the ripples near the base have relatively short wave lengths, the stoss-laminae are usually not preserved, and the shape of the foreset laminae almost straight or very weakly asymptotic. As the ripples climb upward and forward through

FIG. 8.

(i), (ii) and (iii) Grain size distribution across three ripples

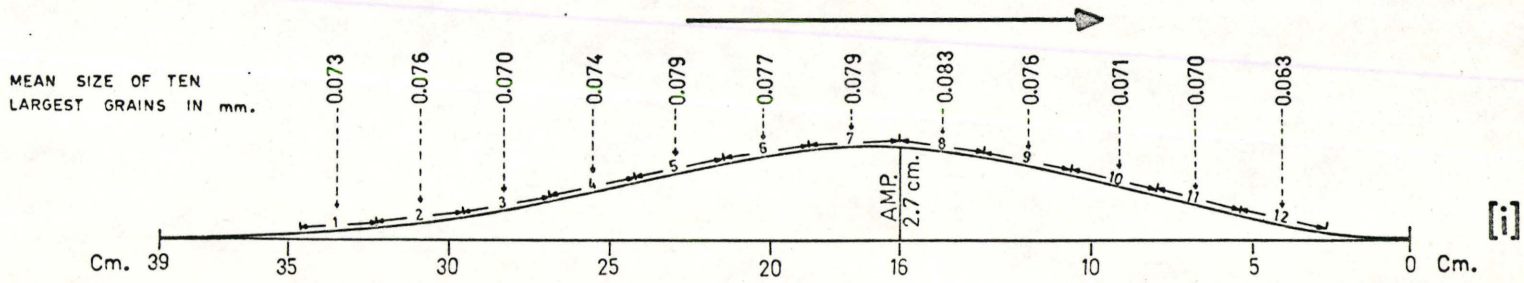

[i]

LOCATION: St. Maurice, Bed – 477, 0′ Ft. POINT, 63 Cm. above the base of the bed.

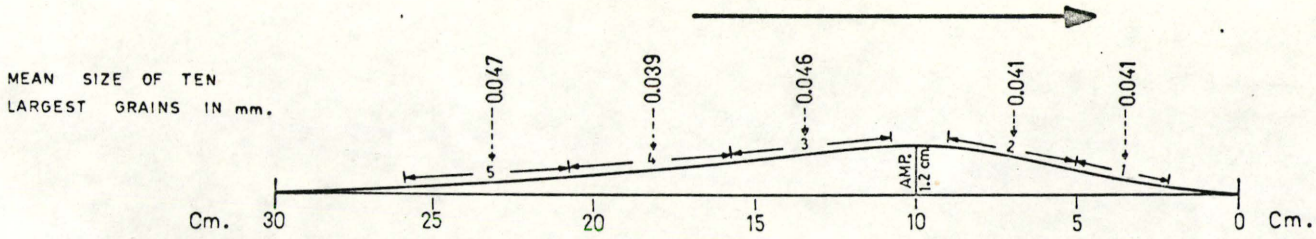

[ii]

LOCATION : Grande Vallée, Bed – 2, 200′ Ft. POINT, From the top of the bed.

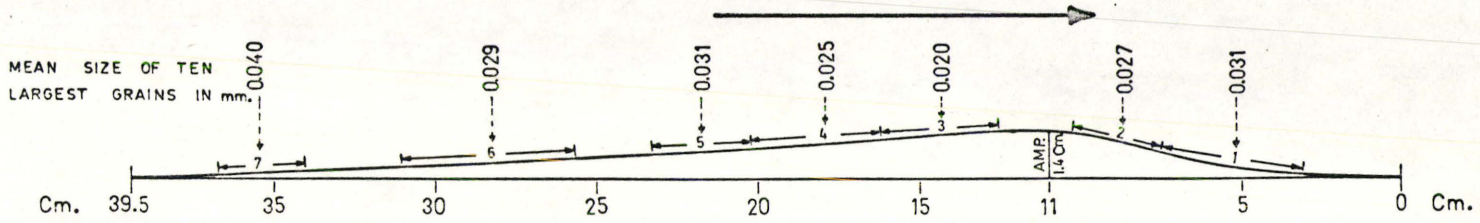

[iii]

LOCATION : Petite Vallée, Bed – 8, 62′ Ft. POINT, From the top of the bed.

FIG. 8

FIG. 9.

Detailed grain size analysis across a ripple

SIZE GRADES ø UP TO	mm. UP TO	1	2	3	4	5	6	7	8	9	10	11	12	← SLIDE NO.
		PERCENT GRAINS												
6.0	0.0156	36	22	32	24	30	26	44	50	58	60	64	70	MATRIX
5.5	0.0220	26	20	18	26	24	20	14	12	16	16	16	10	
5.0	0.0310	22	32	30	20	26	20	16	20	14	14	14	8	
4.5	0.0440	12	16	12	18	8	20	14	6	2	8	2	4	
4.0	0.0625	4	10	4	6	8	10	6	8	6	2	2	6	
3.5	0.0880	0	0	4	6	4	4	6	4	4	0	2	2	
% MATRIX ARGILLITE + CARBONATE		62	42	50	50	54	46	58	62	74	76	80	80	

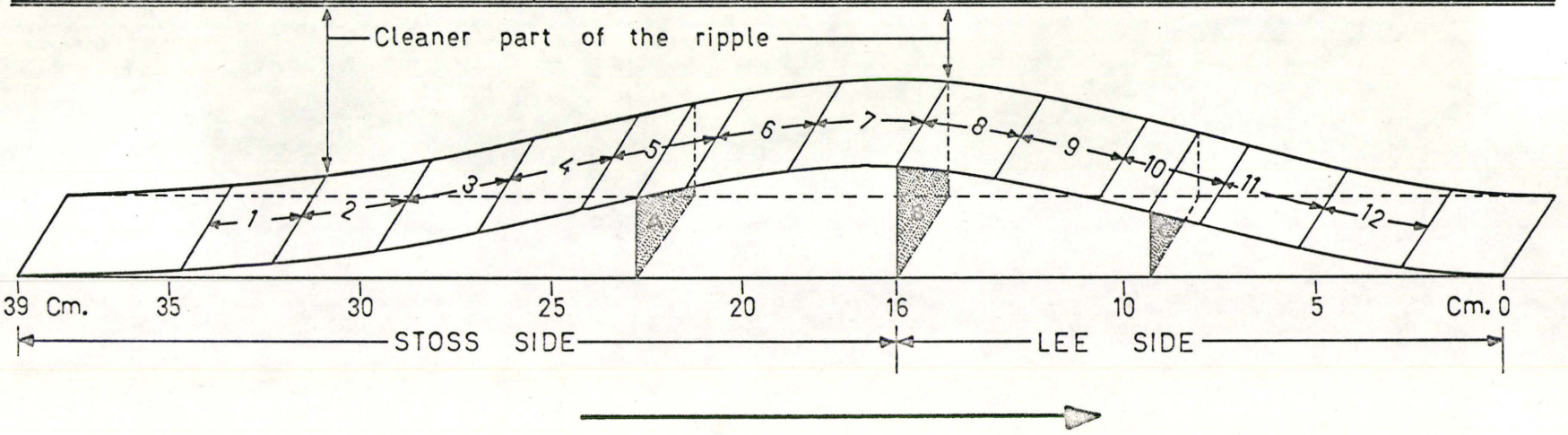

FIG. 9

PLATE 35.

Thin section photographs of rocks, at the positions A, B and C in figure 9, showing lamination characteristics. Note the burrowing in C.

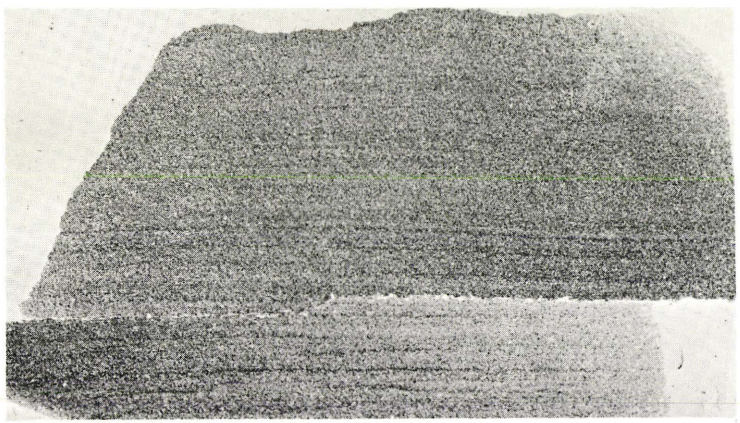

A

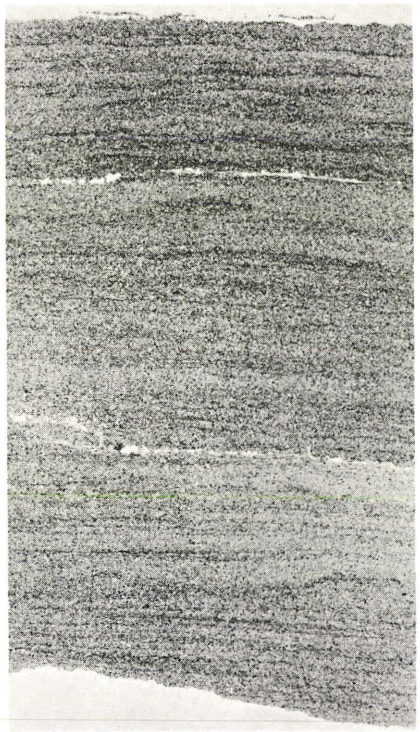

B

C

the coset, the angle of climb increases and concomitantly the ripples also increase in size due to increasing values of W, A, β and α. The size is maximum where the angle of climb attains a maximum value. The shape of the foreset laminae at this point is strongly sigmoidal and values of the parameters A, β, α and ϵ are maximum. Beyond this point A, β, α and ϵ start decreasing until the bed is plane. During the decreasing stage, W does not usually decrease.

Fig. 10B shows a thicker coset exhibiting a sinuous climb. It is to be noted here that (i) as long as ϵ keeps increasing, the ripple size also increases in exactly the same manner as shown in fig. 10A, but (ii) at the middle, where the climb angle flattens out temporarily, the ripple profile becomes a smooth arc with a rare increase in W at this point.

Fig. 10C shows a thinner coset exhibiting a straight climb. In these cosets ripple size continues to increase from the base upwards to near the top and the shape of the foreset laminae simultaneously become more and more sigmoidal. In the top 1 cm of these cosets ripple relief decreases rapidly but instead of being fully levelled, the bed-tops still retain the rippled relief.

Merging of Climbing Bands:

Merging of climbing bands, due to overtaking of a set of dying ripples by their live upstream neighbours, is spectacularly displayed in the upper part of bed 477 (see Pl. 15, 18). It was observed that almost every alternate ripple, in the entire exposed bed length, was overtaken by its upstream neighbour. This feature was also observed at some places in the beds 5 and 7 of Petite Vallée (see Pl. 36).

3.4. Down-Current Changes in Lamination Characteristics

It can be seen in fig. 11 and in Pl. 38, that in bed 2 of Grande Vallée an isolated coset of ripple-drift, 36 m long and 11 cm thick, occurs within a 14 cm thick parallel laminated bed. Initially the bed is very thin and the sediments are deformed into isolated load-balls. As soon as the continuous bed begins, parallel lamination develops in very fine sand and silt. In all probability, these parallel laminations belong to Bouma division B rather than B+D. The parallel lamination in the lower part of the bed is mainly fine sand, and in the upper part of the bed, it is dominantly silty; it does not consist of alternations of very fine silt and clay. Therefore, this parallel lamination, although Bouma's D by definition, has more affinities with Bouma's B. At the 90' point (see Pl. 38) ripple-drift cross-lamination begins; here the lower parallel lamination is 6.5 cm thick. At the 220' point the lower

FIG. 10.

A. Sequence of ripple-shapes and sizes in a thick coset with Concave-upward Climb (diagrammatic)

B. Sequence of ripple-shapes and sizes in a thick coset with Sinuous Climb (diagrammatic)

C. Sequence of ripple-shapes and sizes in a thin coset with Straight Climb (diagrammatic)

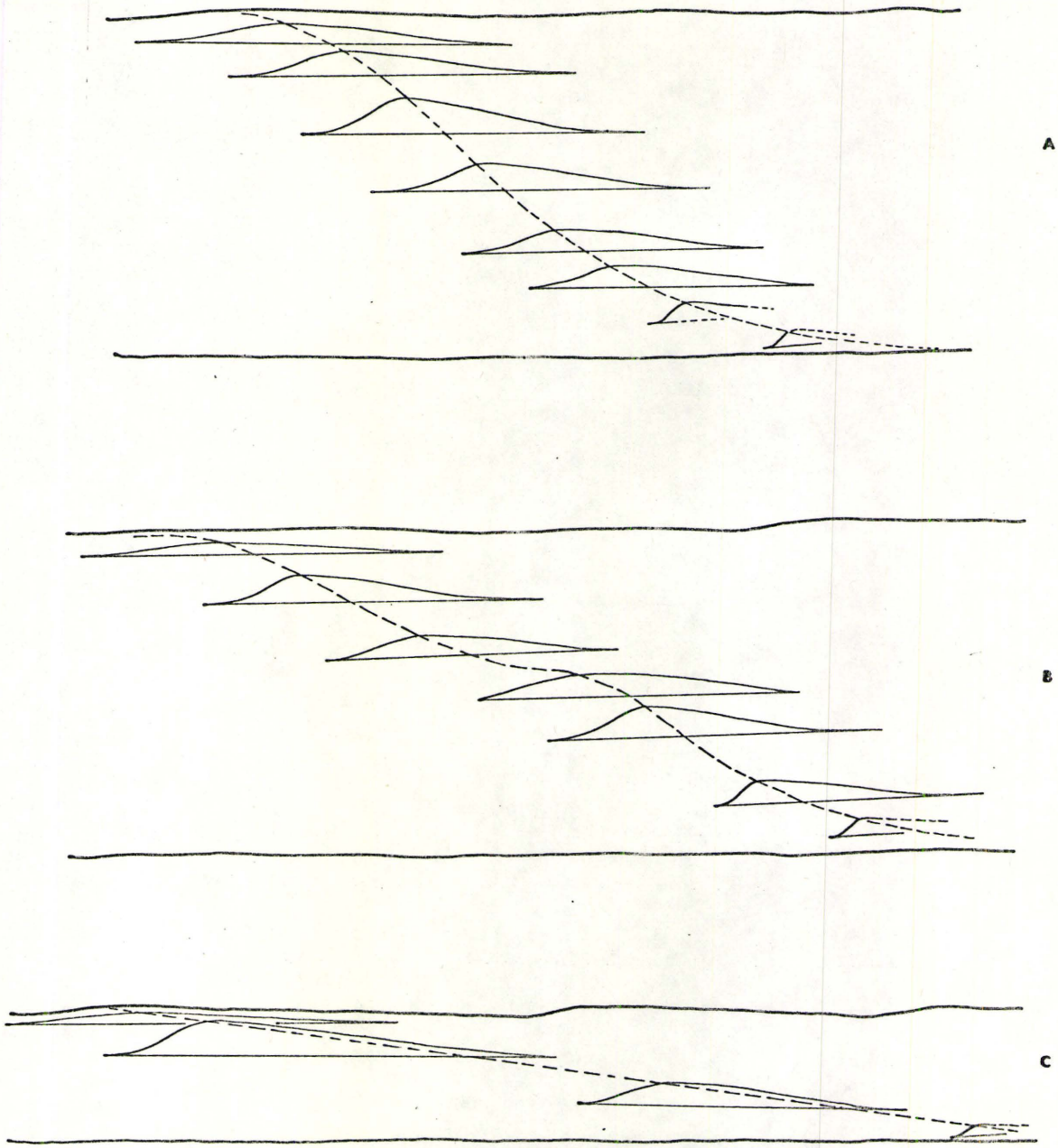

FIG. 10

PLATE 36.

Merging of climbing bands due to overtaking, bed, 5, Petite Vallee.

PLATE 37.

Weak sinuousity in the alignment of the crest line at the top of bed 477, St. Maurice.

FIG. 11

Lateral changes in type of stratification in three beds at Grande Vallée. Fully discussed in the text.

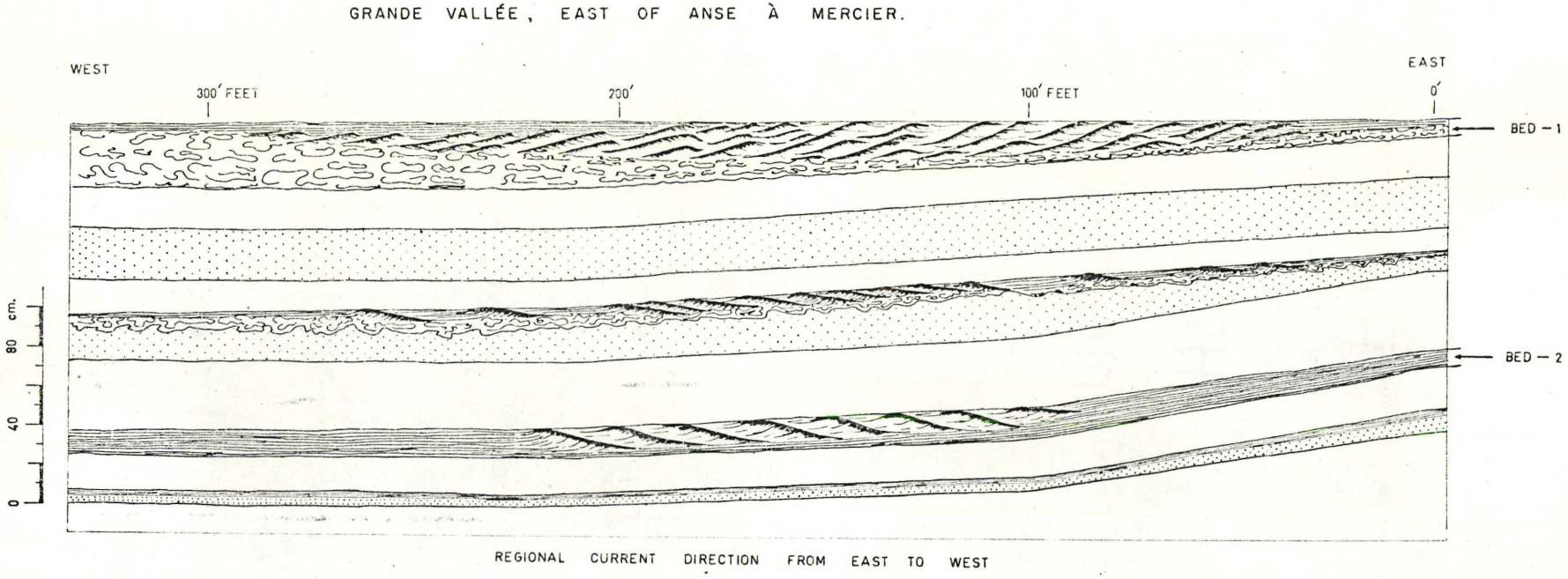
GRANDE VALLÉE, EAST OF ANSE À MERCIER.
WEST
EAST
300' FEET
200'
100' FEET
0'
BED — 1
BED — 2
0
40
80 cm.
REGIONAL CURRENT DIRECTION FROM EAST TO WEST

FIG. 11

PLATE 38.

A through G, illustrate down-current changes in lamination types in bed 2, Grande Vallée. A (upcurrent end) at -13', B at -9', C at 0', D at 68', E at 105', F at 215' and G (downcurrent end) at 230'. For distances refer to fig. 11.

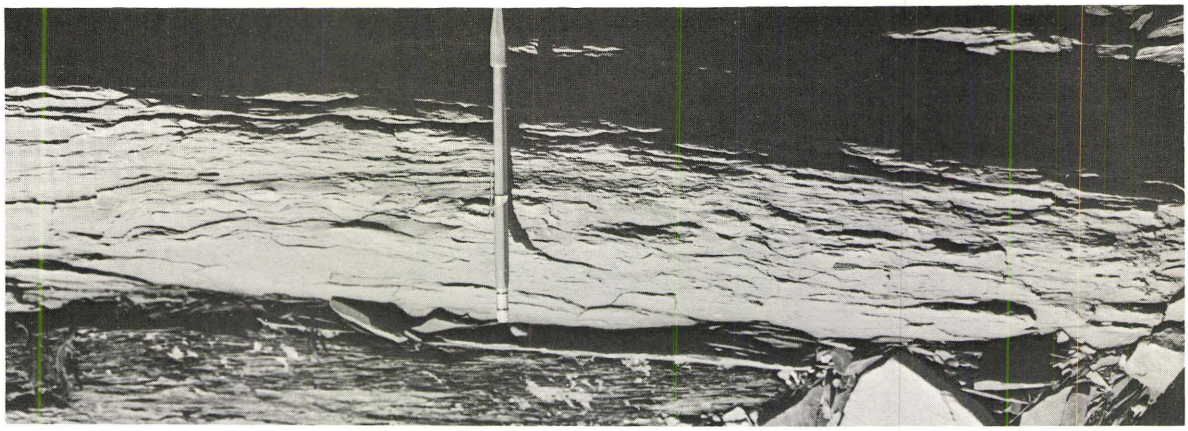

A

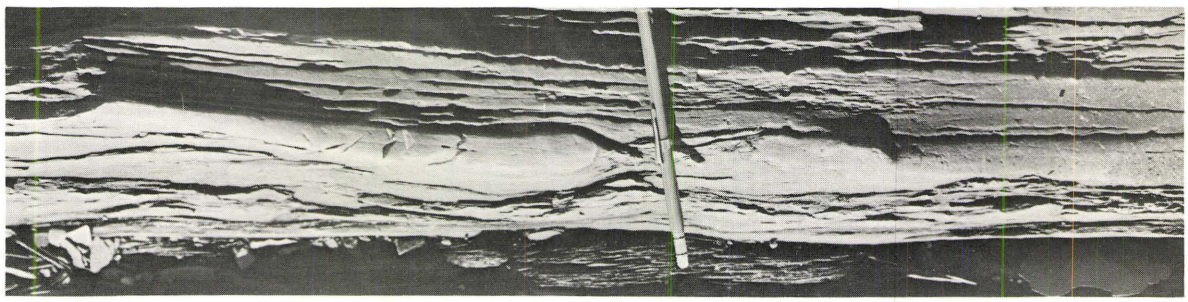

B

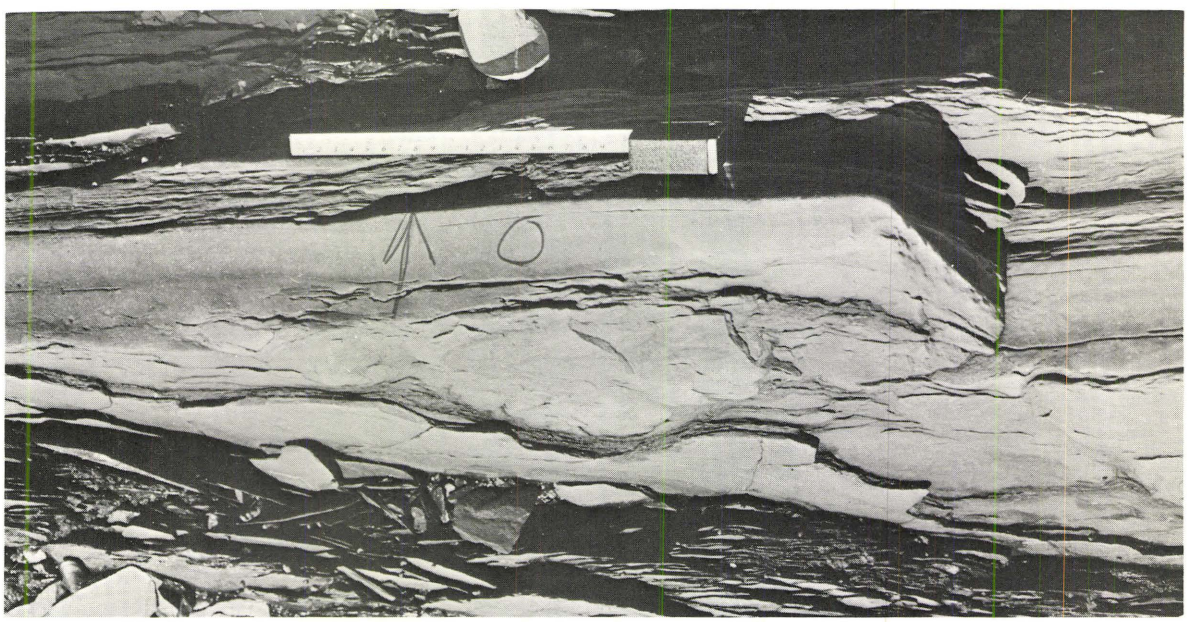

C

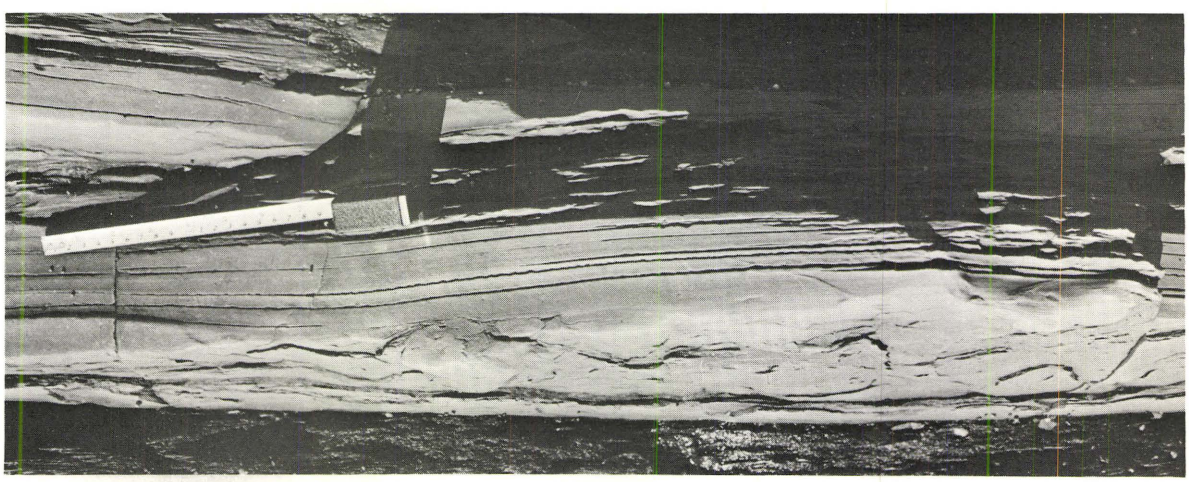

D

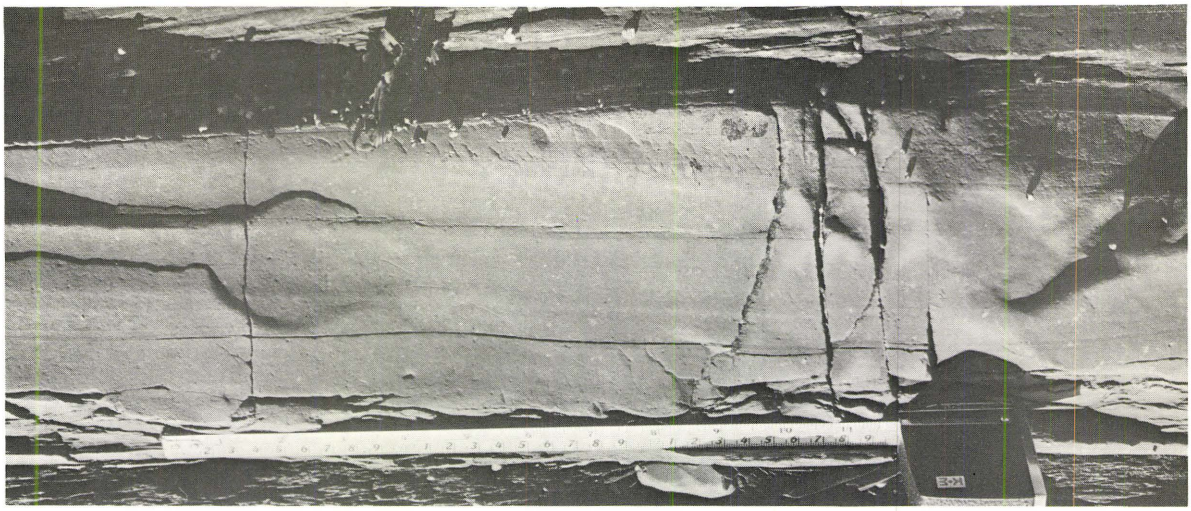

E

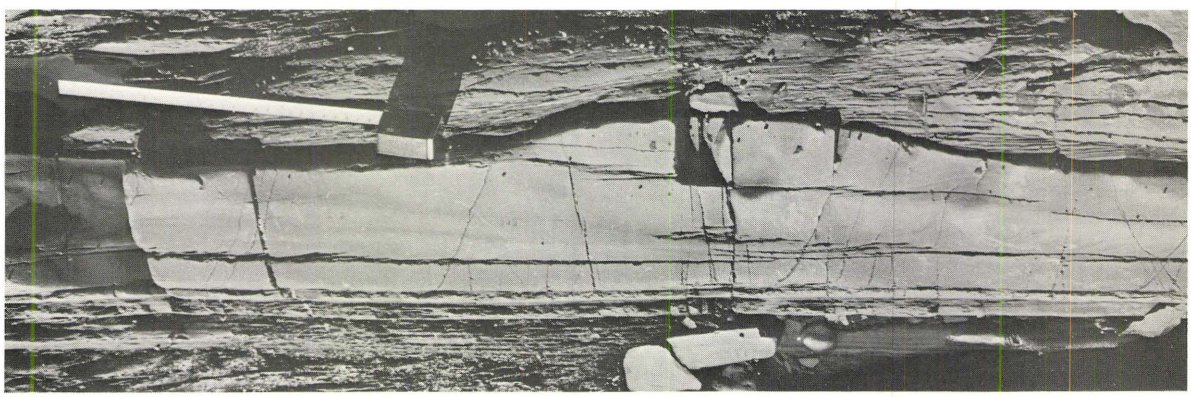

F

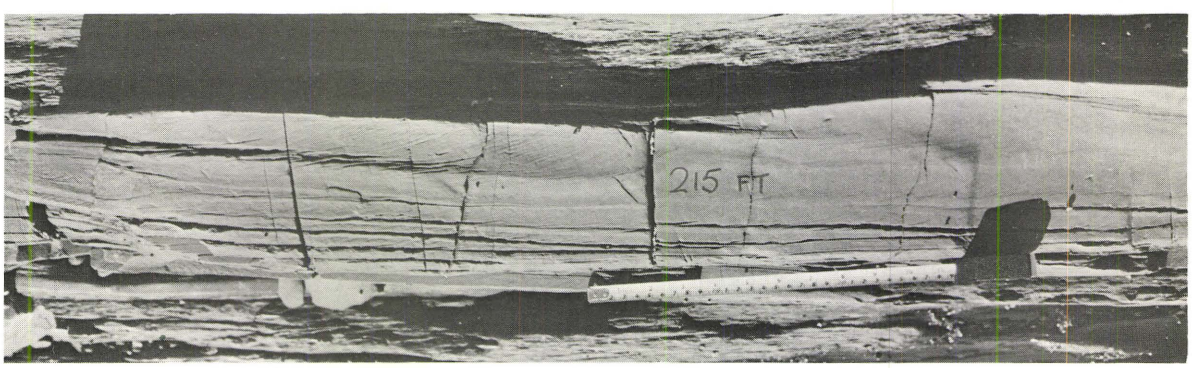

G

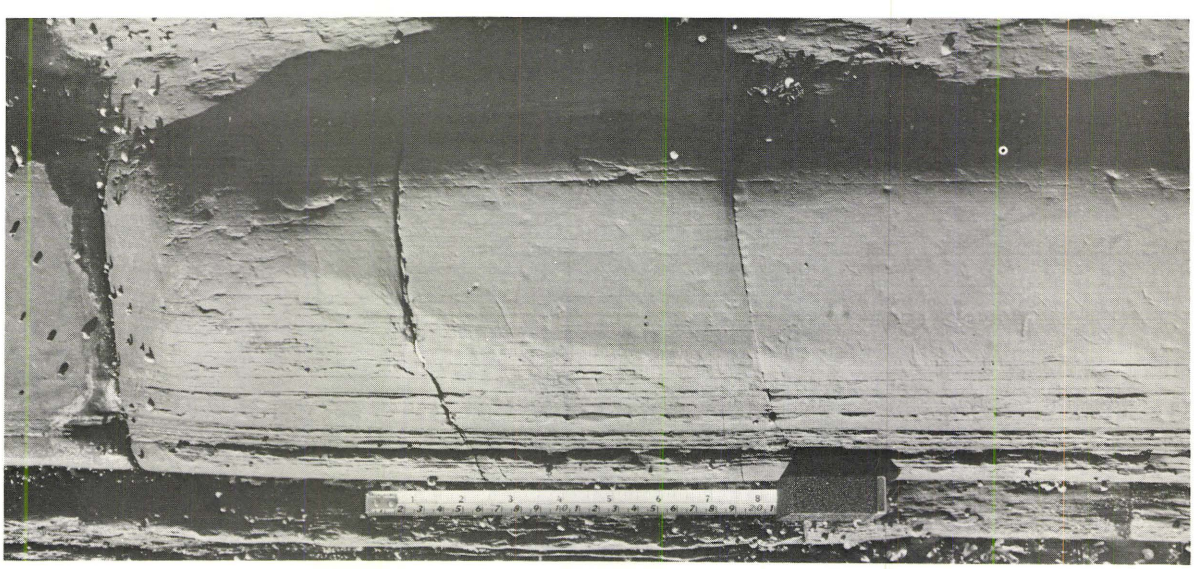

H

PLATE 39.

Down-current changes in internal structures in bed 8, Petite Vallee. Details are explained in the text. Current from A (East) towards C (West).


B
A


C
B

parallel laminated part of the bed is 3.5 cm thick; the ripple-drift cross-lamination ends here abruptly and passes into parallel lamination again. Beyond the 220' point the bed shows parallel lamination only and continues for about 250 ft. before it disappears under the sea. This parallel lamination also has more affinities with Bouma's B. It can be seen in fig. 11 that at the bottom of the ripple-drift coset at the 220' point, parallel lamination first passes into ripples. In successive layers parallel laminations pass into ripples in positions farther and farther upstream. This resulted in a gradual increase in thickness of the parallel laminated part and a corresponding decrease in thickness of the ripple-drift coset in the upstream direction, and implies that the first-formed ripples were at the 220' point, but that higher in the bed ripples were generated in positions farther and farther upstream.

In the same figure, the unnumbered bed above bed 2 shows that in the lower part of the bed, the sediments are deformed into isolated load-balls. In the upper part, the centrally located (between 100'-200' points) regularly ripple-drifted part is preceded and followed by parallel lamination. Within the parallel laminated part a few isolated bands of ripple-drift also occur.

Bed 1 in fig. 11 shows a reversed current direction. In the upstream part of bed 1, sediments are deformed into load-balls and the bed is about 27 cm thick. Thickness of the deformed part of the bed gradually decreases downcurrent, giving place to parallel lamination and then to ripple-drift. Farther downcurrent the bed gradually thins out and the sediments are again deformed into load balls. Finally, the bed dies out eastwards at a distance of 100' from the 0' point shown in fig. 11.

In Petite Vallée, bed 8 (33 cm thick) shows the following downcurrent changes in lamination characteristics (see Pl. 39). The bed as a whole is an amalgamation (vertically) of Bouma's BCB divisions. The lower BC part usually constitutes about 22 cm of the bed. An erosional line between C and the upper B is sometimes distinctly visible (see Pl. 39). At the upstream end, i.e. to the right of the point A in Plate 39, the bed is parallel laminated and is exposed for a length of about 200'. Between the points A and C (length 40', see Pl. 39) the bed shows a lower parallel laminated part, a middle ripple-drifted part and an upper parallel laminated part. Farther downcurrent, i.e. to the left of the point C, the bed contains only parallel laminations for a distance of 30' and then the middle ripple-drift part appears again.

After a short disappearance under beach gravel, the bed (with lower parallel lamination 4 cm, ripple-drift 10 cm, upper parallel lamination 17 cm) again crops out 100' downcurrent and continues unchanged until it disappears under the Petite Vallée wharf. Between the points A and C, it can be seen in Pl. 39 that at the upcurrent end the angle of climb is low and the thickness of the lower parallel laminated part is considerable; in between the points A and B the angle of climb is irregular; near the point B the angle of climb is very steep and the thickness of the lower parallel laminated part is minimum; from B towards C the angle of climb gradually decreases and thickness of the lower parallel laminated part increases again.

3.5. Lateral and Vertical Variation of Parameters and other Features of Ripple-Drift

Coset Thickness:

Fig. 12 shows the lateral variations in thickness of the cosets which were studied in detail. At St. Maurice bed 477, 78 cm thick at the upcurrent end, measured 70 cm at a downcurrent distance of 900' feet. This reduction in thickness is due to elimination of 8 cm of parallel lamination from the basal part of the bed, otherwise the coset thickness remains uniform throughout the exposed length.

The beds measured in β_1 Member at Fame Point, West, could not be traced laterally due to the restricted width of the exposure.

In Petite Vallée beds 1, 2, 3 and 4 (see Pl. 4) and beds 5, 6, and 7 (see Pl. 1) are spectacularly parallel sided and do not show any significant change in coset thickness up and down the exposed length of the beds.

A deviation from this common trend is observed in beds 8 and 9 (Fig. 12A) and 10 and an unnumbered bed (current direction same as bed 10) occurring below bed 10 (Fig. 12B), at Petite Vallée and beds 1 and 2 (Fig. 11) at Grande Vallée. Plate 39 depicts nicely a very unusual sequence of downcurrent changes in ripple-drift coset thickness.

Angle of Climb:

The different types (A to F) of the angle of climb have already been described. It was observed in the field that in some cosets some of these types may show some preferred combinations of lateral and vertical changes. Type-D is excluded for the present purposes of generalisations, because of its extremely rare occurrence.

FIG. 12.

Thickness variation diagram of ripple-drift cosets (not beds).

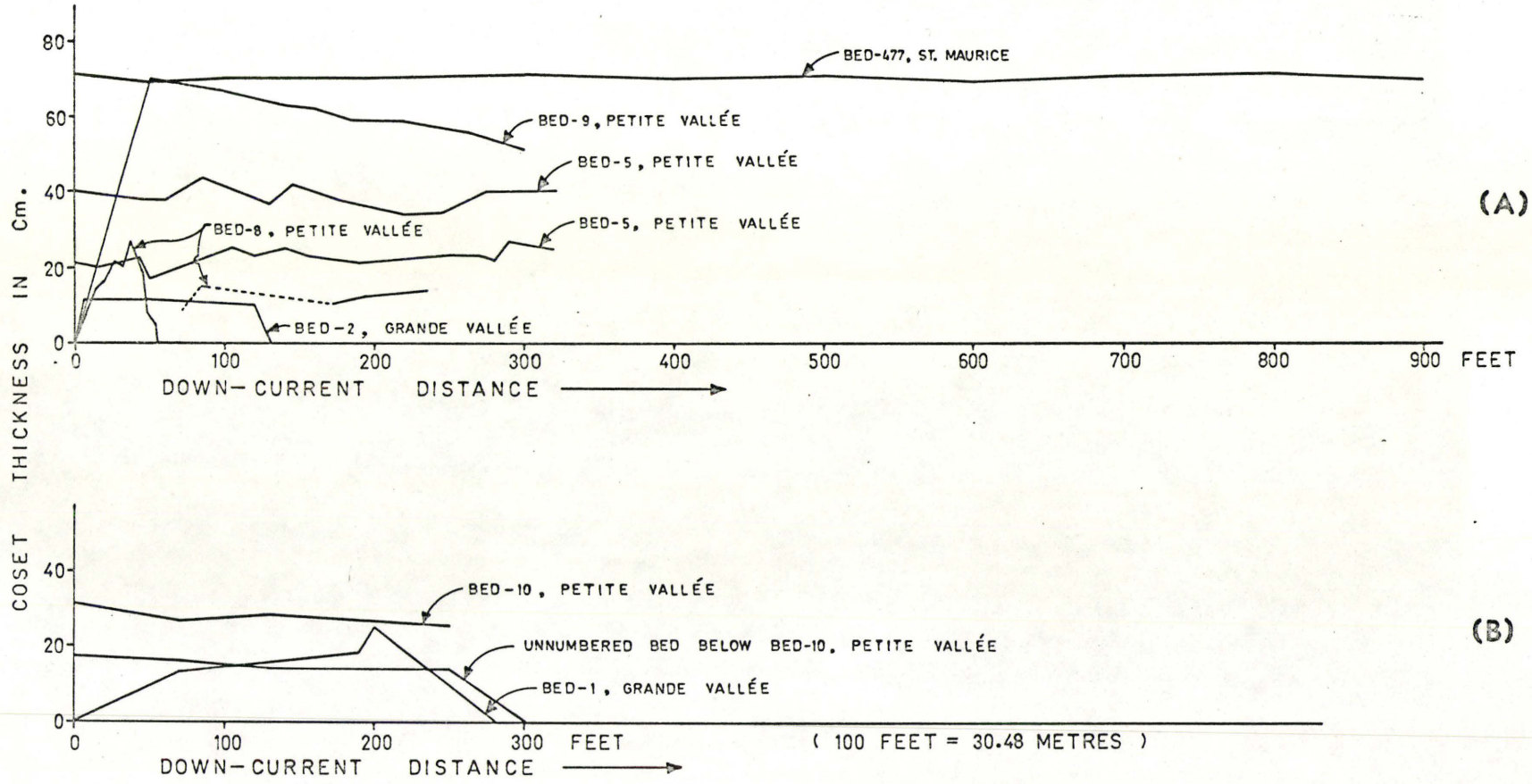
COSET THICKNESS IN Cm.
80
60
40
20
0
BED-477, ST. MAURICE
BED-9, PETITE VALLÉE
BED-5, PETITE VALLÉE
BED-8, PETITE VALLÉE
BED-5, PETITE VALLÉE
BED-2, GRANDE VALLÉE
0
100
200
300
400
500
600
700
800
900
FEET
DOWN-CURRENT DISTANCE
(A)
40
20
0
BED-10, PETITE VALLÉE
UNNUMBERED BED BELOW BED-10, PETITE VALLÉE
BED-1, GRANDE VALLÉE
0
100
200
300
FEET
DOWN-CURRENT DISTANCE
(100 FEET = 30.48 METRES)
(B)

FIG. 12

Vertically, passage of type-E and/or type-F to type A, B or C were observed in several cases (e.g. beds 1, 2, 5, 7, Petite Vallée; bed 477, St. Maurice; see Pls. 33, 16).

Laterally, the following sequences were observed:

(i) In the upper part of the bed 5, Petite Vallée:

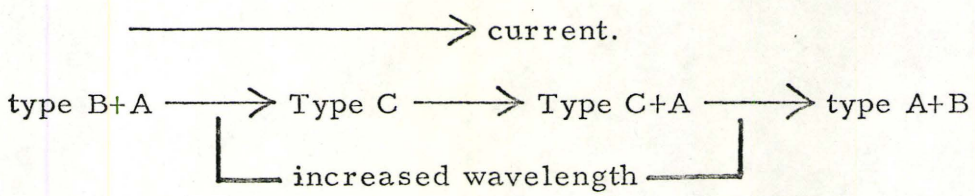

Between 265' and 212' points in fig. 16.

(ii) In bed 7, Petite Vallée (lies 24 cm below bed 5):

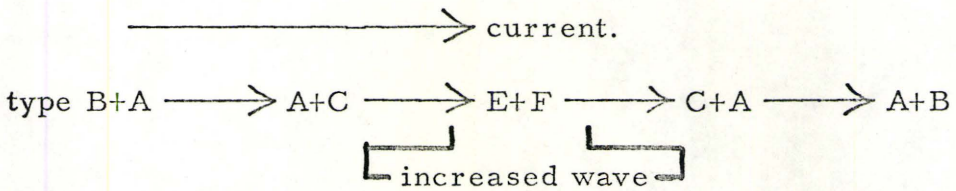

length. Between 265' and 212' points in fig. 18.

(iii) In bed 9, Petite Vallée:

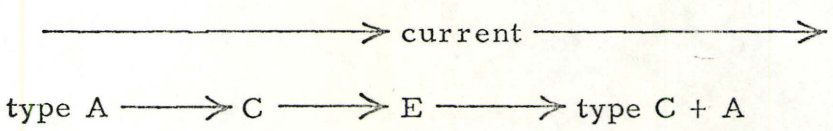

Details of vertical and lateral increase and decrease in the amount of the angle of climb, in the five beds studied in detail, are shown graphically in fig. 13 through fig. 22. It appears that the exposed lengths of the beds are not enough to show any significant lateral change. But regarding vertical changes it can be generalised that thicker cosets exhibit steeper angles of climb and the pattern of climb is predominantly of the type-A (i.e. concave upward climb, might be with a small convexity at the top).

t_L/t_S:

Details of vertical and lateral changes in t_L/t_S are shown in fig. 13 through fig. 22. It appears that t_L/t_S generally decreases upward through a coset. Laterally t_L/t_S does not show any significant change. However, in bed 10 of Petite Vallée a steady downcurrent decrease in average values of the t_L/t_S is clearly noticeable.

Wave Length:

Fig. 13 through fig. 22 depicts vertical and lateral changes in wave length in 5 beds measured in three different localities. A general tendency is that the wave length increases upward through the cosets. In only a few cases vertical changes in wave length are irregular. No lateral change is apparent from the graphs, except in bed 10 of Petite Vallée, where a downcurrent decrease in average values of the wave length is noticeable.

FIG. 13.

Vertical variability of parameters W, A, β, α, ϵ and t_L/t_S in bed 477 at St. Maurice. Part of the bed below the dashed line is parallel laminated.

Note - in plots of Angle of Climb, triangles indicate computed ϵ' and dots indicate measured ϵ.

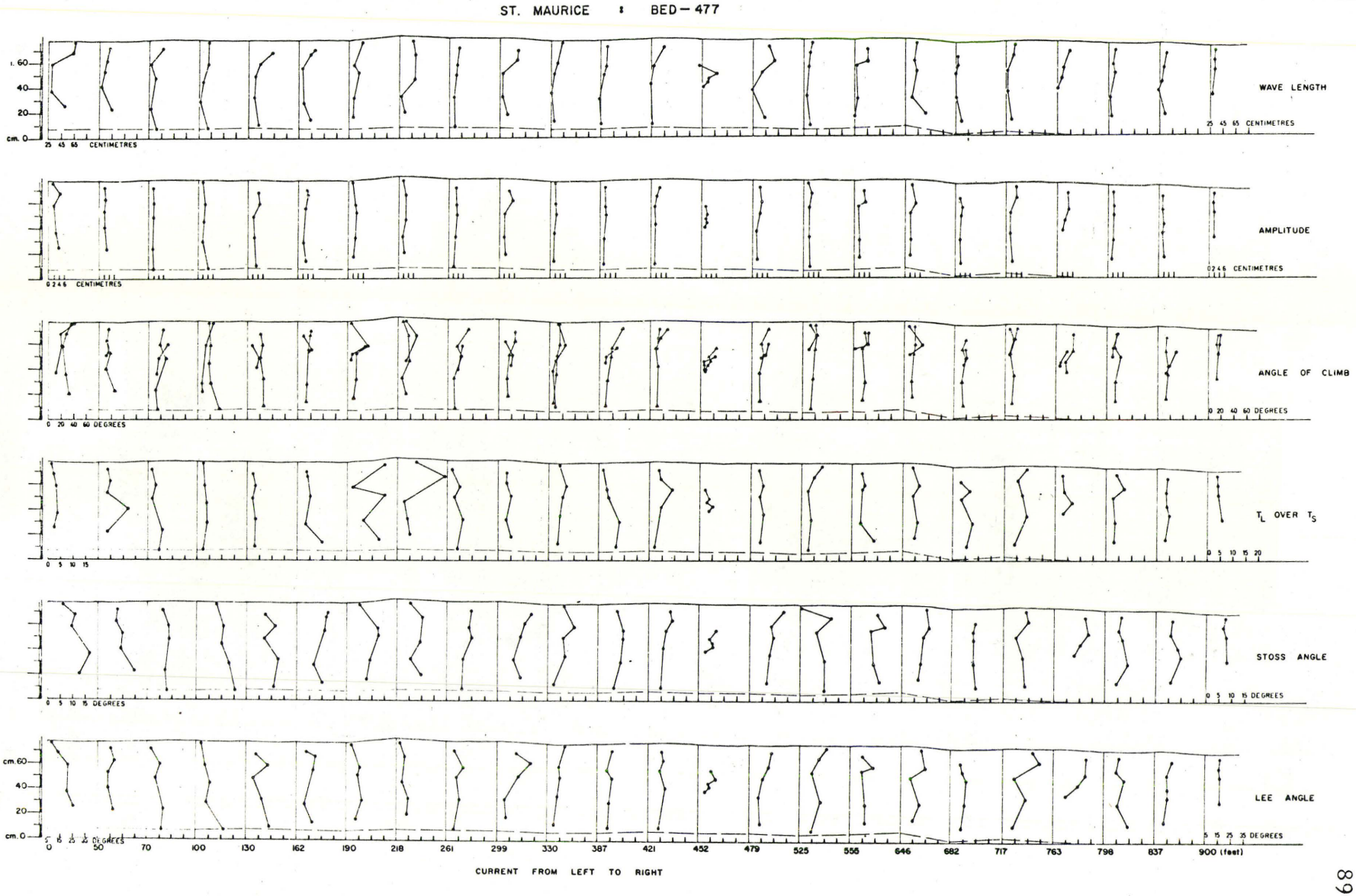
ST. MAURICE : BED – 477
WAVE LENGTH
AMPLITUDE
ANGLE OF CLIMB
T_L OVER T_S
STOSS ANGLE
LEE ANGLE
CENTIMETRES
DEGREES
CURRENT FROM LEFT TO RIGHT
0 50 70 100 130 162 190 218 261 299 330 387 421 452 479 525 555 646 682 717 763 798 837 900 (feet)

FIG. 13

FIG. 14.

Horizontal variability of parameters W, A, β, α, ϵ and t_L/t_S in bed 477 at St. Maurice. Note the average values of the parameters of the upper regularly drifted part and the lower irregularly drifted part have been plotted separately.

Note - in plots of Angle of Climb, triangles indicate computed ϵ' and dots indicate measured ϵ.

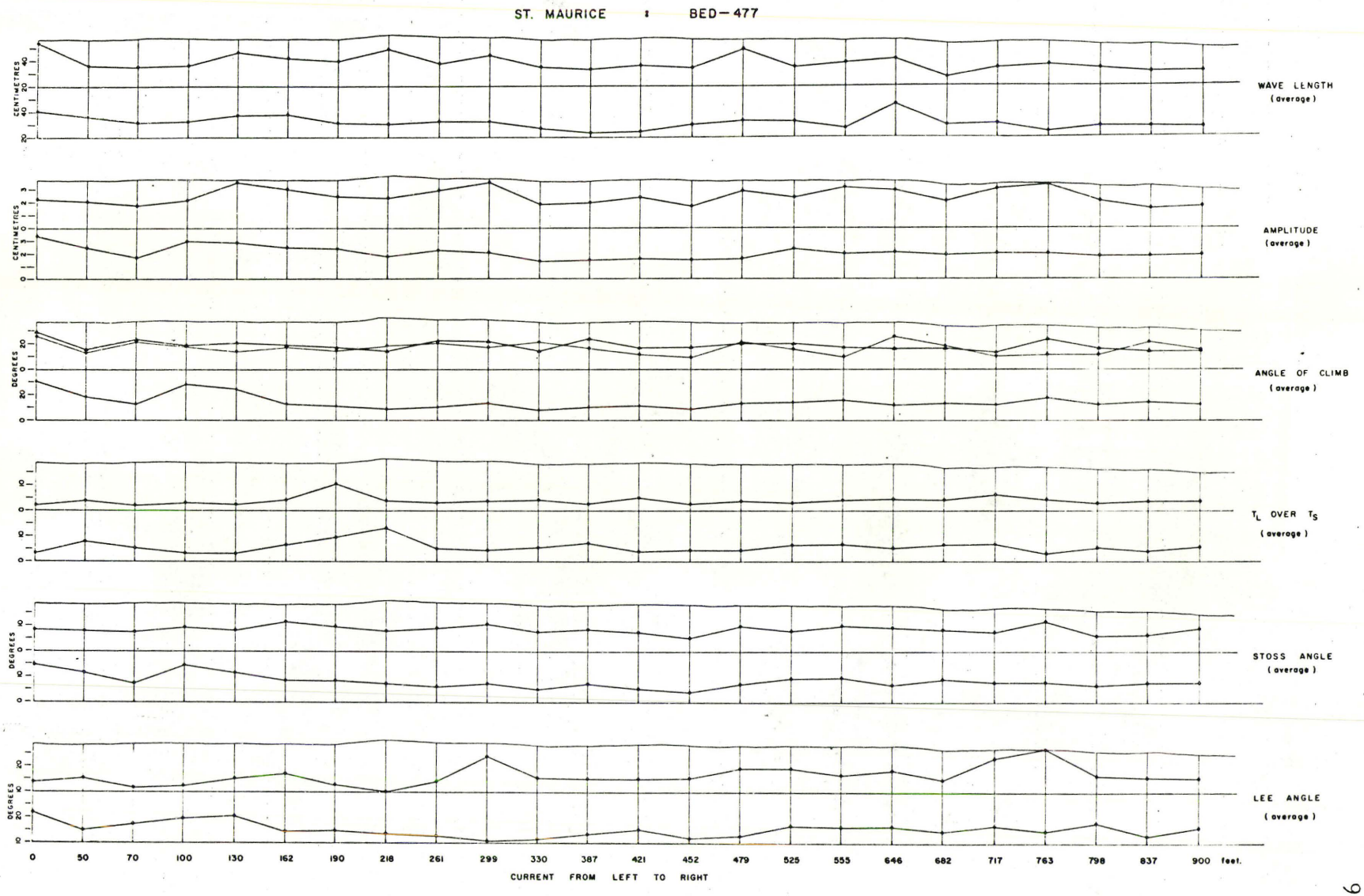
ST. MAURICE : BED—477
CENTIMETRES
WAVE LENGTH
(average)
CENTIMETRES
AMPLITUDE
(average)
DEGREES
ANGLE OF CLIMB
(average)
T_L OVER T_S
(average)
DEGREES
STOSS ANGLE
(average)
DEGREES
LEE ANGLE
(average)
0 50 70 100 130 162 190 218 261 299 330 387 421 452 479 525 555 646 682 717 763 798 837 900 feet.
CURRENT FROM LEFT TO RIGHT

FIG. 14

FIG. 15.

Vertical variability of parameters W, A, β, α, ϵ and t_L/t_S in bed 5 at Petite Vallée.

Note - in plots of Angle of Climb, triangles indicate computed ϵ' and dots indicate measured ϵ.


PETITE VALLÉE : BED-5
CM.
0 10 20 30
25 45 65 85 CENTIMETRES
WAVE LENGTH
0 2 4 6 CENTIMETRES
AMPLITUDE
0 5 10 15
T_L OVER T_S
0 20 40 DEGREES
ANGLE OF CLIMB
0 5 10 15 DEGREES
STOSS ANGLE
0 5 10 15 DEGREES
LEE ANGLE
10 31 48 76 102 112 130 148 164 177 192 200 212 261 277 293 322 (feet)
CURRENT FROM RIGHT TO LEFT

FIG. 15

FIG. 16.

Horizontal variability of parameters W, A, β, α, ϵ and t_L/t_S in bed 5 at Petite Vallée.

Note - in plots of Angle of Climb, triangles indicate computed ϵ' and dots indicate measured ϵ.

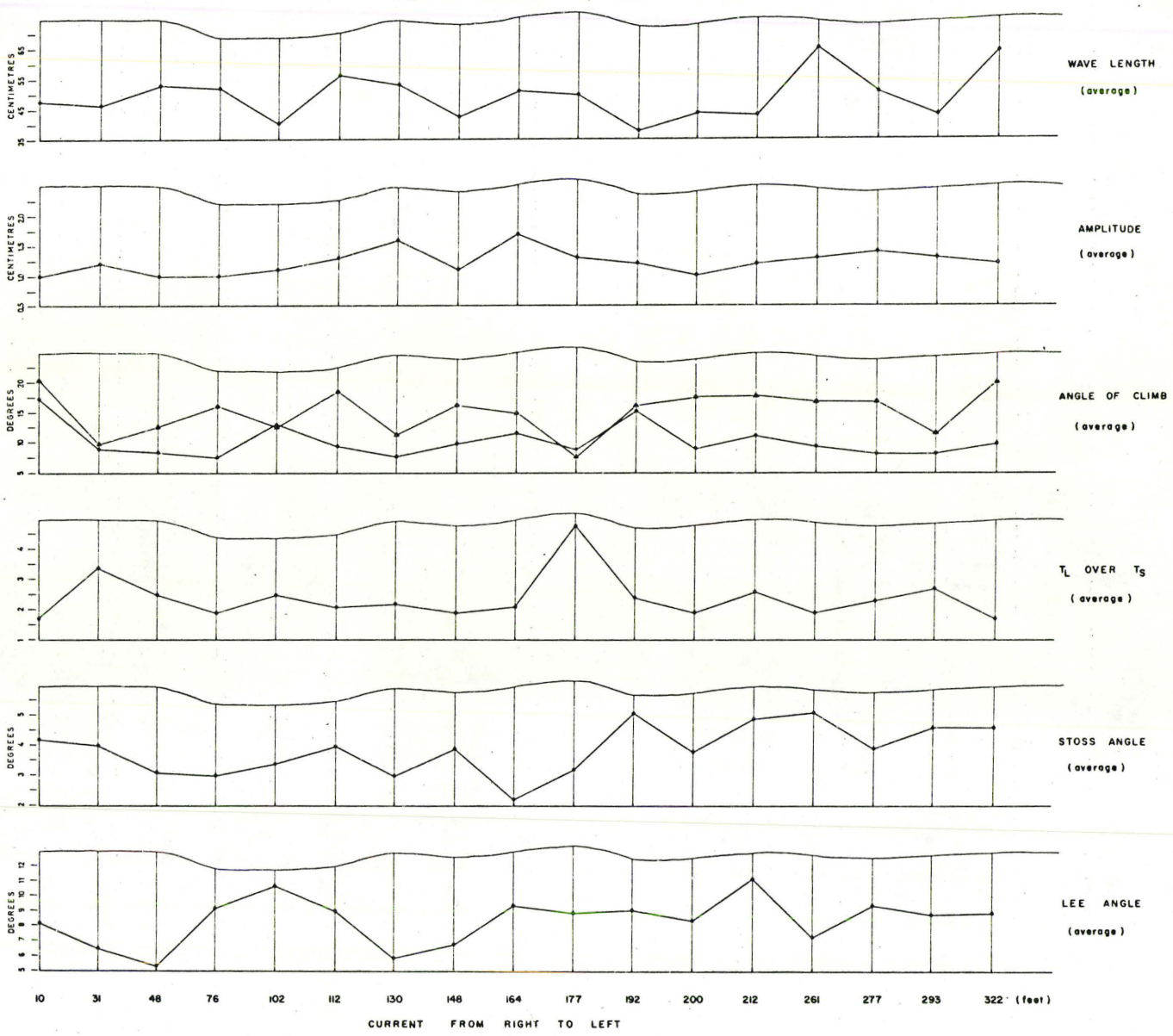
PETITE VALLÉE : BED-5
CENTIMETRES
WAVE LENGTH
(average)
CENTIMETRES
AMPLITUDE
(average)
DEGREES
ANGLE OF CLIMB
(average)
T_L OVER T_S
(average)
DEGREES
STOSS ANGLE
(average)
DEGREES
LEE ANGLE
(average)
10 31 48 76 102 112 130 148 164 177 192 200 212 261 277 293 322 (feet)
CURRENT FROM RIGHT TO LEFT

FIG. 16

FIG. 17.

Vertical variability of parameters W, A, β, α, ϵ and t_L/t_S in bed 7 at Petite Vallée.

Note - in plots of Angle of Climb, triangles indicate computed ϵ' and dots indicate measured ϵ.

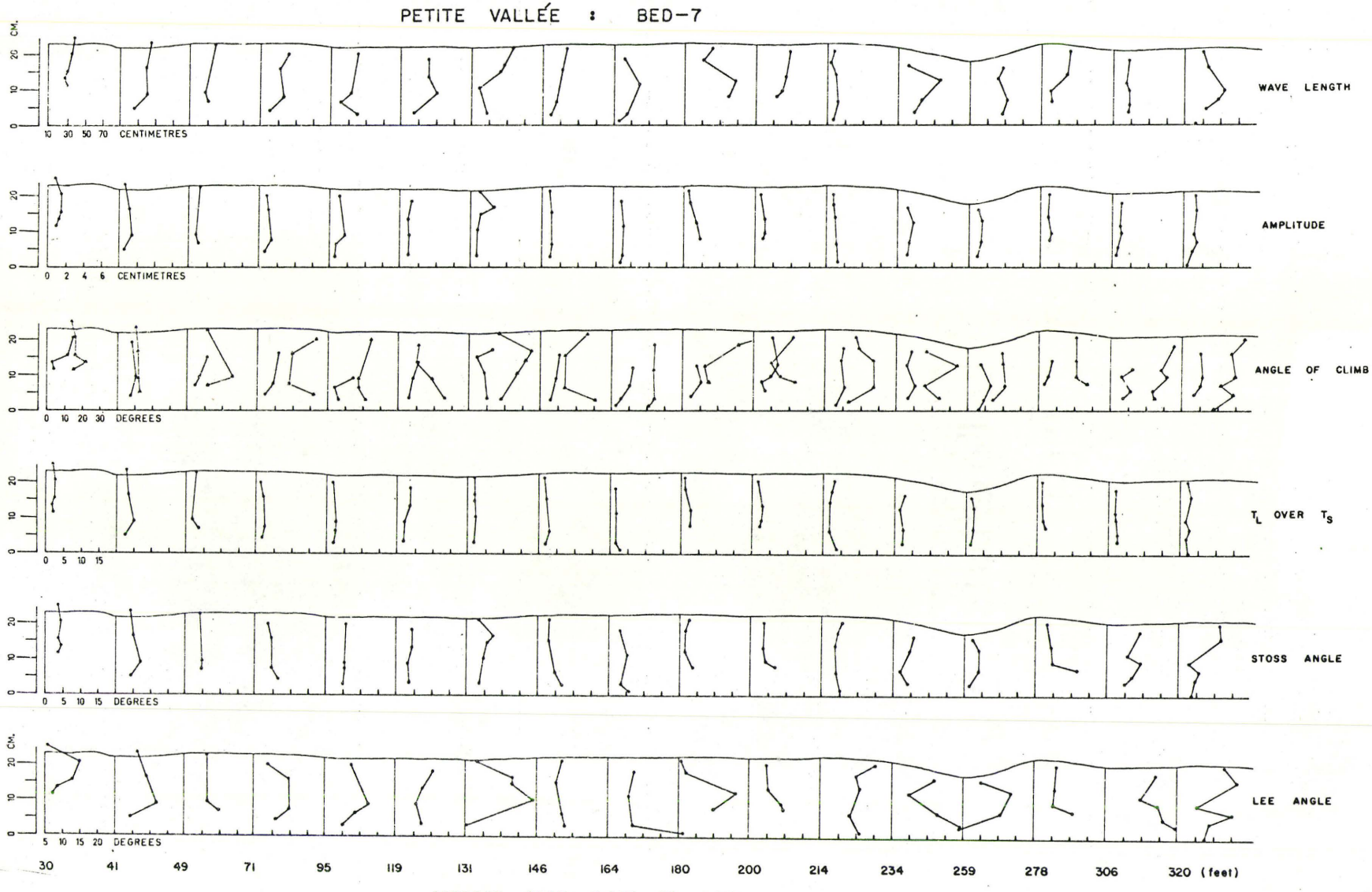
PETITE VALLÉE : BED-7
CM.
20
10
0
10 30 50 70 CENTIMETRES
WAVE LENGTH
0 2 4 6 CENTIMETRES
AMPLITUDE
0 10 20 30 DEGREES
ANGLE OF CLIMB
0 5 10 15
T_L OVER T_S
0 5 10 15 DEGREES
STOSS ANGLE
5 10 15 20 DEGREES
LEE ANGLE
30 41 49 71 95 119 131 146 164 180 200 214 234 259 278 306 320 (feet)
CURRENT FROM RIGHT TO LEFT

FIG. 17

FIG. 18.

Horizontal variability of parameters W, A, β, α, ϵ and t_L/t_S in bed 7 at Petite Vallée.

Note - in plots of Angle of Climb, triangles indicate computed ϵ' and dots indicate measured ϵ.

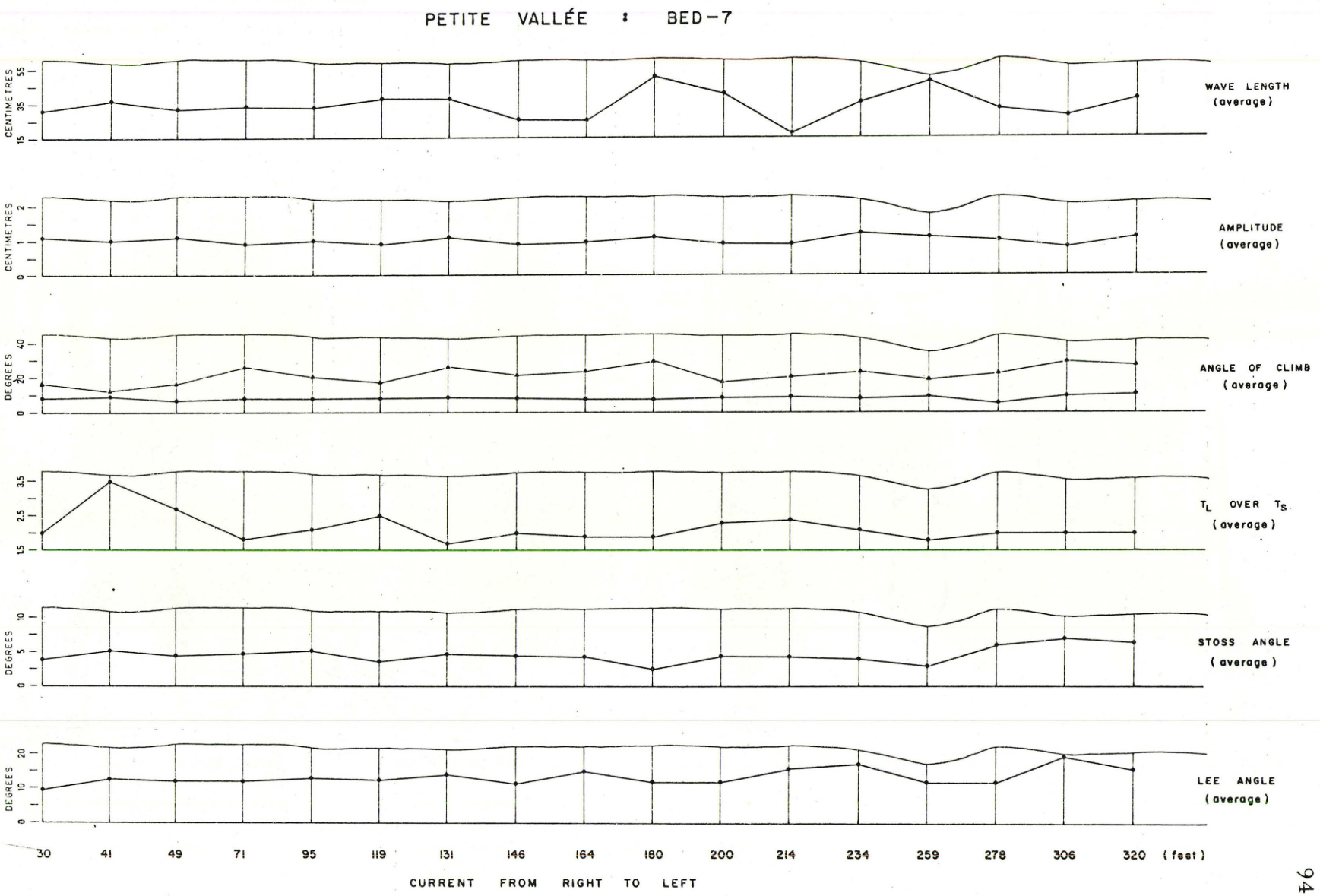
PETITE VALLÉE : BED-7
CENTIMETRES
15
35
55
WAVE LENGTH
(average)
CENTIMETRES
0
1
2
AMPLITUDE
(average)
DEGREES
0
20
40
ANGLE OF CLIMB
(average)
1.5
2.5
3.5
T_L OVER T_S
(average)
DEGREES
0
5
10
STOSS ANGLE
(average)
DEGREES
0
10
20
LEE ANGLE
(average)
30
41
49
71
95
119
131
146
164
180
200
214
234
259
278
306
320
(feet)
CURRENT FROM RIGHT TO LEFT

FIG. 18

FIG. 19.

Vertical variability of parameters W, A, β, α, ϵ and t_L/t_S in bed 10 at Petite Vallée.

Note - in plots of Angle of Climb, triangles indicate computed ϵ' and dots indicate measured ϵ.

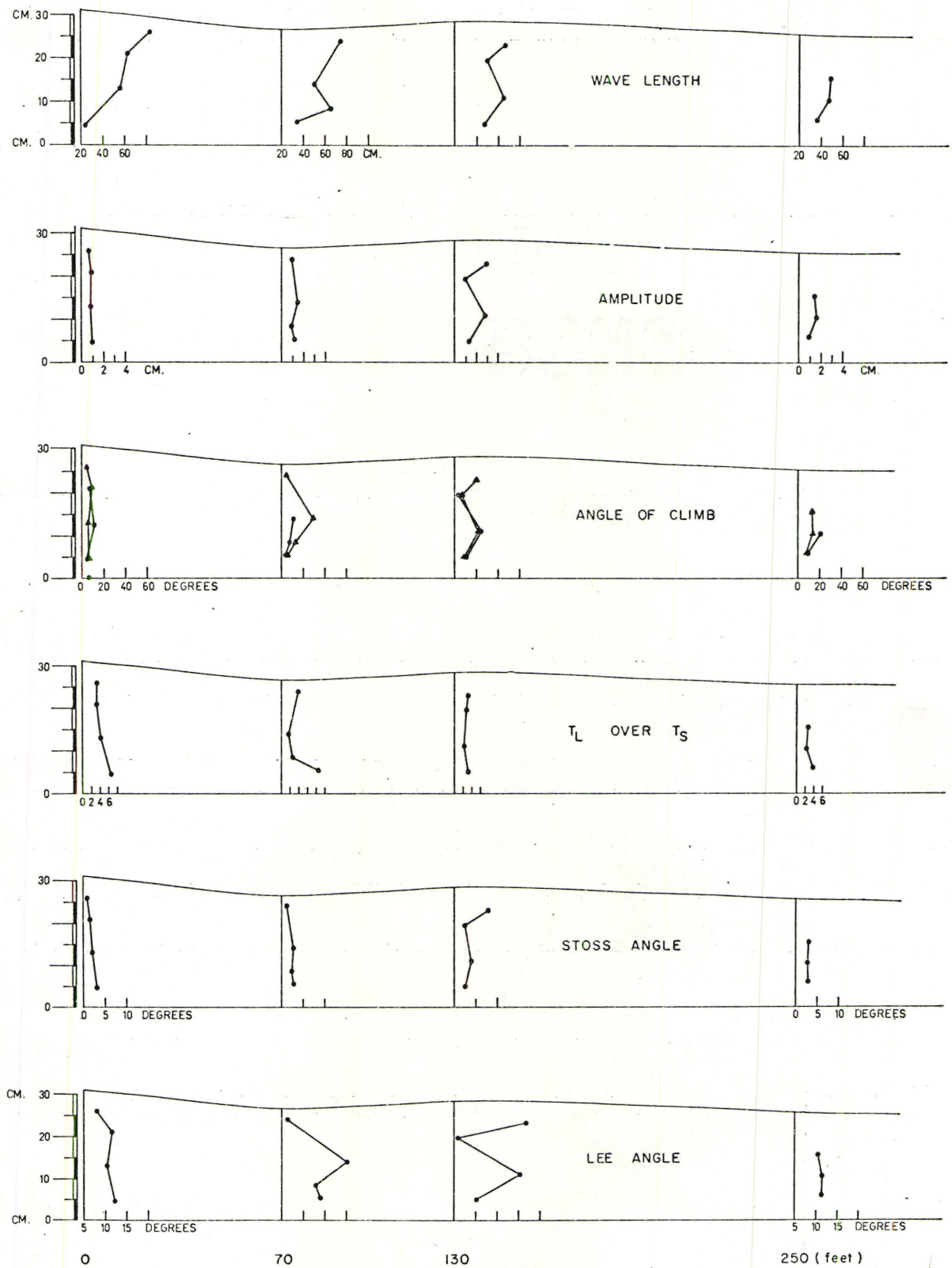

CURRENT FROM LEFT TO RIGHT.

FIG. 19

FIG. 20.

Horizontal variability of parameters W, A, β, α, ϵ and t_L/t_S in bed 10 at Petite Vallée.

Note - in plots of Angle of Climb, triangles indicate computed ϵ' and dots indicate measured ϵ.

PETITE VALLÉE : BED—10

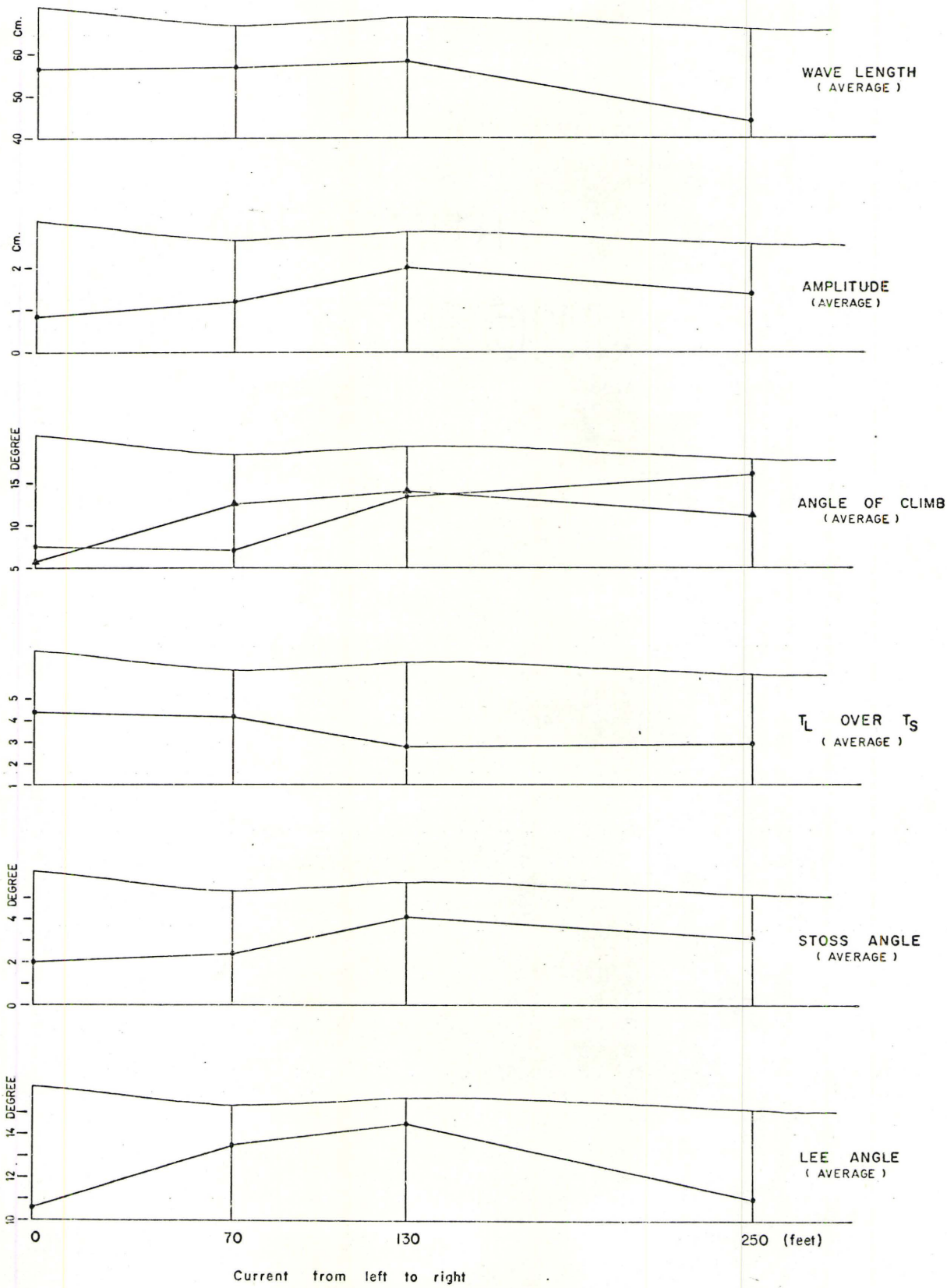

FIG. 20

FIG. 21.

Vertical variability of parameters W, A, β, α, ϵ and t_L/t_S in bed 2 at Grande Vallée. Part of the bed below the dashed line is parallel laminated.

Note - in plots of Angle of Climb, triangles indicate computed ϵ' and dots indicate measured ϵ.

GRANDE VALLÉE BED – 2

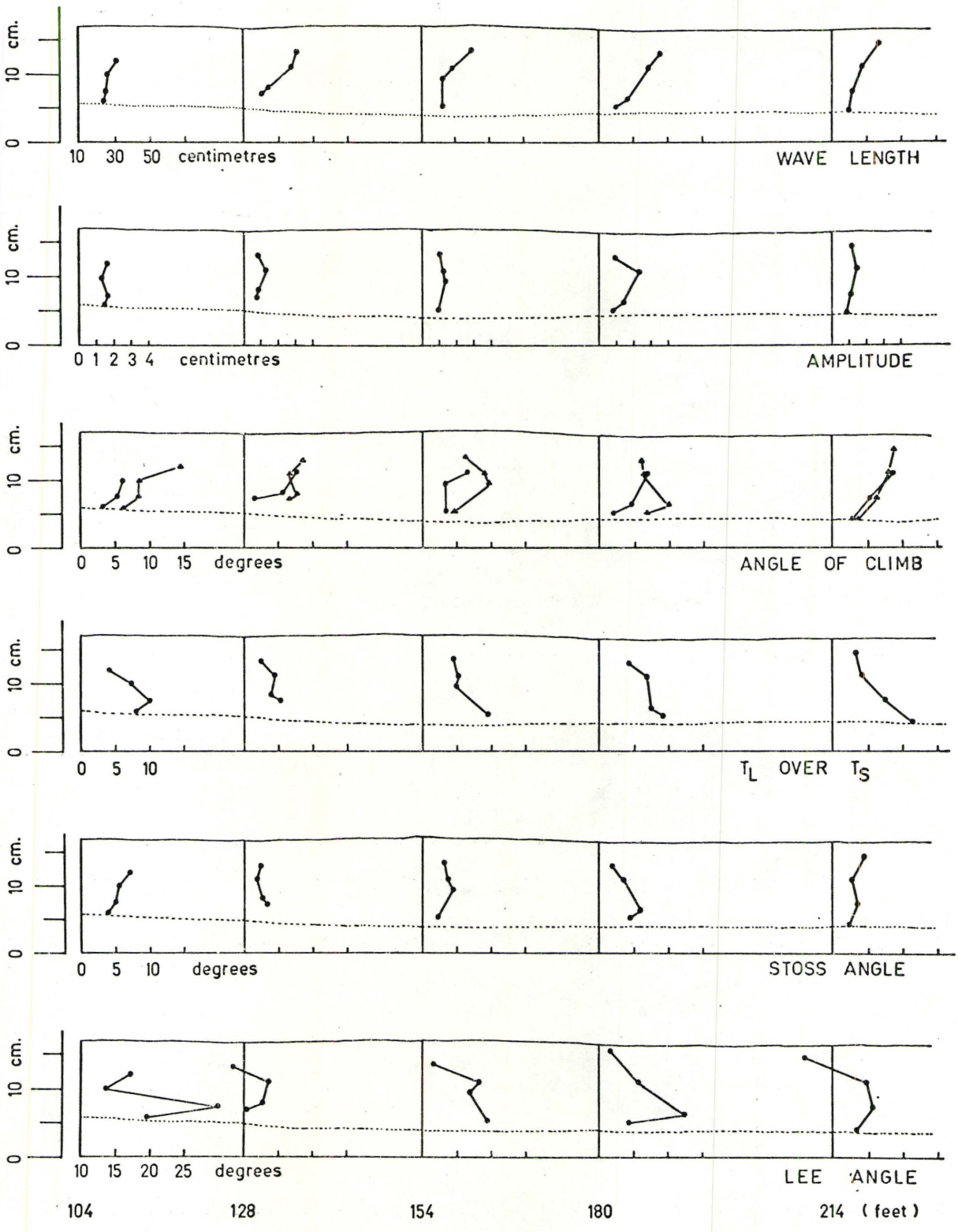

FIG. 21

FIG. 22.

Horizontal variability of parameters W, A, β, α, ϵ and t_L/t_S in bed 2 at Grande Vallee. Part of the bed below the dashed line is parallel laminated.

Note - in plots of Angle of Climb, triangles indicate computed ϵ' and dots indicate measured ϵ.

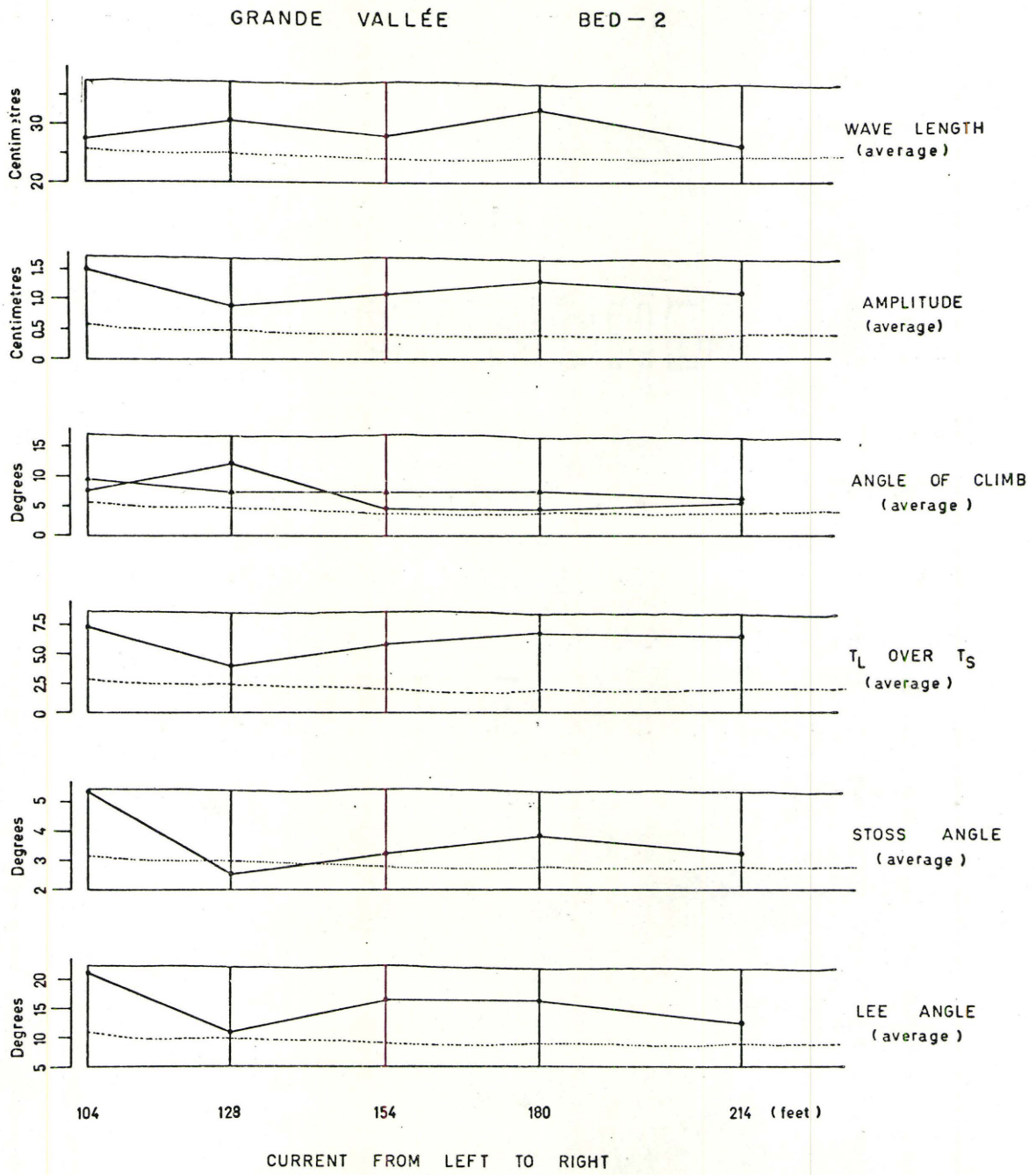
GRANDE VALLÉE
BED — 2
Centimetres
20
30
WAVE LENGTH
(average)
Centimetres
0
0.5
1.0
1.5
AMPLITUDE
(average)
Degrees
0
5
10
15
ANGLE OF CLIMB
(average)
0
2.5
5.0
7.5
T_L OVER T_S
(average)
Degrees
2
3
4
5
STOSS ANGLE
(average)
Degrees
5
10
15
20
LEE ANGLE
(average)
104
128
154
180
214 (feet)
CURRENT FROM LEFT TO RIGHT

FIG. 22

Amplitude:

Amplitude generally increases upward up to about the middle or upper middle of a coset and then decreases (see figs. 13 through fig. 22). In bed 477 (which does not fit in the above generalisations), initially the amplitude decreases (from 4.0 to 1.5 cm) upward in the Lower half (irregularly drifted) of the bed, then it gradually increases (from 1.5 to 5 cm) in the upper half (regularly drifted) of the bed and then again decreases a little in the top 3 or 4 cm of the bed. No significant lateral changes are shown by the graphs.

Stoss-Angle:

Data on this parameter when plotted (see fig. 13 through fig. 22) shows that the stoss-angle in most cases gradually increases up to about the middle or upper middle of a coset and then decreases. Laterally, a slow downcurrent decrease in the average values of β is noticeable in some beds. Behaviour of β closely follows that of amplitude.

Lee-Angle:

Graphs of this parameter (figs. 13 through 22) do not show any recognisable pattern in its behaviour laterally. Vertically, however, α has a tendency to increase gradually up to about the middle or upper middle of a coset, whereafter it decreases.

Grain Size:

Table VI lists the data of grain size analysis. It shows that almost all the ripple-drift cosets exhibit coarse-tail-grading both vertically and laterally. It also appears that the cosets are normally graded too; as in some cases normal grading can be identified megascopically from the colour changes from base (pale greenish brown) to top (greenish grey; due to an increase in clay content along with finer grains) of the cosets.

3.6. Relation Between Parameters

Coset Thickness vs. Angle of Climb:

Field observations revealed that the thicker cosets generally exhibit steeper angles of climb. A plot of coset thickness versus average measured-angle-of-climb of the collected data (Table V) is given in Fig. 23. It demonstrates that a fairly strong relationship exists between the two parameters.

Walker (1969, p. 385, Fig. 6) also demonstrated that angle of climb increases as coset thickness increases.

It was observed that in some of the thicker cosets (e.g. bed 477, see Pl. 15; bed 5, 7, 8, and 9 of Petite Vallée, see Pl. 1, 2, 24) the angle of climb gradually steepens upward through the coset. In con-

trast thinner cosets (e.g. beds of Fame Point, West, see Pl. 28) generally show a straight line pattern of the angle of climb.

Coset Thickness Vs. Grain Size:

Field observation suggested the possible existence of a relationship between coset thickness and grain size. Fig. 24A is a scatter diagram of the collected data (see Table VI). As the rocks are very fine grained (mostly medium to fine silt), the mean size of the 10 largest grains has been used for plot purposes. Good, significant correlations are shown in both the graphs.

Angle of Climb Vs. t_L/t_S:

An examination of fig. 25A, B reveals that the angle of climb tends to increase as t_L/t_S decreases. Fig. 25A shows a scatter plot of t_L/t_S vs. ϵ' (i.e. computed angle of climb) and illustrates the expected relationship between the two parameters related by equation [1] (Walker, 1969).

After a careful examination of the collected data, it was found that the 'position within bed' of 158 readings of the 'measured angle of climb' (out of a total of 306 readings, covering all the 49 beds) correspond closely to the 'position within bed' of 158 measured ripples (out of 523 in total). Fig. 25B shows a plot of t_L/t_S vs. ϵ of these 158 points.

FIG. 23.

Plot of Coset thickness vs. average Angle of Climb. The correlation coefficient is statistically significant.

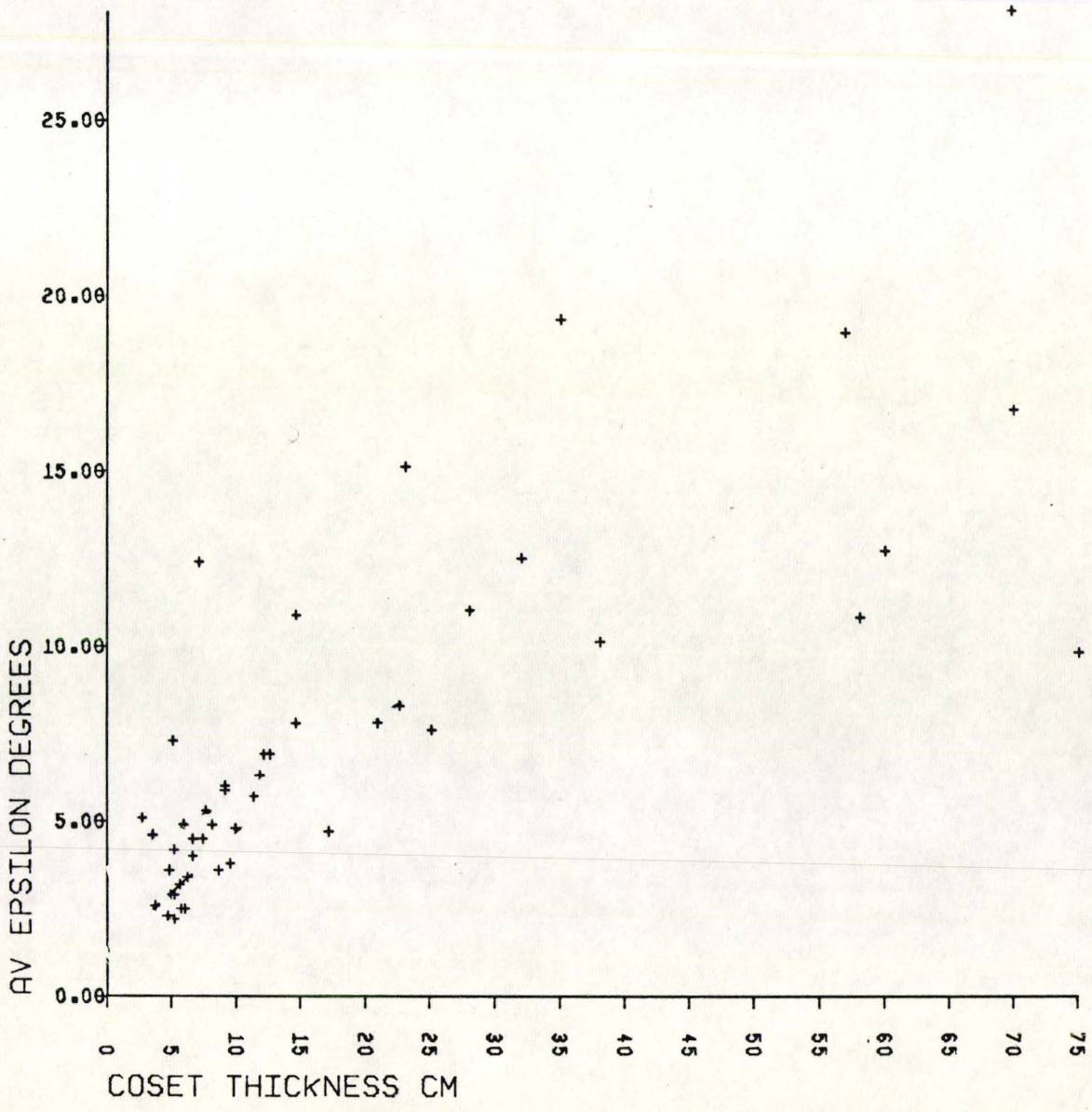
N = 47
r = .78
S
AV EPSILON DEGREES
25.00
20.00
15.00
10.00
5.00
0.00
0
5
10
15
20
25
30
35
40
45
50
55
60
65
70
75
COSET THICKNESS CM

FIG. 23

FIG. 24

A. Plot of Coset thickness vs. Maximum Grain Size.

The correlation coefficient is statistically significant.

B. Plot of average Angle of Climb vs. Maximum Grain Size.

The correlation coefficient is statistically significant.

A

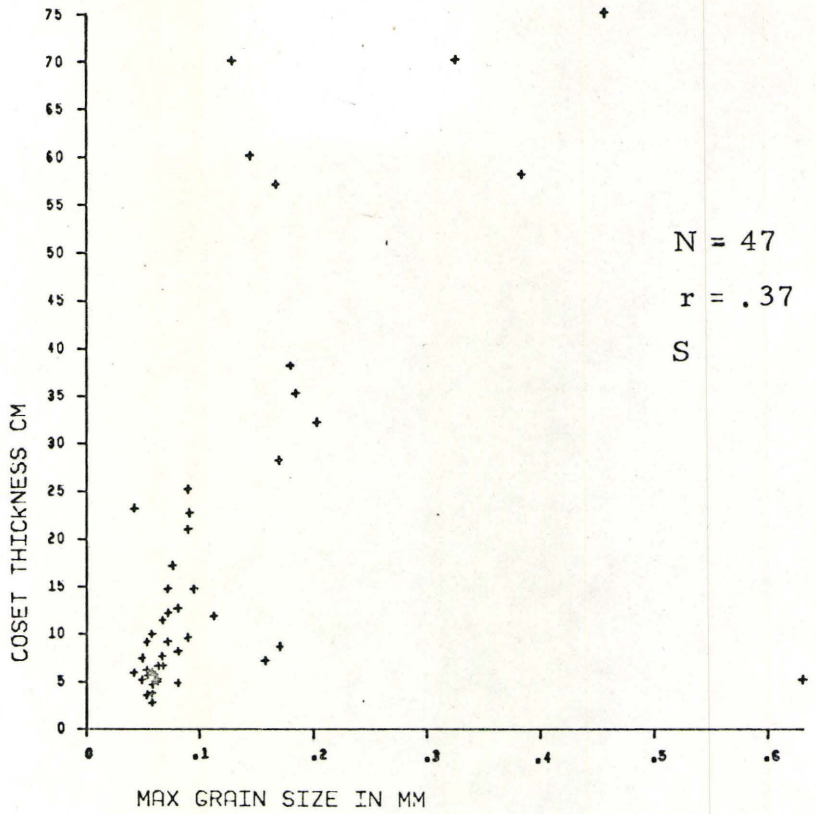
COSET THICKNESS CM
MAX GRAIN SIZE IN MM
N = 47
r = .37
S

B

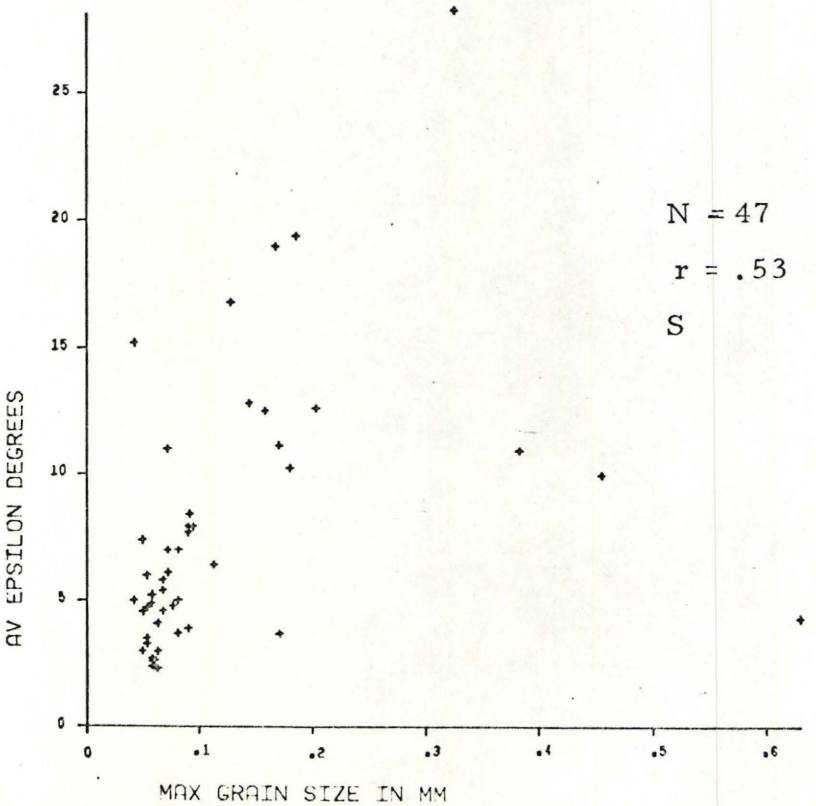
AV EPSILON DEGREES
MAX GRAIN SIZE IN MM
N = 47
r = .53
S

FIG. 25.

A. Plot of Computed Angle of Climb vs. t_L/t_S

The linear correlation coefficient, although significant, is inapplicable to these data.

B. Plot of Measured Angle of Climb vs. t_L/t_S

Correlation coefficient is not statistically significant.

A

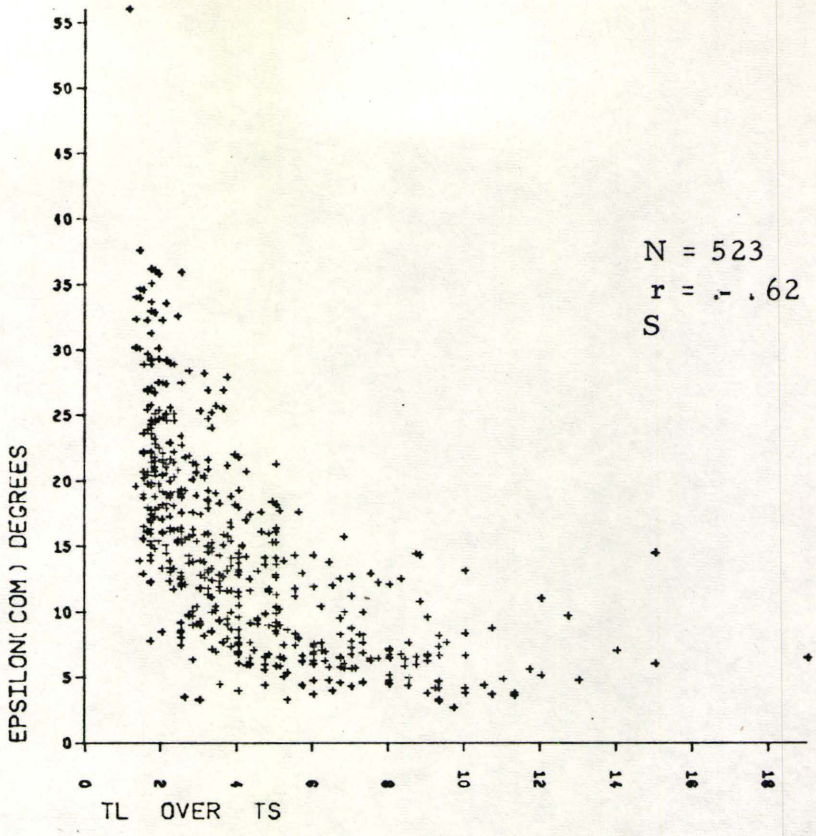
N = 523
r = - .62
S
EPSILON(COM) DEGREES
TL OVER TS

B

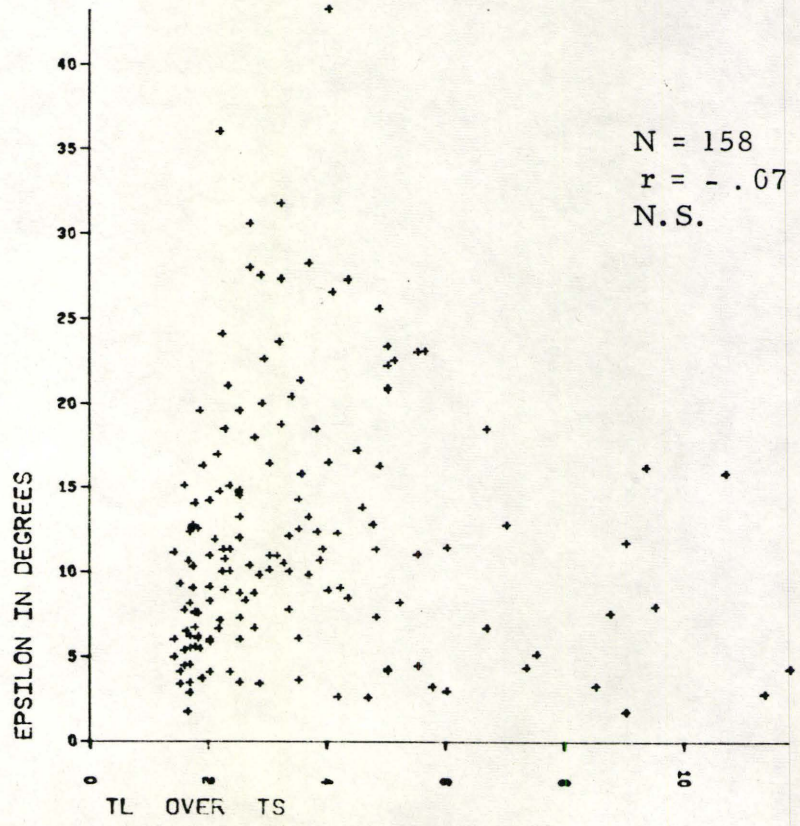
N = 158
r = - .07
N.S.
EPSILON IN DEGREES
TL OVER TS

FIG. 25

FIG. 26.

A. Plot of Computed Angle of Climb vs. Wave length. The correlation coefficient is not statistically significant.

B. Plot of Measured Angle of Climb vs. Wave length. The correlation coefficient is statistically significant.

A

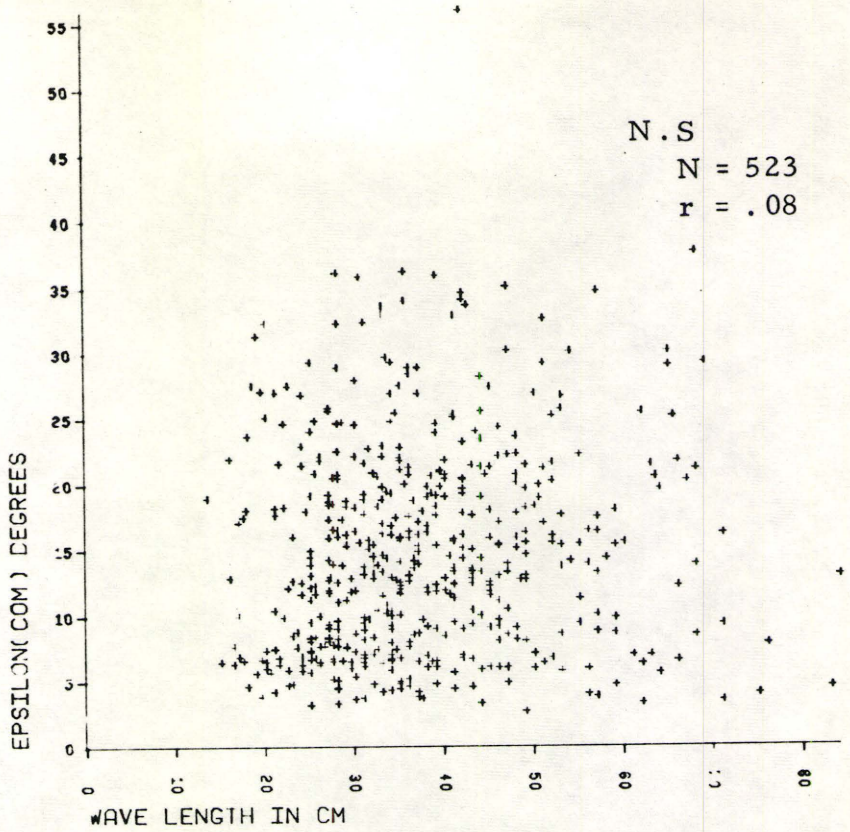
N.S
N = 523
r = .08
EPSILON(COM) DEGREES
WAVE LENGTH IN CM

B

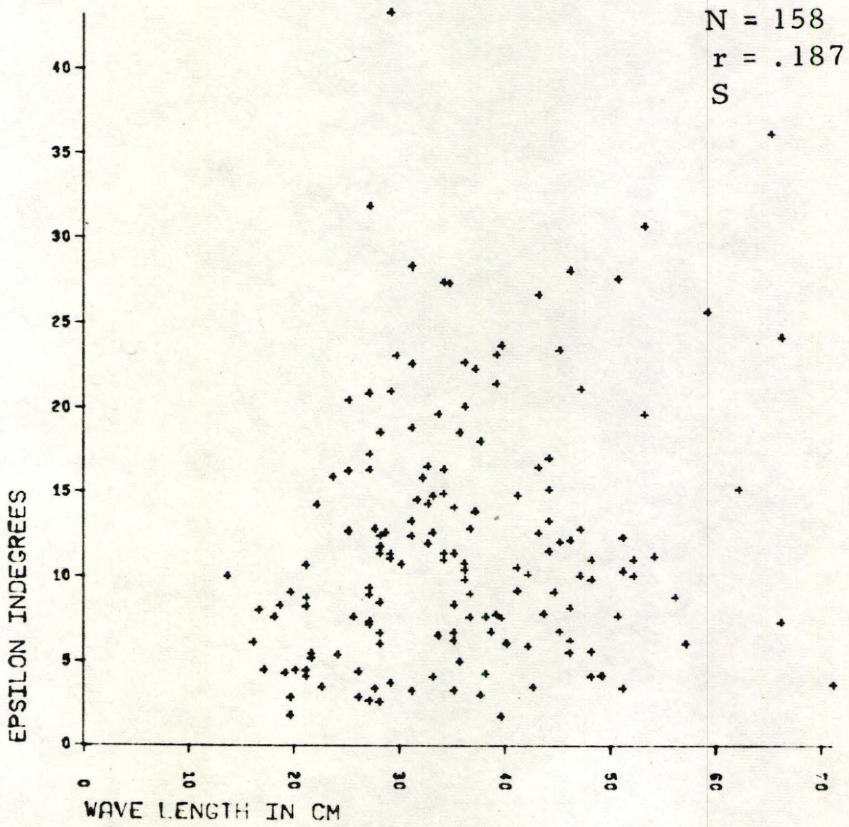
N = 158
r = .187
S
EPSILON INDEGREES
WAVE LENGTH IN CM

FIG. 26

FIG. 27.

A. Plot of Computed Angle of Climb vs. Amplitude.

The correlation coefficient is statistically significant.

B. Plot of Measured Angle of Climb vs. Amplitude.

The correlation coefficient is statistically significant.

A

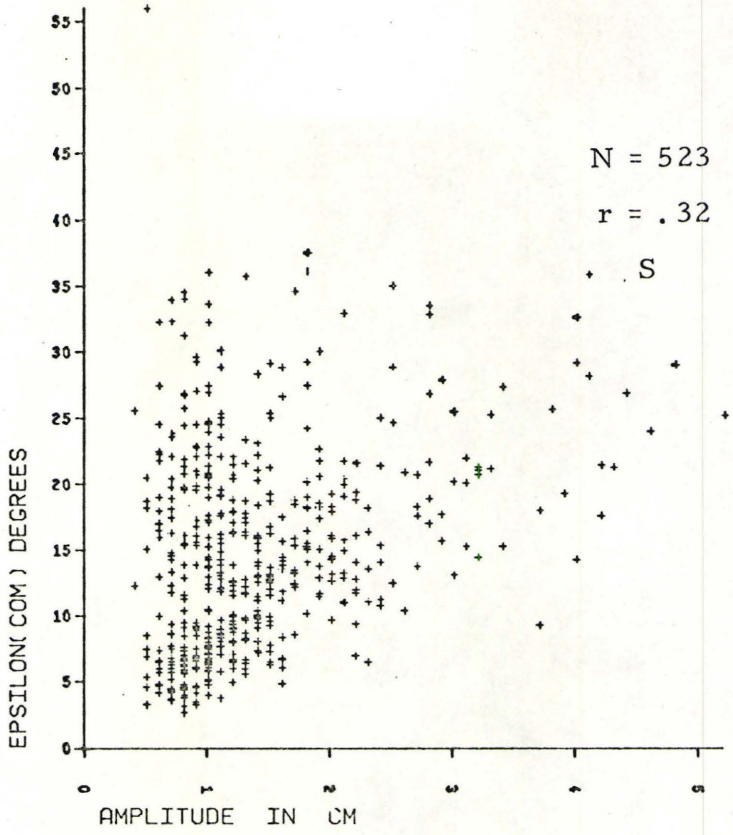
N = 523
r = .32
S
EPSILON(COM) DEGREES
AMPLITUDE IN CM

B

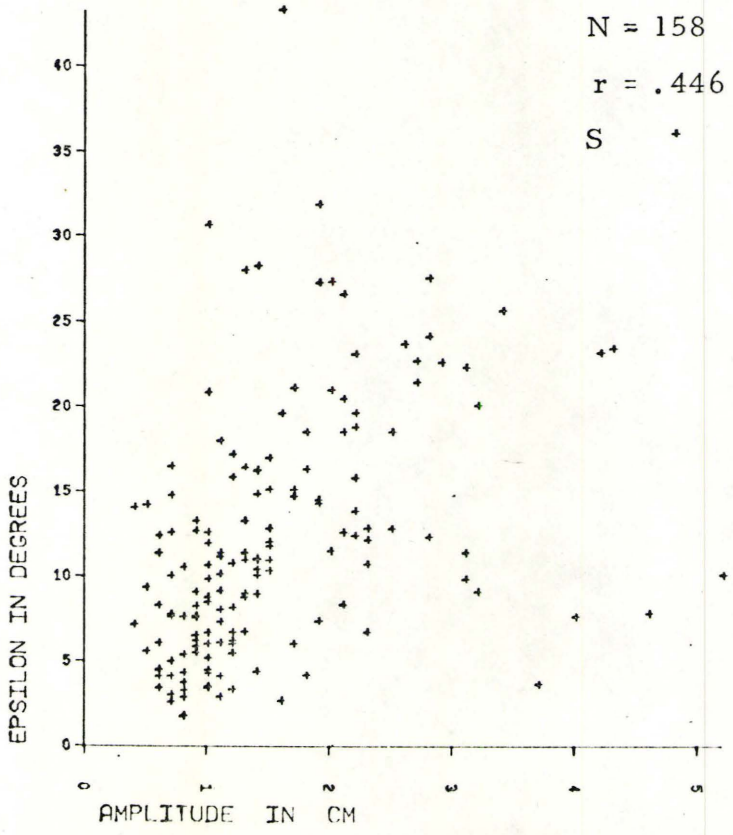
N = 158
r = .446
S
EPSILON IN DEGREES
AMPLITUDE IN CM

FIG. 27

FIG. 28.

A. Plot of Computed Angle of Climb vs. Stoss-angle.

The correlation coefficient is statistically significant.

B. Plot of Measured Angle of Climb vs. Stoss-angle.

The correlation coefficient is statistically significant.

A

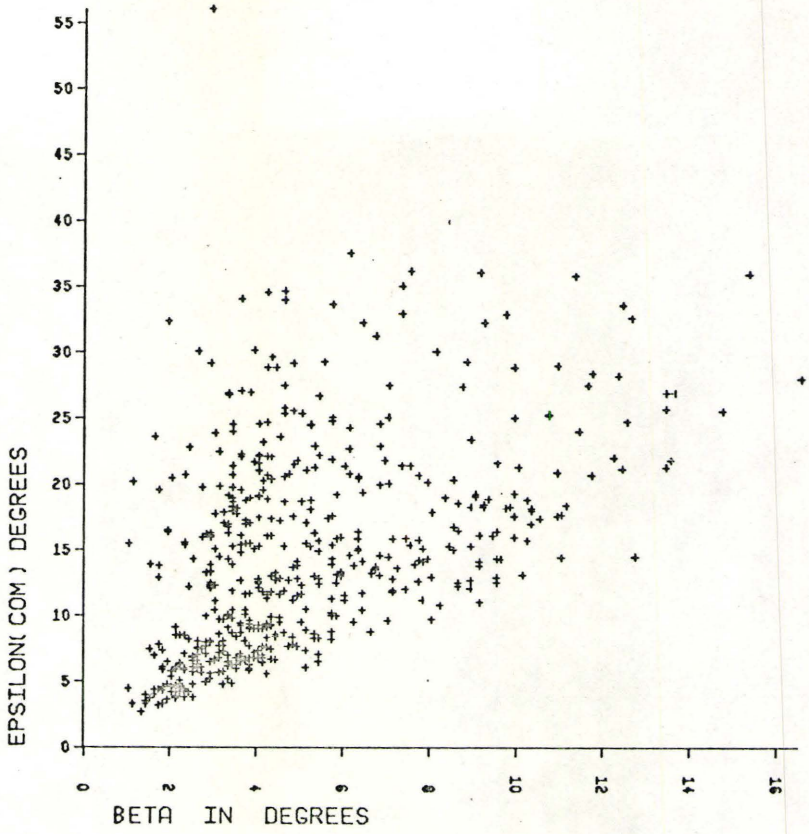

N = 523

r = .47

S

B

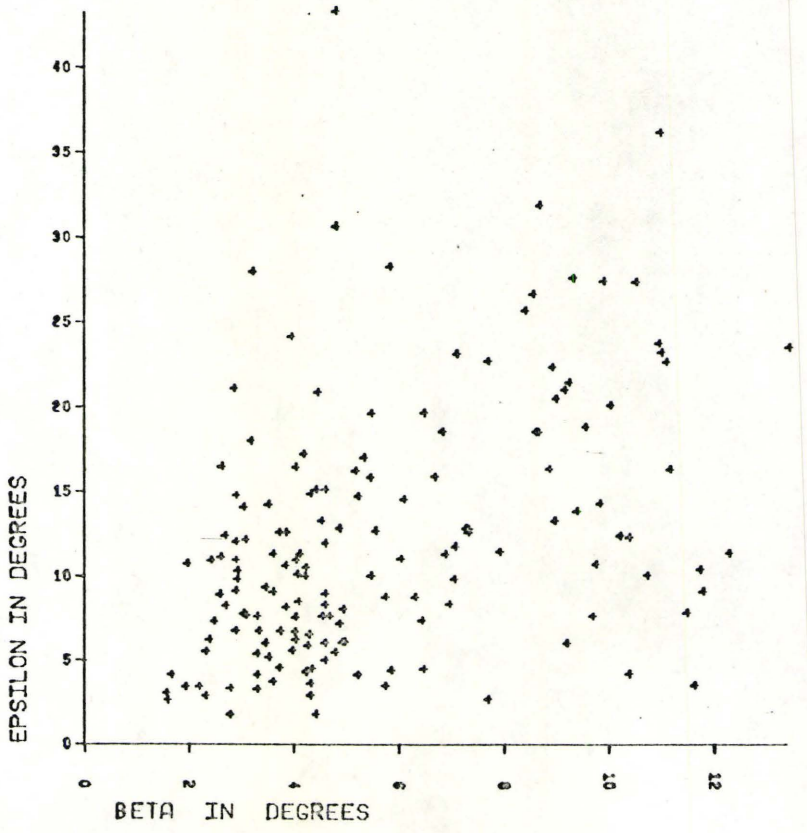

N = 158

r = .41

S

FIG. 28

FIG. 29.

A. Plot of Computed Angle of Climb vs. Lee-angle. The correlation coefficient is statistically significant.

B. Plot of Measured Angle of Climb vs. Lee-angle. The correlation coefficient is not statistically significant.

A

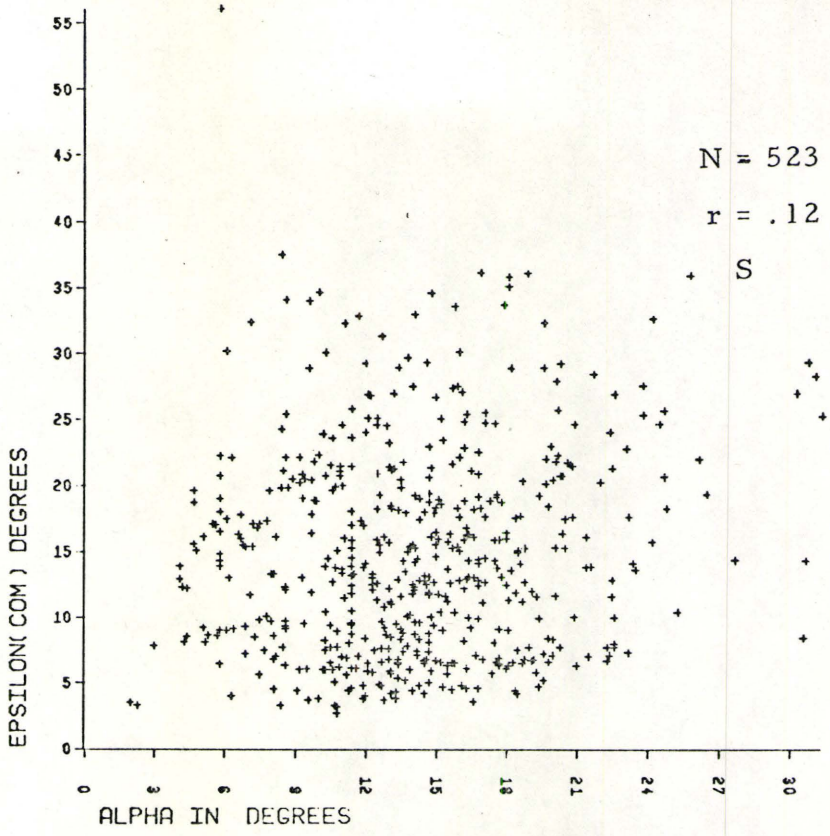
N = 523
r = .12
S
EPSILON(COM) DEGREES
ALPHA IN DEGREES

B

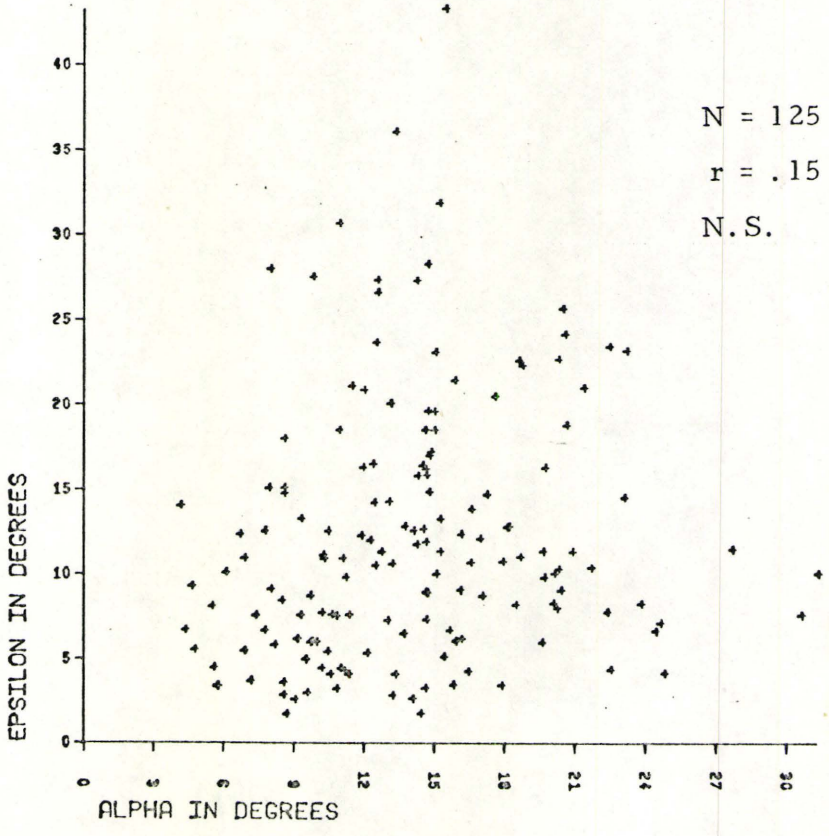
N = 125
r = .15
N.S.
EPSILON IN DEGREES
ALPHA IN DEGREES

FIG. 29

It, however, does not show up the relationship as nicely as it does in fig. 25A.

Angle of Climb Vs. β, α, A and W:

Plots of each of the parameters β, α, A and W versus both ϵ (measured) and ϵ'(computed) are given in figs. 26 through 29. Of them, β and A appear to be very sensitive (r values are significant even at 99.9%). Both β and A increase as ϵ increases. The parameters α and W did not correlate significantly with ϵ.

Angle of Climb Vs. Grain Size:

Mean size of ten largest grains (see Table VI) when plotted (see fig. 24B) against average values of the measured angle of climb shows that ϵ increases as maximum grain size increases.

t_L/t_S Vs. β, α, W and A:

Scatter diagrams (see figs. 30 and 31) obtained from plots of the parameters β, α, W and A versus t_L/t_S reveal that good relationship exists between t_L/t_S and W, and t_L/t_S and α.

β Vs. α, W and A:

A plot of β vs. A (see fig. 33B) shows a strong linear relationship. Good correspondence also exists between β and α (see fig. 32B), but apparently no relationship exists between β and W(see fig. 32A).

FIG. 30.

A. Plot of t_L/t_S vs. Wave length.

The correlation coefficient is statistically significant.

B. Plot of t_L/t_S vs. Amplitude.

The correlation coefficient is not statistically significant.

A

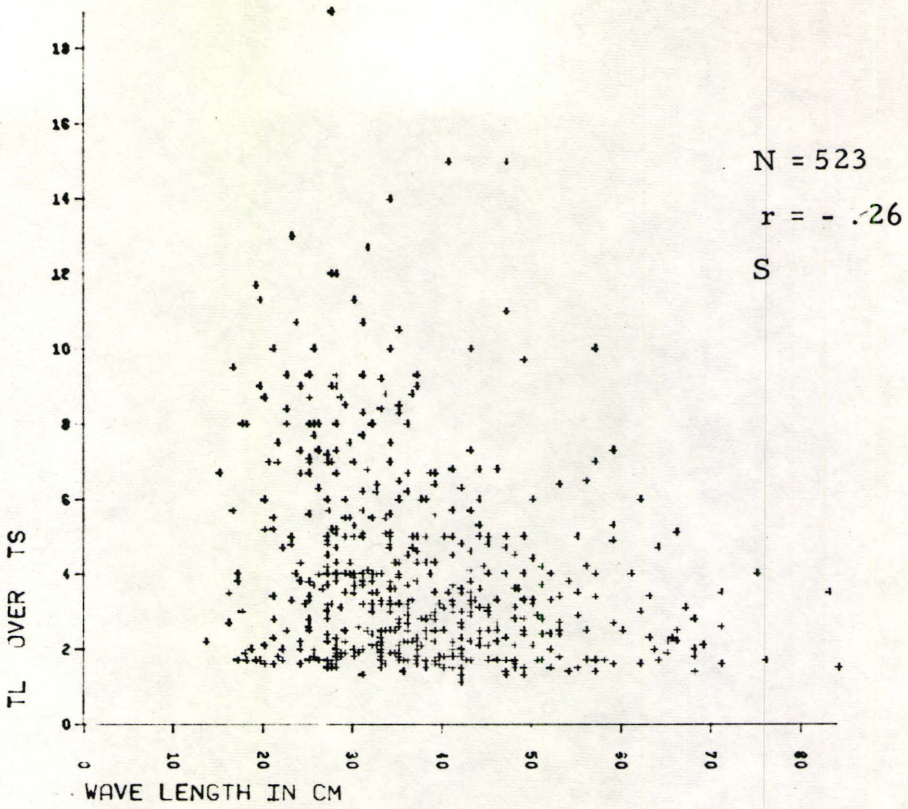
N = 523
r = - .26
S
TL OVER TS
WAVE LENGTH IN CM

B

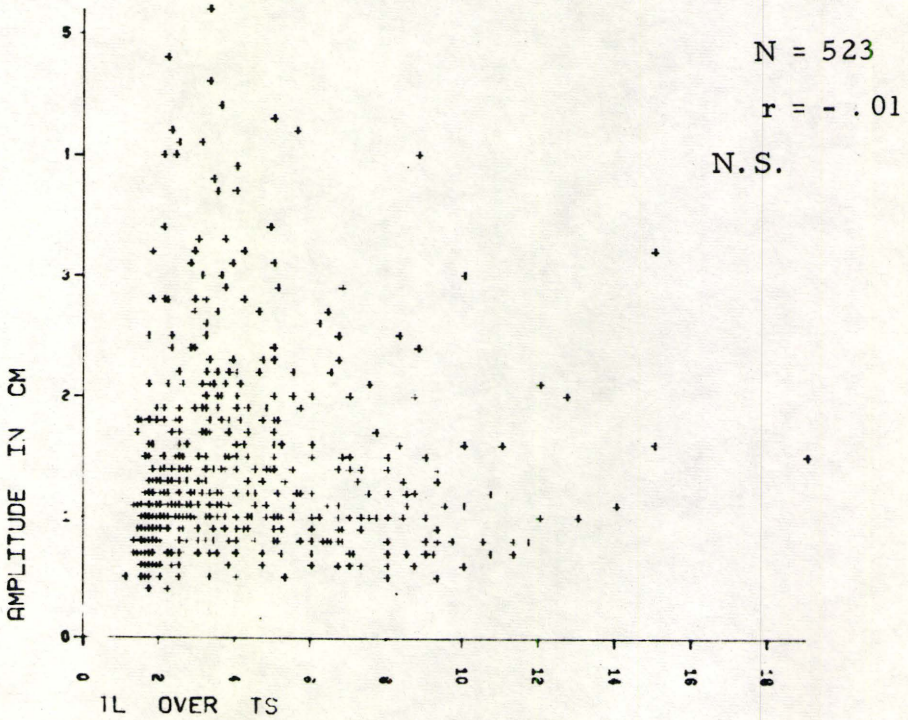
N = 523
r = - .01
N.S.
AMPLITUDE IN CM
TL OVER TS

FIG. 30

FIG. 31.

A. Plot of t_L/t_S vs. Stoss-angle. The correlation coefficient is not statistically significant.

B. Plot of t_L/t_S vs. Lee-angle. The correlation coefficient is statistically significant.

A

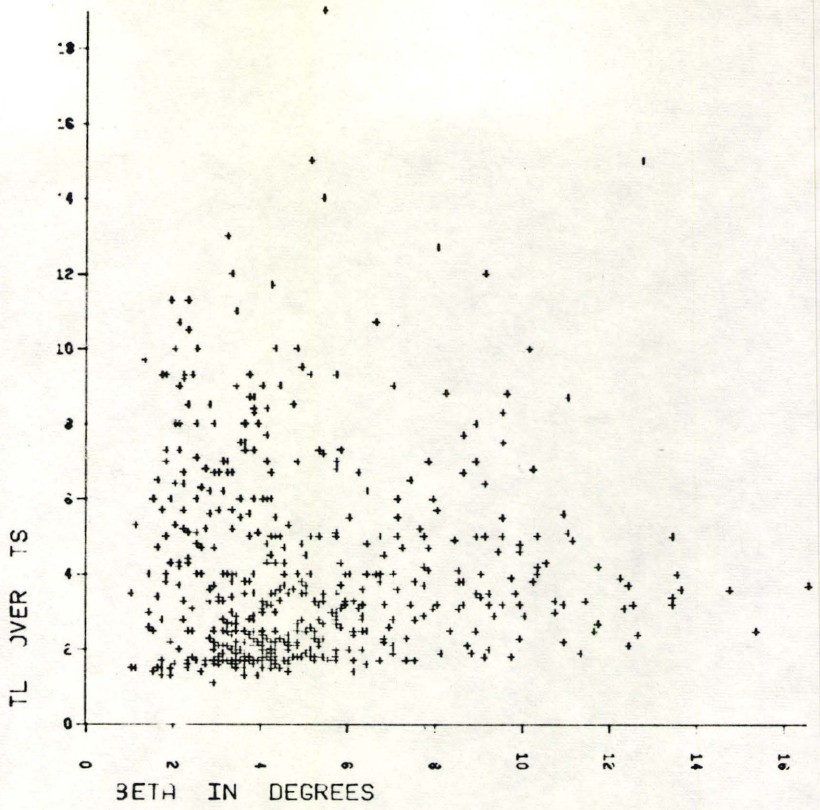

N = 523

r = - .001

N.S.

B

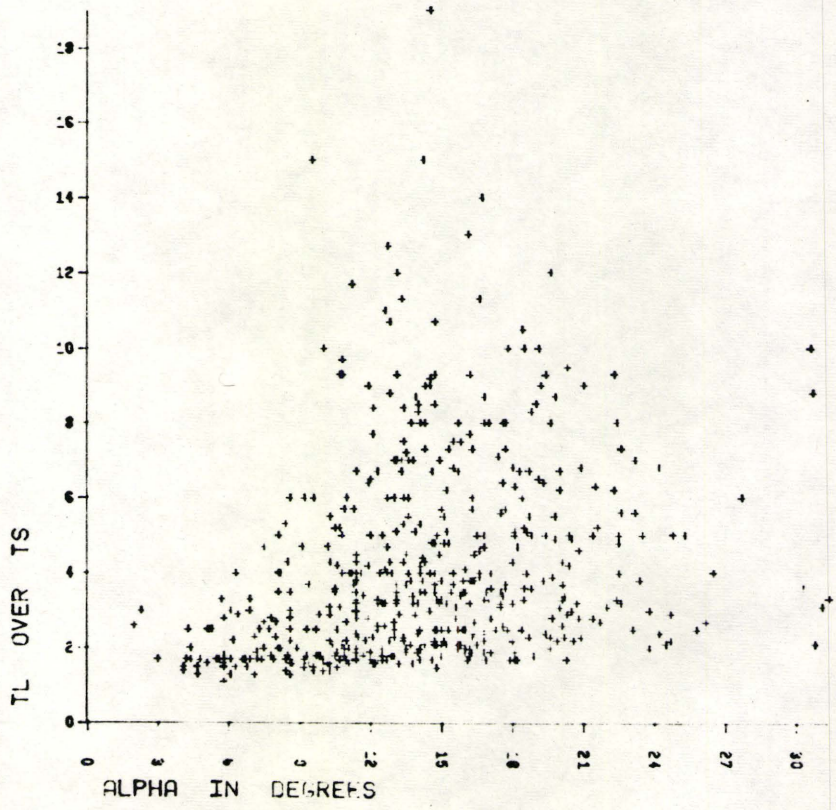

N = 523

r = .28

S

FIG. 31

FIG. 32.

A. Plot of Stoss-angle vs. Wave Length. The correlation coefficient is not statistically significant.

B. Plot of Stoss-angle vs. Lee-angle. The correlation coefficient is statistically significant.

A

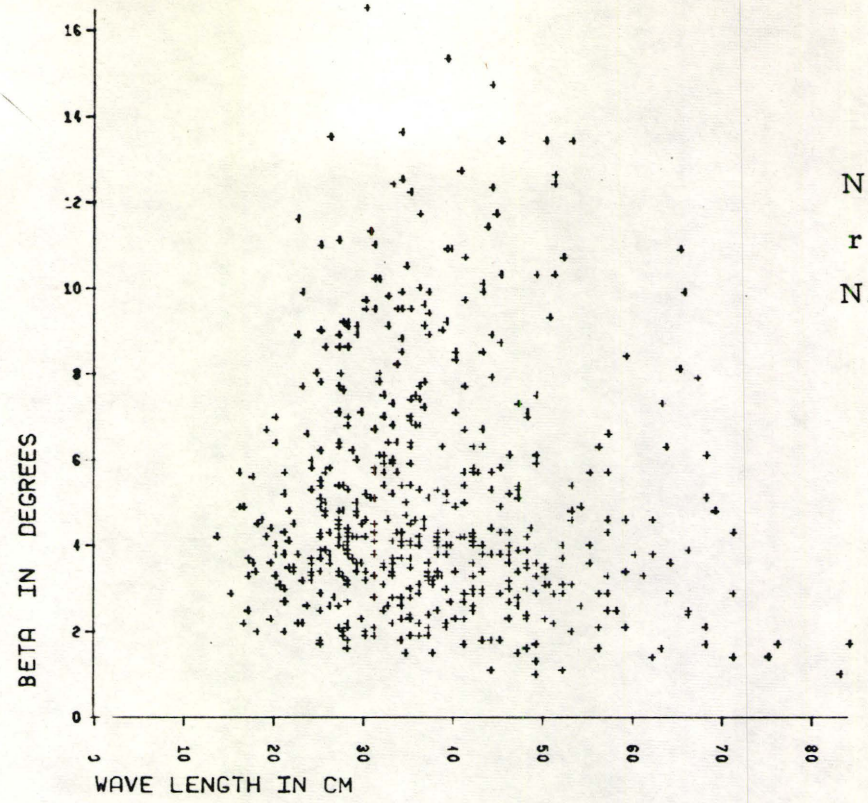

N = 523

r = - .07

N.S.

B

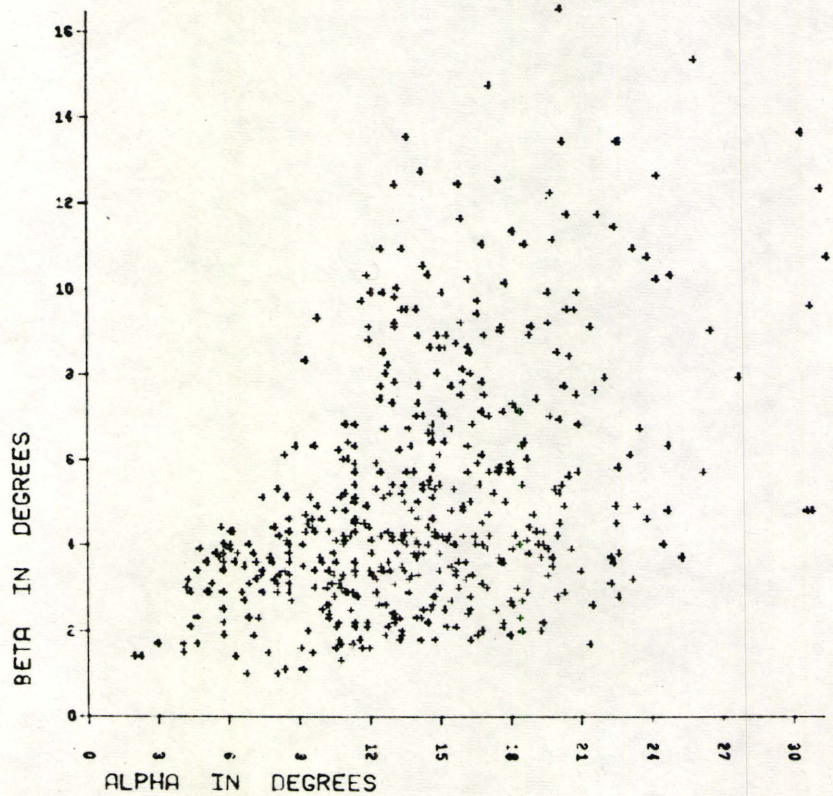

N = 523

r = .24

S

FIG. 32

FIG. 33.

A. Plot of Lee-angle vs. Wave Length. The correlation coefficient is statistically significant.

B. Plot of Stoss-angle vs. Amplitude. The correlation coefficient is statistically significant.

A

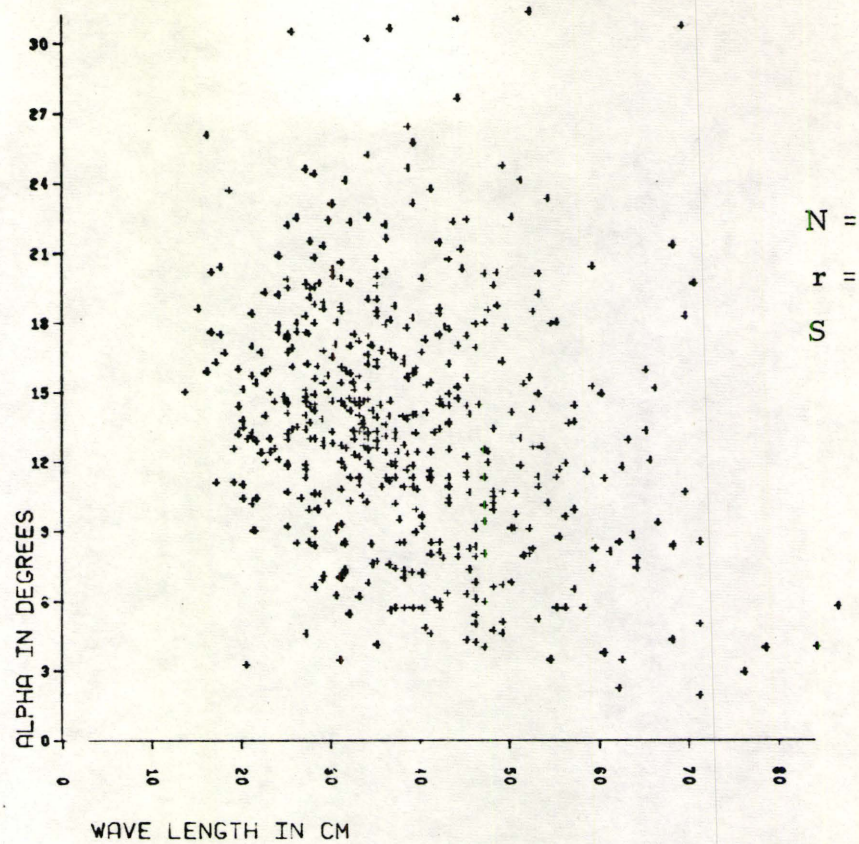
ALPHA IN DEGREES
WAVE LENGTH IN CM
N = 523
r = - .24
S

B

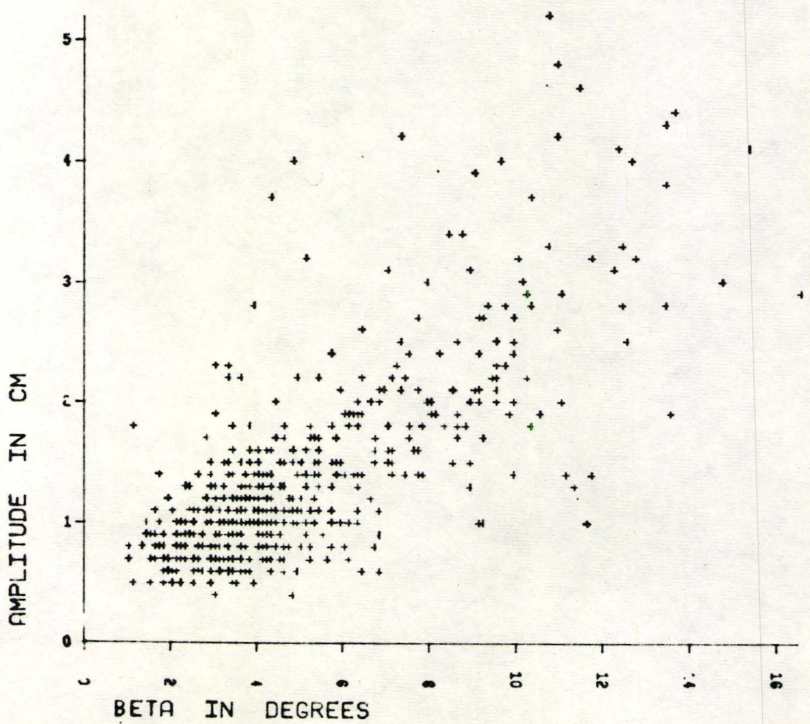
AMPLITUDE IN CM
BETA IN DEGREES
N = 523
r = .75
S

FIG. 33

FIG. 34.

A. Plot of Amplitude vs. Lee-angle. The correlation coefficient is statistically significant.

B. Plot of Amplitude vs. Wave Length. The correlation coefficient is statistically significant.

A

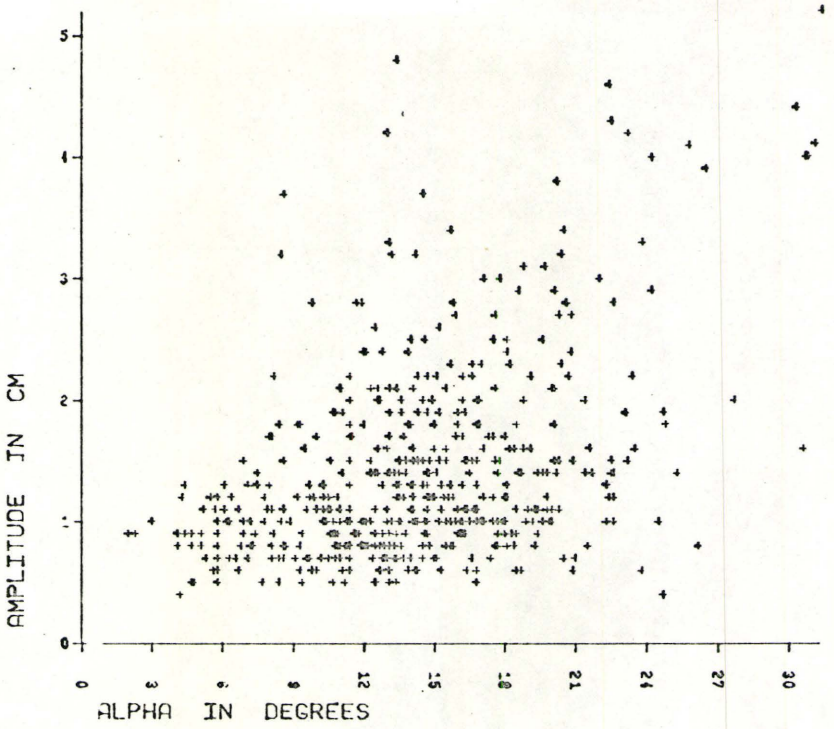

N = 523

r = .44

S

B

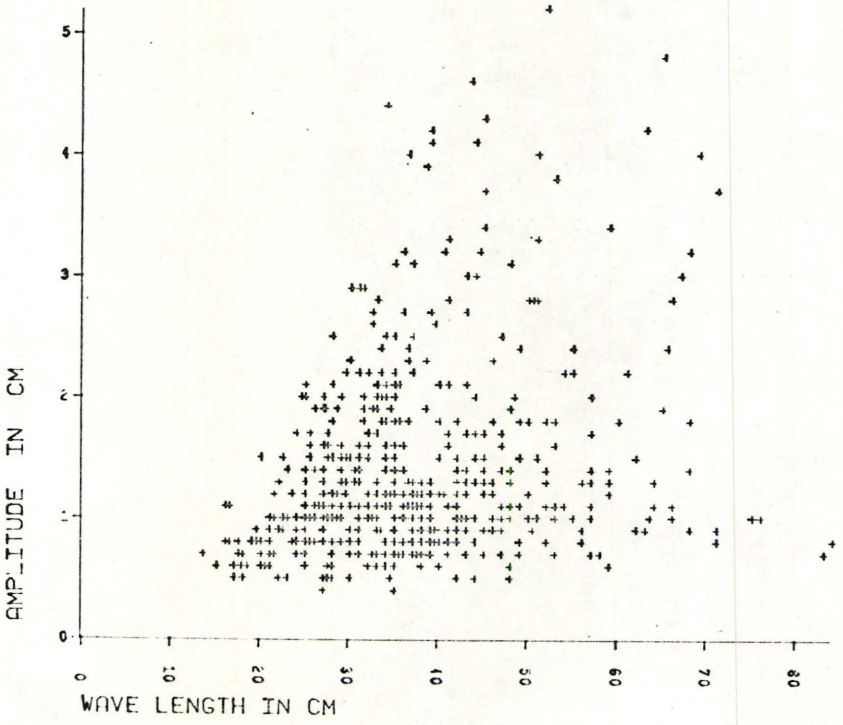

N = 523

r = .25

S

FIG. 34

α Vs. W and A:

It seems (see fig. 33A and fig. 34A) that α correlates significantly to both W and A.

W Vs. A:

The scatter diagram (fig. 34B) apparently shows a positive linear relationship between the two parameters. The low r value and the wide scatter, points to the fact that the relationship is subject to considerable variability.

Grain Size Vs. W, A and RI:

The values of wave length measurements (see Table VII) taken from near the base and top of the cosets at a particular station are plotted (fig. 35) against the corresponding values of the mean size of ten largest grains obtained from samples collected from near the base and the top of the cosets at the respective stations. Fig. 36A, B are plots of maximum grain size (i. e. mean of ten largest grains) versus amplitude and ripple index respectively.

The relation between (i) maximum grain size and A and (ii) maximum grain size and RI are barely, statistically significant at the 95% level, and that between (iii) maximum grain size and W is not statistically significant. However, fig. 36B clearly shows that RI becomes smaller as maximum grain size increases. In non-

turbidite ripples (Reineck and Wunderlich, 1968, fig. 5, p. 329) it has been demonstrated that the RI becomes smaller as mean grain size increases. Fig. 37 shows the frequency distribution of ripple index and ripple symmetry index in the Cloridorme turbidites.

TABLE VII

Data on grain-size corresponding to wave length, amplitude and ripple-index

TABLE VII

LOCATION	Bed Number	Bed Thickness in Centimeters A - B - C	NEAR THE BASE OF THE COSET: Wave Length in cm.	Amplitude in cm.	Ripple Index	Grain size in mm (Mean Size of Ten Largest Grains)	NEAR THE TOP OF THE COSET: Wave Length in cm.	Amplitude in cm.	Ripple Index	Grain Size in mm. (Mean Size of Ten Largest Grains)	Station Locations on the Bed.
St. Maurice (North of Church)	477	0 8 70	36.5	2.4	15.21	0.14	53.0	3.8	13.95	0.05	300'
			57.0	2.0	28.50	0.16	43.0	2.7	15.93	0.07	600'
			27.2	1.9	14.32	0.15	32.0	1.7	18.82	0.08	900'
West of Fame Point	666	0 0 11.2	25.5	1.0	25.50	0.07	34.0	1.6	21.25	0.04	-
	700	0 0 9.4	25.0	1.3	19.23	0.09	37.0	0.8	46.25	0.07	-
	701	0 0 7.5	31.0	1.3	23.85	0.07	38.0	0.9	42.22	0.04	-
	702	0 0 14.5	20.0	0.6	33.33	0.07	35.0	0.6	58.33	0.07	-
	759	0 0 6.5	20.0	0.8	25.00	0.07	34.0	0.6	56.67	0.05	-
	765	0 0 8.0	25.0	1.2	20.83	0.08	44.0	0.8	55.00	0.07	-
	772	0 0 5.9	24.0	0.7	34.29	0.06	42.0	0.8	52.50	0.04	-
	773	0 0 4.8	31.0	0.7	44.29	0.06	56.0	0.8	70.00	0.04	-
	774	0 0 5.1	24.0	0.9	26.67	0.05	42.0	1.0	42.00	0.04	-
	790	0 0 9.8	35.0	0.8	43.75	0.06	59.0	0.6	98.33	0.04	-
	791	0 0 14.5	28.0	0.8	35.00	0.09	43.0	1.2	35.83	0.07	-
	793	0 0 12.5	30.0	0.7	42.86	0.08	37.0	0.9	41.11	0.06	-
	794	0 0 8.5	26.0	1.0	26.00	0.17	49.0	0.8	61.25	0.08	-
	795	0 0 11.7	29.0	1.1	26.36	0.11	50.0	1.0	50.00	0.04	-
	798	0 0 9.0	26.0	1.0	26.00	0.07	35.0	0.7	50.00	0.06	-
	799	0 0 6.5	20.0	0.6	34.17	0.06	38.0	0.9	42.22	0.06	-
	800	0 0 5.5	23.0	1.0	23.00	0.05	39.0	0.8	48.75	0.04	-
	801	0 0 7.3	41.0	0.8	51.25	0.05	66.0	1.0	66.00	0.04	-
	899	0 0 23.0	30.0	0.7	42.86	0.04	35.0	1.4	25.00	0.04	-
	1013	0 0 5.8	23.0	0.5	46.00	0.04	36.0	0.8	45.00	0.08	-
	1014	0 0 2.6	30.0	0.5	60.00	0.06	34.0	0.7	48.57	0.04	-
	1015	0 0 4.7	27.0	0.9	30.00	0.08	41.0	0.8	51.25	0.06	-
	1021	0 0 5.0	17.0	0.5	34.00	0.05	25.0	0.6	41.67	0.04	-
	1030	0 0 5.6	16.0	0.8	20.63	0.06	32.0	0.6	53.33	0.04	-
	1031	0 0 6.1	15.0	0.6	25.00	0.05	33.0	0.7	47.14	0.04	-
	1033	0 0 9.0	17.0	0.6	28.33	0.05	47.0	0.7	67.14	0.04	-
	1034	0 0 5.1	18.0	0.5	36.00	0.06	28.0	0.5	56.00	0.05	-
	1035	0 0 4.6	25.0	0.8	31.25	0.06	34.0	0.8	42.00	0.05	-
	1036	0 0 3.6	26.0	0.8	32.50	0.06	44.0	0.5	88.00	0.05	-
	1038	0 0 5.1	22.5	1.0	22.50	0.63	38.0	0.8	47.50	0.11	-
Petite Valée Harbour, East.	1	0 0 32.0	16.5	1.1	15.00	0.20	34.5	0.5	69.00	0.16	-
	2	0 0 57.0	28.0	1.0	28.00	0.17	48.0	1.1	43.64	0.15	-
	3	0 0 35.0	34.0	1.1	30.91	0.18	54.0	2.2	24.55	0.15	-
	4	0 0 7.0	19.0	0.8	23.75	0.16	25.0	1.1	22.73	0.14	-
	5	0 0 38.0	32.0	1.1	29.09	0.08	71.0	0.9	78.89	0.06	48'
			56.0	0.8	70.00	0.18	71.0	0.8	88.75	0.04	322'
	6	0 0 3.4	21.0	0.9	23.33	0.05	43.0	0.9	47.78	0.05	-
	7	52 2 22.5	30.0	1.1	27.27	0.08	39.0	1.3	30.00	0.04	49'
			22.0	0.5	44.00	0.09	30.0	1.3	23.46	0.06	320'
	8	0 5 20.8	17.8	0.6	29.67	0.09	24.0	1.0	24.00	0.03	-
	9	0 0 60.0	42.0	1.0	42.00	0.10	47.0	1.0	47.00	0.08	0'D
			28.0	1.2	23.33	0.14	31.0	1.4	22.14	0.17	246'
	10	0 0 28.0	24.0	1.0	24.00	0.17	83.0	0.7	118.57	0.08	0'U
			36.0	1.0	36.00	0.07	49.0	1.5	32.67	0.07	250'
East of Anse à Mercier Grande Vallée	1	0 2 25.0	28.0	1.0	28.00	0.09	50.0	1.2	41.67	0.08	-
	2	0 5 12.0	20.0	0.7	28.57	0.07	40.0	0.8	50.00	0.05	-
	3	0 0 17.0	31.8	0.8	38.75	0.08	52.0	0.8	65.00	0.07	-
Anse à Mercier West, Grande Vallée	4	8 2 70.0	27.0	1.2	22.50	0.32	35.0	1.8	19.44	0.29	-
	5	0 0 58.0	27.0	1.4	19.29	0.38	68.0	3.2	21.25	0.36	-
	6	0 0 75.0	27.0	1.9	14.21	0.45	69.0	4.0	17.25	0.09	-

FIG. 35.

Plot of Wave Length vs. Maximum Grain Size

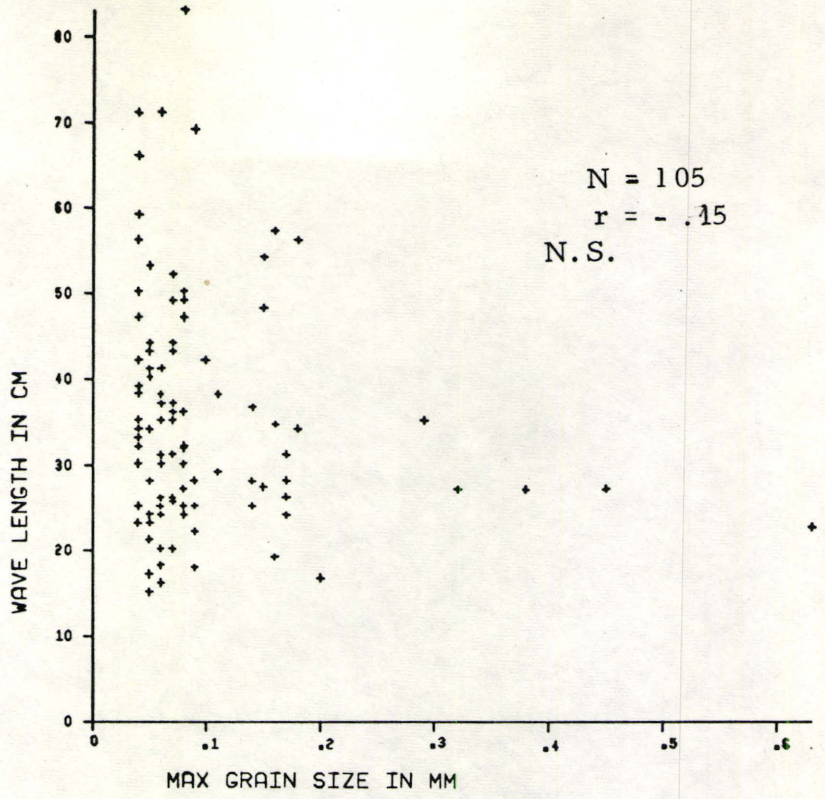
N = 105
r = - .15
N.S.
WAVE LENGTH IN CM
MAX GRAIN SIZE IN MM
0
10
20
30
40
50
60
70
80
.1
.2
.3
.4
.5
.6

FIG. 35

FIG. 36.

A. Plot of Amplitude vs. Maximum Grain Size

B. Plot of Ripple-index vs. Maximum Grain Size

A

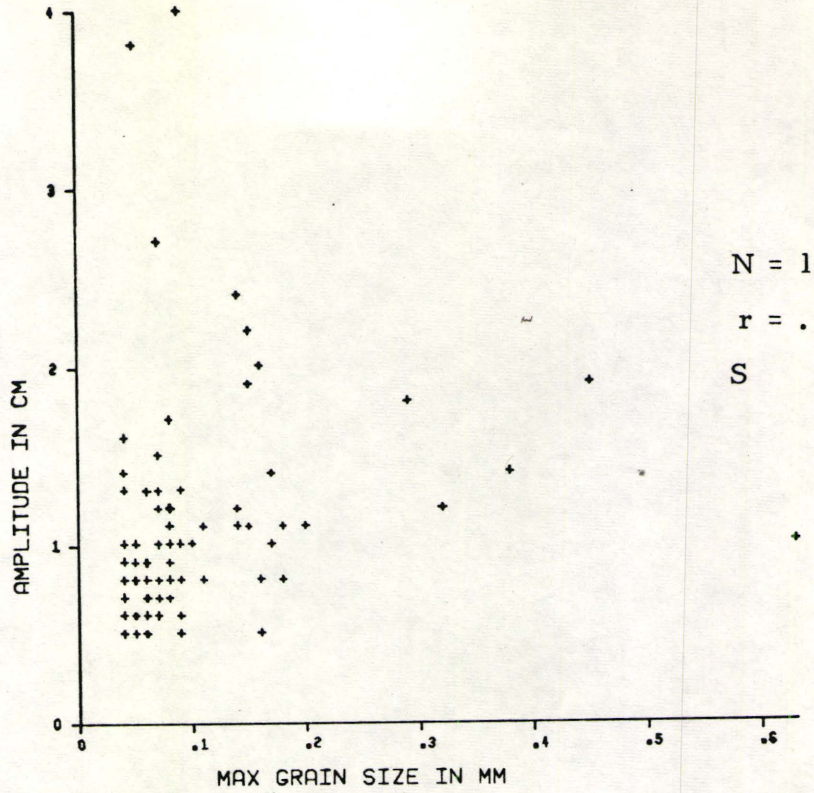

N = 105

r = .22

S

B

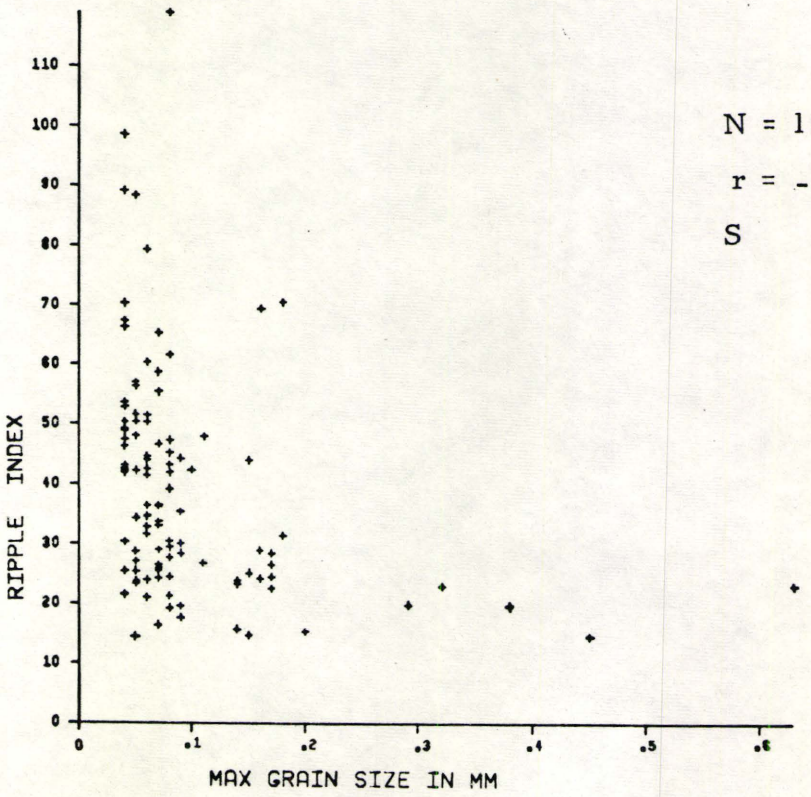

N = 105

r = - .32

S

FIG. 36

FIG. 37

A. Frequency distribution of Ripple-index

B. Frequency distribution of Ripple-symmetry-index

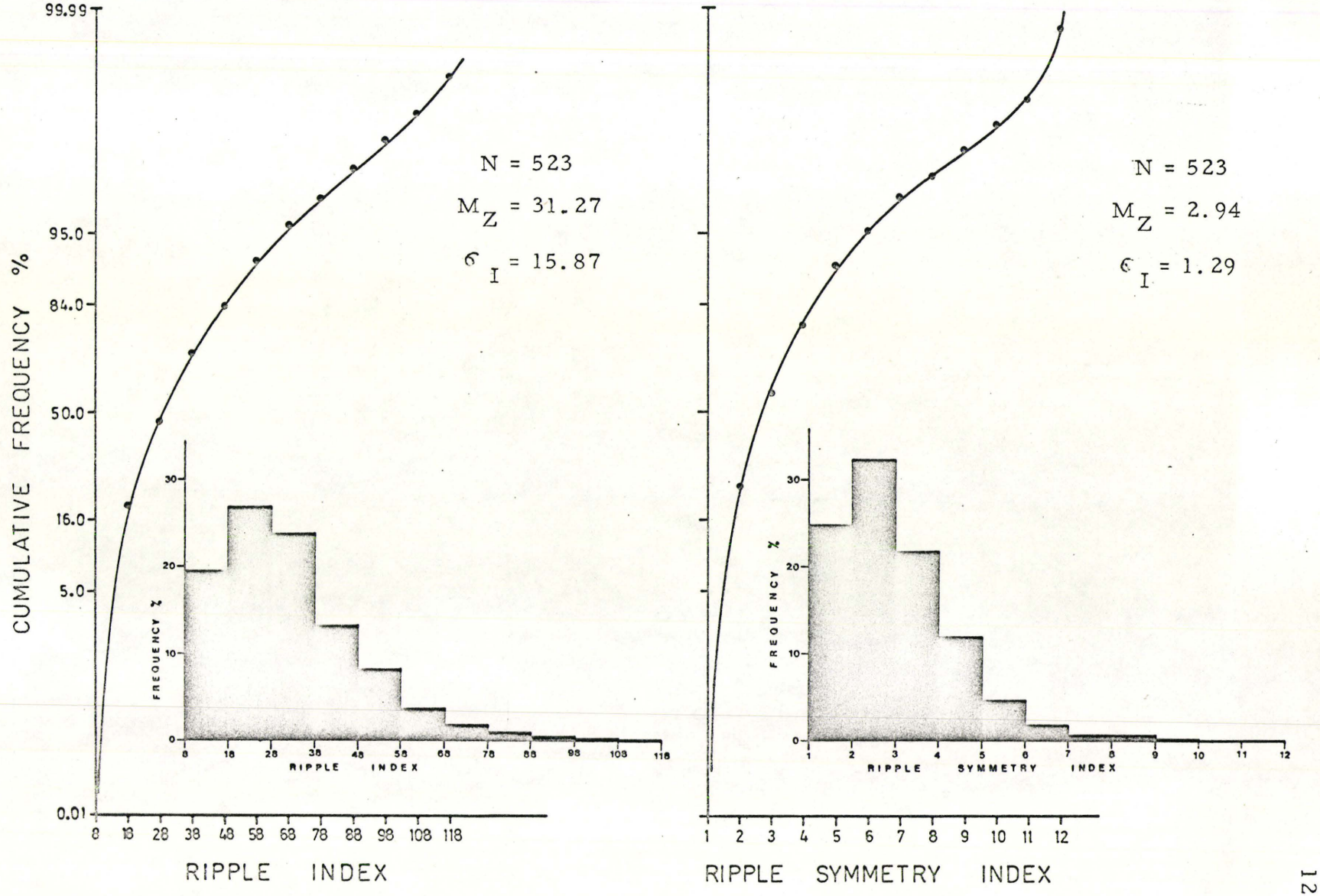
99.99
95.0
84.0
50.0
16.0
5.0
0.01
CUMULATIVE FREQUENCY %
N = 523
M_Z = 31.27
σ_I = 15.87
FREQUENCY %
RIPPLE INDEX
8 18 28 38 48 58 68 78 88 98 108 118
RIPPLE INDEX
A
N = 523
M_Z = 2.94
σ_I = 1.29
FREQUENCY %
RIPPLE SYMMETRY INDEX
1 2 3 4 5 6 7 8 9 10 11 12
RIPPLE SYMMETRY INDEX
B

FIG. 37

CHAPTER FOUR. DISCUSSION AND SUMMARY

4.1. Vertical Variation of Parameters, Sequence of Ripple Shapes and the Phenomenon of Overtaking

The problem of the first appearance of ripples in a system of either increasing or decreasing flow power is still unknown and reasons for ripples becoming more irregular with time, even without a further increase in the existing shear stress, is still unknown (Briggs and Middleton, 1965, p. 15). Similarly, the reasons for changes in the regularity of ripple-formed cross-lamination with time are also unknown.

Walker (1963, 1969) has implied that there is a certain regularity in the shape of ripple-drift laminae and attempted to explain this. In 1965 he suggested (Walker, 1965, p. 15) that "After the initial formation of a rippled surface (perhaps under condition of a clear bed current interface), sedimentation continues but the current velocity is such that the sand grains falling on the stoss-side can not be moved by the current once deposited. Mud, however, is winnowed on to the lee-side and deposited on to the trough. The winnowing probably takes

place in the laminar boundary layer. The result is a set of climbing ripples (Type-3, Walker, 1963, p. 177) whose amplitude gradually decreases upward until the lamination is horizontal. Much of this rippling probably occurs at shear velocities less than those required for the initiation of ripples, and merely represents the fall out of sediment on to a rippled surface under the influence of a gentle forward current".

However, the field data collected by the author does not support Walker's (1965) observation that amplitude and stoss-angle gradually decrease upward through a coset. In fact, in the Cloridorme ripple-drift a common observation is that the amplitude, the stoss-angle, the lee-angle and the angle of climb, all increase gradually up to about 1/2 or 3/4 the thickness of a coset and then decrease until the bed is levelled. However, Pl. 40 and many others do support the assumed process of mud winnowing.

Figs. 13, 15, 17, 19 and 21 show that the parameters A, β, α and ϵ show a general tendency to increase gradually from the base upward through a coset to about 1/2 or 3/4 the thickness of the coset; W continues to increase up to the top and t_L/t_S gradually decreases upward through a coset. Two other important features to be noted here are (i) the overtaking of ripples that results in the merging of climbing bands, as has been observed in bed 477 of St. Maurice and beds 5 and 7 of Petite

PLATE 40.

Increase in mud in the trough up through a coset, bed 2, Petite Vallée.

FIG. 38. Diagram showing vertical variation of parameters, sequence of ripple-shapes and conditions just prior to overtaking. Details explained in the text.

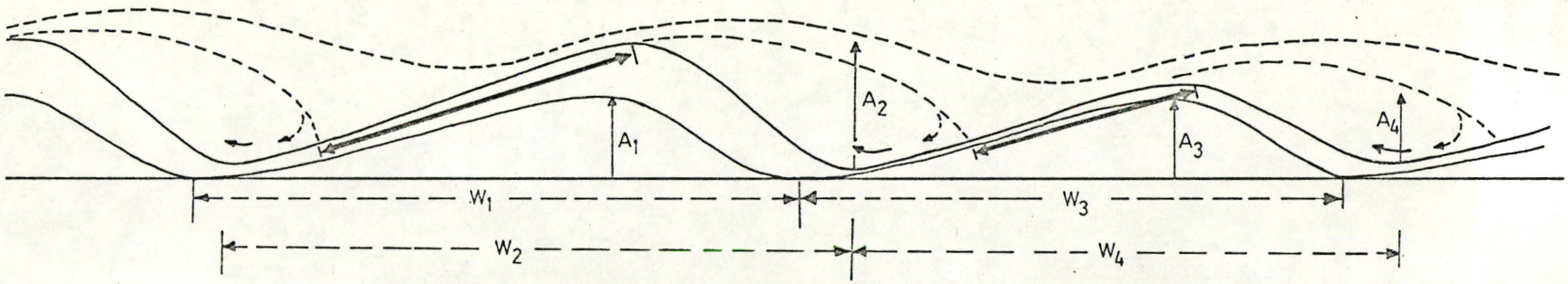

FIG. 38

Vallée, and (ii) change in ripple shapes upward through a coset (see fig. 10). An attempt has been made below to visualize the possible mechanism that can correlate all these observations.

In fig. 38 the ripple lamina defined by A_1W_1 and A_2W_2 shows the most commonly observed shape of a lamina sitting in a band of climbing ripples in the middle or upper middle part of a coset. The lamina illustrates the following features: (i) upward increase in W, A, β, α and ϵ, (ii) lamina thickest near the crest and (iii) t_L/t_S value approximately 2.

For a bed deposited from a decelerating overloaded suspension current, it is assumed that (i) flow strength decreases upward through a coset, (ii) deposition from a suspension current imparts grading characteristics (upward fining of sediment), (iii) clay concentration increases towards the top of a coset, causing an increase in cohesiveness (upward) of the deposited sediment, and (iv) gradual increase in the suspension/traction ratio upward through a coset. The term "suspension/traction ratio" is here taken to imply the Rate of transfer of suspended load to bed load/Rate of transport of bed load.

Figs. 26-29 and 32-35 indicate that in most cases a significant direct positive relationship exists between the parameters W, A, β, α and ϵ. However, figs. 25, 30 and 31 confirm that t_L/t_S is inversely related to these other parameters.

At the bottom of a coset the angle of climb, ϵ has been observed to be generally low, t_L/t_S is high, the stoss-side of a ripple is generally not preserved, and the shape of the foreset laminae is very weakly asymptotic. All these indicate that in the initial stages of deposition of a coset, sediment is less cohesive and there is a dominance of traction. The fallout is moderate, i.e. sufficient to make the ripples climb but insufficient for stoss-side preservation. Higher t_L/t_S indicates a relatively rapid rate of ripple migration.

With an increasing rate of fallout due to declining flow strength, the sediment probably becomes more cohesive due to an increasing proportion of clay and a progressive decrease in grain size, the suspension/traction ratio increases, stoss-laminae begin to be preserved, t_L/t_S starts decreasing, the rate of ripple migration decreases and the angle of climb increases. Declining flow strength results in preservation of more and more sediment on the stoss-side in successive laminae. Due to decreasing traction, grains fail to travel longer distances over the stoss-side and are eventually deposited slightly upstream from the crest. Increasing cohesiveness helps to maintain an increase in lee-angle, α. The trough starts receiving progressively more and more winnowed mud. The overall result is an increase in W, A, β, α and ϵ, and a decrease in t_L/t_S. Plate 40 illustrates increased deposition of mud in the trough. Fig. 9 illustrating

the distribution of grain/matrix ratio across a ripple from bed-477, supports the assumed process. Unusually high β, α and ϵ recorded from bed 477 (see Appendix) and the strongly sigmoidal shape of the foreset laminae (Jopling and Walker, 1968) provides further evidence.

It is suggested that the increase of the parameters W, A, β, α and ϵ continues as long as the rate of fallout keeps increasing and it is reversed, as mentioned earlier, at about 1/2 or 3/4 the thickness of a coset, depending on the availability of sediment in the current. Experiments (Rees, 1966, fig. 9, p. 226) with fine silt show that in the presence of excess material the parameters W, A, β, α and ϵ have a tendency to increase continuously to approach a mature ripple profile (i. e. when β of the ripples does not increase any further).

When the rate of fallout starts decreasing and bed traction decreases more rapidly, while the suspension/traction ratio and cohesiveness continue to increase, the ratio t_L/t_S tends to be 1:1; however, the trough continues to receive a little more sediment through mud winnowing. As a result A, β and α will decrease. ϵ will not decrease substantially because of slow ripple migration. Decrease in W will be compensated by increasing thicknesses of the lee-laminae at the trough. The irregular pattern of grain-size distribution across ripple at the top of the beds (see fig. 8(i) and (ii)) implies that the sediment-size-sorting power of the current deteriorates significantly towards the top.

This eventually supports the assumption that a ripple-drift coset reflects deposition from a gradually decelerating current.

The ripple lamina in fig. 38 defined by A_3W_3 and A_4W_4 represents a ripple lamina belonging to a dying ripple. It is to be noted here that $W_1 > W_3$. The dashed lines over the ripples represent the free stream line and the zone of separation. The fat arrows on the stoss-sides of the ripples indicate the distances available to the grains to travel on the stoss-slope of the respective ripples. The dying ripple lamina shows the following features: (i) upward decrease in A, β, and α, (ii) slight decrease in ϵ upward, (iii) W continues to increase slowly upward, (iv) t_L/t_S value approximately 2, (v) lamina thickest in the trough and (vi) $A_1 = A_3$ but $A_2 > A_4$.

Following the lines of argument presented before, it can be envisaged that as the coset thickness increases, the travelling distance of the grains on the stoss-slope of the longer upstream ripple continues to increase, but that on the stoss-slope of the shorter downstream ripple it continues to decrease. As a result, the trough receives, in addition to the winnowed mud, a little more of the tractive load (in spite of the increasing cohesiveness, which is balanced by the preserved momentum of the grains that tracted a relatively shorter distance). As the height (i.e. amplitude) of the upstream ripple continues

to increase upward through the coset, the free streamline, at a certain stage, will bypass the dying ripple and will reattach on to the stoss-side of the next ripple downstream. The dying ripple under such conditions will be buried more quickly. It appears that the phenomenon of overtaking, once started, will effect the downstream ripples over a certain bed length, and this is precisely the case with bed 477 of St. Maurice.

The phenomenon of overtaking has also been observed at two or three places in the beds 5 and 7 of Petite Vallée, but no down-current effect was observed in those cases. It appears that a mere initial difference in wave length is not the only clue to overtaking. It seems that a certain grain-size range of the sediment (see table VI for the coarse tail measurements of the beds 5, 7 and 477) and a fairly fast rate of deposition (indicated by unusually high ϵ) for a considerable length of time, are also important. The supporting evidence comes from the facts that (i) in beds 5 and 7 of Petite Vallée the grain-size range is the same as in bed 477 but average ϵ (see Table V) is much higher in bed 477, (ii) overtaking has not been observed in the thinner cosets and (iii) overtaking has not been observed in coarser-grained beds. Rees' (1966) observation, mentioned earlier, also lends support to the postulated mechanism.

4.2. Classification of Ripple-Drift

The revised classification of ripple-drift proposed by Jopling and Walker (1968) is reproduced in fig. 39. The ripple-drift they described was deposited, at least in part, by density currents, and the different types of ripple-drift exhibited a complete spectrum between two end members (i) Type-A (stoss eroded) and (ii) sinusoidal ripple lamination. The trend from A to sinusoidal indicates a gradual increase in the suspension/traction ratio of the load. Type-C, an "off shoot" of the spectrum has been described by Jopling and Walker as a turbidite type. Type-C represents swift climb and rapid deposition from suspension onto both stoss and lee sides, resulting in both upward and forward climb, a graded coset passing upward into mudstone, a gradual decrease in amplitude upward and a segregation of mud and mica flakes on to the lee side of the ripples.

In his first classification, Walker (1963) suggested that the type-A is formed in fluvial and shallow water environments. However, in a second paper, Walker (1965, p. 15) cited a few examples of the occurrence of type-A in turbidites of the Ordovician Martinsburg Formation (McBride, 1962, fig. 9, p. 51) and the Devonian Jennings Formation (McIver, 1961, fig. 31, p. 95) and concluded that "The apparent rarity of type-1 (i.e. type-A) ripple-drift in turbidites

suggests that a slow rate of fallout of sand grade particles over a fairly long interval is an uncommon process of deposition from turbidity currents". In a third paper (Walker, 1969, p. 391) he suggested that "the type-A ripple-drift would imply sufficient fallout to make the ripples climb but insufficient for stoss-side preservation".

In the Cloridorme turbidites, the author noticed many occurrences of type-A ripple-drift. This type does not generally form a complete coset, but is found in the lower part of almost every coset. The angle of climb in this part is low. The upper parts of the cosets consist of stoss-preserved ripple-drift. From what has been discussed earlier and from the available field evidence, it appears that the formation of type-A ripple-drift by turbidity currents is commoner than was implied by Walker.

Recently, Allen (1970b) proposed a classification which in essence is a theoretical treatment of the descriptive classification of Jopling and Walker (1968). Fig. 40, taken from Allen's paper, shows in detail the types of climbing-ripple cross-lamination and the predicted patterns of climbing-ripple cross-lamination types resulting from non-uniform flow, unsteady flow and simultaneous non-uniform and unsteady flow. All these types or varieties of climbing-ripple cross-lamination belong to a continuous morphological series. The classification does not

FIG. 39. Classification of ripple-drift cross-lamination proposed by Jopling and Walker (1968), based upon ratio of fallout from suspension to bed-load moved by traction.

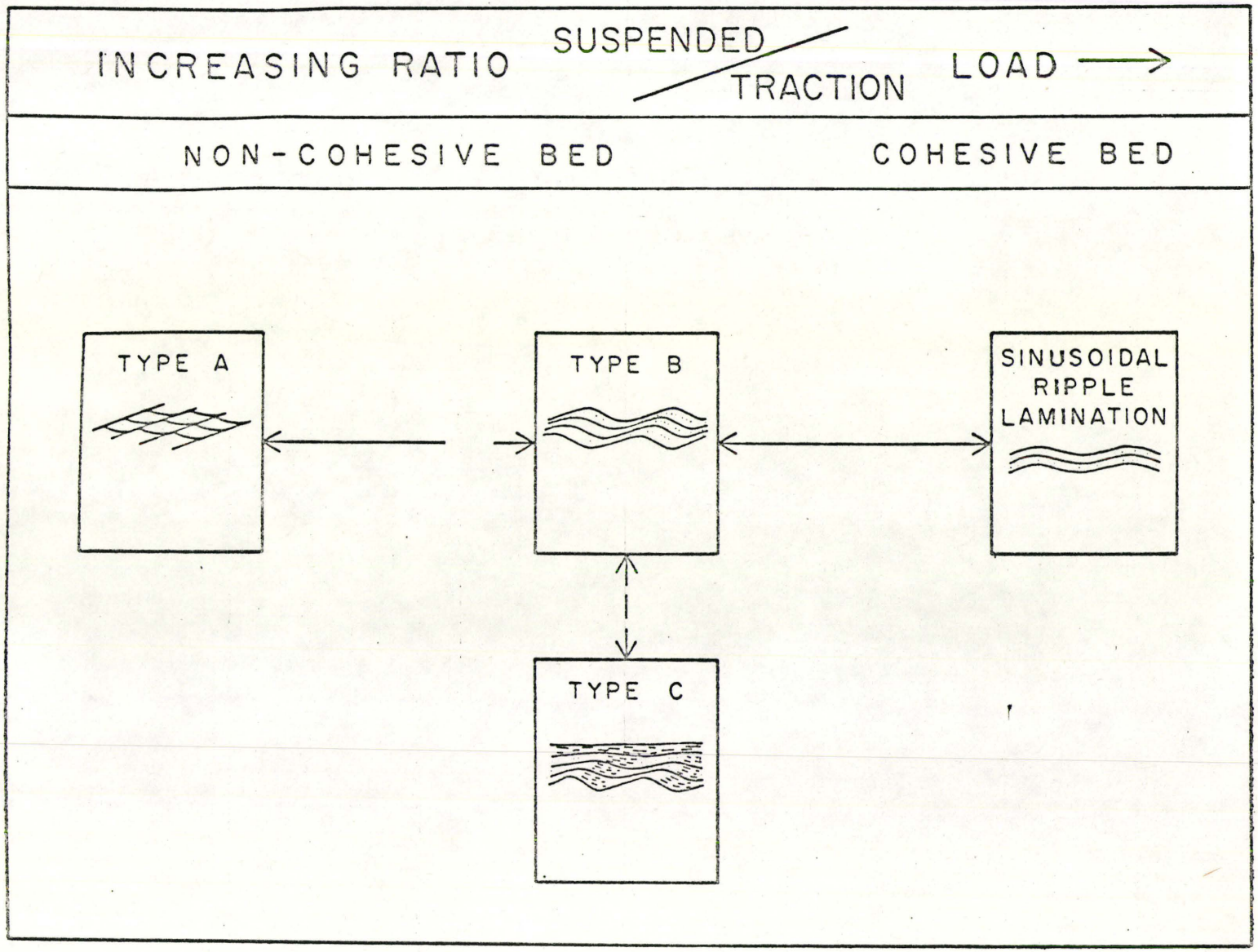
INCREASING RATIO
SUSPENDED
TRACTION
LOAD
NON-COHESIVE BED
COHESIVE BED
TYPE A
TYPE B
SINUSOIDAL RIPPLE LAMINATION
TYPE C

FIG. 39

FIG. 40.

Types and patterns of climbing-ripple cross-lamination after Allen (1970b, fig. 7):

a. main types of climbing ripple cross-lamination;

b. schematic predicted horizontal sequences of cross-lamination types resulting from non-uniform flow;

c. schematic predicted temporal sequences of cross-lamination types resulting from unsteady flow;

d. schematic predicted space-time patterns of cross-lamination types resulting from simultaneous non-uniform and unsteady flow.

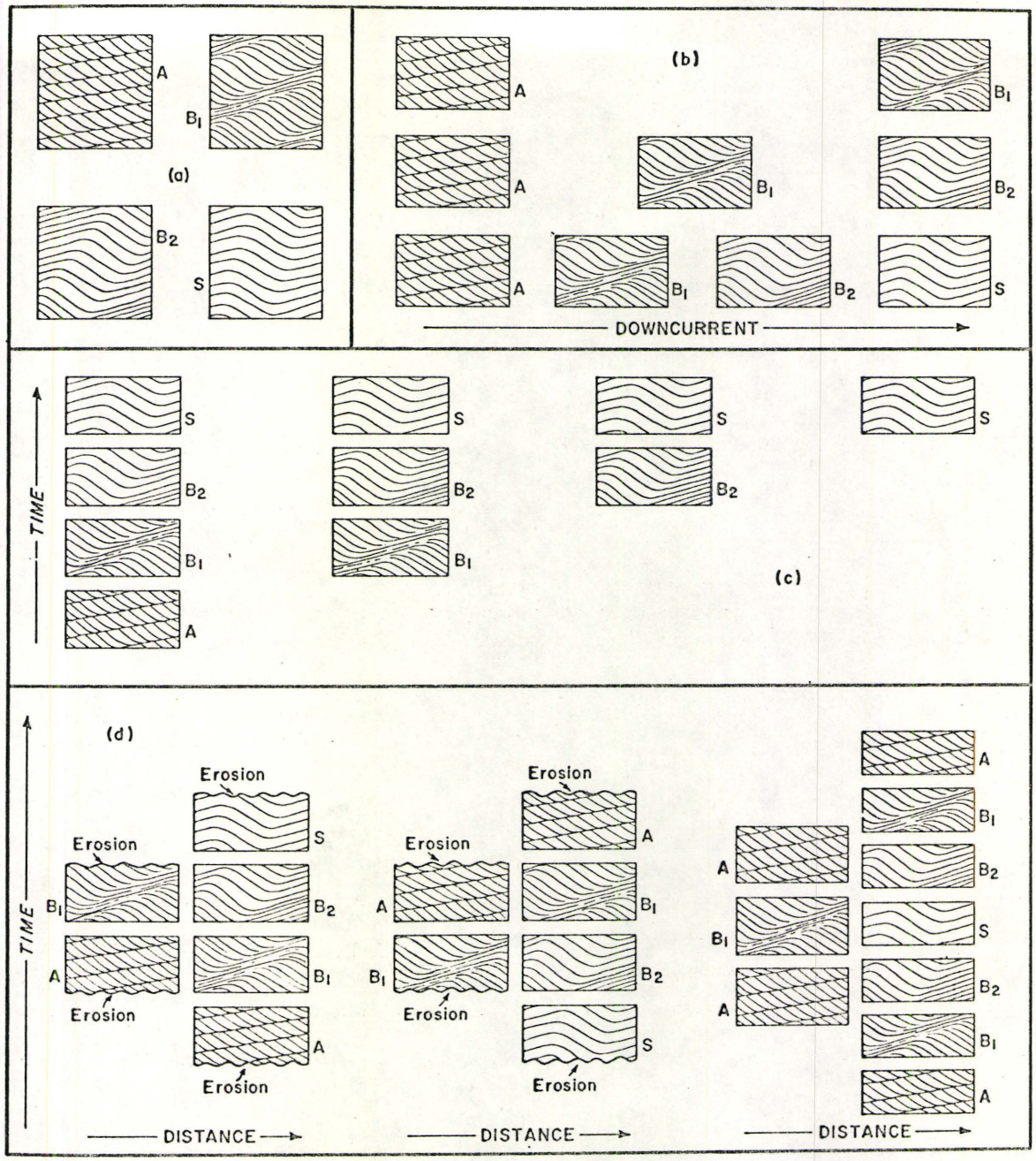
A
B1
(a)
B2
S
(b)
A
A
A
B1
B1
B2
S
DOWNCURRENT
TIME
S
B2
B1
A
(c)
(d)
Erosion
S
B2
B1
A
DISTANCE
TIME

FIG. 40

distinguish a separate turbidite type like 'type-C' of Jopling and Walker (1968). Allen (1970b, p. 24-5) states, "Depositional systems which are simultaneously non-uniform and unsteady give deposits in which both horizontal and vertical variations of type of cross-lamination are apparent. If the unsteadiness is periodic, the cross-lamination types can occur vertically in cyclical patterns. ... A selection of possible sequences of structures is sketched in fig. 7d' (see fig. 40 in this text) 'from which it is seen that the vertical pattern of types at a station depends on the position of that station in the system. Generally speaking, the range of cross-lamination types is greater in distal than in proximal positions.'

'Cross-laminated deposits showing patterns related to those in fig. 7d appear, rather unexpectedly, to be uncommon. From the Langdale Slates, however, Sorby (1908, plate 16) figured a bed in which the angle of climb changes upward from moderately steep (type-B) to gentle (type-A) and then reverts to moderately steep and finally steep (type B and S). This sequence means an increase of current velocity followed by a decrease. ... Perhaps the most important examples are afforded by Jopling and Walker (1968, fig. 4, 7, 8) from their studies of a proglacial lake delta. ... They describe from the 'foreset' deposits of the delta a sequence in bed of which the principal succession of

cross-lamination types is S $\longrightarrow B_2 \longrightarrow B_1 \longrightarrow$ A, the type A cross-lamination at the top of one bed generally passing rapidly up into the type S beginning the next.".

In the Cloridorme Formation, the vertical sequences observed by the author are, in Allen's terminology, A, A $\longrightarrow B_1 \longrightarrow B_2$ and $B_1 \longrightarrow B_2$; type S is apparently absent. However, Allen's classification is not so applicable to turbidity-current-formed ripple-drift cross-lamination as that of Jopling and Walker.

All these examples show that the predicted patterns in vertical sequence can be found in the geological record. The author does not know of any example of the predicted downstream variation of the patterns (see fig. 40d). In the Cloridorme Formation, ripple-drift beds are sometimes found exposed for several hundreds of feet (e.g. bed 477 of St. Maurice exposed for a length of about 1200 feet), but no downcurrent variation of the patterns were noticed in any of the beds. However, Allen does not predict over what downcurrent distances these changes are to be expected. From experience, we know that the ripple-drift beds do not continue laterally for great distances. For example, in the Cloridorme Formation, the lateral continuity is less than 1 kilometre; in that case one might expect to find some of the predicted lateral changes if the beds are exposed for several hundred feet.

In conclusion, these classifications, which in essence are one and the same, give us an idea about the environmental significance of deposits with ripple-drift, in terms of hydraulics. But, given only the geometry of ripple-drift structures, Allen concludes, "we can not say, what was the absolute total-load sediment transport rate, nor can we estimate the sediment deposition rate".

4.3. Grain Size

In the present study it has been found that the rocks containing ripple-drift are very fine grained (see Table-VI), mainly silts and clays and subordinately fine sand. Enos (1969a) also noted this characteristic feature of the sediments. The ripple-drift of Langdale Slates (Sorby, 1908), Gamlan Flags (Kuenen, 1967) and many other examples of both the climbing and the non-climbing turbidite ripples also reveal this characteristic feature.

It appears that the fine grain size is typical of turbidites (Kuenen & Humbert, 1969), whereas in rivers and tidal channels, many examples of coarse-grained ripples and megaripples exist. But a river in flood, when waning, closely follows the flow-properties of a decelerating turbidity current and examples of ripple-drift from the flood-plain deposits of the Colorado River (McKee, 1965, fig. 3c, d; p. 75) also show that the upper limit of grain-size is fine sand.

Experimental studies indicate that rippling does not start until the velocity of an overloaded suspension current drops below Gilbert's second critical velocity (Kuenen, 1967, p. 222). The capacity for fine sand is then decreasing and the finer grains start to reach the bottom.

In a recent paper Kuenen and Humbert (1969) have demonstrated that the turbidite ripples show good sorting and a log-normal grain-size distribution restricted to medians of very fine sand to silt, and claimed that these features are not exhibited so consistently by very many current ripples.

Table-VI reveals that the Cloridorme ripple-drift cosets in general show a gradual decrease in the maximum grain-size from base to top. Downcurrent decrease in the maximum grain-size is not very apparent. Middleton (1962, 1967) has demonstrated that the maximum size values emphasize the grading characteristics of the bed as shown by the mean size, with a few exceptions.

At a particular place a bed of ripple-drift is deposited by the parts of the tail of a turbidity current progressively further behind in the current, and the process results in a vertical grading (Kuenen and Migliorini, 1950; Kuenen, 1967). In the present study, measurements of maximum grain-size (i.e. mean of 10 largest grains) have been

carried out only from two positions of every bed, i.e. top and bottom. However, it appears the ripple-drift beds in general show good normal vertical grading. Downcurrent decrease in grain-size, attributed to decrease in velocity, did not show up in the present study, probably because of the short exposed bed lengths.

Ripple-drift indicates relatively swift deposition. However, normal grading may also result from rapid deposition provided the suspended material in the turbidity current is normally graded (Kuenen, 1966). Deposition of a ripple-drift bed from a turbidity current takes place in the later stages of flow; the suspended material thus gets sufficient time to become normally graded.

The grain-size distribution across three ripples, shown in fig. 8, reveals that (i) at the top of the beds the distribution is haphazard but (ii) at a lower level, the distribution shows a definite pattern with coarsest grain-size near the crest. This implies that the size sorting power of the current gradually decreases upward through a coset and near the top sediments are deposited mainly from suspension. However, winnowing of mud presumably continues even in an extremely low current strength.

Many workers (Sestini and Curcio, 1965; Potter and Scheidegger, 1966) have observed that in graded turbidites, the total bed thickness increases as the maximum grain-size in a bed increases. In the present study a correlation coefficient of 0.53 with a sample size of 47 proves to be significant at the 95% level (fig. 24A), and hence the relationship between maximum grain size and bed thickness described by Scheidegger & Potter, and others, is confirmed.

The positive relationship between the maximum grain-size and the angle of climb (see fig. 24B) is obvious because the relationships between (i) ϵ and coset thickness, and (ii) coset thickness and grain-size, are also positive.

An examination of figs. 35 and 36A, B reveals that each of the parameters W, A and RI decreases as the maximum grain-size increases. Studies of ripples from various other environments (Reineck and Wunderlich, 1968) have revealed that the RI becomes smaller with the increasing values of mean grain-size, i.e. the ripples in coarser sand increase in amplitude in relation to wave length. Experimental studies (Guy et al., 1966) with materials coarser than fine sand show that W increases as grain-size increases. From what has been discussed earlier, it follows that the increase in W with decrease in grain-size is mainly due to an increase in cohesiveness of the deposited sediment.

FIG. 41.

Changes in ripple geometry, after Walker (1969, fig. 12).

A = changing ripple amplitude due to sedimentation in the ripple troughs. B = changing wavelengths due to different rates of deposition and hence different t_L/t_S values. C = changing angles of climb downstream as a result of increasing the wavelength.

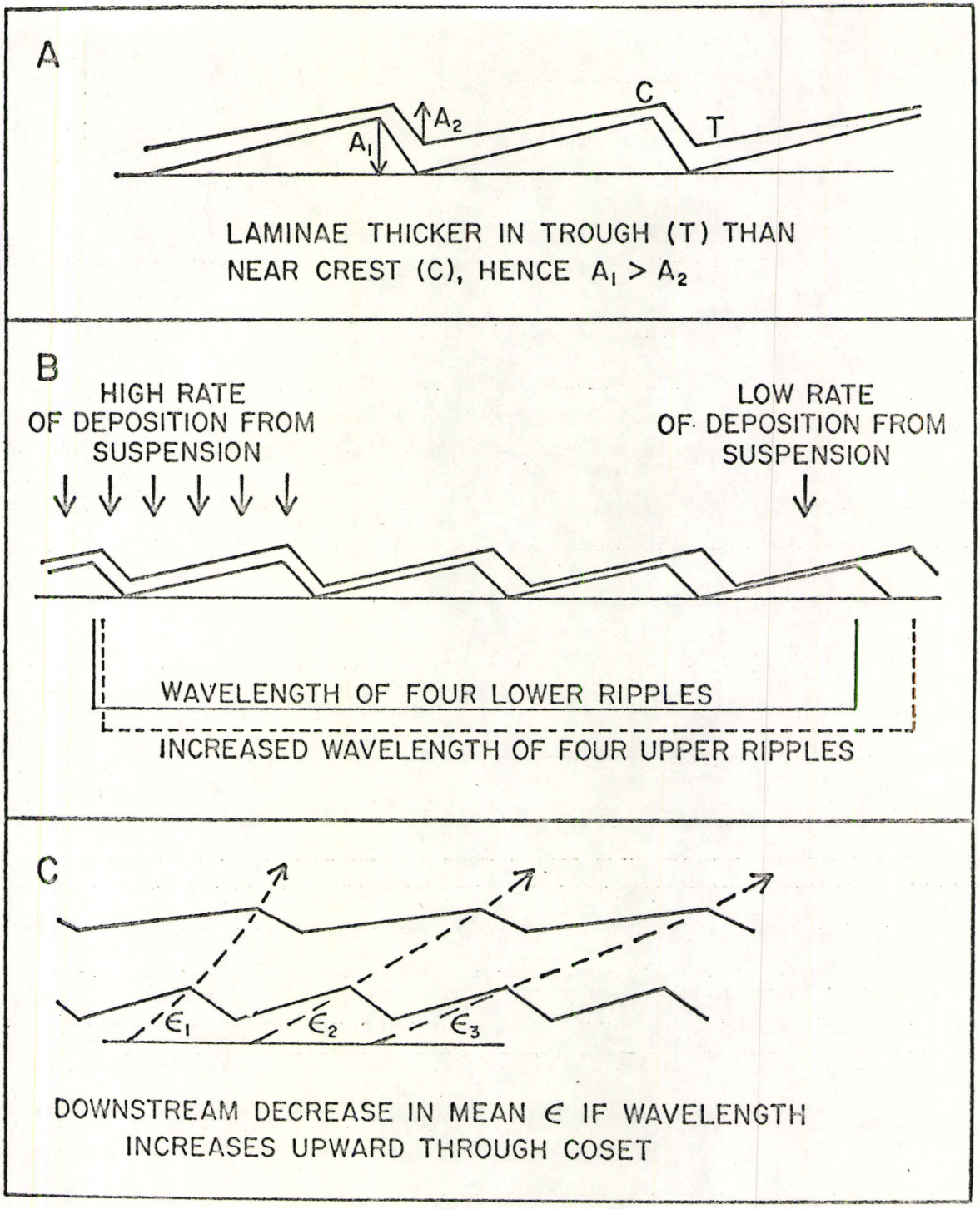
A
A2
A1
C
T
LAMINAE THICKER IN TROUGH (T) THAN
NEAR CREST (C), HENCE A1 > A2
B
HIGH RATE
OF DEPOSITION FROM
SUSPENSION
LOW RATE
OF DEPOSITION FROM
SUSPENSION
WAVELENGTH OF FOUR LOWER RIPPLES
INCREASED WAVELENGTH OF FOUR UPPER RIPPLES
C
ϵ1
ϵ2
ϵ3
DOWNSTREAM DECREASE IN MEAN ϵ IF WAVELENGTH
INCREASES UPWARD THROUGH COSET

FIG. 41

4.4. Coset Thickness, Lateral Continuity and Rate of Deposition

The average coset thickness of the Cloridorme ripple-drift is 20 cm and the range is 2 - 75 cm. Still higher values (98 cm) have been reported by Walker (1969). These spectacularly high values of coset thickness as against the low downcurrent continuity of beds (approximately 1/2 km) pose an interesting problem.

The ripple-drift cosets are sometimes traceable (see fig. 12) laterally for up to 1200 feet (e.g. bed 177). Some of the cosets die out within short distances (e.g. bed 1 and 2 of Grande Vallée). Continuity of ripple-drift beds for up to 1200 feet does not seem to be very surprising, particularly when the cosets are several tens of centimetres thick. However, the field evidence suggests that the ripple-drift beds are not as laterally continuous as other Cloridorme turbidites.

Walker (1969, p. 390) attributed this short lateral continuance of the ripple-drift beds to (i) an increase in wave length upward which "implies a decreasing mean value of ϵ downstream until climbing ripples could no longer be recognised. Also, continuous lengthening of the wave length downstream would imply impossibly great thicknesses of lee-side laminae, and instead of ripple-drift, normal ripple cross-lamination would be formed", and (ii) "it is unlikely that a natural turbidity current could flow for tens of hours in the ripple regime continuously depositing sediment".

The first explanation is based on a very idealised situation arising out of a purely geometrical analysis. In fig. 4lc, taken from Walker (1969), if the wave lengths of the ripples at the base of the coset are assumed to be unequal, then ϵ may not necessarily decrease downstream. Conversely, in spite of unequal wave length at the base ϵ may decrease downstream. Figs. 14, 16, 18, 20 and 22 reveal that neither W nor ϵ show any regular pattern of variation downcurrent. Bed 2 of Grande Vallee (see fig. 11 and 22), however, does show a little decrease in the mean value of ϵ and a correspondingly very small increase in W; but these changes are not very apparent. Rather surprisingly, the ripple-drift ends abruptly. Fig. 35 again shows that grain-size is one of the factors that control wave length. The relation (increase in wave length with decrease in grain-size) supports the idea of Walker.

The lateral relationship of ripple-drift passing upstream and downstream into parallel lamination is difficult to explain. A recent theoretical paper by Allen (1970a) suggests a possible answer. In his figure 4, which plots flow power against grain size, it can be seen that very slight fluctuations in grain size (at sizes smaller than 0.2 mm) could cause fluctuations in the bed form from current ripples to upper regime plane bed. However, Allen's replotting of the data of Guy et al. (1966) disagrees with the original plot of Guy et al. (in

Simons et al., 1965). In using conclusions from a theoretical paper of Bagnold (1966), Allen has ignored the fact that "grain size" in turbidity currents cannot simply be related to settling velocity because of complications of high grain concentrations during the depositional stages of turbidity currents. He has also ignored the fact that viscosity in turbidity currents bears an unknown relationship to the viscosity of pure water. There is, therefore, no well established theory or experiment which may be used to explain this abrupt lateral relationship of parallel lamination and ripple-drift.

Great thicknesses of cosets indicate that large quantities of sediment were suspended by the turbidity currents before they started depositing ripple-drift beds. High proportion of extremely fine grained material (see fig. 9 for modal analyses) in the sediment provides support for the assumption that large quantities of silt and fine sand could be maintained in high-mud-suspension currents because of the increased density of the currents. Such a suspension current, overloaded with fines, presumably up on reaching a certain combination of flow power and grain size would deposit a thick bed of ripple-drift.

This hypothesis of increased density implies a greater continuity of beds, but the Cloridorme ripple-drift beds appear to be continuous for only about 1 /2 kilometre. Apparently 'continuity of bed' does not have any relation with 'coset thickness'. However, from the

experimentally determined rate of ripple migration and the rate of deposition, we can have some idea about the continuity of the ripple-drift beds.

Sorby (1908) first showed that the rate of deposition can be estimated from the angle of climb combined with the probable current velocity, and his estimate for the growth rate of the ripple-drift beds of the Langdale Slates was 0.017 to 0.082 cm/sec. On the basis of experimental data and field evidence, Kuenen (1967, p. 219) suggested a growth rate of 10 min/cm, assuming that the turbidite ripple-drift beds generally exhibit an average ϵ of 12^{o} (1:5). He also states that "Ripples resembling those of flysch formations formed between 80 and 30 cm/sec and the respective travel velocities were 6 and 0.1 cm/min. Let is be assumed that upward growth in natural beds varies roughly between 1 and 1/15 time the travel distance and that the former value belongs to slow, the latter to swift currents. In these combinations the 30 cm current would deposit at 0.1 cm/min or 50 minutes for 5 cm, the 80 cm current at 0.4 cm/min or 12 minutes for 5 cm. The average rate of deposition is probably less because most ripples climb at moderate angles. The average slope of 1:5 could be the product of ripples migrating at 0.5 cm/min and climbing 0.1 cm/min".

In the Cloridorme Formation it has been observed that the ripples climb a vertical distance of 50 cm within a horizontal distance of 150 cm, i.e. the mean slope of the climb angle is 1:3. Kuenen's (1967, Table 1) experimental data show that in a current strength of 50 cm/sec ripples migrate at the rate of 20 m/day = 1.5 cm/min. Relating this value to the slope, 1:3, we get a vertical growth rate of 0.5 cm/min. It means that a 50 cm coset will take approximately 100 minutes to form, and during this time the 50 cm/sec current will travel a distance of about 3 Km. It may therefore be considered that with an average 50 cm current and an average ϵ of 20° (= 1:3), a 50 cm thick bed would show a lateral continuity of approximately 3 Km. But as mentioned earlier, the Cloridorme ripple-drift beds do not even continue for a kilometre. Bed 2 of Grande Vallée offers a good example. Fig. 11 shows that the coset is 36 m long and 11 cm thick (average). Assuming a vertical growth of 0.5 cm/min and an average 50 cm current, this 11 cm coset would theoretically have shown a lateral continuity of 0.6 Km. These calculations, based on little experimental work, raise some doubt as to the validity of the suggested growth rate of 0.1 cm/min. (Kuenen, 1967). Even a growth rate as high as 0.5 cm/min does not help much to resolve the problem.

4.5. Angle of Climb

The various types of angle of climb have been mentioned earlier (see fig. 6). It is emphasized that the types were distinguished solely for the purposes of field description. It can be seen that the difference between type-A and type-C is very little, the latter being distinctly sigmoidal in shape with the upper infliction point lying at a much lower level than it is in the former. Likewise, it is possible that in type-B, the line appears to be straight because curving is too subtle to recognise when the ϵ is very low and the coset is very thin. Type-D was observed in bed 6 of Petite Vallée only. Types-E and-F are, however, distinctly different, the former shows sinuousity in the line of climb without any sign of erosion, whereas the latter emphasizes breaks in the line with visible signs of erosion (see Pl. 33).

Type-A climb suggests that (i) in the initial stages of deposition of a coset, a relatively less cohesive character of the deposited sediment and a relatively high current strength contribute towards a moderate fallout and a faster rate of ripple migration (evidenced by high values of t_L/t_S) resulting in a slow increase in the angle of climb, (ii) with progressive decrease in current strength, the rate of fallout increases and a progressive increase in cohesiveness concomitantly retards the rate of ripple migration (evidenced by de-

crease in grain size and t_L/t_S) resulting in a fast increase in the angle of climb and (iii) finally near the top of a coset the angle of climb may again decrease a little if a virtually unloaded weak current still exists and continues winnowing mud on to the trough until the bed profile is levelled.

If, however, during the deposition of the middle or upper middle part of a coset the rate of fallout decreases more rapidly than the relative decrease of the current strength, the pattern of climb would show a distinctly sigmoidal shape (type-C). Similarly, the straight pattern of climb (type-B) might possibly have resulted from a delicate balance between the decreasing current strength and the rate of fallout. The sinuous climb (type-E) is probably due to deposition from successive pulses of a flow. Pulses causing slight erosive periods may produce a disconnected irregular climb (type-F).

If type-B climb is considered as an ideal case of balance between the current strength and the rate of fallout, then any change in the configuration of the straight line pattern would imply that some mechanism, possibly external to the turbidity current, regulates this change. It is again tentatively concluded that the most likely mechanism is the basin floor irregularity. The supporting evidence is provided by the facts that the thicker cosets (range 3-75 cm) with larger maximum

grain size (range 0.05 - 0.45 mm) and steeper angles of climb (range 1^{o} - 43^{o}) are more frequently encountered in the β_7 Member (ABC index 59%) than in the β_1 Member (ABC index 11%) where the cosets are thinner (range 2 - 23 cm), the angles of climb, showing a straight pattern, are less steep (range 1^{o} - 16^{o}) and the maximum grain size is smaller (range 0.04 - 0.17 mm).

Vertical passage of type E and/or type F to types A, B or C, and downcurrent passage of types A $\longrightarrow$ C $\longrightarrow$ E or F $\longrightarrow$ C $\longrightarrow$ A were observed in some beds of Petite Vallée. If in a vertical sequence, the occurrence of type E and/or type F in the lower part of a coset is attributable to a combined effect of relatively high current strength and moderate fallout, then the appearance of type E and/or F in a downcurrent sequence must also be attributable to the same process. If so, the possible mechanism can be envisaged as follows: the flow initially passing over a relatively low slope and producing type A climb, would, on encountering a locally steeper slope, accelerate and produce type C and type E and/or F in succession and then trace back during the decelerating phase through type C to type A after the resumption of the slope.

4.6. Sole Marks and Current Direction

The sole marks in the ripple-drift beds are mainly of one type, namely L-ridges, which show a poor to fair development with occasional cuspate crossing bars (see Pl. 6).

The data on current directions (see Table I) indicate that the current direction measured from the ripple-drift is close to the mean direction of flow given by sole marks in all the localities and also close to the individual sole marks of the ripple-drifted beds. This suggests that the sole marks, in all probability, were produced by the same current that deposited the beds. The consistency of the current directions along the length of the beds and the fairly straight intersection of the erosion laminae (Pl. 5) at the base of the beds indicate that the ripples are fairly straight crested. Weak sinuousity (Pl. 37) of the crest observed at the top of the bed-477 is perhaps due to the prolonged existence of a weak current after the supply ran out. Experimental studies demonstrate that the irregularity is a function of time (Briggs and Middleton, 1965, p. 15).

Occurrence of adjacent beds of ripple-drift showing opposite current directions were noted at several places. The idea of debouchment of turbidity currents from two sources helps to resolve the problem. There is no reason why a turbidity current debouched from a secondary

source and at an angle to the main flow direction, can not travel in the opposite direction and deposit beds of ripple-drift, especially when the slopes are assumed to be extremely low. It is surprising that the characteristics (great thicknesses of cosets, grain-size, continuity of beds, etc.) of both kinds of beds do not exhibit any apparently recognisable disparity. However, it has been observed in the field that the beds showing opposite current directions do exhibit, in general, a sinuous and/or disconnected pattern of climb; concave-upward climb is extremely rare and other types of climb are absent.

4.7. Summary

1. The Cloridorme ripple-drift beds mostly occur singly (i.e. entire bed ripple-drifted). Occurrence of cosets of ripple-drift with Bouma's B laminations and/or graded division A are rare.

2. Vertical sequence of the types of ripple-drift cross-lamination observed in the field are (in Allen's (1970b) terminology): A, A $\longrightarrow B_1 \longrightarrow B_2$, $B_1 \longrightarrow B_2$. Type S is apparently absent. The classification of Jopling and Walker (1968) fits in well with these sequences, except for the fact that type A ripple-drift is more abundant than they thought it to be.

3. According to Allen (1970b), ripple-drift beds are supposed to show some lateral changes in sequences of the types of ripple-drift cross-lamination; but presently we do not know over what distances these changes are to be expected. However, in the Cloridorme turbidites, no lateral changes were observed despite the fact that the ripple-drift beds are exposed for up to 1200 feet.

4. The three most interesting observations of the present study are: (i) the geometrical parameters W, A, β, α, ϵ and t_L/t_S show a definite pattern of change upward through a coset. Walker (1969) noted that A gradually decreases upward through a coset. The present study shows that W continues to increase up through a coset; A, β and α increase as long as ϵ keeps increasing (usually up to about 1/2 or 3/4 the thickness of a coset) and then they decrease until the bed is plane; and t_L/t_S decreases upward. It is suggested that these changes are possibly attributable to the combined effect of upward increase in cohesiveness due to fining upward of the grain size, rate of fallout, and upward decrease in current velocity. (ii) concomitant with the increase in ripple size and ϵ, the shape of the foreset laminae of the ripples also show a systematic change (almost straight to strongly sigmoidal) upward through the coset.

(iii) the overtaking of ripples, resulting in the merging of climbing bands, is another important phenomenon which possibly owes its origin to several factors, viz. initial difference in wave length, a specific grain size range and current strength, and prolonged and sufficient supply. The phenomenon was also observed by Rees (1966) in his flume experiments with fine silt.

5. The geometrical parameters W, A, β, α, ϵ and t_L/t_S, do not show any regularity in their downcurrent variability.

6. Six types of climbing patterns were recognised in the field viz. type A (concave-upward climb), type B (straight climb), type C (sigmoidal climb), type D (convex-upward climb), type E (sinuous climb) and type F (disconnected-irregular climb). Of these, types C, E and F, are normally restricted to thicker cosets. Type B is restricted to thinner cosets. Its low angle of climb probably indicates a lower ratio of suspension/traction deposition than types C, E and F. Type A occurs commonly but type D is very rare.

7. (a) The coarsest grain size in the ripple-beds of the Cloridorme Formation is 0.63 mm. The mean size of the grains is about 0.02 mm. This confirms the observation of Kuenen and Humbert (1969) that turbidite ripples usually have a grain size below 150μ.

(b) There is a good correlation between maximum grain size and coset thickness, which agrees with previous studies (e.g. Sestini and Curcio, 1965; Potter and Scheidegger, 1966).

(c) Studies of non-turbidite ripples in sand (Reineck and Wunderlich, 1968) show that W and A increase as the mean grain size increases. The present study shows that W, A and RI have a tendency to decrease with increase in maximum grain size. This possibly is a function of the fine grain size range and the upward increase in cohesiveness due to normal grading of the sediment.

8. An abrupt flattening of the gradient of the basinfloor, as suggested by Walker (1969) might possibly account for the short lateral continuity (1 Km) of the ripple-drift cosets and the high values of coset thicknesses (e.g. 98 cm). The rate of growth (0.1 cm/min) of turbidite ripple-drift beds, suggested by Kuenen (1967) does not appear applicable to the cosets in the Cloridorme Formation.

9. The lateral change in lamination characteristics noted in the present study are: Parallel lamination $\longrightarrow$ Parallel lamination + ripple-drift $\longrightarrow$ Parallel lamination. There is

presently no well established theoretical or experimental work which can be used to interpret this lateral relationship.

BIBLIOGRAPHY

Allen, J.R.L., 1960, The Mam Tor Sandstones: A turbidite facies of the Namurian deltas of Derbyshire, England. Jour. Sed. Petrol., 30:193-208.

_____, 1963, Depositional features of Dittonian rocks: Pembrokeshire compared with the Welsh Borderland. Geol. Mag., 100: 385-400.

_____, 1968, Current Ripples. North-Holland, Amsterdam, 433 p.

_____, 1969, Some recent advances in the physics of sedimentation. Proc. Geol. Ass., 80:1-42.

_____, 1970a, The sequence of sedimentary structures in turbidites, with special reference to dunes. Scott. J. Geol. 6(2): 146-161.

_____, 1970b, A quantitative model of climbing ripples and their cross-laminated deposits. Sedimentology, 14:5-26.

Bagnold, R.A., 1962, Auto-suspension of transported sediment; turbidity currents. Roy. Soc. London, Proc., Ser. A, 265:315-319.

_____, 1966, An approach to the sediment transport problem from general physics. Prof. Paper U.S. Geol. Surv. 422-1, 1-37.

Ballance, P. F., 1964, The sedimentology of the Waitemata Group in the Takapuna Section, Auckland. New Zealand J. Geol. Geophys., 7:466-499.

Basset, D. A. and Walton, E. K., 1960, Cambrian greywackes in St. Tudwal's Peninsula, North Wales. Geol. Soc. London, Qtly. Jour., 116:85-110.

Berry, W. B. N., 1960, Graptolite faunas of the Marathon region, West Texas. Univ. Texas Publ. 6005, pp. 1-179.

_____, 1962, Stratigraphy, zonation and age of Schaghticoke, Deepkill and Normánskill Shales, Eastern New York. Bull. Geol. Soc. Am., 73:695-718.

Bouma, A. H., 1962, Sedimentology of some flysch deposits. Elsevier, Amsterdam, 168 p.

Briggs, L. I. and Middleton, G. V., 1965, Hydromechanical principles of sediment structure formation. Soc. Econ. Pal. Min., Spec. Publ. 12, 5-16.

Bucher, W. H., 1919, On ripples and related sedimentary surface forms and their paleogeographic interpretations. Am. Jour. Sci., 47:149-210, 241-269.

Cline, L. M., 1960, Late Palaeozoic rocks of the Ouachita Mountains. Oklahoma Geol. Surv. Bull., 113 p.

Coleman, J.M. and Gagliano, S.M., 1965, Sedimentary Structures: Mississippi River deltaic plain, in G.V. Middleton, ed., Primary Sed. Structures and their hydrodynamic interpretations. Soc. Econ. Pal. Min., Spec. Publ. 12, 133-148.

_____, _____ and Webb, J.E., 1964, Minor sedimentary structures in a prograding distributary. Marine Geol., 1: 240-258.

Crowell, J.C., 1955, Directional current structures from the Prealpine Flysch, Switzerland. Geol. Soc. Am. Bull., 66:1351-1384.

_____, Hope, R.A., Kahle, J.E., Ovenshine, A.T. and Sans, R.A. 1966, Deep water sedimentary structures of the Pliocene Pico Formation, Santa Paula Creek, Ventura Basin, California. Calif. Dept. Nat. Resources, Div. Mines, Spec. Rept. 89, 1-40.

Cotera, A.S., 1962, Petrology and petrography of Mississippian-Pennsylvanian Tesnus Formation, Marathon Basin, Trans-Pecos, Texas. Ph.D. thesis, The Univ. of Texas, Austin, Texas.

Davies, D.K., 1966, Sedimentary structures and subfacies of a Mississippi River Point Bar. Jour. Geol., 74:234-239.

De Raaf, J.F.M., Reading, H.G. and Walker, R.G., 1964, Cyclic sedimentation in the Upper Carboniferous of North Devon, England. Sedimentology, 3.

Dixon, W.J. and Massey, F.J., 1957, Introduction to statistical analysis. McGraw-Hill, second ed.

Dzulynski, S., 1965, New data on experimental production of sedimentary structures. Jour. Sed. Petrol., 35:196-212.

_____, 1966, Sedimentary structures resulting from convection like pattern of motion. Ann. de la Societe Geologique de Pologne, XXXVI:3-21.

_____ and Simpson, F., 1966a, Influence of bottom irregularities and transported tools upon experimental scour markings. Ann. de la Soc. Geol. de Pologne, XXXVI:285-294.

_____ and _____, 1966b, Experiments on interfacial current markings. Geol. Romana, V:197-214.

_____ and Walton, E.K., 1963, Experimental production of sole marks. Trans. Edin. Geol. Soc., 19:279-305.

_____ and _____, 1965, Sedimentary features of flysch and greywackes. Elsevier, Amsterdam, 274 p.

Emery, K.O., 1956, Deep standing internal waves in California basins. Jour. Limnology and Oceanography, 1:35-41.

Enos, P., 1965, Anatomy of a flysch: Cloridorme Formation (Mid. Ordovician), Northern Gaspe Peninsula, Quebec. Ph. D. Thesis, Yale Univ., 145 p.

_____, 1969a, Cloridorme Formation Middle Ordovician flysch, northern Gaspe Peninsula, Quebec. Geol. Soc. Amer. Spec. Paper 117, 66 p.

_____, 1969b, Anatomy of a flysch. Jour. Sed. Petrol., 39:680-723.

Ericson, D. B., Ewing, W. M., Heezen, B. C. and Wollin, G., 1955, Sediment deposition in the deep Atlantic. Geol. Soc. Amer., Spec. Paper 62, 205-419.

Folk, R. L., 1968, Petrology of Sedimentary Rocks. Hemphill's, Austin, Texas, 170 p.

Friend, P. F., 1965, Fluviatile sedimentary structures in the Wood Bay Series (Devonian) of Spitsbergen. Sedimentology, 5:39-68.

Gilbert, G. K., 1899, Ripple-marks and cross-bedding. Geol. Soc. Amer. Bull., 10:135-140.

Guy, H. P., Simons, D. B. and Richardson, E. V., 1966, Summary of alluvial channel data from flume experiments, 1956-61. Prof. Pap. U. S. Geol. Surv. 462-1, 1-96.

Harms, J. C., 1969, Hydraulic significance of some sand ripples. Bull. Geol. Soc. Am., 80:363-396.

Harms, J.C. and Fahnstock, R.K., 1965, Stratification, bed forms and flow phenomena (with an example from Rio Grande). Spec. Publ. Soc. Econ. Pal. Min., 12, 84-115.

Heezen, B.C. and Hollister, C., 1964, Deep-sea current evidence from abyssal sediments. Marine Geol., 1:141-174.

Hsu, K.J., 1960, Palaeocurrent structures and palaeogeography of the Ultrahelvetic Flysch Basins, Switzerland. Geol. Soc. Amer. Bull., 71:577-610.

_____, 1964, Cross-laminations in graded bed sequences. Jour. Sed. Petrol., 34(2):379-388.

Hubert, J.F., 1966, Modification of model for internal structures in graded beds to include a dune division. Nature, London, 211:614-615.

Jopling, A.V. and Walker, R.G., 1968, Morphology and origin of ripple-drift cross-lamination, with examples from the Pleistocene of Massachusetts. Jour. Sed. Petrol., 38(4):971-984.

Kelling, G., 1958, Ripple-marks in the Rhinns of Galloway. Trans. Edin. Geol. Soc., 17:117-132.

Kopstein, F.P.H.W., 1954, Graded bedding of the Harlech Dome. Geol. Inst. Groningen, Netherlands, Publ. 81, 97 p.

Kuenen, Ph. H., 1951, Properties of turbidity currents of high density. Soc. Econ. Pal. Min., Spec. Publ. 2:14-33.

_____, 1953, Graded bedding with observations on Lower Palaeozoic rocks of Britain. Verhandel. Konikl. Ned. Akad. Wetenschap., Afd. Natuurk., 20(3):1-47.

_____, 1965, Experiments in connection with turbidity currents. Univ. Bristol., Colston Papers, 17:47-74.

_____, 1966, Experimental turbidite lamination in a circular flume. Jour. Geol., 74:523-545.

_____, 1967, Emplacement of flysch-type sand beds. Sedimentology, 9:203-243.

_____ and Humbert, F. L., 1969, Grain size of turbidite ripples. Sedimentology, 13:253-261.

_____ and Migliorini, C. I., 1950, Turbidity currents as cause of graded bedding. Jour. Geol., 58:91-127.

_____ and Sanders, J. E., 1956, Sedimentation phenomena in Kulm and Flözleeres greywackes, Sauerland and Oberharz, Germany. Am. J. Sci., 254:649-671.

McBride, E. F., 1962, Flysch and associated beds of the Martinsburg Formation (Ordovician), central Appalachians. J. Sed. Petrol., 32:39-91.

McBride, E. F., 1966, Sedimentary petrology and history of the Haymond Formation (Pennsylvanian), Marathon Basin, Texas. Texas, Bureau of Economic Geology, Rept. Invest. No. 57, 101 p.

McGerrigle, H. W., 1959, Madeleine River area. Quebec Dept. of Mines Geol., Rpt. 77, 50 p.

McIver, N. L., 1961, Upper Devonian marine sedimentation in the Central Appalachians. Ph. D. Thesis, Johns Hopkins Univ., Baltimore.

McKee, E. D., 1938, Original structures in Colorado River flood deposits of Grand Canyon. J. Sed. Petrol., 8:77-83.

_____, 1939, Some types of bedding in the Colorado River delta. Jour. Geol., 47:64-81.

_____, 1965, Experiments on ripple-lamination. Soc. Econ. Pal. Min., Spec. Publ. 12:66-83.

_____, 1966, Significance of climbing ripple structure. U.S. Geol. Surv. Prof. Pap. 550-D, 94-103.

Menard, H. W., 1952, Deep ripple marks in the sea. J. Sed. Petrol., 22:3-9.

Middleton, G. V., 1962, Size and sphericity of quartz grains in two turbidite formations. J. Sed. Petrol., 32:725-742.

Middleton, G. V., 1966a, Small-scale models of turbidity currents and the criterion for autosuspension. J. Sed. Petrol., 36:202-208.

_____, 1966b, Experiments on density and turbidity currents. I. Motion of the head. Canadian Jour. Earth Sci., 3:523-545.

_____, 1966c, Experiments on density and turbidity currents. II Uniform flow of density currents. Canadian Jour. Earth Sci., 3:627-637.

_____, 1967, Experiments on density and turbidity currents. III. Deposition of sediment. Canadian Jour. Earth Sci., 4:475-505.

Natland, M. L. and Kuenen, Ph. H., 1951, Sedimentary history of the Ventura Basin, California, and the action of turbidity currents. Soc. Econ. Pal. Min., Spec. Publ. 2, 76-107.

Parkash, B., 1969, Depositional mechanism of greywackes, Cloridorme Formation (Middle Ordovician), Gaspe, Quebec. Ph. D. Thesis, McMaster Univ., 238 p.

Pett, J. W., 1970, The morphology of flutes. M. Sc. Thesis, McMaster Univ., 121 p.

Pett, J. W. and Walker, R. G., 1971, Relationship of flute cast morphology to internal sedimentary structures in turbidites. Jour. Sed. Petr., 41.

Potter, P. E. and Scheidegger, A. E., 1966, Bed thickness and grain size: Graded beds. Sedimentology, 7:233-240.

Prentice, J. E., 1960, Flow structures in sedimentary rocks. J. Geol., 68:217-225.

Reading, H. G., 1963, A sedimentological comparison of the Bude Sandstones with the Northam and Abbotsham Beds of Westward Ho. Proc. Ussher Soc., 2.

Rees, A. I., 1966, Some flume experiments with a fine silt. Sedimentology, 6:209-240.

Reineck, H.-E. and Wunderlich, F., 1968, Zur unterscheidung von asymmetrischen oszillationsrippeln und strömungsrippeln. Senckenbergiana lethaea, 49(4):321-345.

Riva, J., 1968, Graptolite faunas from the Middle Ordovician of the Gaspe north shore. Extrait du Naturaliste canadien, 95(6):1379-1400.

Sanders, J. E., 1963, Concepts of fluid mechanics provided by primary sedimentary structures. J. Sed. Petrol., 33(1):173-179.

Sanders, J.E., 1965, Primary sedimentary structures formed by turbidity currents and related resedimentation mechanisms. Soc. Econ. Pal. Min., Spec. Publ. 12, 192-219.

Scheidegger, A.E. and Potter, P.E., 1965, Textural studies of graded bedding: Observation and theory. Sedimentology, 5:289-325.

Sestini, G. and Curcio, M., 1965, Aspetti quantitativi delle impronte di fondo da corrente nelle torbiditi dell'Appennini tosca-emiliano. Boll. del. Soc. Geol. Ital., 84:1-26.

Shepard, F.P. and Dill, R.F., 1966, Submarine canyons and other sea valleys. Rand McNally & Co., Chicago, 381 p.

Simons, D.B., Richardson, E.V. and Nordin, Jr. C.F., 1965, Sedimentary structures generated by flow in alluvial channels. Soc. Econ. Pal. Min., Spec. Publ. 12, 34-52.

Skipper, K., 1970, Depositional mechanics of atypical turbidites. M.Sc. Thesis, McMaster Univ., 137 p.

Sorby, H.C., 1859, On the structures produced by the currents present during the deposition of stratified rocks. Geologist, 2: 137-147.

_____, 1908, On the application of quantitative methods to the study of the structure and history of rocks. Qtly. J. Geol. Soc. London, 64:171-233.

Spurr, J.E., 1894, False bedding in stratified drift deposits. Am. Geologist, 13:43-47, 201-206.

Stanley, D.J. and Kelling, G., 1967, Sedimentation patterns in the Wilmington submarine canyon area. Trans. Marine Technology Soc., Philadelphia, March 19-20, 127-142.

Walker, R.G., 1963, Distinctive types of ripple-drift cross-lamination. Sedimentology, 2:173-188.

_____, 1965, The origin and significance of the internal sedimentary structures of turbidites. Proc. Yorkshire Geol. Soc., 35: 1-32.

_____, 1967, Turbidite sedimentary structures and their relationship to proximal and distal depositional environments. J. Sed. Petrol., 37:25-43.

_____, 1969, Geometrical analysis of ripple-drift cross-lamination. Canadian Jour. Earth Sci., 6(3):383-391.

_____ and Sutton, R.G., 1967, Quantitative analysis of turbidites in the Upper Devonian Sonyea Group, New York. J. Sed. Petrol., 37(4):1012-1022.

Walton, E.K., 1967, The sequence of internal structures in turbidites. Scott. J. Geol., 3:306-317.

Wood, A. and Smith, A. J., 1959, The sedimentation and sedimentary history of the Aberystwyth Grits (Upper Llandoverian). Q. J. Geol. Soc. London, 114:163-190.

Woodworth, J. B., 1901, Original micaceous cross-banding of strata by current action. Amer. Geologist, 27:281-283.

APPENDIX

APPENDIX 1A: SPECIMEN DATA SHEET

DATE: Aug. 23, 1969

LOCALITY — Grande Vallée

BED NO. 2 | POSITION ON BED 104' west of 0' point

BED THICKNESS Cm. | A = 0 | B = 6·0 | C = 11·0 | INTER = 36·0

ANGLE OF CLIMB

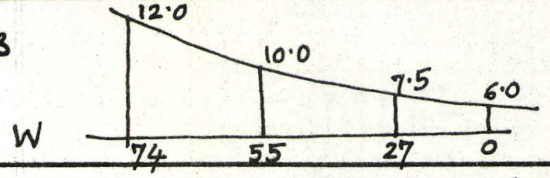

heights from base of the bed.

DIRECTION (RIPPLES): (MAGNETIC) N 69° W

SOLE MARKS: DIRECTION (MAG.) N 66° W

L-ridges with small cuspate crossing bars.

NOTES: Angle of climb low.
Stoss laminae often truncated near the base.
Troughs are highly clayey.

NOTES: Coarsest grain appear to be near the crest.

PHOTOS: Roll-21 No. 6.

SPECIMENS:

POSITION WITHIN BED	6·0/0	7·5/27·0	10·0/55·0	12·0/74·0
WAVELENGTH	25·0	25·5	27·0	32·0
AMPLITUDE	1·4	1·6	1·3	1·6
STOSS ANGLE	0·8/11·6	0·8/9·5	1·7/18·0	2·1/17·1
LEE ANGLE	4·1/11·6	5·6/9·5	4·3/18·0	3·4/11·1
STOSS THICKNESS	0·15	0·2	0·25	0·2
LEE THICKNESS	1·2	2·0	1·8	0·8
RIPPLE SHAPE 0	0	0	0	0
5	1·2	1·5	0·6	0·9
10	1·0	1·4	1·3	1·6
15	0·6	0·95	0·9	1·4
20	0·35	0·4	0·5	1·0
25		0·05	0·1	0·55
30				0·1
35				
40				
45				
50				
55				
60				
65				
70				
75				
80				
85				
90				
L. TO CREST	6·0	5·5	9·0	8·5
AMP	1·4	1·6	1·3	1·6

Lee Length

KEY TO APPENDIX 1B (ANGLE OF CLIMB)

Columns	Format	Content
1-4	I4	Bed Number
5-10	F6.1	Position on Bed
11-45	7F5.1	Horizontal distances from the 'Position on Bed'
46-80	7F5.1	Vertical distances at points corresponding to Horizontal distances (in the same order)

Note, 999.9 is a false figure; ignore it.

APPENDIX 1B: ANGLE OF CLIMB

ST. MAURICE (NORTH OF CHURCH)

477	0.0	0.0	18.0	46.0	57.0	99.9	99.9	99.9	9	53.5	58.5	68.0	76.0	99.9	99.9	99.9	9
477	50.0	0.0	12.0	47.5	89.5	99.9	99.9	99.9	9	51.0	53.5	62.5	72.0	99.9	99.9	99.9	9
477	70.0	0.0	53.0	90.0	110.0	99.9	99.9	99.9	9	36.0	48.5	59.3	71.7	99.9	99.9	99.9	9
477	100.0	0.0	64.0	104.0	99.9	99.9	99.9	99.9	9	45.0	59.0	76.5	99.9	99.9	99.9	99.9	9
477	130.0	0.0	28.0	58.0	124.0	99.9	99.9	99.9	9	41.5	49.0	59.0	68.0	99.9	99.9	99.9	9
477	162.0	0.0	4.5	31.0	53.0	99.9	99.9	99.9	9	54.0	55.5	66.5	70.0	99.9	99.9	99.9	9
477	190.0	0.0	43.0	90.0	123.0	99.9	99.9	99.9	9	47.5	52.0	58.0	76.0	99.9	99.9	99.9	9
477	218.0	0.0	8.5	46.5	99.0	99.9	99.9	99.9	9	44.5	46.5	66.3	77.7	99.9	99.9	99.9	9
477	261.0	0.0	36.5	58.5	91.5	99.9	99.9	99.9	9	39.5	50.0	58.0	71.5	99.9	99.9	99.9	9
477	299.0	0.0	23.5	51.0	93.5	99.9	99.9	99.9	9	43.0	51.0	61.5	69.0	99.9	99.9	99.9	9
477	330.0	0.0	29.0	49.0	81.0	99.9	99.9	99.9	9	45.0	50.0	58.5	75.0	99.9	99.9	99.9	9
477	387.0	0.0	29.5	64.0	94.0	99.9	99.9	99.9	9	44.5	49.5	56.0	71.5	99.9	99.9	99.9	9
477	421.0	0.0	36.0	74.5	103.0	99.9	99.9	99.9	9	50.0	56.0	64.0	71.0	99.9	99.9	99.9	9
477	452.0	0.0	11.0	45.0	75.0	115.0	131.0	99.9	9	38.3	39.5	43.0	46.0	49.5	56.0	99.9	9
477	479.0	0.0	8.0	31.0	55.0	99.9	99.9	99.9	9	48.5	50.5	59.5	71.0	99.9	99.9	99.9	9
477	525.0	0.0	24.0	55.0	95.0	99.9	99.9	99.9	9	48.5	55.0	66.0	74.0	99.9	99.9	99.9	9
477	555.0	0.0	11.0	76.0	98.0	99.9	99.9	99.9	9	55.6	56.0	59.0	68.5	99.9	99.9	99.9	9
477	646.0	0.0	21.0	36.0	70.0	99.9	99.9	99.9	9	42.5	51.0	58.5	73.0	99.9	99.9	99.9	9
477	682.0	0.0	19.5	37.0	58.0	99.9	99.9	99.9	9	43.0	48.5	55.0	62.0	99.9	99.9	99.9	9
477	717.0	0.0	9.0	62.0	126.0	99.9	99.9	99.9	9	49.5	51.0	63.0	71.5	99.9	99.9	99.9	9
477	763.0	0.0	20.0	85.0	126.0	99.9	99.9	99.9	9	42.5	45.0	53.5	66.5	99.9	99.9	99.9	9
477	798.0	0.0	14.0	62.0	101.0	99.9	99.9	99.9	9	47.0	49.0	56.0	67.0	99.9	99.9	99.9	9
477	837.0	0.0	22.5	55.5	76.0	99.9	99.9	99.9	9	36.5	42.0	53.0	64.0	99.9	99.9	99.9	9
477	900.0	0.0	19.0	43.5	67.5	99.9	99.9	99.9	9	47.0	51.0	58.5	66.0	99.9	99.9	99.9	9

WEST OF FAME POINT

666	0.0	0.0	25.0	99.9	99.9	99.9	99.9	99.9	9	0.0	2.5	99.9	99.9	99.9	99.9	99.9	9
700	0.0	0.0	27.2	99.9	99.9	99.9	99.9	99.9	9	0.0	1.8	99.9	99.9	99.9	99.9	99.9	9
701	0.0	0.0	40.0	99.9	99.9	99.9	99.9	99.9	9	0.0	3.7	99.9	99.9	99.9	99.9	99.9	9
702	0.0	0.0	30.0	99.9	99.9	99.9	99.9	99.9	9	0.0	5.7	99.9	99.9	99.9	99.9	99.9	9
759	0.0	0.0	23.9	99.9	99.9	99.9	99.9	99.9	9	0.0	1.9	99.9	99.9	99.9	99.9	99.9	9
765	0.0	0.0	23.0	99.9	99.9	99.9	99.9	99.9	9	0.0	2.0	99.9	99.9	99.9	99.9	99.9	9
772	0.0	0.0	39.0	44.0	99.9	99.9	99.9	99.9	9	0.6	3.2	3.3	99.9	99.9	99.9	99.9	9
773	0.0	0.0	48.0	99.9	99.9	99.9	99.9	99.9	9	1.4	3.8	99.9	99.9	99.9	99.9	99.9	9
774	0.0	0.0	30.5	46.5	99.9	99.9	99.9	99.9	9	1.0	3.5	3.8	99.9	99.9	99.9	99.9	9
790	0.0	0.0	28.5	99.9	99.9	99.9	99.9	99.9	9	0.0	2.4	99.9	99.9	99.9	99.9	99.9	9
791	0.0	0.0	55.0	99.9	99.9	99.9	99.9	99.9	9	0.0	7.5	99.9	99.9	99.9	99.9	99.9	9
793	0.0	0.0	35.0	99.9	99.9	99.9	99.9	99.9	9	0.0	4.2	99.9	99.9	99.9	99.9	99.9	9
794	0.0	0.0	30.5	99.9	99.9	99.9	99.9	99.9	9	0.0	1.9	99.9	99.9	99.9	99.9	99.9	9
795	0.0	0.0	25.5	99.9	99.9	99.9	99.9	99.9	9	0.0	2.8	99.9	99.9	99.9	99.9	99.9	9
798	0.0	0.0	29.5	99.9	99.9	99.9	99.9	99.9	9	0.0	3.1	99.9	99.9	99.9	99.9	99.9	9
799	0.0	0.0	30.0	99.9	99.9	99.9	99.9	99.9	9	0.0	2.1	99.9	99.9	99.9	99.9	99.9	9
800	0.0	0.0	26.5	99.9	99.9	99.9	99.9	99.9	9	0.0	1.5	99.9	99.9	99.9	99.9	99.9	9
801	0.0	0.0	26.5	99.9	99.9	99.9	99.9	99.9	9	0.0	2.1	99.9	99.9	99.9	99.9	99.9	9
899	0.0	0.0	24.5	39.5	99.9	99.9	99.9	99.9	9	9.2	15.3	19.5	99.9	99.9	99.9	99.9	9
1013	0.0	0.0	52.0	99.9	99.9	99.9	99.9	99.9	9	0.0	4.5	99.9	99.9	99.9	99.9	99.9	9
1014	0.0	0.0	28.0	99.9	99.9	99.9	99.9	99.9	9	0.0	2.5	99.9	99.9	99.9	99.9	99.9	9
1015	0.0	0.0	58.0	99.9	99.9	99.9	99.9	99.9	9	0.0	3.6	99.9	99.9	99.9	99.9	99.9	9
1021	0.0	0.0	23.5	99.9	99.9	99.9	99.9	99.9	9	0.0	3.0	99.9	99.9	99.9	99.9	99.9	9
1030	0.0	0.0	126.0	99.9	99.9	99.9	99.9	99.9	9	0.0	5.5	99.9	99.9	99.9	99.9	99.9	9
1031	0.0	0.0	50.0	99.9	99.9	99.9	99.9	99.9	9	0.0	3.0	99.9	99.9	99.9	99.9	99.9	9
1033	0.0	0.0	70.0	99.9	99.9	99.9	99.9	99.9	9	0.0	7.3	99.9	99.9	99.9	99.9	99.9	9
1034	0.0	0.0	34.0	99.9	99.9	99.9	99.9	99.9	9	0.0	1.3	99.9	99.9	99.9	99.9	99.9	9
1035	0.0	0.0	70.0	99.9	99.9	99.9	99.9	99.9	9	0.0	2.8	99.9	99.9	99.9	99.9	99.9	9
1036	0.0	0.0	40.0	99.9	99.9	99.9	99.9	99.9	9	0.0	1.8	99.9	99.9	99.9	99.9	99.9	9
1038	0.0	0.0	55.0	99.9	99.9	99.9	99.9	99.9	9	0.0	4.0	99.9	99.9	99.9	99.9	99.9	9

PETITE VALLEE HARBOUR,EAST.

1	0.0	0.0	37.0	82.0	92.0111	.0133	.0999	.9	4.3	9.5	13.0	16.8	20.5	27.0999.9
2	0.0	0.0	37.0	71.0	89.0106	.0122	.0999	.9	9.0	14.5	22.5	30.0	35.5	44.0999.9
3	0.0	0.0	20.0	38.0	60.0999	.9999	.9999	.9	11.5	15.5	19.5	32.5999	.9999	.9999.9
4	0.0	0.0	16.0	26.0	32.0999	.9999	.9999	.9	0.0	1.2	4.1	5.8999	.9999	.9999.9
5	10.0	0.0	44.0	75.0999	.9999	.9999	.9999	.9	16.0	27.0	38.0999	.9999	.9999	.9999.9
5	31.0	0.0	87.5	138.0169	.0999	.9999	.9999	.9	15.5	24.0	33.0	39.0999	.9999	.9999.9
5	48.0	0.0	58.0	95.0162	.0198	.0999	.9999	.9	10.5	17.5	24.0	31.0	37.5999	.9999.9
5	76.5	0.0	56.0	96.0142	.0999	.9999	.9999	.9	15.5	19.5	28.0	33.0999	.9999	.9999.9
5	102.6	0.0	19.0	36.0	74.0999	.9999	.9999	.9	18.0	23.0	28.0	32.0999	.9999	.9999.9
5	112.3	0.0	28.0	54.0	80.0999	.9999	.9999	.9	21.0	23.0	27.0	34.0999	.9999	.9999.9
5	130.8	0.0	48.0	82.0114	.0999	.9999	.9999	.9	15.5	26.0	30.0	32.0999	.9999	.9999.9
5	148.0	0.0	28.0	54.0	93.0999	.9999	.9999	.9	19.0	23.0	30.0	34.0999	.9999	.9999.9
5	164.0	0.0	29.0	57.0	77.0100	.0999	.9999	.9	22.0	22.5	24.0	33.5	39.5999	.9999.9
5	177.5	0.0	26.0	45.0	68.0	84.0999	.9999	.9	21.0	24.0	26.5	33.0	34.5999	.9999.9
5	192.2	0.0	30.0	46.5	52.0	58.0	73.0	85.5	17.0	20.5	23.5	27.2	29.0	32.0 33.5
5	200.4	0.0	15.0	43.0	60.0	86.0999	.9999	.9	19.0	21.0	25.5	29.5	32.0999	.9999.9
5	212.5	0.0	40.0	56.0	72.0106	.0999	.9999	.9	16.5	20.5	23.0	28.0	35.0999	.9999.9
5	261.0	0.0	32.0	46.0	58.0	77.0103	.0124	.0	17.0	18.4	19.5	20.2	24.0	34.5 38.5
5	277.0	0.0	33.0	52.0	81.0	94.0105	.0999	.9	19.0	20.5	22.5	26.0	27.0	31.0999.9
5	293.0	0.0	25.0	43.0	73.0100	.0140	.0999	.9	15.0	16.5	18.5	25.0	31.0	35.0999.9
5	322.0	0.0	35.0	53.0	74.0	98.0130	.0999	.9	16.5	20.0	23.0	26.0	33.0	38.0999.9
6	0.0	0.0	9.0	24.5	34.0999	.9999	.9999	.9	0.0	1.3	2.0	2.5999	.9999	.9999.9
7	30.0	0.0	31.0	71.0	96.0113	.0999	.9999	.9	11.5	13.5	15.5	20.5	25.0999	.9999.9
7	41.0	0.0	42.0	93.0128	.0999	.9999	.9999	.9	4.0	9.5	19.0	24.5999	.9999	.9999.9
7	49.0	0.0	35.0	80.0120	.0999	.9999	.9999	.9	7.0	9.5	15.0	23.0999	.9999	.9999.9
7	71.0	0.0	41.0	95.0114	.0999	.9999	.9999	.9	4.3	7.5	16.0	20.0999	.9999	.9999.9
7	95.8	0.0	33.0	68.0110	.0999	.9999	.9999	.9	3.0	6.5	9.0	20.0999	.9999	.9999.9
7	119.3	0.0	58.5	92.0119	.0999	.9999	.9999	.9	3.5	9.0	13.5	18.5999	.9999	.9999.9
7	131.0	0.0	44.0	75.0105	.0128	.0999	.9999	.9	3.3	10.5	15.0	16.8	22.0999	.9999.9
7	146.0	0.0	63.0	105.0137	.0999	.9999	.9999	.9	3.0	9.0	15.5	21.5999	.9999	.9999.9
7	164.3	0.0	42.0	84.0109	.0142	.0999	.9999	.9	1.2	3.2	7.0	11.5	18.5999	.9999.9
7	180.7	0.0	46.0	70.0110	.0154	.0999	.9999	.9	4.0	8.0	12.5	18.2	21.5999	.9999.9
7	200.0	0.0	20.5	39.5	63.0	94.0105	.0999	.9	5.5	8.0	9.5	13.5	20.5	22.5999.9
7	214.0	0.0	47.0	87.0109	.0126	.0999	.9999	.9	1.5	6.5	14.0	17.5	20.5999	.9999.9
7	234.5	0.0	30.0	59.0	97.0123	.0999	.9999	.9	3.5	7.0	12.5	16.5	20.5999	.9999.9
7	259.0	0.0	27.0	51.5	77.0100	.0999	.9999	.9	0.0	3.0	7.0	13.0	16.0999	.9999.9
7	278.0	0.0	33.0	80.0129	.0999	.9999	.9999	.9	7.5	9.5	14.0	20.5999	.9999	.9999.9
7	306.0	0.0	16.0	36.0	55.0	84.0999	.9999	.9	3.5	5.5	9.5	11.5	18.0999	.9999.9
7	320.0	0.0	17.0	39.0	52.0	86.0109	.0999	.9	0.2	4.5	7.0	9.3	16.0	20.2999.9
8	43.0	0.0	35.0	55.0	69.0	83.0	98.0999	.9	0.0	3.0	3.8	6.0	8.5	12.0999.9
8	62.0	0.0	19.0	47.0	61.0	71.0999	.9999	.9	0.0	0.5	2.2	6.2	9.5999	.9999.9
8	151.0	0.0	23.0	38.0	61.0999	.9999	.9999	.9	6.5	8.5	10.5	17.5999	.9999	.9999.9
8	172.0	0.0	31.0	62.0999	.9999	.9999	.9999	.9	0.5	3.4	6.5999	.9999	.9999	.9999.9
8	182.8	0.0	25.5	38.0	48.0999	.9999	.9999	.9	0.0	1.5	3.2	3.5999	.9999	.9999.9
8	187.8	0.0	16.0	35.0	58.0999	.9999	.9999	.9	0.0	1.0	2.5	6.0999	.9999	.9999.9
8	194.7	0.0	38.0	90.5	106.0999	.9999	.9999	.9	1.5	4.5	11.5	14.5999	.9999	.9999.9
8	203.0	0.0	48.0	90.0122	.0190	.0999	.9999	.9	0.0	0.5	5.0	9.5	19.0999	.9999.9
8	209.0	0.0	23.0	50.0	81.0999	.9999	.9999	.9	3.0	5.5	11.5	19.5999	.9999	.9999.9
8	215.8	0.0	41.0	71.0	81.0116	.0999	.9999	.9	0.0	2.5	9.7	12.5	17.0999	.9999.9
8	223.0	0.0	40.0	62.5	85.0114	.0999	.9999	.9	0.0	2.3	6.0	9.5	12.0999	.9999.9
8	228.0	0.0	38.0	69.0	82.0999	.9999	.9999	.9	0.0	4.0	10.5	12.5999	.9999	.9999.9

```
   9 449.0   0.0 55.0104.0131.0178.0999.9999.9   0.0   9.0 21.5 27.5 30.0999.9999.9
   9 484.0   0.0 60.0169.0211.0284.0374.0999.9   0.0   4.5 20.0 26.0 30.0 48.0999.9
   9 528.0   0.0 30.0 86.0154.0191.0250.0999.9   0.0   4.0 21.5 42.0 49.0 57.0999.9
   9 562.0   0.0 34.0 72.0116.0180.0270.0999.9   0.0   1.5 14.0 32.0 36.0 53.0999.9
   9 587.0   0.0 52.0102.0179.0238.0282.0999.9   0.0   7.0 18.5 34.0 45.0 58.0999.9
   9 607.0   0.0 40.0 84.0111.0151.0185.0224.0   0.0  12.5 17.5 29.5 39.0 49.0 55.0
   9 630.0   0.0 20.0 67.0101.0122.0149.0999.9   0.0   1.8 17.5 34.0 44.0 53.0999.9
   9 647.0   0.0 56.0105.0153.0204.0259.0999.9   0.0  14.0 22.5 33.5 48.0 62.0999.9
   9 667.0   0.0 35.0 90.0138.0164.0232.0273.0   0.0   3.5 12.5 23.5 35.0 57.0 65.5
   9 691.0   0.0 78.0114.0169.0197.0230.0276.0   0.0  13.0 20.5 31.0 38.5 46.0 53.0

  10   0.0   0.0 40.0155.0196.0232.0999.9999.9   0.0   4.7 13.0 21.0 26.0999.9999.9
  10  70.0   0.0 52.0 95.0150.0999.9999.9999.9   5.5   8.5 14.0 24.0999.9999.9999.9
  10 130.0   0.0 31.0 50.0109.0999.9999.9999.9   5.0  11.0 19.5 23.0999.9999.9999.9
  10 250.0   0.0 26.0 39.0999.9999.9999.9999.9   6.0  10.5 15.5999.9999.9999.9999.9

EAST OF ANSE A MERCIER, GRANDE VALLEE
   1  90.0   0.0 84.0999.9999.9999.9999.9999.9   0.0  11.2999.9999.9999.9999.9999.9

   2 104.0   0.0 27.0 55.0 74.0999.9999.9999.9   6.0   7.5 10.0 12.0999.9999.9999.9
   2 128.0   0.0 24.5 52.5 85.0101.0999.9999.9   0.0   7.3  8.0 11.1 13.2999.9999.9
   2 154.0   0.0  8.5 77.0103.0125.0999.9999.9   0.0   5.4  9.5 11.0 13.5999.9999.9
   2 180.0   0.0 35.5 97.0114.0999.9999.9999.9   5.2   6.3 11.0 13.0999.9999.9999.9
   2 214.0   0.0 69.0111.0132.0999.9999.9999.9   4.0   7.4 11.2 14.5999.9999.9999.9

   3   0.0   0.0 16.0 45.0 92.0999.9999.9999.9   4.7   5.6  9.0 12.5999.9999.9999.9

ANSE A MERCIER WEST, GRANDE VALLEE
   4   0.0   0.0 68.0 85.0112.0999.9999.9999.9  20.0  41.0 57.0 63.0999.9999.9999.9

   5   0.0   0.0 24.0113.0265.0999.9999.9999.9  16.0  23.0 41.0 52.0999.9999.9999.9

   6   0.0   0.0 62.0114.0170.0999.9999.9999.9  14.0  22.0 31.0 43.0999.9999.9999.9

GRANDE VALLEE HARBOUR, EAST
   7   0.0   0.0 50.0180.0999.9999.9999.9999.9  10.0  12.0 17.0999.9999.9999.9999.9

   8   0.0   0.0120.0290.0425.0999.9999.9999.9  24.0  31.0 35.0 52.0999.9999.9999.9
```

KEY TO APPENDIX 1C (RAW DATA)

Columns	Format	Contents
1-4	I4	Bed Number
5-10	F6.1	Position on Bed
11-15	F5.1	Horizontal distance (from the 'Position on Bed') for locating the 'Position within Bed'
16-20	F5.1	Vertical distance at the point corresponding to the horizontal distance
21-25	F5.1	Wave Length
26-30	F5.1	Amplitude
31-35	F5.1	Vertical distance for the measurement of stoss-angle
36-40	F5.1	Horizontal distance for the measurement of stoss-angle
41-45	F5.1	Vertical distance for the measurement of lee-angle
46-50	F5.1	Horizontal distance for the measurement of lee-angle
51-55	F5.2	t_S
56-60	F5.2	t_L
61-65	F5.1	Lee length

APPENDIX 1C: RAW DATA

ST MAURICE, NORTH OF CHURCH

477	0.0	25.5	0.0	51.0	4.0	5.0	22.3	7.5	16.8	0.45	1.10	14.0	1
477	0.0	37.0	0.0	30.0	2.9	3.5	11.8	5.1	14.0	1.20	4.50	12.0	1
477	0.0	58.5	18.0	31.0	2.2	3.1	18.5	6.0	16.0	0.50	1.60	9.0	1
477	0.0	68.0	46.0	65.0	4.8	2.7	14.0	2.9	12.3	0.60	1.30	32.0	1
477	0.0	76.0	57.0	68.0	1.8	1.5	14.0	1.8	12.3	0.80	1.10	29.0	1
477	50.0	23.0	0.0	44.0	3.0	4.5	17.2	5.9	19.3	1.50	5.40	17.0	1
477	50.0	40.5	0.0	28.0	2.1	3.9	24.4	4.0	17.3	0.10	1.20	12.0	1
477	50.0	53.0	12.0	32.5	1.9	4.0	23.2	4.2	18.2	0.20	0.70	12.0	1
477	50.0	62.5	47.5	36.5	2.3	4.0	31.5	5.5	16.8	0.20	0.95	9.5	1
477	50.0	72.0	89.5	41.0	2.1	2.6	19.2	3.5	12.7	0.15	0.55	19.0	1
477	70.0	7.3	0.0	36.5	1.8	2.4	17.5	5.1	17.0	0.30	1.40	8.0	1
477	70.0	23.7	0.0	27.0	1.6	2.5	20.0	6.6	20.0	0.25	1.50	8.5	1
477	70.0	48.5	53.0	34.0	1.8	4.5	29.0	6.1	29.0	2.50	4.70	11.0	1
477	70.0	59.3	90.0	27.0	1.9	4.1	27.0	7.3	27.0	1.00	3.20	9.0	1
477	70.0	71.7	110.0	46.0	1.8	1.6	15.0	2.2	15.0	1.10	1.90	20.0	1
477	100.0	7.5	0.0	39.0	4.1	8.0	29.3	14.1	29.3	0.60	1.50	14.5	1
477	100.0	29.5	0.0	26.0	1.9	4.8	20.0	4.8	20.0	0.30	1.20	12.0	1
477	100.0	45.0	0.0	31.0	2.2	3.3	18.4	5.3	18.4	1.10	4.20	13.5	1
477	100.0	59.0	64.0	39.5	2.6	4.1	21.3	4.7	21.3	0.60	1.90	16.5	1
477	100.0	76.5	104.0	40.0	1.8	2.5	17.2	2.8	17.2	1.10	2.80	18.0	1
477	130.0	10.5	0.0	41.0	3.3	3.6	19.0	6.6	15.0	0.90	2.70	12.0	1
477	130.0	32.5	0.0	34.0	2.5	5.3	24.0	7.5	24.0	0.60	1.90	12.0	1
477	130.0	49.0	28.0	35.5	2.1	2.3	19.3	3.7	19.3	0.80	1.80	12.5	1
477	130.0	59.0	58.0	43.5	4.6	3.4	16.8	6.9	16.8	0.90	3.00	19.5	1
477	130.0	68.0	124.0	63.0	4.2	2.5	19.6	4.5	19.6	1.30	3.00	27.0	1
477	162.0	14.0	0.0	43.0	3.0	4.2	23.5	7.5	23.5	0.20	2.00	13.5	1
477	162.0	28.3	0.0	33.0	2.0	3.0	25.0	5.0	25.0	0.40	1.30	10.5	1
477	162.0	55.5	4.5	31.0	2.9	3.9	20.0	6.7	20.0	0.45	2.30	9.5	1
477	162.0	66.5	31.0	44.5	3.2	3.7	17.8	6.6	17.8	0.50	2.10	16.0	1
477	162.0	70.0	53.0	51.0	3.3	4.4	20.0	4.4	19.0	0.30	1.10	17.0	1
477	190.0	17.0	0.0	31.5	2.0	2.8	20.0	5.2	23.3	0.15	1.90	11.0	1
477	190.0	32.0	0.0	32.5	2.7	4.2	26.2	6.0	19.0	0.25	1.60	12.2	1
477	190.0	52.0	43.0	40.5	3.2	4.5	20.0	6.3	25.0	0.20	3.00	14.5	1
477	190.0	58.0	90.0	33.0	2.8	4.8	21.8	6.5	23.1	2.00	4.20	16.0	1
477	190.0	76.0	123.0	47.0	1.6	2.7	30.5	3.2	19.3	0.10	1.50	14.5	1
477	218.0	20.5	0.0	34.0	2.1	4.8	28.7	6.8	28.7	0.20	1.50	10.0	1
477	218.0	33.0	0.0	27.5	1.5	2.2	23.3	6.0	23.3	0.10	1.90	10.5	1
477	218.0	46.5	8.5	50.5	2.8	3.1	19.0	3.4	19.8	0.70	2.00	23.5	1
477	218.0	66.3	46.5	51.0	2.8	4.8	26.3	4.5	21.5	0.65	2.70	18.0	1
477	218.0	77.7	99.0	47.0	1.7	2.2	23.5	3.3	23.5	0.10	0.50	22.0	1
477	261.0	9.0	0.0	33.0	1.9	1.8	17.0	3.3	17.0	0.25	1.00	10.2	1
477	261.0	32.5	0.0	32.5	2.6	2.2	19.7	5.3	19.7	1.10	6.80	10.3	1
477	261.0	50.0	36.5	36.0	3.2	2.2	12.5	2.9	12.5	0.80	2.30	14.0	1
477	261.0	58.0	58.5	37.0	3.1	3.0	19.2	6.5	19.2	0.20	1.00	11.0	1
477	261.0	71.5	91.5	41.0	2.8	2.9	17.0	3.5	17.0	0.90	1.60	17.5	1
477	299.0	18.5	0.0	36.5	2.4	2.8	17.5	3.7	17.5	0.25	1.25	15.2	1
477	299.0	32.5	0.0	28.5	1.9	2.7	25.0	4.7	25.0	0.40	1.25	10.0	1
477	299.0	51.0	23.5	29.0	2.0	3.5	21.8	8.5	21.8	0.30	1.50	10.5	1
477	299.0	61.5	51.0	52.0	5.2	3.3	17.5	7.6	12.5	0.90	3.00	20.0	1
477	299.0	69.0	93.5	53.0	3.8	3.1	13.0	4.9	13.4	0.55	1.85	18.0	1
477	330.0	13.0	0.0	29.5	1.3	0.6	15.0	2.7	15.0	0.35	1.50	10.5	1
477	330.0	35.0	0.0	25.0	1.4	2.2	16.0	3.7	16.0	0.20	1.40	9.2	1
477	330.0	50.0	29.0	29.5	2.2	3.2	25.8	6.9	25.8	0.40	2.20	11.3	1
477	330.0	58.5	49.0	34.5	1.9	4.1	22.2	5.6	22.2	0.30	1.30	11.2	1
477	330.0	75.0	81.0	42.0	1.8	1.3	11.7	3.9	11.7	0.80	2.90	11.5	1
477	387.0	10.5	0.0	25.0	1.4	2.5	23.0	5.4	23.0	0.15	1.00	8.2	1
477	387.0	30.5	0.0	22.5	1.5	2.7	17.2	4.3	17.2	0.15	1.20	7.0	1
477	387.0	49.5	29.5	30.0	2.3	2.6	15.2	4.5	15.2	0.70	2.70	11.2	1
477	387.0	56.0	64.0	34.0	2.0	2.9	16.7	3.7	16.7	0.50	1.60	12.5	1
477	387.0	71.5	94.0	35.5	1.8	1.8	13.6	3.3	10.9	1.20	2.00	11.5	1

477	421.0	10.5	0.0	25.5	1.5	1.5	17.2	4.1	17.2	0.30	1.10	6.5	1
477	421.0	42.0	0.0	24.0	1.7	1.6	15.8	5.1	15.8	0.30	1.30	7.0	1
477	421.0	56.0	3.0	28.0	1.5	2.1	17.0	4.3	17.0	0.25	2.25	6.0	1
477	421.0	64.0	41.5	37.0	2.2	2.8	17.0	5.1	17.2	0.35	1.60	9.5	1
477	421.0	71.0	70.0	45.0	3.4	2.9	19.0	5.3	19.0	0.80	1.70	18.5	1
477	452.0	39.5	11.0	26.5	1.1	1.0	20.2	3.7	20.2	1.10	4.00	7.5	1
477	452.0	43.0	45.0	33.5	1.8	1.9	19.2	4.7	19.2	0.80	4.10	11.7	1
477	452.0	46.0	75.0	35.0	1.6	2.7	28.4	6.5	28.4	1.30	3.50	11.5	1
477	452.0	49.5	115.0	48.4	2.0	1.6	21.0	7.1	21.0	0.50	1.80	10.8	1
477	452.0	56.0	131.0	20.0	1.5	2.1	17.0	4.6	17.0	0.60	1.25	7.5	1
477	479.0	14.5	0.0	43.0	1.7	1.4	12.0	2.9	12.0	0.25	0.95	12.5	0
477	479.0	36.5	0.0	23.0	1.4	3.1	22.8	5.0	22.8	0.15	0.75	7.5	1
477	479.0	50.5	8.0	39.0	2.7	5.1	31.5	8.9	31.5	0.85	3.00	13.5	1
477	479.0	59.5	31.0	59.0	3.4	3.1	21.1	6.4	17.2	0.70	3.40	12.0	1
477	479.0	71.0	55.0	50.0	2.8	5.0	21.0	8.7	21.0	0.40	1.30	12.0	1
477	525.0	8.5	0.0	35.0	2.5	2.5	15.0	3.7	15.0	0.70	5.80	11.0	1
477	525.0	32.0	0.0	30.0	2.3	4.0	23.8	8.8	23.8	0.50	2.50	8.2	1
477	525.0	55.0	24.0	33.5	2.2	1.3	11.5	3.0	11.5	1.80	4.50	11.0	1
477	525.0	66.0	55.0	35.0	3.1	3.1	14.3	5.8	16.3	1.10	4.30	13.0	1
477	525.0	74.0	95.0	38.5	1.9	1.5	13.5	4.8	10.5	0.80	2.30	10.5	0
477	555.0	15.5	0.0	25.0	2.0	3.8	19.6	3.6	12.0	0.15	1.30	9.0	1
477	555.0	29.5	0.0	29.0	2.0	3.8	24.4	5.0	16.6	0.80	2.80	8.5	1
477	555.0	56.0	11.0	27.0	1.6	2.8	20.8	5.2	20.8	0.60	2.50	8.5	1
477	555.0	59.0	76.0	45.0	4.3	3.8	16.0	3.5	8.5	0.80	4.00	21.0	1
477	555.0	68.5	98.0	45.0	3.7	2.2	12.1	3.1	12.1	1.00	4.00	17.5	1
477	646.0	17.5	0.0	57.0	2.0	2.6	22.5	5.2	20.3	0.25	1.00	20.0	1
477	646.0	30.0	0.0	35.0	2.2	2.8	21.5	7.4	21.5	0.20	1.30	10.5	1
477	646.0	51.0	21.0	43.0	2.1	4.4	29.4	6.3	28.4	0.70	2.85	10.5	1
477	646.0	58.5	36.0	39.0	4.2	2.9	15.0	6.4	15.0	0.80	4.50	12.5	1
477	646.0	73.0	70.0	43.0	2.7	3.0	17.2	6.5	17.2	0.50	2.30	11.0	1
477	682.0	11.0	0.0	33.5	2.0	2.5	15.0	3.6	15.0	0.20	1.10	8.0	1
477	682.0	29.5	0.0	25.5	1.7	3.8	25.0	7.2	25.0	0.30	2.30	7.5	1
477	682.0	48.5	19.5	25.0	2.1	2.6	16.5	5.2	16.5	0.80	2.70	8.0	1
477	682.0	55.0	37.0	28.0	2.5	2.5	16.6	4.3	16.6	0.30	2.00	9.5	1
477	682.0	62.0	58.0	27.5	1.7	2.6	16.0	3.7	16.0	0.40	1.30	9.0	1
477	717.0	12.5	0.0	33.5	2.4	2.6	18.0	2.7	12.0	0.25	2.20	12.5	1
477	717.0	34.5	0.0	27.5	1.6	2.2	16.5	7.1	18.0	0.40	2.10	6.8	1
477	717.0	51.0	9.0	27.5	1.5	1.6	18.9	4.6	18.9	0.20	1.40	7.5	1
477	717.0	63.0	62.0	36.5	4.0	2.6	15.3	6.5	11.0	0.40	3.50	8.5	1
477	717.0	71.5	126.0	38.5	3.9	2.6	16.4	5.7	11.5	0.60	2.40	9.5	1
477	763.0	37.0	0.0	24.5	2.0	2.4	17.0	4.5	17.0	0.60	1.90	7.5	1
477	763.0	45.0	20.0	31.5	2.9	3.2	17.7	4.7	10.5	0.40	2.70	8.0	1
477	763.0	53.5	85.0	34.0	4.4	4.8	19.8	9.9	17.0	1.70	6.20	11.5	1
477	763.0	66.5	126.0	44.0	4.1	3.5	16.0	8.7	14.5	1.40	4.40	10.0	1
477	798.0	14.5	0.0	29.5	1.5	0.8	10.2	4.2	10.2	0.60	2.40	7.5	1
477	798.0	29.5	0.0	27.0	2.0	2.4	15.3	4.3	16.3	0.10	0.70	9.5	1
477	798.0	49.0	14.0	35.0	2.1	1.7	14.0	5.1	14.0	0.50	1.30	7.5	1
477	798.0	56.0	62.0	32.0	2.2	1.5	15.8	4.0	15.8	1.10	3.90	9.5	1
477	798.0	67.0	101.0	35.0	2.0	2.0	18.0	5.2	18.0	1.10	3.50	12.0	1
477	837.0	16.0	0.0	33.0	2.1	2.1	20.3	4.4	20.3	0.60	2.00	11.5	1
477	837.0	35.0	0.0	23.0	1.4	2.4	13.8	3.7	13.8	0.50	2.40	7.0	1
477	837.0	42.0	22.5	28.0	1.8	2.5	16.5	4.4	16.5	1.50	5.70	8.5	1
477	837.0	53.0	55.5	31.0	1.4	1.4	13.8	3.6	13.8	0.60	2.20	7.0	1
477	837.0	64.0	76.0	35.0	1.4	2.6	23.3	7.8	23.3	0.60	2.40	6.7	1
477	900.0	31.5	0.0	27.2	1.9	3.1	22.0	6.4	22.0	0.70	4.00	9.0	1
477	900.0	51.0	19.0	31.5	1.8	3.3	24.0	5.0	17.5	0.55	2.25	8.3	1
477	900.0	58.5	43.5	31.0	1.5	1.8	15.3	4.2	15.3	0.70	2.80	7.5	1
477	900.0	66.0	67.0	32.0	1.7	2.0	15.2	4.3	15.2	0.80	3.00	9.7	1

WEST OF FAME POINT

666	0.0	0.7	7.0	25.5	1.0	0.9	13.2	4.0	13.2	0.20	1.60	6.2	1
666	0.0	5.0	50.0	34.0	1.1	1.5	15.8	4.2	14.1	0.15	2.10	8.2	1
666	0.0	9.5	95.0	34.0	1.6	1.1	14.8	5.1	14.8	0.20	2.00	10.0	1
700	0.0	0.4	5.4	25.0	1.3	1.3	20.0	6.0	14.7	0.15	1.40	5.5	1
700	0.0	3.6	54.5	28.5	1.2	1.4	21.8	4.0	11.2	0.30	2.60	7.5	1
700	0.0	8.0	120.0	37.0	0.8	0.6	16.7	3.5	16.7	0.20	1.80	7.0	1
701	0.0	0.4	4.0	31.0	1.3	1.8	18.0	5.2	18.0	0.30	2.80	7.2	1
701	0.0	3.7	40.0	33.0	1.3	1.0	14.0	3.3	14.0	0.25	2.10	7.6	1
701	0.0	7.1	80.0	38.0	0.9	1.2	16.0	3.6	16.0	0.15	0.65	8.0	1
702	0.0	6.3	33.0	20.0	0.6	0.8	12.2	3.0	12.2	0.15	1.30	5.0	1
702	0.0	9.5	50.0	24.0	0.8	0.9	13.8	4.8	13.8	0.20	0.75	4.5	1
702	0.0	12.8	66.0	35.0	0.6	0.5	14.8	3.3	14.8	0.10	0.60	3.5	1
759	0.0	0.7	9.0	20.0	0.8	1.0	14.3	2.9	12.1	0.20	1.20	6.2	1
759	0.0	2.6	33.5	21.5	0.7	1.0	14.0	3.2	14.0	0.10	0.70	5.0	1
759	0.0	5.7	71.5	34.0	0.6	0.6	13.0	2.9	13.0	0.20	0.95	6.0	1
765	0.0	1.0	11.5	25.0	1.2	0.9	14.0	4.4	14.0	0.25	1.40	5.5	1
765	0.0	3.0	44.0	30.0	1.5	0.4	7.2	2.3	5.4	0.20	1.40	5.5	1
765	0.0	7.0	80.0	44.0	0.8	0.5	15.6	4.1	15.6	0.30	1.50	7.0	1
772	0.0	0.7	11.0	24.0	0.7	1.0	17.0	6.5	17.0	0.30	2.70	4.5	1
772	0.0	2.8	45.0	36.0	1.0	1.2	22.1	8.6	21.1	0.45	2.80	6.0	1
772	0.0	4.6	74.0	42.0	0.8	0.6	13.0	5.1	13.0	0.20	1.25	7.0	1
773	0.0	0.5	9.8	31.0	0.7	0.6	16.0	3.6	16.0	0.15	1.60	5.0	1
773	0.0	2.4	48.0	39.0	0.9	1.1	21.0	2.5	7.6	0.15	1.00	6.0	1
773	0.0	4.0	79.5	56.0	0.8	0.4	14.7	3.1	14.7	0.20	1.30	7.5	1
774	0.0	1.0	0.0	24.0	0.9	0.9	14.2	4.5	14.2	0.15	1.10	4.5	1
774	0.0	2.0	24.5	29.0	1.0	0.9	12.2	2.8	12.2	0.20	1.20	7.0	1
774	0.0	3.8	46.5	42.0	1.0	0.8	18.6	4.8	18.6	0.25	1.20	7.5	1
790	0.0	0.8	8.9	35.0	0.8	0.8	20.0	6.6	20.0	0.10	1.05	4.5	1
790	0.0	4.3	51.3	46.0	0.9	1.1	23.6	7.6	23.6	0.25	1.70	5.5	1
790	0.0	8.2	103.0	59.0	0.6	0.9	25.0	6.8	25.0	0.15	1.10	6.0	1
791	0.0	0.7	5.5	28.0	0.8	0.4	11.1	3.1	11.1	0.15	1.20	4.5	1
791	0.0	7.5	55.0	34.0	1.2	0.6	12.1	5.0	12.1	0.25	1.40	6.0	1
791	0.0	13.7	99.9	43.0	1.2	0.8	15.4	4.1	15.4	0.15	0.85	7.5	1
793	0.0	0.4	3.5	30.0	0.7	0.5	15.2	4.5	15.2	0.30	3.40	4.0	1
793	0.0	4.6	38.5	32.0	1.2	0.9	14.4	5.9	14.4	0.20	1.60	5.0	1
793	0.0	9.5	78.5	37.0	0.9	0.7	16.5	3.8	16.5	0.15	1.40	6.5	1
794	0.0	1.1	18.3	26.0	1.0	0.9	14.5	4.6	14.5	0.20	1.60	5.0	1
794	0.0	2.5	40.0	32.0	1.1	1.0	16.5	5.9	16.5	0.20	1.10	5.5	1
794	0.0	7.6	122.0	49.0	0.8	0.4	17.5	3.3	17.5	0.15	1.45	6.0	1
795	0.0	1.4	12.7	29.0	1.1	1.1	13.4	4.6	13.4	0.20	1.70	5.0	1
795	0.0	5.6	51.0	34.0	1.4	1.0	15.3	7.2	15.3	0.20	1.00	5.0	1
795	0.0	9.9	90.0	50.0	1.0	0.7	17.1	4.3	17.1	0.25	1.10	7.0	1
798	0.0	3.1	29.5	26.0	1.0	1.0	15.0	6.2	15.0	0.15	1.10	4.0	1
798	0.0	8.0	75.0	35.0	0.7	0.6	15.0	3.7	15.0	0.20	1.70	5.0	1
799	0.0	0.2	3.0	20.5	0.6	0.8	14.8	3.4	14.7	0.10	0.70	4.5	1
799	0.0	2.9	42.5	31.0	1.0	0.7	14.1	5.1	14.1	0.30	1.85	5.5	1
799	0.0	5.7	84.0	38.0	0.9	0.8	18.3	5.3	18.3	0.15	0.90	5.0	1
800	0.0	0.3	5.3	23.0	1.0	1.0	17.8	5.4	18.8	0.15	1.95	6.0	1
800	0.0	1.8	31.8	27.5	1.0	1.0	17.6	2.9	8.2	0.15	1.80	5.5	1
800	0.0	4.5	78.0	39.0	0.8	0.8	20.6	4.3	20.6	0.25	1.60	6.5	1
801	0.0	0.7	8.0	41.0	0.8	0.6	12.8	2.7	9.8	0.20	1.35	5.0	1
801	0.0	4.2	53.0	53.0	1.1	0.7	19.8	6.9	19.8	0.25	1.60	5.5	1
801	0.0	6.3	79.5	66.0	1.0	0.7	16.3	4.4	16.3	0.35	1.80	6.5	1
899	0.0	9.2	0.0	30.0	0.7	0.9	15.0	3.4	15.0	0.40	1.60	5.8	1
899	0.0	15.3	24.5	34.5	1.2	1.4	17.0	5.2	17.0	0.70	2.50	6.0	1
899	0.0	19.5	39.5	35.0	1.4	1.2	17.0	5.0	17.0	1.30	2.70	9.5	1
1013	0.0	0.9	13.5	23.0	0.5	0.5	13.0	3.0	13.0	0.30	1.00	4.0	1
1013	0.0	2.5	28.0	31.0	1.6	0.8	12.0	2.1	6.2	0.30	2.50	7.5	1
1013	0.0	4.5	52.0	36.0	0.8	0.7	18.0	3.6	18.0	0.15	1.00	6.5	1
1014	0.0	0.0	0.0	30.0	0.5	0.6	17.4	4.1	17.4	0.15	0.80	5.5	1

1014	0.0	0.8	7.5	27.5	1.0	1.6	23.0	2.6	7.5	0.10	0.90	6.2	1
1014	0.0	1.6	24.0	34.0	0.7	0.5	15.8	3.7	15.8	0.10	0.70	7.5	1
1015	0.0	0.0	0.0	27.0	0.9	0.6	16.1	5.1	16.1	0.35	1.30	4.0	1
1015	0.0	1.9	22.2	29.5	1.2	1.5	23.6	1.8	6.4	0.10	0.75	7.7	1
1015	0.0	3.3	50.5	41.0	0.8	0.6	20.2	4.0	20.2	0.15	0.85	7.2	1
1021	0.0	1.5	12.0	17.0	0.5	0.4	9.2	1.8	9.2	0.15	0.60	5.0	1
1021	0.0	2.4	18.5	21.0	0.8	0.6	11.3	2.3	8.2	0.35	1.20	4.5	1
1021	0.0	4.0	31.5	25.0	0.6	0.4	12.7	3.2	12.7	0.20	0.75	4.5	1
1030	0.0	0.3	2.5	16.5	0.8	0.7	18.0	5.7	18.0	0.30	1.70	4.0	1
1030	0.0	2.2	50.5	25.0	0.7	0.4	9.0	2.8	9.0	0.35	2.50	5.0	1
1030	0.0	5.0	114.0	32.0	0.6	0.5	11.5	2.9	11.5	0.25	2.00	5.5	1
1031	0.0	0.6	10.0	15.0	0.6	0.4	8.0	2.7	8.0	0.30	2.00	4.8	1
1031	0.0	2.2	36.0	17.5	0.8	0.7	11.0	3.4	10.8	0.35	2.80	5.2	1
1031	0.0	5.3	90.0	33.0	0.7	0.5	13.2	3.4	13.2	0.25	2.30	6.0	1
1033	0.0	0.7	0.0	17.0	0.6	0.8	14.0	4.1	14.0	0.45	1.70	4.0	0
1033	0.0	3.6	35.0	35.0	0.9	0.9	14.8	2.8	11.8	0.35	2.10	8.0	0
1033	0.0	7.3	70.0	47.0	0.7	0.5	11.2	2.0	11.2	0.30	1.40	8.5	0
1034	0.0	0.4	10.5	18.0	0.5	0.6	17.0	3.5	11.7	0.30	2.40	6.4	1
1034	0.0	2.6	68.0	21.0	0.6	0.4	11.6	3.9	11.7	0.20	2.00	5.2	1
1034	0.0	4.6	120.0	28.0	0.5	0.4	12.5	2.1	11.2	0.20	1.85	7.5	1
1035	0.0	0.3	7.0	25.0	0.8	0.5	17.0	1.7	9.0	0.15	1.40	7.5	1
1035	0.0	2.8	70.0	28.0	1.0	0.3	7.9	2.8	15.0	0.80	4.20	8.0	1
1035	0.0	4.0	99.0	34.0	0.8	0.4	10.0	2.3	10.0	0.45	2.30	9.8	1
1036	0.0	0.4	8.0	26.0	0.8	0.9	20.0	4.1	12.6	0.30	1.90	5.0	1
1036	0.0	1.8	40.0	36.0	0.7	0.6	12.0	2.9	12.0	0.15	1.20	6.5	1
1036	0.0	3.0	68.0	44.0	0.5	0.4	20.0	2.9	20.0	0.30	1.60	8.0	1
1038	0.0	0.3	4.0	22.5	1.0	0.8	12.0	3.2	15.0	0.25	2.10	4.5	1
1038	0.0	2.1	27.0	31.0	1.0	1.2	16.8	3.4	16.0	0.30	2.30	5.0	1
1038	0.0	4.0	55.0	38.0	0.8	1.1	15.5	2.9	15.0	0.10	0.60	6.0	1
PETITE VALLEE HARBOUR, EAST													
1	0.0	4.3	0.0	16.5	1.1	1.1	12.8	4.7	12.8	0.10	0.95	5.5	1
1	0.0	9.5	37.0	21.0	1.0	0.8	10.6	1.9	10.6	0.20	1.10	6.5	1
1	0.0	13.0	82.0	27.0	1.0	1.1	14.2	3.0	14.2	0.15	0.75	6.7	1
1	0.0	16.8	92.0	29.0	1.4	1.0	9.5	3.2	9.5	0.20	1.10	6.0	1
1	0.0	20.5	111.0	32.5	0.7	0.5	11.0	2.4	11.0	0.25	1.00	7.2	1
1	0.0	27.0	133.0	34.5	0.5	0.3	11.3	1.5	11.3	0.50	1.25	7.8	1
2	0.0	9.0	0.0	28.0	1.0	1.1	15.5	2.3	15.5	0.30	1.30	10.0	1
2	0.0	14.5	37.0	31.0	0.9	1.4	17.8	2.9	17.8	0.30	1.10	11.0	1
2	0.0	22.5	71.0	36.0	2.7	2.3	17.1	6.3	17.1	1.10	3.20	12.0	1
2	0.0	30.0	89.0	37.5	1.1	1.1	20.0	3.0	20.0	0.40	1.10	8.5	1
2	0.0	35.5	106.0	46.0	1.3	1.0	18.0	2.5	18.0	0.30	0.80	13.0	1
2	0.0	44.0	122.0	48.0	1.1	1.1	18.2	2.1	18.2	0.60	1.00	16.0	1
3	0.0	11.5	0.0	34.0	1.1	0.5	7.0	1.9	7.0	0.50	2.40	15.0	1
3	0.0	15.5	20.0	43.0	0.7	0.8	12.0	2.2	12.0	0.40	1.40	9.0	1
3	0.0	19.5	38.0	53.0	1.0	1.0	12.0	2.3	12.0	0.60	1.60	14.5	1
3	0.0	32.5	60.0	54.0	2.2	1.2	14.0	4.3	10.0	0.50	1.90	13.0	1
4	0.0	0.0	0.0	19.0	0.8	1.2	16.3	3.2	16.3	0.20	2.35	7.0	1
4	0.0	1.2	16.0	25.0	1.4	1.8	20.0	5.2	20.0	0.15	1.40	8.0	1
4	0.0	4.1	26.5	23.5	1.2	1.9	16.3	4.5	17.3	0.15	1.60	8.5	1
4	0.0	5.8	32.0	25.0	1.1	1.0	13.5	4.9	13.5	0.15	1.00	9.0	1
5	10.0	16.0	0.0	35.0	0.4	0.5	9.5	0.5	7.000	.2000	.35	13.5	1
5	10.0	27.0	44.0	53.0	1.6	1.0	10.5	0.8	3.000	.3000	.55	20.0	1
5	10.0	38.0	75.0	55.0	1.0	0.7	10.0	0.5	5.000	.3000	.45	21.5	1
5	31.0	15.5	0.0	48.0	0.5	2.1	30.5	2.3	28.000	.4000	.70	16.0	1
5	31.0	24.0	87.5	42.0	1.1	0.6	8.5	0.9	8.500	.2000	.60	15.5	1
5	31.0	33.0	138.0	34.0	1.5	0.7	10.0	1.2	10.000	.1000	.30	13.0	1

```
5  31.0 39.0169.0 62.0  1.5  1.0 15.0  1.5 10.000.1000.60 19.0 1
5  48.0 39.0192.0 71.0  0.9  1.0 40.0  1.0 30.000.0500.13 24.0 1
5  48.0 19.5 88.5 47.0  1.1  1.1 16.0  1.1 10.500.1500.20 18.0 1
5  48.0 26.5144.0 62.0  0.9  0.5 20.0  0.6 15.500.0500.15 22.0 1
5  48.0 10.5  0.0 32.0  1.1  1.0 10.0  0.8  4.000.1500.45  8.0 1
5  76.5 15.5  0.0 33.0  0.6  0.4  7.0  1.4  7.000.1000.20 12.0 1
5  76.5 19.5 56.0 45.0  1.5  0.3  6.0  1.3  6.000.1000.25 17.0 1
5  76.5 28.0 96.0 46.0  1.2  0.7 10.0  1.6 10.000.3000.50 19.0 1
5  76.5 33.0142.0 84.0  0.8  0.3 10.0  0.7 10.000.1000.15 37.0 1
5 102.8 18.0  0.0 41.0  0.7  0.5 10.0  1.5 10.000.6001.30 16.0 1
5 102.8 23.0 19.0 43.0  1.3  0.7 10.0  1.8  7.000.3000.90 15.0 1
5 102.8 28.0 36.0 40.0  1.2  0.6 10.0  1.7 10.000.2000.50 14.5 1
5 102.8 32.0 74.0 37.0  1.2  0.6 10.0  1.8 10.000.2000.45 13.0 1
5 112.3 21.0  0.0 48.0  1.1  0.2  7.0  1.3  7.000.3000.45 16.0 1
5 112.3 23.0 28.0 56.0  1.3  1.1 10.0  1.7 10.001.0002.50 20.0 1
5 112.3 27.0 54.0 62.0  1.5  0.8 10.0  1.5 10.000.7001.10 21.0 1
5 112.3 34.0 80.0 59.0  1.4  0.6 10.0  1.3 10.000.1500.40 17.0 1
5 130.8 15.5  0.0 28.0  0.6  0.2  4.3  0.5  4.300.3000.50 10.5 1
5 130.8 26.0 48.0 45.0  1.3  0.4  8.0  0.6  8.000.2000.35 17.0 1
5 130.8 30.0 82.0 71.0  3.7  0.6  8.0  1.2  8.000.8002.80 27.0 1
5 130.8 32.0114.0 68.0  0.9  0.3  8.0  0.6  8.000.5001.00 22.0 1
5 148.0 19.0  0.0 46.0  1.2  1.0 15.0  1.0 10.500.3000.50 17.0 1
5 148.0 23.0 28.0 44.0  1.7  0.5  6.5  0.9  6.500.3000.70 17.0 1
5 148.0 30.0 54.0 42.0  0.9  1.0 13.5  1.0  7.000.3000.60 11.5 1
5 148.0 34.0 93.0 38.0  0.6  0.5  8.5  1.0 10.001.0001.55 14.0 1
5 164.0 22.1  9.0 52.0  1.8  0.2 10.0  1.6 10.001.0001.50 16.5 1
5 164.0 24.5 26.5 55.0  2.2  0.6  9.5  1.9  9.500.2000.70 19.0 1
5 164.0 29.3 33.0 48.0  1.9  0.5  9.5  1.8  9.500.6001.25 18.0 1
5 164.0 38.0 65.5 49.0  0.8  0.2 12.0  1.4 12.000.1000.15 16.0 1
5 177.5 21.5  0.0 46.0  1.2  0.3  5.4  0.4  5.400.1000.25 16.0 1
5 177.5 26.0 26.0 49.0  1.1  0.5 10.0  0.9 10.000.4001.00 17.0 1
5 177.5 31.0 45.0 57.0  1.4  0.4  7.0  1.7  7.000.2500.85 14.0 1
5 177.5 35.0 68.0 47.0  1.6  1.0 17.0  1.0  4.500.0500.55 16.0 1
5 192.2 20.5  0.0 40.0  0.9  0.6 10.0  1.0 10.000.1000.15 16.0 1
5 192.2 23.5 16.5 37.0  1.3  0.9 10.0  1.3 10.000.1000.20 15.5 1
5 192.2 27.2 22.0 36.0  1.4  1.3 10.0  2.2 10.000.2500.80  7.0 1
5 192.2 29.0 28.0 34.0  1.5  1.5 10.0  2.9 10.0 0.25 0.95  6.5 1
5 192.2 32.0 43.0 38.0  1.1  0.7 10.0  1.5 10.000.1000.25  8.5 1
5 192.2 33.5 55.5 41.0  0.9  0.4 10.0  0.8 10.000.1000.15 14.0 1
5 200.4 19.0  0.0 38.0  0.9  0.4  7.0  0.9  7.000.2000.35  8.0 1
5 200.4 21.0 15.0 41.0  1.1  0.5 10.0  1.4 10.000.3500.70  8.4 1
5 200.4 25.5 43.0 44.0  1.3  1.1  7.0  1.9  7.000.1000.25  9.0 1
5 200.4 29.5 60.0 46.0  0.9  0.4 10.0  1.2 10.000.1500.25 12.0 1
5 200.4 32.0 86.0 49.0  0.8  0.3 10.0  0.8 10.000.3000.40 15.0 1
5 212.5 20.5  0.0 42.0  0.8  0.7  9.5  2.5  9.500.8001.20 14.0 1
5 212.5 23.0 16.0 43.0  1.4  1.0  9.0  2.2  9.000.5001.60 13.0 1
5 212.5 28.0 32.0 41.0  1.7  1.0 10.5  2.1 10.500.3001.00 12.5 1
5 212.5 35.0 66.0 46.0  0.9  0.5  8.0  0.7  8.000.2000.50 20.5 1
5 261.0 22.0 14.0 58.0  0.7  0.3  7.0  0.7  7.000.3000.50 23.0 1
5 261.0 27.0 26.0 63.5  1.0  1.0  9.0  1.4  9.000.6001.20 19.0 1
5 261.0 30.0 45.0 65.5  2.4  1.4  8.0  1.7  8.001.0002.30 22.0 1
5 261.0 37.5 71.0 76.0  1.0  0.3 10.0  0.4  8.000.2000.35 26.0 1
5 277.0 20.0  0.0 33.0  0.7  0.7 11.0  1.2 11.000.1000.15 14.0 1
5 277.0 22.2 33.5 42.0  1.2  0.6  8.0  1.9  8.000.1000.20 13.5 1
5 277.0 25.0 52.0 53.0  1.8  0.4  5.0  1.0  5.000.5001.20 14.0 1
5 277.0 29.0 81.0 61.0  2.2  0.2  3.5  0.5  3.500.3001.20 15.5 1
5 277.0 31.7 94.0 64.0  1.1  0.5  8.0  1.1  8.000.1500.25 20.0 1
5 293.0 17.0  0.0 38.0  1.3  0.6  9.0  1.1  9.000.3000.70 13.0 1
5 293.0 19.5 25.0 39.0  1.2  0.8 12.0  1.2 12.000.5001.40 14.5 1
5 293.0 23.0 43.0 40.0  2.1  1.2  8.0  2.9  8.000.7002.20 12.0 1
5 293.0 30.5 73.0 45.0  1.2  0.6  9.0  1.0  9.000.5001.45 11.5 1
```

5	293.0	37.5	100.0	53.0	0.7	0.6	11.0	1.0	11.000	.1000	.25	14.0	1
5	322.0	21.0	0.0	56.0	0.8	0.4	8.0	0.8	8.000	.2000	.35	13.5	1
5	322.0	28.5	53.0	65.0	1.9	1.0	7.0	2.0	7.001	.3002	.50	11.5	1
5	322.0	38.0	98.0	71.0	0.8	0.4	8.0	0.7	8.000	.3500	.55	15.0	1
6	0.0	0.0	0.0	21.0	0.9	0.7	15.0	5.0	15.0	0.25	1.30	4.0	1
6	0.0	1.3	9.0	28.0	0.7	0.5	18.3	2.9	18.3	0.15	0.70	5.5	1
6	0.0	2.0	24.5	37.5	0.7	0.4	14.9	2.5	14.9	0.20	1.20	4.0	1
6	0.0	2.5	34.0	43.0	0.9	0.4	12.7	3.7	12.7	0.15	1.10	5.5	1
7	30.0	11.5	0.0	29.0	0.8	0.5	8.0	1.0	8.000	.1500	.28	6.0	1
7	30.0	13.5	31.0	26.0	1.1	0.6	8.0	1.2	8.000	.6001	.00	10.5	1
7	30.0	15.5	71.0	29.0	1.3	0.5	8.0	1.8	8.000	.4501	.00	11.5	1
7	30.0	20.5	96.0	34.0	1.4	0.6	8.0	2.1	8.000	.4001	.00	9.0	1
7	30.0	25.0	113.0	37.0	0.7	0.5	8.0	0.8	8.000	.1000	.18	9.5	1
7	41.0	5.0	0.0	25.0	0.6	0.6	8.0	1.3	8.000	.1000	.25	7.0	1
7	41.0	9.0	30.0	40.0	1.5	1.0	8.0	2.4	8.000	.3001	.50	8.0	1
7	41.0	16.5	82.0	39.0	1.2	0.7	8.0	2.0	8.000	.1000	.35	6.5	1
7	41.0	23.5	122.0	45.0	0.7	0.6	8.0	1.6	8.000	.1000	.30	10.5	1
7	49.0	7.0	0.0	30.0	1.1	0.4	5.0	1.3	5.000	.2000	.70	5.0	1
7	49.0	9.5	35.0	27.0	0.8	0.6	7.5	1.5	7.500	.3000	.50	8.0	1
7	49.0	23.0	120.0	39.0	1.3	0.6	8.0	1.6	8.000	.2000	.60	10.5	1
7	71.0	4.3	0.0	20.0	0.6	0.7	6.2	1.2	6.200	.3500	.55	6.0	1
7	71.0	7.5	41.0	36.5	1.3	0.4	5.0	1.3	5.000	.2000	.45	10.0	1
7	71.0	16.0	95.0	32.5	1.0	0.8	10.0	2.6	10.001	.2002	.50	6.5	1
7	71.0	20.0	114.0	42.0	0.8	0.5	8.0	1.2	8.000	.1500	.20	7.5	1
7	95.8	3.0	0.0	40.0	0.6	0.3	3.5	0.6	3.500	.2500	.45	9.0	1
7	95.8	6.5	33.0	21.0	0.7	0.5	5.5	1.3	5.500	.3000	.70	7.0	1
7	95.8	9.0	68.0	33.0	1.7	0.5	5.5	1.7	5.500	.1000	.25	7.5	1
7	95.8	20.0	110.0	41.0	1.1	0.5	5.0	1.1	5.000	.3000	.55	9.5	1
7	119.3	3.5	0.0	24.0	0.8	0.4	7.0	1.5	7.000	.3500	.55	8.0	1
7	119.3	9.0	58.5	50.5	0.9	0.4	7.5	1.4	7.500	.2000	.35	9.0	1
7	119.3	13.5	92.0	41.0	0.8	0.5	6.8	1.5	6.800	.2000	.65	7.5	1
7	119.3	18.5	119.0	40.5	1.2	0.4	5.5	1.5	5.500	.2000	.70	9.5	1
7	131.0	3.3	0.0	27.0	0.5	0.3	5.0	0.4	5.000	.1000	.15	5.0	1
7	131.0	10.5	44.0	18.5	0.6	0.4	5.0	2.2	5.000	.4000	.80	4.5	1
7	131.0	15.0	75.0	42.5	1.0	0.5	5.0	0.9	2.800	.3000	.50	11.3	1
7	131.0	16.8	105.0	47.0	2.5	1.1	8.6	2.8	8.600	.3500	.60	14.0	1
7	131.0	22.0	128.0	57.0	0.7	0.7	14.0	1.6	14.000	.1500	.25	11.5	1
7	146.0	3.0	0.0	19.0	0.8	1.0	8.5	1.9	8.500	.1500	.25	6.0	1
7	146.0	6.5	63.0	25.0	1.0	0.9	10.5	2.2	10.500	.2500	.70	9.0	1
7	146.0	15.5	105.0	32.0	1.0	0.3	5.5	2.0	11.000	.4000	.85	9.6	1
7	146.0	21.5	137.0	37.0	0.8	0.7	12.0	1.7	8.000	.3500	.55	11.5	1
7	164.3	1.2	0.0	16.0	0.8	1.0	10.0	4.9	10.000	.1500	.40	3.0	1
7	164.3	3.2	42.0	25.0	1.0	0.6	10.0	2.1	10.000	.6001	.00	7.5	1
7	164.3	11.5	109.0	39.0	1.1	0.8	8.8	1.7	8.800	.2000	.35	13.5	1
7	164.3	18.5	142.0	22.0	0.9	0.6	10.0	2.2	10.000	.3000	.50	6.5	1
7	180.7	8.0	46.0	60.0	1.8	1.0	15.0	4.0	15.000	.6001	.50	12.5	1
7	180.7	12.5	70.0	68.0	1.4	0.3	10.0	3.9	10.000	.4001	.10	6.0	1
7	180.7	18.2	110.0	31.0	0.7	0.3	9.0	1.1	9.000	.4000	.50	9.0	1
7	180.7	21.5	154.0	42.0	0.5	0.5	10.0	1.0	10.000	.5000	.55	20.5	1
7	200.0	8.0	20.5	33.0	0.9	1.2	10.0	2.6	10.000	.2500	.55	9.5	1
7	200.0	9.5	39.5	39.0	1.0	0.7	10.0	2.5	10.000	.7001	.75	10.5	1
7	200.0	13.5	63.0	43.0	1.0	0.6	10.0	1.8	10.000	.5001	.45	10.0	1
7	200.0	20.5	94.0	48.0	0.6	0.4	6.3	1.1	6.300	.1500	.25	8.5	1
7	214.0	1.5	0.0	16.0	1.1	0.7	8.1	2.3	8.100	.2000	.70	5.0	1
7	214.0	6.5	47.0	21.0	1.0	0.6	9.0	2.1	9.000	.5500	.90	7.0	1
7	214.0	14.0	87.0	19.5	0.9	0.5	8.0	2.3	8.000	.7001	.20	5.5	1
7	214.0	17.5	109.0	13.5	0.7	0.6	8.2	2.2	8.200	.5001	.10	4.5	1
7	214.0	20.5	126.0	17.5	0.7	0.5	5.1	1.9	5.100	.1000	.30	4.5	1
7	234.5	3.5	0.0	28.0	1.0	0.6	8.6	3.9	8.600	.3500	.75	5.7	1

7	234.5	7.0	30.0	36.0	1.2	0.6	17.7	5.7	17.700	.2000	.45	5.8	1
7	234.5	12.5	59.0	57.0	1.7	1.6	20.0	3.5	20.000	.5000	.70	18.5	1
7	234.5	16.5	97.0	21.0	1.0	1.8	18.0	5.5	18.000	.2000	.55	5.2	1
7	259.0	3.0	0.0	47.0	0.9	0.3	11.5	0.8	11.500	.3500	.50	14.5	1
7	259.0	7.0	24.5	52.0	1.3	0.7	10.0	2.8	10.000	.7001	.40	10.5	1
7	259.0	13.0	50.0	42.0	1.4	0.7	9.8	3.3	9.801	.0002	.25	7.0	1
7	259.0	16.0	73.0	48.0	1.0	0.4	10.0	1.8	10.000	.4000	.65	11.0	1
7	278.0	7.5	0.0	22.5	1.0	1.6	7.8	2.2	7.800	.2000	.50	6.0	1
7	278.0	9.5	33.0	21.5	1.2	0.5	6.0	1.1	6.000	.3000	.55	8.5	1
7	278.0	14.0	80.0	39.5	0.9	0.7	10.0	1.9	10.000	.5000	.90	15.5	1
7	278.0	20.5	129.0	43.0	1.0	0.6	10.0	2.0	10.000	.4000	.70	16.5	1
7	306.0	3.5	0.0	27.0	0.4	0.5	5.9	2.7	5.900	.3000	.65	3.0	1
7	306.0	5.5	16.0	28.0	0.6	1.2	10.0	3.8	10.000	.1500	.35	4.0	1
7	306.0	9.5	36.0	28.0	1.0	1.0	6.2	2.2	6.200	.2000	.40	5.0	1
7	306.0	11.5	55.0	25.0	0.9	0.6	6.2	1.6	6.200	.3500	.60	5.5	1
7	306.0	18.0	84.0	28.0	1.0	1.6	10.0	3.4	10.000	.2500	.45	4.5	1
7	320.0	0.2	0.0	22.0	0.5	0.5	8.2	1.8	8.200	.2500	.50	4.0	1
7	320.0	4.5	17.0	33.5	0.9	0.8	10.7	2.6	10.701	.0001	.60	5.0	1
7	320.0	7.0	39.0	47.0	1.4	0.6	6.3	2.3	6.300	.3000	.70	8.5	1
7	320.0	9.3	52.0	54.0	1.1	0.4	8.9	1.6	8.901	.5002	.10	7.0	1
7	320.0	16.0	86.0	36.0	1.4	1.2	5.8	2.3	5.800	.6001	.60	7.5	1
7	320.0	20.2	109.0	30.5	1.3	0.8	4.0	1.3	4.000	.9001	.75	7.0	1
8	43.0	3.8	20.0	28.0	1.2	0.8	12.0	3.0	12.000	.1000	.40	9.0	1
8	43.0	6.0	34.0	30.0	0.9	0.7	9.5	2.7	9.500	.3000	.60	6.5	1
8	43.0	8.5	48.0	38.0	1.2	1.2	13.0	3.6	13.000	.4001	.10	11.0	1
8	43.0	12.0	63.0	45.0	1.4	1.3	15.3	6.3	15.300	.2501	.20	7.5	1
8	62.0	0.5	19.0	27.0	0.8	0.7	12.0	1.8	12.000	.1000	.30	10.0	1
8	62.0	2.2	47.0	41.0	1.6	1.4	12.0	5.2	12.000	.2001	.00	8.5	1
8	62.0	6.2	61.0	49.0	1.5	1.5	14.5	4.3	14.500	.7002	.80	11.5	1
8	62.0	9.5	71.0	52.0	1.1	0.8	12.5	3.1	12.500	.5001	.20	12.0	1
8	151.0	6.5	0.0	35.5	0.7	1.2	15.0	2.5	15.000	.2500	.35	11.0	1
8	151.0	8.5	23.0	18.0	0.7	1.5	19.0	3.8	19.000	.2000	.35	6.0	1
8	151.0	10.5	38.0	44.0	1.5	1.8	19.4	5.1	19.400	.7501	.60	10.0	1
8	151.0	17.5	61.0	37.0	2.5	3.5	20.0	7.1	20.000	.5001	.15	10.5	1
8	172.0	3.4	31.0	28.0	0.7	1.2	16.0	2.7	16.000	.2500	.45	10.0	1
8	172.0	6.5	62.0	28.0	1.1	0.7	9.0	1.5	9.000	.4000	.60	11.3	1
8	182.8	0.0	0.0	27.5	0.6	0.4	12.0	1.2	12.000	.2000	.30	7.5	1
8	182.8	1.5	25.5	39.0	0.7	0.5	9.5	1.7	9.500	.3500	.55	11.0	1
8	182.8	3.2	38.0	39.5	0.8	0.6	12.5	1.9	12.500	.4000	.65	8.5	1
8	187.8	1.0	0.0	17.8	0.6	0.6	10.0	2.0	10.000	.1800	.35	4.0	1
8	187.8	2.5	19.0	27.0	1.1	0.4	5.7	2.0	5.700	.4000	.95	5.0	1
8	187.8	6.0	42.0	24.0	1.0	1.4	15.0	5.4	15.000	.4000	.90	5.5	1
8	194.7	1.5	0.0	17.0	0.6	1.0	15.5	1.5	15.500	.3000	.50	4.3	1
8	194.7	4.5	38.0	25.5	0.8	0.7	8.6	1.4	8.600	.5000	.90	7.0	1
8	194.7	11.5	90.5	52.0	1.4	1.0	20.0	3.9	20.000	.4500	.90	11.0	1
8	194.7	14.5	106.0	50.0	1.8	1.5	25.5	6.8	25.500	.4000	.85	11.5	1
8	203.0	0.5	0.0	27.5	0.5	0.5	14.0	2.3	14.0	0.35	0.55	5.0	1
8	203.0	5.0	42.0	28.0	0.6	0.8	15.0	4.5	15.0	0.50	0.95	5.5	1
8	203.0	9.5	74.0	29.0	1.5	1.3	15.0	4.8	15.000	.4001	.00	10.5	1
8	203.0	19.0	142.0	57.0	1.3	1.0	13.3	1.4	13.300	.4000	.70	21.0	1
8	209.0	3.0	0.0	35.0	0.9	0.4	9.7	2.8	9.700	.2500	.45	5.5	1
8	209.0	5.5	23.0	28.5	1.0	1.0	15.5	2.1	15.500	.2500	.45	9.0	1
8	209.0	11.5	50.0	31.5	1.9	1.2	11.3	4.8	11.300	.6001	.50	7.5	1
8	209.0	19.5	81.0	34.5	1.1	0.6	6.9	2.0	6.900	.5000	.95	6.0	1
8	215.8	2.5	0.0	30.0	0.8	1.0	11.0	2.5	11.000	.6001	.10	6.5	1
8	215.8	9.7	30.0	36.0	1.6	0.8	11.0	3.6	11.000	.8001	.40	11.0	1
8	215.8	12.5	40.0	25.5	1.0	0.9	9.0	2.6	9.000	.5001	.00	8.5	1
8	215.8	17.0	75.0	28.5	1.0	0.7	9.5	2.9	9.500	.2000	.38	8.0	1
8	223.0	2.3	0.0	31.0	1.1	0.8	14.0	3.5	14.000	.3000	.60	7.5	1
8	223.0	6.0	22.5	37.5	1.2	0.7	12.4	3.0	12.400	.8001	.65	9.0	1

```
 8 223.0  9.5 45.0 33.0  1.0  0.8 13.4  3.2 13.400.9001.75  8.0   1
 8 228.0  1.0 17.0 36.0  1.2  0.9 13.0  3.6 13.000.3501.10  7.0   1
 8 228.0  5.0 41.0 44.0  1.5  1.0 10.0  3.8 10.000.2501.70  9.0   1
 8 228.0 11.0 62.0 59.0  1.2  0.6 10.0  1.0 10.001.0001.60 23.0   1

 9 449.0  9.0  0.0 42.0  1.0  0.8  8.0  2.5  8.000.2000.70 12.0   1
 9 449.0 21.5 49.0 46.0  1.0  1.0 13.2  1.4 13.200.3000.65 14.0   1
 9 449.0 27.5 76.0 41.0  0.8  1.0 11.5  2.3 11.500.1000.45  9.0   1
 9 449.0 30.0123.0 47.0  1.0  0.9 10.0  2.0 10.000.1500.60 14.5   1
 9 484.0  4.5  0.0 37.0  1.1  0.6  9.5  1.9  9.500.2500.96 12.0   1
 9 484.0 20.0109.0 55.0  2.4  1.2 12.0  3.9 12.000.2001.00 12.0   1
 9 484.0 26.0151.0 43.0  0.7  0.6 12.0  2.3 12.000.2000.45 11.0   1
 9 484.0 30.0224.0 49.0  1.5  0.7 12.0  3.5 12.000.5001.20 14.0   1
 9 484.0 48.0314.0 57.0  1.1  0.5 11.5  2.0 11.500.1001.00 11.5   1
 9 528.0  4.0  0.0 27.0  0.9  0.8 10.1  2.1 10.101.0002.20  8.5   1
 9 528.0 21.5 56.0 42.0  1.5  1.1 10.8  3.4 10.800.7001.80 11.0   1
 9 528.0 42.0124.0 48.0  1.4  0.9 12.2  2.9 12.200.2000.90 13.0   1
 9 528.0 49.0161.0 64.0  1.3  0.5 10.0  1.3 10.000.1500.70 15.0   1
 9 528.0 57.0220.0 50.0  1.0  0.4  7.5  0.9  7.500.3001.00 18.0   1
 9 562.0  1.5 24.0 36.0  1.1  1.8 15.0  4.4 15.000.2000.90  7.0   1
 9 562.0 14.0 62.0 48.0  1.4  1.5 12.0  3.8 12.000.8002.90  9.0   1
 9 562.0 32.0106.0 49.0  0.7  0.8  7.5  2.0  7.500.1500.50  7.0   1
 9 562.0 36.0170.0 53.0  1.1  1.1 13.0  3.7 13.000.4001.00 10.0   1
 9 562.0 53.0260.0 57.0  1.0  1.0 10.0  2.4 10.000.2001.40 12.0   1
 9 587.0  7.0 27.0 27.0  1.1  1.0  9.0  1.8  9.000.4001.10  5.5   1
 9 587.0 18.5 77.0 33.0  1.2  0.6  9.3  1.6  9.300.6001.10 10.0   1
 9 587.0 34.0154.0 36.0  1.4  0.6  6.5  1.4  6.500.3000.95 10.5   1
 9 587.0 45.0213.0 35.0  1.0  1.6 15.5  5.0 15.500.6001.90  8.5   1
 9 587.0 58.0257.0 43.0  1.0  0.7 10.0  3.0 10.000.3001.00  9.0   1
 9 607.0 12.5  0.0 29.0  1.0  0.6 10.0  2.8 10.000.2000.50  8.5   1
 9 607.0 17.5 44.0 35.0  1.5  0.7  8.8  3.2  8.800.2000.85  8.5   1
 9 607.0 29.5 71.0 37.0  1.0  0.8 14.5  1.8 14.501.0001.70 13.5   1
 9 607.0 39.0111.0 42.0  1.1  0.8 14.0  4.1 14.000.1500.40  9.5   1
 9 607.0 49.0145.0 38.0  0.7  0.7 11.7  1.7 11.700.1500.25 11.0   1
 9 607.0 55.0184.0 42.0  0.9  0.5  7.0  1.3  7.000.8001.50  8.0   1
 9 630.0  1.8  0.0 24.0  0.8  1.1 10.5  2.0 10.500.4000.80  7.5   1
 9 630.0 17.5 47.0 32.0  1.0  1.5 14.0  4.2 14.000.2500.60  8.0   1
 9 630.0 34.0 81.0 36.0  1.6  0.9 13.0  4.3 13.000.6001.50  9.0   1
 9 630.0 44.0102.0 33.0  1.1  0.7 14.5  4.2 14.500.5001.15 11.0   1
 9 630.0 53.0129.0 44.0  1.0  1.0 15.0  3.8 15.001.1002.30 11.5   1
 9 647.0 14.0 11.0 25.0  1.0  0.6 12.0  2.6 12.000.3500.90  5.5   1
 9 647.0 22.5 60.0 34.0  1.2  0.6 12.2  3.2 12.200.3001.00  8.0   1
 9 647.0 33.5108.0 39.0  1.1  0.7 10.0  3.0 10.000.8001.80  8.0   1
 9 647.0 48.0159.0 46.0  1.8  1.0 11.0  4.0 11.000.7002.30 10.5   1
 9 647.0 62.0214.0 31.0  0.9  0.8  9.0  1.7  9.000.1500.75  6.5   1
 9 667.0  3.5  0.0 28.0  0.7  0.7 12.7  2.4 12.700.1000.40  5.5   1
 9 667.0 12.5 55.0 35.0  1.3  1.1 15.3  3.8 15.300.4001.30 10.0   1
 9 667.0 23.5103.0 42.0  1.4  1.0 14.0  3.2 14.000.2500.45  9.0   1
 9 667.0 35.0129.0 49.0  2.4  1.4 10.6  4.0 10.600.1000.28 12.0   1
 9 667.0 57.0197.0 55.0  2.4  1.1 11.0  2.7 11.000.4501.30 15.5   1
 9 667.0 65.5238.0 59.0  1.3  0.8 10.0  2.5 10.000.1500.80 18.0   1
 9 691.0 13.0 13.0 28.0  1.2  0.8 11.0  2.1 11.000.3000.55 12.0   1
 9 691.0 20.5 49.0 30.5  1.4  0.8  9.0  2.0  9.000.5001.30  9.0   1
 9 691.0 31.0104.0 42.0  1.3  0.5  9.5  1.6  9.500.5000.90 14.0   1
 9 691.0 38.5132.0 25.0  1.1  1.0 10.5  3.5 10.500.3001.00  6.0   1
 9 691.0 46.0165.0 31.0  1.4  0.6  8.0  2.8  8.000.1800.90  6.5   1

10   0.0  4.7  0.0 24.0  1.0  1.0 18.0  3.9 18.0 0.15 1.00  7.0   1
10   0.0 13.0115.0 56.0  0.9  0.8 22.2  4.1 22.2 1.20 5.00 10.0   1
10   0.0 21.0156.0 63.0  0.9  0.6 21.0  4.3 21.0 0.35 1.20 10.0   1
10   0.0 26.0192.0 83.0  0.7  0.4 23.5  3.3 23.5 0.20 0.70  6.5   1
```

10	70.0	5.5	0.0	35.0	1.2	1.0	20.8	5.4	20.8	0.20	1.70	9.0	1
10	70.0	8.5	52.0	66.0	1.1	1.0	23.5	5.4	23.5	1.00	2.50	8.0	1
10	70.0	14.0	95.0	51.0	1.5	1.0	19.8	7.3	19.8	1.40	2.40	10.0	1
10	70.0	24.0	150.0	75.0	1.0	0.7	27.8	3.0	27.8	0.30	1.20	13.0	1
10	130.0	5.0	0.0	48.0	1.3	0.9	21.6	3.9	21.6	0.80	2.50	16.0	1
10	130.0	11.0	31.0	66.0	2.8	1.3	19.0	7.1	19.0	1.00	2.20	19.0	1
10	130.0	19.5	50.0	51.0	1.0	0.8	21.2	2.1	21.2	0.60	1.70	18.0	1
10	130.0	23.0	109.0	67.0	3.0	2.8	20.2	8.1	20.2	0.70	2.20	17.0	1
10	250.0	6.0	0.0	36.0	1.0	1.1	21.8	4.3	21.8	0.60	2.20	7.0	1
10	250.0	10.5	26.0	47.0	1.7	1.2	24.3	4.9	24.3	1.00	2.30	12.0	1
10	250.0	15.5	39.0	49.0	1.5	1.4	22.1	4.1	22.1	1.00	2.50	11.0	1
EAST OF ANSE A MERCIER, GRANDE VALLEE													
1	90.0	8.0	0.0	28.0	1.0	1.0	10.7	2.7	10.7	0.15	1.10	6.0	1
1	90.0	10.0	16.0	32.0	1.5	1.5	14.6	1.9	9.5	0.40	1.30	12.0	1
1	90.0	20.5	95.0	45.0	1.7	1.2	11.8	3.7	11.8	0.35	1.10	11.0	1
1	90.0	23.0	114.0	50.0	1.2	1.1	18.1	1.9	11.8	0.10	0.60	12.5	1
2	104.0	6.0	0.0	25.0	1.4	0.8	11.6	4.1	11.6	0.15	1.20	6.0	1
2	104.0	7.5	27.0	25.5	1.6	0.8	9.5	5.6	9.5	0.20	2.00	5.5	1
2	104.0	10.0	55.0	27.0	1.3	1.7	18.0	4.3	18.0	0.25	1.80	9.0	1
2	104.0	12.0	74.0	32.0	1.6	2.1	17.1	3.4	11.1	0.20	0.80	8.5	1
2	128.0	7.3	24.5	20.0	0.7	0.9	15.8	2.9	15.8	0.25	1.30	4.5	1
2	128.0	8.0	52.5	23.5	0.8	0.6	13.0	2.9	13.0	0.35	1.40	6.4	1
2	128.0	11.1	85.0	37.0	1.2	0.4	11.8	2.8	11.8	0.35	1.50	7.5	1
2	128.0	13.2	101.0	40.0	0.8	1.2	30.0	1.2	9.5	0.10	0.25	9.5	1
2	154.0	5.4	8.5	22.5	0.9	0.4	10.3	3.6	10.3	0.30	2.80	4.0	1
2	154.0	9.5	77.0	22.0	1.3	1.1	14.0	4.2	14.0	0.40	1.90	5.5	1
2	154.0	11.0	103.0	28.0	1.2	1.0	14.5	4.7	14.5	0.35	1.80	7.3	1
2	154.0	13.5	125.0	39.0	1.0	0.4	11.0	2.2	11.0	0.20	0.85	7.5	1
2	180.0	5.2	0.0	19.5	0.8	1.2	15.6	4.0	15.6	0.10	0.90	4.5	1
2	180.0	6.3	35.5	26.0	1.4	1.5	14.7	3.1	7.5	0.15	1.10	6.5	1
2	180.0	11.0	97.0	38.5	2.3	0.6	10.4	2.9	10.4	0.30	2.00	11.5	1
2	180.0	13.0	114.0	45.0	0.9	0.3	9.8	2.0	9.8	0.15	0.60	7.5	1
2	214.0	4.0	0.0	19.5	0.8	0.6	15.0	2.2	9.4	0.15	1.70	3.5	1
2	214.0	7.4	69.0	21.5	1.0	0.8	13.1	3.6	13.1	0.20	1.50	5.0	1
2	214.0	11.2	111.0	27.0	1.4	0.6	13.4	3.5	13.4	0.50	2.00	7.5	1
2	214.0	14.5	132.0	36.5	1.1	1.6	20.7	2.0	20.5	0.15	0.50	16.0	1
3	0.0	4.7	0.0	31.0	0.8	0.6	10.5	2.0	10.5	0.20	1.15	7.5	1
3	0.0	5.6	16.0	35.0	1.2	1.3	20.0	2.7	20.0	0.40	1.10	12.0	1
3	0.0	9.0	45.0	38.0	1.0	0.5	6.8	2.0	6.8	0.20	1.00	5.5	1
3	0.0	12.5	92.0	52.0	0.8	0.7	12.8	1.8	12.8	0.30	1.20	7.5	1
ANSE A MERCIER WEST, GRANDE VALLEE													
4	0.0	20.0	0.0	27.0	1.2	0.8	11.0	2.9	11.0	00.200	0.90	7.0	1
4	0.0	41.0	68.0	29.0	1.6	1.0	12.0	3.3	12.0	00.400	1.60	11.0	1
4	0.0	57.0	85.0	33.0	2.1	2.3	18.0	4.5	18.0	03.500	5.90	11.5	1
4	0.0	63.0	112.0	35.0	1.8	0.9	7.3	1.8	7.3	00.900	1.70	12.5	1
5	0.0	16.0	0.0	27.0	1.4	1.1	5.6	2.0	5.6	00.700	3.40	8.0	1
5	0.0	23.0	24.0	44.0	2.0	1.8	13.0	6.8	13.0	00.500	3.00	10.0	1
5	0.0	41.0	113.0	49.0	1.8	2.1	11.5	5.3	11.5	00.500	2.50	12.5	1
5	0.0	52.0	265.0	68.0	3.2	2.4	27.0	4.0	27.0	00.700	1.25	28.0	1
6	0.0	14.0	0.0	27.0	1.9	2.2	19.6	5.1	19.6	00.500	2.40	8.5	1
6	0.0	22.0	62.0	48.0	3.1	2.8	22.7	8.1	22.7	01.200	3.40	16.0	1
6	0.0	31.0	114.0	46.0	2.3	1.0	18.8	5.7	18.8	00.600	2.00	13.0	1
6	0.0	43.0	170.0	69.0	4.0	1.4	16.7	9.9	16.7	02.200	4.60	16.5	1

KEY TO APPENDIX 1D (PROCESSED DATA)

Columns	Format	Contents
1-6	I4	Bed Number
7-12	F6.1	Position on Bed
13-18	F6.2	Horizontal distance (from the 'Position on Bed') for locating the 'Position within Bed'
19-24	F6.2	Vertical distance at the point corresponding to the horizontal distance
25-30	F6.2	Wave length
31-36	F6.2	Amplitude
37-42	F6.2	Stoss-angle in degrees
43-48	F6.2	Lee-angle in degrees
49-54	F6.2	t_L/t_S
55-60	F6.2	Angle of climb in degrees
61-66	F6.2	Ripple Index
67-72	F6.2	Ripple Symmetry Index
73-78	F6.2	Projected Stoss length

APPENDIX 1D: PROCESSED DATA

ST. MAURICE (NORTH OF CHURCH)

477	0.0	25.50	0.00	51.00	4.00	12.64	24.06	2.44	14.00	32.63	12.75	2.64
477	0.0	37.00	0.00	30.00	2.90	16.52	20.02	3.75	12.00	27.94	10.34	1.50
477	0.0	58.50	18.00	31.00	2.20	9.51	20.56	3.20	9.00	21.63	14.09	2.44
477	0.0	68.00	46.00	65.00	4.80	10.92	13.27	2.17	32.00	29.00	13.54	1.03
477	0.0	76.00	57.00	68.00	1.80	6.12	8.33	1.38	29.00	37.64	37.78	1.34
477	50.0	23.00	0.00	44.00	3.00	14.66	17.00	3.60	17.00	25.47	14.67	1.59
477	50.0	40.50	0.00	28.00	2.10	9.08	13.02	12.00	12.00	11.03	13.33	1.33
477	50.0	53.00	12.00	32.50	1.90	9.78	12.99	3.50	12.00	18.32	17.11	1.71
477	50.0	62.50	47.50	36.50	2.30	7.24	18.13	4.75	9.50	13.59	15.87	2.84
477	50.0	72.00	89.50	41.00	2.10	7.71	15.41	3.67	19.00	15.85	19.52	1.16
477	70.0	7.30	0.00	36.50	1.80	7.81	16.70	4.67	8.00	14.11	20.28	3.56
477	70.0	23.70	0.00	27.00	1.60	7.13	18.26	6.00	8.50	11.93	16.88	2.18
477	70.0	48.50	53.00	34.00	1.80	8.82	11.88	1.88	11.00	29.34	18.89	2.09
477	70.0	59.30	90.00	27.00	1.90	8.63	15.13	3.20	9.00	18.64	14.21	2.00
477	70.0	71.70	110.00	46.00	1.80	6.09	8.34	1.73	20.00	24.27	25.56	1.30
477	100.0	7.50	0.00	39.00	4.10	15.27	25.70	2.50	14.50	35.87	9.51	1.69
477	100.0	29.50	0.00	26.00	1.90	13.50	13.50	4.00	12.00	21.80	13.68	1.17
477	100.0	45.00	0.00	31.00	2.20	10.17	16.07	3.82	13.50	18.77	14.09	1.30
477	100.0	59.00	64.00	39.50	2.60	10.90	12.44	3.17	16.50	20.89	15.19	1.39
477	100.0	76.50	104.00	40.00	1.80	8.27	9.25	2.55	18.00	18.98	22.22	1.22
477	130.0	10.50	0.00	41.00	3.30	10.73	23.75	3.00	12.00	25.31	12.42	2.42
477	130.0	32.50	0.00	34.00	2.50	12.45	17.35	3.17	12.00	24.65	13.60	1.83
477	130.0	49.00	28.00	35.50	2.10	6.80	10.85	2.25	12.50	19.95	16.90	1.84
477	130.0	59.00	58.00	43.50	4.60	11.44	22.33	3.33	19.50	23.97	9.46	1.23
477	130.0	68.00	124.00	63.00	4.20	7.27	12.93	2.31	27.00	21.42	15.00	1.33
477	162.0	14.00	0.00	43.00	3.00	10.13	17.70	10.00	13.50	13.07	14.33	2.19
477	162.0	28.30	0.00	33.00	2.00	6.84	11.31	3.25	10.50	14.56	16.50	2.14
477	162.0	55.50	4.50	31.00	2.90	11.03	18.52	5.11	9.50	17.67	10.69	2.26
477	162.0	66.50	31.00	44.50	3.20	11.74	20.34	4.20	16.00	20.75	13.91	1.78
477	162.0	70.00	53.00	51.00	3.30	12.41	13.04	3.67	17.00	21.24	15.45	2.00
477	190.0	17.00	0.00	31.50	2.00	7.97	12.58	12.67	11.00	9.68	15.75	1.86
477	190.0	32.00	0.00	32.50	2.70	9.11	17.53	6.40	12.20	13.76	12.04	1.66
477	190.0	52.00	43.00	40.50	3.20	12.68	14.14	15.00	14.50	14.51	12.66	1.79
477	190.0	58.00	90.00	33.00	2.80	12.42	15.72	2.10	16.00	33.58	11.79	1.06
477	190.0	76.00	123.00	47.00	1.60	5.06	9.41	15.00	14.50	6.08	29.38	2.24
477	218.0	20.50	0.00	34.00	2.10	9.49	13.33	7.50	10.00	12.87	16.19	2.40
477	218.0	33.00	0.00	27.50	1.50	5.39	14.44	19.00	10.50	6.47	18.33	1.62
477	218.0	46.50	8.50	50.50	2.80	9.27	9.74	2.86	23.50	18.94	18.04	1.15
477	218.0	66.30	46.50	51.00	2.80	10.34	11.82	4.15	18.00	17.01	18.21	1.83
477	218.0	77.70	99.00	47.00	1.70	5.35	7.99	5.00	22.00	8.63	27.65	1.14
477	261.0	9.00	0.00	33.00	1.90	6.04	10.99	4.00	10.20	11.54	17.37	2.24
477	261.0	32.50	0.00	32.50	2.60	6.37	15.06	6.18	10.30	10.35	12.50	2.16
477	261.0	50.00	36.50	36.00	3.20	9.98	13.06	2.87	14.00	21.31	11.25	1.57
477	261.0	58.00	58.50	37.00	3.10	8.88	18.70	5.00	11.00	15.30	11.94	2.36
477	261.0	71.50	91.50	41.00	2.80	9.68	11.63	1.78	17.50	32.93	14.64	1.34
477	299.0	18.50	0.00	36.50	2.40	9.09	11.94	5.00	15.20	14.13	15.21	1.40
477	299.0	32.50	0.00	28.50	1.90	6.16	10.65	3.13	10.00	13.76	15.00	1.85
477	299.0	51.00	23.50	29.00	2.00	9.12	21.30	5.00	10.50	16.10	14.50	1.76
477	299.0	61.50	51.00	52.00	5.20	10.68	31.30	3.33	20.00	25.16	10.00	1.60
477	299.0	69.00	93.50	53.00	3.80	13.41	20.09	3.36	18.00	25.72	13.95	1.94
477	330.0	13.00	0.00	29.50	1.30	2.29	10.20	4.29	10.50	6.03	22.69	1.81
477	330.0	35.00	0.00	25.00	1.40	7.83	13.02	7.00	9.20	11.19	17.86	1.72
477	330.0	50.00	29.00	29.50	2.20	7.07	14.97	5.50	11.30	11.76	13.41	1.61
477	330.0	58.50	49.00	34.50	1.90	10.46	14.16	4.33	11.20	17.40	18.16	2.08
477	330.0	75.00	81.00	42.00	1.80	6.34	18.43	3.63	11.50	15.11	23.33	2.65
477	387.0	10.50	0.00	25.00	1.40	6.20	13.21	6.67	8.20	9.53	17.86	2.05
477	387.0	30.50	0.00	22.50	1.50	8.92	14.04	8.00	7.00	12.07	15.00	2.21
477	387.0	49.50	29.50	30.00	2.30	9.71	16.49	3.86	11.20	18.19	13.04	1.68

477	387.0	56.00	64.00	34.00	2.00	9.85	12.49	3.20	12.50	19.34	17.00	1.72
477	387.0	71.50	94.00	35.50	1.80	7.54	16.84	1.67	11.50	36.18	19.72	2.09
477	421.0	10.50	0.00	25.50	1.50	4.98	13.41	3.67	6.50	11.61	17.00	2.92
477	421.0	42.00	0.00	24.00	1.70	5.78	17.89	4.33	7.00	12.48	14.12	2.43
477	421.0	56.00	3.00	28.00	1.50	7.04	14.19	9.00	6.00	9.61	18.67	3.67
477	421.0	64.00	41.50	37.00	2.20	9.35	16.52	4.57	9.50	16.13	16.82	2.89
477	421.0	71.00	70.00	45.00	3.40	8.68	15.59	2.13	18.50	27.39	13.24	1.43
477	452.0	39.50	11.00	26.50	1.10	2.83	10.38	3.64	7.50	7.74	24.09	2.53
477	452.0	43.00	45.00	33.50	1.80	5.65	13.76	5.13	11.70	10.19	18.61	1.86
477	452.0	46.00	75.00	35.00	1.60	5.43	12.89	2.69	11.50	15.65	21.88	2.04
477	452.0	49.50	115.00	48.40	2.00	4.36	18.68	3.60	10.80	12.67	24.20	3.48
477	452.0	56.00	131.00	20.00	1.50	7.04	15.14	2.08	7.50	25.11	13.33	1.67
477	479.0	14.50	0.00	43.00	1.70	6.65	13.59	3.80	12.50	13.55	25.29	2.44
477	479.0	36.50	0.00	23.00	1.40	7.74	12.37	5.00	7.50	12.58	16.43	2.07
477	479.0	50.50	8.00	39.00	2.70	9.20	15.78	3.53	13.50	18.34	14.44	1.89
477	479.0	59.50	31.00	59.00	3.40	8.36	20.41	4.86	12.00	15.25	17.35	3.92
477	479.0	71.00	55.00	50.00	2.80	13.39	22.50	3.25	12.00	26.90	17.86	3.17
477	525.0	8.50	0.00	35.00	2.50	9.46	13.86	8.29	11.00	12.54	14.00	2.18
477	525.0	32.00	0.00	30.00	2.30	9.54	20.29	5.00	8.20	16.40	13.04	2.66
477	525.0	55.00	24.00	33.50	2.20	6.45	14.62	2.50	11.00	19.37	15.23	2.05
477	525.0	66.00	55.00	35.00	3.10	12.23	19.59	3.91	13.00	22.01	11.29	1.69
477	525.0	74.00	95.00	38.50	1.90	6.34	24.57	2.87	10.50	20.63	20.26	2.67
477	555.0	15.50	0.00	25.00	2.00	10.97	16.70	8.67	9.00	14.39	12.50	1.78
477	555.0	29.50	0.00	29.00	2.00	8.85	16.76	3.50	8.50	18.30	14.50	2.41
477	555.0	56.00	11.00	27.00	1.60	7.67	14.04	4.17	8.50	14.18	16.88	2.18
477	555.0	59.00	76.00	45.00	4.30	13.36	22.38	5.00	21.00	21.30	10.47	1.14
477	555.0	68.50	98.00	45.00	3.70	10.30	14.37	4.00	17.50	18.00	12.16	1.57
477	646.0	17.50	0.00	57.00	2.00	6.59	14.37	4.00	20.00	13.25	28.50	1.85
477	646.0	30.00	0.00	35.00	2.20	7.42	18.99	6.50	10.50	11.96	15.91	2.33
477	646.0	51.00	21.00	43.00	2.10	8.51	12.51	4.07	10.50	15.03	20.48	3.10
477	646.0	58.50	36.00	39.00	4.20	10.94	23.11	5.63	12.50	17.60	9.29	2.12
477	646.0	73.00	70.00	43.00	2.70	9.89	20.70	4.60	11.00	17.65	15.93	2.91
477	682.0	11.00	0.00	33.50	2.00	9.46	13.50	5.50	8.00	14.33	16.75	3.19
477	682.0	29.50	0.00	25.50	1.70	8.64	16.07	7.67	7.50	12.18	15.00	2.40
477	682.0	48.50	19.50	25.00	2.10	8.95	17.49	3.38	8.00	19.14	11.90	2.13
477	682.0	55.00	37.00	28.00	2.50	8.56	14.52	6.67	9.50	12.47	11.20	1.95
477	682.0	62.00	58.00	27.50	1.70	9.23	13.02	3.25	9.00	18.48	16.18	2.06
477	717.0	12.50	0.00	33.50	2.40	8.22	12.68	8.80	12.50	10.82	13.96	1.68
477	717.0	34.50	0.00	27.50	1.60	7.59	21.53	5.25	6.80	13.94	17.19	3.04
477	717.0	51.00	9.00	27.50	1.50	4.84	13.68	7.00	7.50	7.84	18.33	2.67
477	717.0	63.00	62.00	36.50	4.00	9.64	30.58	8.75	8.50	14.27	9.13	3.29
477	717.0	71.50	126.00	38.50	3.90	9.01	26.37	4.00	9.50	19.31	9.87	3.05
477	763.0	37.00	0.00	24.50	2.00	8.04	14.83	3.17	7.50	17.85	12.25	2.27
477	763.0	45.00	20.00	31.50	2.90	10.25	24.11	6.75	8.00	15.69	10.86	2.94
477	763.0	53.50	85.00	34.00	4.40	13.63	30.21	3.65	11.50	26.95	7.73	1.96
477	763.0	66.50	126.00	44.00	4.10	12.34	30.96	3.14	10.00	28.19	10.73	3.40
477	798.0	14.50	0.00	29.50	1.50	4.48	22.38	4.00	7.50	12.76	19.67	2.93
477	798.0	29.50	0.00	27.00	2.00	8.91	14.78	7.00	9.50	12.69	13.50	1.84
477	798.0	49.00	14.00	35.00	2.10	6.92	20.02	2.60	7.50	21.77	16.67	3.67
477	798.0	56.00	62.00	32.00	2.20	5.42	14.21	3.55	9.50	12.78	14.55	2.37
477	798.0	67.00	101.00	35.00	2.00	6.34	16.11	3.18	12.00	15.94	17.50	1.92
477	837.0	16.00	0.00	33.00	2.10	5.91	12.23	3.33	11.50	13.35	15.71	1.87
477	837.0	35.00	0.00	23.00	1.40	9.87	15.01	4.80	7.00	16.03	16.43	2.29
477	837.0	42.00	22.50	28.00	1.80	8.62	14.93	3.80	8.50	16.50	15.56	2.29
477	837.0	53.00	55.50	31.00	1.40	5.79	14.62	3.67	7.00	13.08	22.14	3.43
477	837.0	64.00	76.00	35.00	1.40	6.37	18.51	4.00	6.70	14.11	25.00	4.22
477	900.0	31.50	0.00	27.20	1.90	8.02	16.22	5.71	9.00	12.91	14.32	2.02
477	900.0	51.00	19.00	31.50	1.80	7.83	15.95	4.09	8.30	15.06	17.50	2.80
477	900.0	58.50	43.50	31.00	1.50	6.71	15.35	4.00	7.50	13.68	20.67	3.13
477	900.0	66.00	67.00	32.00	1.70	7.50	15.80	3.75	9.70	15.45	18.82	2.30

WEST OF FAME POINT

666	0.0	.70	7.00	25.50	1.00	3.90	16.86	8.00	6.20	6.77	25.50	3.11
666	0.0	5.00	50.00	34.00	1.10	5.42	16.59	14.00	8.20	7.07	30.91	3.15
666	0.0	9.50	95.00	34.00	1.60	4.25	19.01	10.00	10.00	6.74	21.25	2.40
700	0.0	.40	5.40	25.00	1.30	3.72	22.20	9.33	5.50	6.69	19.23	3.55
700	0.0	3.60	54.50	28.50	1.20	3.67	19.65	8.67	7.50	6.60	23.75	2.80
700	0.0	8.00	120.00	37.00	.80	2.06	11.84	9.00	7.00	3.77	46.25	4.29
701	0.0	.40	4.00	31.00	1.30	5.71	16.11	9.33	7.20	8.24	23.85	3.31
701	0.0	3.70	40.00	33.00	1.30	4.09	13.26	8.40	7.60	6.38	25.38	3.34
701	0.0	7.10	80.00	38.00	.90	4.29	12.68	4.33	8.00	9.23	42.22	3.75
702	0.0	6.30	33.00	20.00	.60	3.75	13.82	8.67	5.00	5.99	33.33	3.00
702	0.0	9.50	50.00	24.00	.80	3.73	19.18	3.75	4.50	11.57	30.00	4.33
702	0.0	12.80	66.00	35.00	.60	1.93	12.57	6.00	3.50	4.78	58.33	9.00
759	0.0	.70	9.00	20.00	.80	4.00	13.48	6.00	6.20	7.41	25.00	2.23
759	0.0	2.60	33.50	21.50	.70	4.09	12.88	7.00	5.00	6.85	30.71	3.30
759	0.0	5.70	71.50	34.00	.60	2.64	12.58	4.75	6.00	6.61	56.67	4.67
765	0.0	1.00	11.50	25.00	1.20	3.68	17.45	5.60	5.50	8.09	20.83	3.55
765	0.0	3.00	44.00	30.00	1.50	3.18	23.07	7.00	5.50	7.32	20.00	4.45
765	0.0	7.00	80.00	44.00	.80	1.84	14.73	5.00	7.00	5.87	55.00	5.29
772	0.0	.70	11.00	24.00	.70	3.37	20.92	9.00	4.50	6.28	34.29	4.33
772	0.0	2.80	45.00	36.00	1.00	3.11	22.17	6.22	6.00	7.70	36.00	5.00
772	0.0	4.60	74.00	42.00	.80	2.64	21.42	6.25	7.00	7.01	52.50	5.00
773	0.0	.50	9.80	31.00	.70	2.15	12.68	10.67	5.00	3.66	44.29	5.20
773	0.0	2.40	48.00	39.00	.90	3.00	18.21	6.67	6.00	6.61	43.33	5.50
773	0.0	4.00	79.50	56.00	.80	1.56	11.91	6.50	7.50	3.97	70.00	6.47
774	0.0	1.00	0.00	24.00	.90	3.63	17.58	7.33	4.50	6.86	26.67	4.33
774	0.0	2.00	24.50	29.00	1.00	4.22	12.93	6.00	7.00	7.56	29.00	3.14
774	0.0	3.80	46.50	42.00	1.00	2.46	14.47	4.80	7.50	6.80	42.00	4.60
790	0.0	.80	8.90	35.00	.80	2.29	18.26	10.50	4.50	4.39	43.75	6.78
790	0.0	4.30	51.30	46.00	.90	2.67	17.85	6.80	5.50	6.09	51.11	7.36
790	0.0	8.20	103.00	59.00	.60	2.06	15.22	7.33	6.00	4.73	98.33	8.83
791	0.0	.70	5.50	28.00	.80	2.06	15.60	8.00	4.50	4.53	35.00	5.22
791	0.0	7.50	55.00	34.00	1.20	2.84	22.45	5.60	6.00	8.04	28.33	4.67
791	0.0	13.70	99.90	43.00	1.20	2.97	14.91	5.67	7.50	6.70	35.83	4.73
793	0.0	.40	3.50	30.00	.70	1.88	16.49	11.33	4.00	3.62	42.86	6.50
793	0.0	4.60	38.50	32.00	1.20	3.58	22.28	8.00	5.00	7.09	26.67	5.40
793	0.0	9.50	78.50	37.00	.90	2.43	12.97	9.33	6.50	4.25	41.11	4.69
794	0.0	1.10	18.30	26.00	1.00	3.55	17.60	8.00	5.00	6.47	26.00	4.20
794	0.0	2.50	40.00	32.00	1.10	3.47	19.68	5.50	5.50	8.37	29.09	4.82
794	0.0	7.60	122.00	49.00	.80	1.31	10.68	9.67	6.00	2.68	61.25	7.17
795	0.0	1.40	12.70	29.00	1.10	4.69	18.95	8.50	5.00	7.72	26.36	4.80
795	0.0	5.60	51.00	34.00	1.40	3.74	25.20	5.00	5.00	10.43	24.29	5.80
795	0.0	9.90	90.00	50.00	1.00	2.34	14.12	4.40	7.00	7.05	50.00	6.14
798	0.0	3.10	29.50	26.00	1.00	3.81	22.46	7.33	4.00	7.75	26.00	5.50
798	0.0	8.00	75.00	35.00	.70	2.29	13.86	8.50	5.00	4.40	50.00	6.00
799	0.0	.20	3.00	20.50	.60	3.09	13.02	7.00	4.50	5.73	34.17	3.56
799	0.0	2.90	42.50	31.00	1.00	2.84	19.89	6.17	5.50	7.06	31.00	4.64
799	0.0	5.70	84.00	38.00	.90	2.50	16.15	6.00	5.00	6.13	42.22	6.60
800	0.0	.30	5.30	23.00	1.00	3.22	16.03	13.00	6.00	4.78	23.00	2.83
800	0.0	1.80	31.80	27.50	1.00	3.25	19.48	12.00	5.50	5.25	27.50	4.00
800	0.0	4.50	78.00	39.00	.80	2.22	11.79	6.40	6.50	4.78	48.75	5.00
801	0.0	.70	8.00	41.00	.80	2.68	15.40	6.75	5.00	5.75	51.25	7.20
801	0.0	4.20	53.00	53.00	1.10	2.02	19.21	6.40	5.50	5.81	48.18	8.64
801	0.0	6.30	79.50	66.00	1.00	2.46	15.11	5.14	6.50	6.58	66.00	9.15
899	0.0	9.20	0.00	30.00	.70	3.43	12.77	4.00	5.80	8.68	42.86	4.17
899	0.0	15.30	24.50	34.50	1.20	4.71	17.01	3.57	6.00	12.68	28.75	4.75
899	0.0	19.50	39.50	35.00	1.40	4.04	16.39	2.08	9.50	21.06	25.00	2.68
1013	0.0	.90	13.50	23.00	.50	2.20	12.99	3.33	4.00	8.52	46.00	4.75
1013	0.0	2.50	28.00	31.00	1.60	3.81	18.71	8.33	7.50	6.77	19.38	3.13
1013	0.0	4.50	52.00	36.00	.80	2.23	11.31	6.67	6.50	4.58	45.00	4.54
1014	0.0	0.00	0.00	30.00	.50	1.97	13.26	5.33	5.50	5.42	60.00	4.45

1014	0.0	.80	7.50	27.50	1.00	3.98	19.12	9.00	6.20	6.76	27.50	3.44
1014	0.0	1.60	24.00	34.00	.70	1.81	13.18	7.00	7.50	4.27	48.57	3.53
1015	0.0	0.00	0.00	27.00	.90	2.13	17.58	3.71	4.00	9.07	30.00	5.75
1015	0.0	1.90	22.20	29.50	1.20	3.64	15.71	7.50	7.70	6.53	24.58	2.83
1015	0.0	3.30	50.50	41.00	.80	1.70	11.20	5.67	7.20	4.43	51.25	4.69
1021	0.0	1.50	12.00	17.00	.50	2.49	11.07	4.00	5.00	6.92	34.00	2.40
1021	0.0	2.40	18.50	21.00	.80	3.04	15.67	3.43	4.50	10.40	26.25	3.67
1021	0.0	4.00	31.50	25.00	.60	1.80	14.14	3.75	4.50	7.43	41.67	4.56
1030	0.0	.30	2.50	16.50	.80	2.23	17.57	5.67	4.00	6.33	20.63	3.13
1030	0.0	2.20	50.50	25.00	.70	2.54	17.28	7.14	5.00	5.67	35.71	4.00
1030	0.0	5.00	114.00	32.00	.60	2.49	14.15	8.00	5.50	4.82	53.33	4.82
1031	0.0	.60	10.00	15.00	.60	2.86	18.65	6.67	4.80	6.52	25.00	2.12
1031	0.0	2.20	36.00	17.50	.80	3.64	17.47	8.00	5.20	6.56	21.88	2.37
1031	0.0	5.30	90.00	33.00	.70	2.17	14.44	9.20	6.00	4.16	47.14	4.50
1033	0.0	.70	0.00	17.00	.60	3.27	16.32	3.78	4.00	10.01	28.33	3.25
1033	0.0	3.60	35.00	35.00	.90	3.48	13.35	6.00	8.00	6.77	38.89	3.38
1033	0.0	7.30	70.00	47.00	.70	2.56	10.12	4.67	8.50	5.96	67.14	4.53
1034	0.0	.40	10.50	18.00	.50	2.02	16.65	8.00	6.40	4.62	36.00	1.81
1034	0.0	2.60	68.00	21.00	.60	1.97	18.43	10.00	5.20	4.18	35.00	3.04
1034	0.0	4.60	120.00	28.00	.50	1.83	10.62	9.25	7.50	3.33	56.00	2.73
1035	0.0	.30	7.00	25.00	.80	1.68	10.70	9.33	7.50	3.15	31.25	2.33
1035	0.0	2.80	70.00	28.00	1.00	2.17	10.57	5.25	8.00	5.13	28.00	2.50
1035	0.0	4.00	99.00	34.00	.80	2.29	12.95	5.11	9.80	5.92	42.50	2.47
1036	0.0	.40	8.00	26.00	.80	2.58	18.02	6.33	5.00	6.31	32.50	4.20
1036	0.0	1.80	40.00	36.00	.70	2.86	13.59	8.00	6.50	5.17	51.43	4.54
1036	0.0	3.00	68.00	44.00	.50	1.15	8.25	5.33	8.00	3.30	88.00	4.50
1038	0.0	.30	4.00	22.50	1.00	3.81	12.04	8.40	4.50	5.92	22.50	4.00
1038	0.0	2.10	27.00	31.00	1.00	4.09	12.00	7.67	5.00	6.45	31.00	5.20
1038	0.0	4.00	55.00	38.00	.80	4.06	10.94	6.00	6.00	7.00	47.50	5.33

PETITE VALLEE HARBOUR, EAST.

1	0.0	4.30	0.00	16.50	1.10	4.91	20.16	9.50	5.50	7.73	15.00	2.00
1	0.0	9.50	37.00	21.00	1.00	4.32	10.16	5.50	6.50	7.47	21.00	2.23
1	0.0	13.00	82.00	27.00	1.00	4.43	11.93	5.00	6.70	8.42	27.00	3.03
1	0.0	16.80	92.00	29.00	1.40	6.01	18.62	5.50	6.00	11.19	20.71	3.83
1	0.0	20.50	111.00	32.50	.70	2.60	12.31	4.00	7.20	7.45	46.43	3.51
1	0.0	27.00	133.00	34.50	.50	1.52	7.56	2.50	7.80	7.48	69.00	3.42
2	0.0	9.00	0.00	28.00	1.00	4.06	8.44	4.33	10.00	7.75	28.00	1.80
2	0.0	14.50	37.00	31.00	.90	4.50	9.25	3.67	11.00	9.54	34.44	1.82
2	0.0	22.50	71.00	36.00	2.70	7.66	20.22	2.91	12.00	20.66	13.33	2.00
2	0.0	30.00	89.00	37.50	1.10	3.15	8.53	2.75	8.50	9.67	34.09	3.41
2	0.0	35.50	106.00	46.00	1.30	3.18	7.91	2.67	13.00	9.69	35.38	2.54
2	0.0	44.00	122.00	48.00	1.10	3.46	6.58	1.67	16.00	17.80	43.64	2.00
3	0.0	11.50	0.00	34.00	1.10	4.09	15.19	4.80	15.00	8.98	30.91	1.27
3	0.0	15.50	20.00	43.00	.70	3.81	10.39	3.50	9.00	9.35	61.43	3.78
3	0.0	19.50	38.00	53.00	1.00	4.76	10.85	2.67	14.50	13.74	53.00	2.66
3	0.0	32.50	60.00	54.00	2.20	4.90	23.27	3.80	13.00	14.09	24.55	3.15
4	0.0	0.00	0.00	19.00	.80	4.21	11.11	11.75	7.00	5.61	23.75	1.71
4	0.0	1.20	16.00	25.00	1.40	5.14	14.57	9.33	8.00	7.44	17.86	2.13
4	0.0	4.10	26.50	23.50	1.20	6.65	14.58	10.67	8.50	8.78	19.58	1.76
4	0.0	5.80	32.00	25.00	1.10	4.24	19.95	6.67	9.00	8.31	22.73	1.78
5	10.0	16.00	0.00	35.00	.40	3.01	4.09	1.75	13.50	12.28	87.50	1.59
5	10.0	27.00	44.00	53.00	1.60	5.44	14.93	1.83	20.00	26.67	33.13	1.65
5	10.0	38.00	75.00	55.00	1.00	4.00	5.71	1.50	21.50	22.17	55.00	1.56
5	31.0	15.50	0.00	48.00	.50	3.94	4.70	1.75	16.00	15.09	96.00	2.00
5	31.0	24.00	87.50	42.00	1.10	4.04	6.04	3.00	15.50	9.00	38.18	1.71
5	31.0	33.00	138.00	34.00	1.50	4.00	6.84	3.00	13.00	9.33	22.67	1.62
5	31.0	39.00	169.00	62.00	1.50	3.81	8.53	6.00	19.00	6.25	41.33	2.26
5	48.0	39.00	192.00	71.00	.90	1.43	1.91	2.60	24.00	3.52	78.89	1.96
5	48.0	19.50	88.50	47.00	1.10	3.93	5.98	1.33	18.00	30.24	42.73	1.61
5	48.0	26.50	144.00	62.00	.90	1.43	2.22	3.00	22.00	3.25	68.89	1.82

5	48.0	10.50	0.00	32.00	1.10	5.71	11.31	3.00	8.00	13.86	29.09	3.00
5	76.5	15.50	0.00	33.00	.60	3.27	11.31	2.00	12.00	16.98	55.00	1.75
5	76.5	19.50	56.00	45.00	1.50	2.86	12.23	2.50	17.00	12.49	30.00	1.65
5	76.5	28.00	96.00	46.00	1.20	4.00	9.09	1.67	19.00	22.12	38.33	1.42
5	76.5	33.00	142.00	84.00	.80	1.72	4.00	1.50	37.00	12.89	105.00	1.27
5	102.8	18.00	0.00	41.00	.70	2.86	8.53	2.17	16.00	12.32	58.57	1.56
5	102.8	23.00	19.00	43.00	1.30	4.00	14.42	3.00	15.00	12.76	33.08	1.87
5	102.8	28.00	36.00	40.00	1.20	3.43	9.65	2.50	14.50	11.87	33.33	1.76
5	102.8	32.00	74.00	37.00	1.20	3.43	10.20	2.25	13.00	13.89	30.83	1.85
5	112.3	21.00	0.00	48.00	1.10	1.64	10.52	1.50	16.00	23.59	43.64	2.00
5	112.3	23.00	28.00	56.00	1.30	6.28	9.65	2.50	20.00	16.39	43.08	1.80
5	112.3	27.00	54.00	62.00	1.50	4.57	8.53	1.57	21.00	25.35	41.33	1.95
5	112.3	34.00	80.00	59.00	1.40	3.43	7.41	2.67	17.00	9.80	42.14	2.47
5	130.8	15.50	0.00	28.00	.60	2.66	6.63	1.67	10.50	16.03	46.67	1.67
5	130.8	26.00	48.00	45.00	1.30	2.86	4.29	1.75	17.00	12.19	34.62	1.65
5	130.8	30.00	82.00	71.00	3.70	4.29	8.53	3.50	27.00	9.31	19.19	1.63
5	130.8	32.00	114.00	68.00	.90	2.15	4.29	2.00	22.00	8.50	75.56	2.09
5	148.0	19.00	0.00	46.00	1.20	3.81	5.44	1.67	17.00	17.13	38.33	1.71
5	148.0	23.00	28.00	44.00	1.70	4.40	7.88	2.33	17.00	13.31	25.88	1.59
5	148.0	30.00	54.00	42.00	.90	4.24	8.13	2.00	11.50	16.06	46.67	2.65
5	148.0	34.00	93.00	38.00	.60	3.37	5.71	1.55	14.00	19.03	63.33	1.71
5	164.0	22.10	9.00	52.00	1.80	1.15	9.09	1.50	16.50	20.15	28.89	2.15
5	164.0	24.50	26.50	55.00	2.20	3.61	11.31	3.50	19.00	9.42	25.00	1.89
5	164.0	29.30	33.00	48.00	1.90	3.01	10.73	2.08	18.00	15.07	25.26	1.67
5	164.0	38.00	65.50	49.00	.80	.95	6.65	1.50	16.00	15.54	61.25	2.06
5	177.5	21.50	0.00	46.00	1.20	3.18	4.24	2.50	16.00	8.07	38.33	1.88
5	177.5	26.00	26.00	49.00	1.10	2.86	5.14	2.50	17.00	8.13	44.55	1.88
5	177.5	31.00	45.00	57.00	1.40	3.27	13.65	3.40	14.00	10.06	40.71	3.07
5	177.5	35.00	68.00	47.00	1.60	3.37	12.53	11.00	16.00	4.93	29.38	1.94
5	192.2	20.50	0.00	40.00	.90	3.43	5.71	1.50	16.00	20.66	44.44	1.50
5	192.2	23.50	16.50	37.00	1.30	5.14	7.41	2.00	15.50	17.12	28.46	1.39
5	192.2	27.20	22.00	36.00	1.40	7.41	12.41	3.20	7.00	15.94	25.71	4.14
5	192.2	29.00	28.00	34.00	1.50	8.53	16.17	3.80	6.50	16.75	22.67	4.23
5	192.2	32.00	43.00	38.00	1.10	4.00	8.53	2.50	8.50	12.11	34.55	3.47
5	192.2	33.50	55.50	41.00	.90	2.29	4.57	1.50	14.00	15.55	45.56	1.93
5	200.4	19.00	0.00	38.00	.90	3.27	7.33	1.75	8.00	16.75	42.22	3.75
5	200.4	21.00	15.00	41.00	1.10	2.86	7.97	2.00	8.40	13.32	37.27	3.88
5	200.4	25.50	43.00	44.00	1.30	8.93	15.19	2.50	9.00	23.37	33.85	3.89
5	200.4	29.50	60.00	46.00	.90	2.29	6.84	1.67	12.00	15.44	51.11	2.83
5	200.4	32.00	86.00	49.00	.80	1.72	4.57	1.33	15.00	19.62	61.25	2.27
5	212.5	20.50	0.00	42.00	.80	4.21	14.74	1.50	14.00	34.59	52.50	2.00
5	212.5	23.00	16.00	43.00	1.40	6.34	13.74	3.20	13.00	14.97	30.71	2.31
5	212.5	28.00	32.00	41.00	1.70	5.44	11.31	3.33	12.50	12.36	24.12	2.28
5	212.5	35.00	66.00	46.00	.90	3.58	5.00	2.50	20.50	9.21	51.11	1.24
5	261.0	22.00	14.00	58.00	.70	2.45	5.71	1.67	23.00	14.30	82.86	1.52
5	261.0	27.00	26.00	63.50	1.00	6.34	8.84	2.00	19.00	20.54	63.50	2.34
5	261.0	30.00	45.00	65.50	2.40	9.93	12.00	2.30	22.00	25.15	27.29	1.98
5	261.0	37.50	71.00	76.00	1.00	1.72	2.86	1.75	26.00	7.77	76.00	1.92
5	277.0	20.00	0.00	33.00	.70	3.64	6.23	1.50	14.00	22.05	47.14	1.36
5	277.0	22.20	33.50	42.00	1.20	4.29	13.36	2.00	13.50	20.44	35.00	2.11
5	277.0	25.00	52.00	53.00	1.80	4.57	11.31	2.40	14.00	15.35	29.44	2.79
5	277.0	29.00	81.00	61.00	2.20	3.27	8.13	4.00	15.50	7.02	27.73	2.94
5	277.0	31.70	94.00	64.00	1.10	3.58	7.83	1.67	20.00	19.65	58.18	2.20
5	293.0	17.00	0.00	38.00	1.30	3.81	6.97	2.33	13.00	11.70	29.23	1.92
5	293.0	19.50	25.00	39.00	1.20	3.81	5.71	2.80	14.50	9.03	32.50	1.69
5	293.0	23.00	43.00	40.00	2.10	8.53	19.93	3.14	12.00	20.42	19.05	2.33
5	293.0	30.50	73.00	45.00	1.20	3.81	6.34	2.90	11.50	9.07	37.50	2.91
5	293.0	37.50	100.00	53.00	.70	3.12	5.19	2.50	14.00	8.59	75.71	2.79
5	322.0	21.00	0.00	56.00	.80	2.86	5.71	1.75	13.50	13.94	70.00	3.15
5	322.0	28.50	53.00	65.00	1.90	8.13	15.95	1.92	11.50	30.12	34.21	4.65
5	322.0	38.00	98.00	71.00	.80	2.86	5.00	1.57	15.00	16.12	88.75	3.73

6	0.0	0.00	0.00	21.00	.90	2.67	18.43	5.20	4.00	7.50	23.33	4.25
6	0.0	1.30	9.00	28.00	.70	1.57	9.00	4.67	5.50	4.42	40.00	4.09
6	0.0	2.00	24.50	37.50	.70	1.54	9.52	6.00	4.00	3.73	53.57	8.38
6	0.0	2.50	34.00	43.00	.90	1.80	16.24	7.33	5.50	4.58	47.78	6.82
7	30.0	11.50	0.00	29.00	.80	3.58	7.13	1.87	6.00	15.44	36.25	3.83
7	30.0	13.50	31.00	26.00	1.10	4.29	8.53	1.67	10.50	22.08	23.64	1.48
7	30.0	15.50	71.00	29.00	1.30	3.58	12.68	2.22	11.50	16.08	22.31	1.52
7	30.0	20.50	96.00	34.00	1.40	4.29	14.71	2.50	9.00	16.12	24.29	2.78
7	30.0	25.00	113.00	37.00	.70	3.58	5.71	1.80	9.50	14.80	52.86	2.89
7	41.0	5.00	0.00	25.00	.60	4.29	9.23	2.50	7.00	12.99	41.67	2.57
7	41.0	9.00	30.00	40.00	1.50	7.13	16.70	5.00	8.00	12.77	26.67	4.00
7	41.0	16.50	82.00	39.00	1.20	5.00	14.04	3.50	6.50	12.28	32.50	5.00
7	41.0	23.50	122.00	45.00	.70	4.29	11.31	3.00	10.50	11.81	64.29	3.29
7	49.0	7.00	0.00	30.00	1.10	4.57	14.57	3.50	5.00	11.89	27.27	5.00
7	49.0	9.50	35.00	27.00	.80	4.57	11.31	1.67	8.00	25.79	33.75	2.38
7	49.0	23.00	120.00	39.00	1.30	4.29	11.31	3.00	10.50	11.81	30.00	2.71
7	71.0	4.30	0.00	20.00	.60	6.44	10.95	1.57	6.00	32.29	33.33	2.33
7	71.0	7.50	41.00	36.50	1.30	4.57	14.57	2.25	10.00	18.68	28.08	2.65
7	71.0	16.00	95.00	32.50	1.00	4.57	14.57	2.08	6.50	20.64	32.50	4.00
7	71.0	20.00	114.00	42.00	.80	3.58	8.53	1.33	7.50	34.11	52.50	4.60
7	95.8	3.00	0.00	40.00	.60	4.90	9.73	1.80	9.00	21.77	66.67	3.44
7	95.8	6.50	33.00	21.00	.70	5.19	13.30	2.33	7.00	18.09	30.00	2.00
7	95.8	9.00	68.00	33.00	1.70	5.19	17.18	2.50	7.50	18.78	19.41	3.40
7	95.8	20.00	110.00	41.00	1.10	5.71	12.41	1.83	9.50	25.11	37.27	3.32
7	119.3	3.50	0.00	24.00	.80	3.27	12.09	1.57	8.00	26.85	30.00	2.00
7	119.3	9.00	58.50	50.50	.90	3.05	10.57	1.75	9.00	19.90	56.11	4.61
7	119.3	13.50	92.00	41.00	.80	4.21	12.44	3.25	7.50	11.33	51.25	4.47
7	119.3	18.50	119.00	40.50	1.20	4.16	15.26	3.50	9.50	11.57	33.75	3.26
7	131.0	3.30	0.00	27.00	.50	3.43	4.57	1.50	5.00	18.72	54.00	4.40
7	131.0	10.50	44.00	18.50	.60	4.57	23.75	2.00	4.50	27.54	30.83	3.11
7	131.0	15.00	75.00	42.50	1.00	5.71	17.82	1.67	11.30	33.74	42.50	2.76
7	131.0	16.80	105.00	47.00	2.50	7.29	18.03	1.71	14.00	35.11	18.80	2.36
7	131.0	22.00	128.00	57.00	.70	2.86	6.52	1.67	11.50	16.34	81.43	3.96
7	146.0	3.00	0.00	19.00	.80	6.71	12.60	1.67	6.00	31.29	23.75	2.17
7	146.0	6.50	63.00	25.00	1.00	4.90	11.83	2.80	9.00	13.78	25.00	1.78
7	146.0	15.50	105.00	32.00	1.00	3.12	10.30	2.13	9.60	14.52	32.00	2.33
7	146.0	21.50	137.00	37.00	.80	3.34	12.00	1.57	11.50	26.88	46.25	2.22
7	164.3	1.20	0.00	16.00	.80	5.71	26.10	2.67	3.00	21.89	20.00	4.33
7	164.3	3.20	42.00	25.00	1.00	3.43	11.86	1.67	7.50	24.02	25.00	2.33
7	164.3	11.50	109.00	39.00	1.10	5.19	10.93	1.75	13.50	24.58	35.45	1.89
7	164.3	18.50	142.00	22.00	.90	3.43	12.41	1.67	6.50	24.61	24.44	2.38
7	180.7	8.00	46.00	60.00	1.80	3.81	14.93	2.50	12.50	15.51	33.33	3.80
7	180.7	12.50	70.00	68.00	1.40	1.72	21.31	2.75	6.00	13.78	48.57	10.33
7	180.7	18.20	110.00	31.00	.70	1.91	6.97	1.25	9.00	32.41	44.29	2.44
7	180.7	21.50	154.00	42.00	.50	2.86	5.71	1.10	20.50	56.15	84.00	1.05
7	200.0	8.00	20.50	33.00	.90	6.84	14.57	2.20	9.50	22.90	36.67	2.47
7	200.0	9.50	39.50	39.00	1.00	4.00	14.04	2.50	10.50	15.31	39.00	2.71
7	200.0	13.50	63.00	43.00	1.00	3.43	10.20	2.90	10.00	10.41	43.00	3.30
7	200.0	20.50	94.00	48.00	.60	3.63	9.90	1.67	8.50	22.26	80.00	4.65
7	214.0	1.50	0.00	16.00	1.10	4.94	15.85	3.50	5.00	12.82	14.55	2.20
7	214.0	6.50	47.00	21.00	1.00	3.81	13.13	1.64	7.00	27.02	21.00	2.00
7	214.0	14.00	87.00	19.50	.90	3.58	16.04	1.71	5.50	27.07	21.67	2.55
7	214.0	17.50	109.00	13.50	.70	4.18	15.02	2.20	4.50	18.86	19.29	2.00
7	214.0	20.50	126.00	17.50	.70	5.60	20.43	3.00	4.50	17.40	25.00	2.89
7	234.5	3.50	0.00	28.00	1.00	3.99	24.39	2.14	5.70	24.62	28.00	3.91
7	234.5	7.00	30.00	36.00	1.20	1.94	17.85	2.25	5.80	16.44	30.00	5.21
7	234.5	12.50	59.00	57.00	1.70	4.57	9.93	1.40	18.50	34.68	33.53	2.08
7	234.5	16.50	97.00	21.00	1.00	5.71	16.99	2.75	5.20	17.64	21.00	3.04
7	259.0	3.00	0.00	47.00	.90	1.49	3.98	1.43	14.50	13.91	52.22	2.24
7	259.0	7.00	24.50	52.00	1.30	4.00	15.64	2.00	10.50	21.63	40.00	3.95

7	259.0	13.00	50.00	42.00	1.40	4.09	18.61	2.25	7.00	20.29	30.00	5.00
7	259.0	16.00	73.00	48.00	1.00	2.29	10.20	1.62	11.00	20.74	48.00	3.36
7	278.0	7.50	0.00	22.50	1.00	11.59	15.75	2.50	6.00	27.50	22.50	2.75
7	278.0	9.50	33.00	21.50	1.20	4.76	10.39	1.83	8.50	21.52	17.92	1.53
7	278.0	14.00	80.00	39.50	.90	4.00	10.76	1.80	15.50	21.01	43.89	1.55
7	278.0	20.50	129.00	43.00	1.00	3.43	11.31	1.75	16.50	21.44	43.00	1.61
7	306.0	3.50	0.00	27.00	.40	4.84	24.59	2.17	3.00	25.61	67.50	8.00
7	306.0	5.50	16.00	28.00	.60	6.84	20.81	2.33	4.00	24.62	46.67	6.00
7	306.0	9.50	36.00	28.00	1.00	9.16	19.54	2.00	5.00	32.32	28.00	4.60
7	306.0	11.50	55.00	25.00	.90	5.53	14.47	1.71	5.50	29.35	27.78	3.55
7	306.0	18.00	84.00	28.00	1.00	9.09	18.78	1.80	4.50	36.13	28.00	5.22
7	320.0	.20	0.00	22.00	.50	3.49	12.38	2.00	4.00	18.25	44.00	4.50
7	320.0	4.50	17.00	33.50	.90	4.28	13.66	1.60	5.00	29.67	37.22	5.70
7	320.0	7.00	39.00	47.00	1.40	5.44	20.06	2.33	8.50	22.19	33.57	4.53
7	320.0	9.30	52.00	54.00	1.10	2.57	10.19	1.40	7.00	30.06	49.09	6.71
7	320.0	16.00	86.00	36.00	1.40	11.69	21.63	2.67	7.50	28.39	25.71	3.80
7	320.0	20.20	109.00	30.50	1.30	11.31	18.00	1.94	7.00	35.85	23.46	3.36
8	43.0	3.80	20.00	28.00	1.20	3.81	14.04	4.00	9.00	9.56	23.33	2.11
8	43.0	6.00	34.00	30.00	.90	4.21	15.87	2.00	6.50	22.15	33.33	3.62
8	43.0	8.50	48.00	38.00	1.20	5.27	15.48	2.75	11.00	16.32	31.67	2.45
8	43.0	12.00	63.00	45.00	1.40	4.86	22.38	4.80	7.50	11.53	32.14	5.00
8	62.0	.50	19.00	27.00	.80	3.34	8.53	3.00	10.00	9.15	33.75	1.70
8	62.0	2.20	47.00	41.00	1.60	6.65	23.43	5.00	8.50	13.57	25.63	3.82
8	62.0	6.20	61.00	49.00	1.50	5.91	16.52	4.00	11.50	12.98	32.67	3.26
8	62.0	9.50	71.00	52.00	1.10	3.66	13.93	2.40	12.00	15.46	47.27	3.33
8	151.0	6.50	0.00	35.50	.70	4.57	9.46	1.40	11.00	34.01	50.71	2.23
8	151.0	8.50	23.00	18.00	.70	4.51	11.31	1.75	6.00	23.60	25.71	2.00
8	151.0	10.50	38.00	44.00	1.50	5.30	14.73	2.13	10.00	21.31	29.33	3.40
8	151.0	17.50	61.00	37.00	2.50	9.93	19.54	2.30	10.50	28.92	14.80	2.52
8	172.0	3.40	31.00	28.00	.70	4.29	9.58	1.80	10.00	20.41	40.00	1.80
8	172.0	6.50	62.00	28.00	1.10	4.45	9.46	1.50	11.30	28.87	25.45	1.48
8	182.8	0.00	0.00	27.50	.60	1.91	5.71	1.50	7.50	16.52	45.83	2.67
8	182.8	1.50	25.50	39.00	.70	3.01	10.15	1.57	11.00	23.86	55.71	2.55
8	182.8	3.20	38.00	39.50	.80	2.75	8.64	1.62	8.50	19.78	49.38	3.65
8	187.8	1.00	0.00	17.80	.60	3.43	11.31	1.94	4.00	18.03	29.67	3.45
8	187.8	2.50	19.00	27.00	1.10	4.01	19.33	2.37	5.00	19.23	24.55	4.40
8	187.8	6.00	42.00	24.00	1.00	5.33	19.80	2.25	5.50	22.86	24.00	3.36
8	194.7	1.50	0.00	17.00	.60	3.69	5.53	1.67	4.30	16.96	28.33	2.95
8	194.7	4.50	38.00	25.50	.80	4.65	9.25	1.80	7.00	20.81	31.88	2.64
8	194.7	11.50	90.50	52.00	1.40	2.86	11.03	2.00	11.00	16.00	37.14	3.73
8	194.7	14.50	106.00	50.00	1.80	3.37	14.93	2.13	11.50	18.32	27.78	3.35
8	203.0	.50	0.00	27.50	.50	2.05	9.33	1.57	5.00	20.50	55.00	4.50
8	203.0	5.00	42.00	28.00	.60	3.05	16.70	1.90	5.50	22.47	46.67	4.09
8	203.0	9.50	74.00	29.00	1.50	4.95	17.74	2.50	10.50	18.70	19.33	1.76
8	203.0	19.00	142.00	57.00	1.30	4.30	6.01	1.75	21.00	17.45	43.85	1.71
8	209.0	3.00	0.00	35.00	.90	2.36	16.10	1.80	5.50	22.76	38.89	5.36
8	209.0	5.50	23.00	28.50	1.00	3.69	7.72	1.80	9.00	17.26	28.50	2.17
8	209.0	11.50	50.00	31.50	1.90	6.06	23.01	2.50	7.50	22.70	16.58	3.20
8	209.0	19.50	81.00	34.50	1.10	4.97	16.16	1.90	6.00	25.41	31.36	4.75
8	215.8	2.50	0.00	30.00	.80	5.19	12.80	1.83	6.50	24.50	37.50	3.62
8	215.8	9.70	30.00	36.00	1.60	4.16	18.12	1.75	11.00	28.85	22.50	2.27
8	215.8	12.50	40.00	25.50	1.00	5.71	16.11	2.00	8.50	24.84	25.50	2.00
8	215.8	17.00	75.00	28.50	1.00	4.21	16.98	1.90	8.00	24.70	28.50	2.56
8	223.0	2.30	0.00	31.00	1.10	3.27	14.04	2.00	7.50	19.16	28.18	3.13
8	223.0	6.00	22.50	37.50	1.20	3.23	13.60	2.06	9.00	17.91	31.25	3.17
8	223.0	9.50	45.00	33.00	1.00	3.42	13.43	1.94	8.00	19.78	33.00	3.13
8	228.0	1.00	17.00	36.00	1.20	3.96	15.48	3.14	7.00	12.56	30.00	4.14
8	228.0	5.00	41.00	44.00	1.50	5.71	20.81	6.80	9.00	10.03	29.33	3.89
8	228.0	11.00	62.00	59.00	1.20	3.43	5.71	1.60	23.00	17.97	49.17	1.57
9	449.0	9.00	0.00	42.00	1.00	5.71	17.35	3.50	12.00	14.35	42.00	2.50

9	449.0	21.50	49.00	46.00	1.00	4.33	6.05	2.17	14.00	13.00	46.00	2.29
9	449.0	27.50	76.00	41.00	.80	4.97	11.31	4.50	9.00	9.50	51.25	3.56
9	449.0	30.00	123.00	47.00	1.00	5.14	11.31	4.00	14.50	10.46	47.00	2.24
9	484.0	4.50	0.00	37.00	1.10	3.61	11.31	3.84	12.00	8.73	33.64	2.08
9	484.0	20.00	109.00	55.00	2.40	5.71	18.00	5.00	12.00	11.33	22.92	3.58
9	484.0	26.00	151.00	43.00	.70	2.86	10.85	2.25	11.00	13.37	61.43	2.91
9	484.0	30.00	224.00	49.00	1.50	3.34	16.26	2.40	14.00	16.30	32.67	2.50
9	484.0	48.00	314.00	57.00	1.10	2.49	9.87	10.00	11.50	3.85	51.82	3.96
9	528.0	4.00	0.00	27.00	.90	4.53	11.75	2.20	8.50	17.26	30.00	2.18
9	528.0	21.50	56.00	42.00	1.50	5.82	17.47	2.57	11.00	19.27	28.00	2.82
9	528.0	42.00	124.00	48.00	1.40	4.22	13.37	4.50	13.00	9.09	34.29	2.69
9	528.0	49.00	161.00	64.00	1.30	2.86	7.41	4.67	15.00	5.63	49.23	3.27
9	528.0	57.00	220.00	50.00	1.00	3.05	6.84	3.33	18.00	7.24	50.00	1.78
9	562.0	1.50	24.00	36.00	1.10	6.84	16.35	4.50	7.00	13.12	32.73	4.14
9	562.0	14.00	62.00	48.00	1.40	7.13	17.57	3.63	9.00	15.87	34.29	4.33
9	562.0	32.00	106.00	49.00	.70	6.09	14.93	3.33	7.00	14.59	70.00	6.00
9	562.0	36.00	170.00	53.00	1.10	4.84	15.89	2.50	10.00	17.58	48.18	4.30
9	562.0	53.00	260.00	57.00	1.00	5.71	13.50	7.00	12.00	8.82	57.00	3.75
9	587.0	7.00	27.00	27.00	1.10	6.34	11.31	2.75	5.50	15.92	24.55	3.91
9	587.0	18.50	77.00	33.00	1.20	3.69	9.76	1.83	10.00	18.82	27.50	2.30
9	587.0	34.00	154.00	36.00	1.40	5.27	12.15	3.17	10.50	12.98	25.71	2.43
9	587.0	45.00	213.00	35.00	1.00	5.89	17.88	3.17	8.50	16.04	35.00	3.12
9	587.0	58.00	257.00	43.00	1.00	4.00	16.70	3.33	9.00	12.39	43.00	3.78
9	607.0	12.50	0.00	29.00	1.00	3.43	15.64	2.50	8.50	15.30	29.00	2.41
9	607.0	17.50	44.00	35.00	1.50	4.55	19.98	4.25	8.50	11.63	23.33	3.12
9	607.0	29.50	71.00	37.00	1.00	3.16	7.08	1.70	13.50	17.10	37.00	1.74
9	607.0	39.00	111.00	42.00	1.10	3.27	16.32	2.67	9.50	14.27	38.18	3.42
9	607.0	49.00	145.00	38.00	.70	3.42	8.27	1.67	11.00	19.85	54.29	2.45
9	607.0	55.00	184.00	42.00	.90	4.09	10.52	1.88	8.00	19.62	46.67	4.25
9	630.0	1.80	0.00	24.00	.80	5.98	10.78	2.00	7.50	21.45	30.00	2.20
9	630.0	17.50	47.00	32.00	1.00	6.12	16.70	2.40	8.00	20.81	32.00	3.00
9	630.0	34.00	81.00	36.00	1.60	3.96	18.30	2.50	9.00	17.49	22.50	3.00
9	630.0	44.00	102.00	33.00	1.10	2.76	16.15	2.30	11.00	16.23	30.00	2.00
9	630.0	53.00	129.00	44.00	1.00	3.81	14.22	2.09	11.50	19.00	44.00	2.83
9	647.0	14.00	11.00	25.00	1.00	2.86	12.23	2.57	5.50	12.07	25.00	3.55
9	647.0	22.50	60.00	34.00	1.20	2.82	14.70	3.33	8.00	10.02	28.33	3.25
9	647.0	33.50	108.00	39.00	1.10	4.00	16.70	2.25	8.00	19.06	35.45	3.88
9	647.0	48.00	159.00	46.00	1.80	5.19	19.98	3.29	10.50	15.33	25.56	3.38
9	647.0	62.00	214.00	31.00	.90	5.08	10.70	5.00	6.50	8.93	34.44	3.77
9	667.0	3.50	0.00	28.00	.70	3.15	10.70	4.00	5.50	7.68	40.00	4.09
9	667.0	12.50	55.00	35.00	1.30	4.11	13.95	3.25	10.00	11.79	26.92	2.50
9	667.0	23.50	103.00	42.00	1.40	4.09	12.88	1.80	9.00	23.16	30.00	3.67
9	667.0	35.00	129.00	49.00	2.40	7.52	20.67	2.80	12.00	21.36	20.42	3.08
9	667.0	57.00	197.00	55.00	2.40	5.71	13.79	2.89	15.50	15.44	22.92	2.55
9	667.0	65.50	238.00	59.00	1.30	4.57	14.04	5.33	18.00	8.74	45.38	2.28
9	691.0	13.00	13.00	28.00	1.20	4.16	10.81	1.83	12.00	20.74	23.33	1.33
9	691.0	20.50	49.00	30.50	1.40	5.08	12.53	2.60	9.00	15.49	21.79	2.39
9	691.0	31.00	104.00	42.00	1.30	3.01	9.56	1.80	14.00	17.81	32.31	2.00
9	691.0	38.50	132.00	25.00	1.10	5.44	18.43	3.33	6.00	14.94	22.73	3.17
9	691.0	46.00	165.00	31.00	1.40	4.29	19.29	5.00	6.50	9.88	22.14	3.77
10	0.0	4.70	0.00	24.00	1.00	3.18	12.23	6.67	7.00	5.85	24.00	2.43
10	0.0	13.00	115.00	56.00	.90	2.06	10.46	4.17	10.00	5.95	62.22	4.60
10	0.0	21.00	156.00	63.00	.90	1.64	11.57	3.43	10.00	6.95	70.00	5.30
10	0.0	26.00	192.00	83.00	.70	.98	7.99	3.50	6.50	4.53	118.57	11.77
10	70.0	5.50	0.00	35.00	1.20	2.75	14.55	8.50	9.00	5.01	29.17	2.89
10	70.0	8.50	52.00	66.00	1.10	2.44	12.94	2.50	8.00	12.23	60.00	7.25
10	70.0	14.00	95.00	51.00	1.50	2.89	20.24	1.71	10.00	29.19	34.00	4.10
10	70.0	24.00	150.00	75.00	1.00	1.44	6.16	4.00	13.00	3.96	75.00	4.77
10	130.0	5.00	0.00	48.00	1.30	2.39	10.23	3.13	16.00	8.19	36.92	2.00
10	130.0	11.00	31.00	66.00	2.80	3.91	20.49	2.20	19.00	21.68	23.57	2.47
10	130.0	19.50	50.00	51.00	1.00	2.16	5.66	2.83	18.00	6.38	51.00	1.83

10	130.0	23.00	109.00	67.00	3.00	7.89	21.85	3.14	17.00	20.20	22.33	2.94
10	250.0	6.00	0.00	36.00	1.00	2.89	11.16	3.67	7.00	8.03	36.00	4.14
10	250.0	10.50	26.00	47.00	1.70	2.83	11.40	2.30	12.00	13.29	27.65	2.92
10	250.0	15.50	39.00	49.00	1.50	3.62	10.51	2.50	11.00	12.69	32.67	3.45

EAST OF ANSE A MERCIER, GRANDE VALLEE

1	90.0	8.00	0.00	28.00	1.00	5.34	14.16	7.33	6.00	8.33	28.00	3.67
1	90.0	10.00	16.00	32.00	1.50	5.87	11.31	3.25	12.00	13.20	21.33	1.67
1	90.0	20.50	95.00	45.00	1.70	5.81	17.41	3.14	11.00	15.86	26.47	3.09
1	90.0	23.00	114.00	50.00	1.20	3.48	9.15	6.00	12.50	5.97	41.67	3.00
2	104.0	6.00	0.00	25.00	1.40	3.95	19.47	8.00	6.00	7.16	17.86	3.17
2	104.0	7.50	27.00	25.50	1.60	4.81	30.52	10.00	5.50	8.42	15.94	3.64
2	104.0	10.00	55.00	27.00	1.30	5.40	13.44	7.20	9.00	8.35	20.77	2.00
2	104.0	12.00	74.00	32.00	1.60	7.00	17.03	4.00	8.50	14.52	20.00	2.76
2	128.0	7.30	24.50	20.00	.70	3.26	10.40	5.20	4.50	6.46	28.57	3.44
2	128.0	8.00	52.50	23.50	.80	2.64	12.58	4.00	6.40	7.59	29.38	2.67
2	128.0	11.10	85.00	37.00	1.20	1.94	13.35	4.29	7.50	6.48	30.83	3.93
2	128.0	13.20	101.00	40.00	.80	2.29	7.20	2.50	9.50	8.51	50.00	3.21
2	154.0	5.40	8.50	22.50	.90	2.22	19.27	9.33	4.00	4.72	25.00	4.63
2	154.0	9.50	77.00	22.00	1.30	4.49	16.70	4.75	5.50	9.90	16.92	3.00
2	154.0	11.00	103.00	28.00	1.20	3.95	17.96	5.14	7.30	9.00	23.33	2.84
2	154.0	13.50	125.00	39.00	1.00	2.08	11.31	4.25	7.50	6.13	39.00	4.20
2	180.0	5.20	0.00	19.50	.80	4.40	14.38	9.00	4.50	6.69	24.38	3.33
2	180.0	6.30	35.50	26.00	1.40	5.83	22.46	7.33	6.50	10.03	18.57	3.00
2	180.0	11.00	97.00	38.50	2.30	3.30	15.58	6.67	11.50	6.54	16.74	2.35
2	180.0	13.00	114.00	45.00	.90	1.75	11.53	4.00	7.50	6.10	50.00	5.00
2	214.0	4.00	0.00	19.50	.80	2.29	13.17	11.33	3.50	3.76	24.38	4.57
2	214.0	7.40	69.00	21.50	1.00	3.49	15.37	7.50	5.00	6.32	21.50	3.30
2	214.0	11.20	111.00	27.00	1.40	2.56	14.64	4.00	7.50	8.11	19.29	2.60
2	214.0	14.50	132.00	36.50	1.10	4.42	5.57	3.33	16.00	8.65	33.18	1.28
3	0.0	4.70	0.00	31.00	.80	3.27	10.78	5.75	7.50	6.18	38.75	3.13
3	0.0	5.60	16.00	35.00	1.20	3.72	7.69	2.75	12.00	10.10	29.17	1.92
3	0.0	9.00	45.00	38.00	1.00	4.21	16.39	5.00	5.50	9.15	38.00	5.91
3	0.0	12.50	92.00	52.00	.80	3.13	8.00	4.00	7.50	6.79	65.00	5.93

ANSE A MERCIER WEST, GRANDE VALLEE

4	0.0	20.00	0.00	27.00	1.20	4.16	14.77	4.50	7.00	9.37	22.50	2.86
4	0.0	41.00	68.00	29.00	1.60	4.76	15.38	4.00	11.00	11.18	18.13	1.64
4	0.0	57.00	85.00	33.00	2.10	7.28	14.04	1.69	11.50	33.02	15.71	1.87
4	0.0	63.00	112.00	35.00	1.80	7.03	13.85	1.89	12.50	27.50	19.44	1.80
5	0.0	16.00	0.00	27.00	1.40	11.11	19.65	4.86	8.00	18.40	19.29	2.38
5	0.0	23.00	24.00	44.00	2.00	7.88	27.61	6.00	10.00	14.27	22.00	3.40
5	0.0	41.00	113.00	49.00	1.80	10.35	24.74	5.00	12.50	18.18	27.22	2.92
5	0.0	52.00	265.00	68.00	3.20	5.08	8.43	1.79	28.00	21.10	21.25	1.43
6	0.0	14.00	0.00	27.00	1.90	6.40	14.59	4.80	8.50	11.70	14.21	2.18
6	0.0	22.00	62.00	48.00	3.10	7.03	19.64	2.83	16.00	20.06	15.48	2.00
6	0.0	31.00	114.00	46.00	2.30	3.04	16.87	3.33	13.00	11.14	20.00	2.54
6	0.0	43.00	170.00	69.00	4.00	4.79	30.66	2.09	16.50	29.23	17.25	3.18